Markov Chain Analysis for IEEE 802.11 Wireless Networks

by

XIJIE LIU

A dissertation submitted to the Graduate Faculty in Engineering in partial fulfillment of the requirement for the degree of Doctor of Philosophy, The City University of New York

2012

This manuscript has been read and accepted for the
Graduate Faculty in the Engineering in satisfaction of
the dissertation requirement for the degree of Doctor of Philosophy

Professor Tarek N. Saadawi

Date 10/20/2011 Chair of Examining Committee

Professor Mumtaz Kassir

Date 11/3/2011 Executive Officer

Professor Myung J. Lee

Professor Yi Sun

Professor Michael Conner

Professor Mehmet Ulema

Supervisory Committee

THE CITY UNIVERSITY OF NEW YORK

This manuscript has been read and accepted for the
Graduate Faculty in the Engineering in satisfaction of
the dissertation requirement for the degree of Doctor of Philosophy

Professor Tarek N. Saadawi .

Date Chair of Examining Committee .

Professor Mumtaz Kassir .

Date Executive Officer .

Professor Myung J. Lee .

Professor Yi Sun .

Professor Michael Conner .

Professor Mehmet Ulema .

Supervisory Committee

THE CITY UNIVERSITY OF NEW YORK

Abstract

Markov Chain Analysis for IEEE 802.11 Wireless Networks

by

XIJIE LIU

Adviser: Professor Tarek N. Saadawi

In this dissertation, we investigate the Markov chain analytical model, which is applied in three focuses of current interest: the distortion of video quality, the performance of directional MAC (D-MAC) protocols, and the performances of IEEE 802.11 wireless networks in the presence of various greedy behavior strategies.

First, to seek an innovative computable formula to evaluate objective video quality, we discover formulas to estimate the video quality distortion due to packet loss in IEEE 802.11 wireless networks. We also derive the expressions to estimate the video quality where some IEEE 802.11 wireless nodes manipulate their backoff schemes. Based on the formulas, numerical results of video quality are provided for different wireless network scenarios. An optimization of setting parameters of IEEE 802.11 to minimize the distortion is also discussed. As a conclusion, the formulas provide us a transition from setting parameters of IEEE 802.11 wireless networks to the objective video quality of wireless networks and allow us to compute the objective video quality if the parameters of IEEE802.11 wireless networks are given.

Second, we calculate the performance of a D-MAC protocol with a new Markov chain equivalently. As an example, our approach is applied to single-hop wireless networks where nodes are directional and distributed randomly. We obtain theoretical throughput and delays of each node in the D-MAC wireless networks. Numerical results show that the average throughput of wireless network, a 64-node network for example, will increase at a faster pace for the RTS/CTS access mechanism than the basic access mechanism while transmitting antenna elements increase from one to eight. Numerical results also show the performance of D-MAC wireless network depends on the parameters of D-MAC protocol and the number of antennae, as well as the topology.

Third, we provide a series of analytical formula to obtain the performance of the IEEE 802.11 wireless networks in the presence of various greedy behavior strategies. Unlike previous research papers, our improvement provides the performance of nodes where the nodes have different arrival rates under non-saturation conditions. It also provides analytical performances for multi-hop networks, networks with hidden nodes, and networks combining multiple greedy strategies.

Clearly each user may have different applications, and as a result users have different arrival rates. We improve the Markov chain analytical model so that the non-saturation Markov is able to compute performance of wireless networks whose stations have heterogeneous traffic in this dissertation. Our analysis with the Markov chain analytical model is validated in multiple scenarios with heterogeneous traffic, and is proved by simulations.

Acknowledgments

First of all, I am highly grateful to my advisor, Professor Tarek N. Saadawi, for his continuous encouragement, guidance, and financial support during the past five years of my graduate studies. I would never have been able to finish my dissertation without his guidance.

In addition, I would like to thank all my committee members for their constructive criticism and useful feedback. I also would like to thank all of the members in our lab for the time we had in the past couple of years. And I would like to express my genuine gratitude to the City University of New York for the given opportunities, and for its helpful finance support. I would never have chance to finish my dissertation without their support in all ways through.

Finally, I would like to thank my family and wife. I will be able to finish my dissertation with their support.

Table **o**f Contents

List of Figures

List of Tables

1. Introduction

In this dissertation, we investigate the theoretical formula of three focuses of current interest: the distortion of video quality, the performance of D-MAC protocols, and the performances of IEEE 802.11 wireless networks in the presence of various greedy behavior strategies. Our work is motivated by the increased needs of video services over IEEE 802.11 wireless networks.

In order to discover the theoretical formulae of video quality over wireless networks, or the performance of D-MAC protocols, or the performances of IEEE 802.11 wireless networks in the presence of various greedy behavior strategies, the Markov chain analysis model is applied. To the best of my knowledge, the Markov chain model has never been used in analysis of video quality for wireless networks. Neither has it been used in the analysis of performance for D-MAC protocols.

The bi-dimensional Markov chain analysis model, as a tool of analysis of performance of IEEE 802.11 protocols, was introduced by Bianchi [7] in 2000. The model is able to simulate the exponential backoff protocol, and to compute the throughput performance for both standardized Basic and RTS/CTS access mechanisms. In Bianchi's model[7], performance of IEEE 802.11 has been carried out by formulas with simplified backoff assumptions and under saturation conditions. Bianchi's model does not provide performance of IEEE 802.11 wireless network under non-saturation condition or in the presence of the hidden stations. The model does not analyze the IEEE 802.11e, either.

Huang and Liao [33] extend the Bianchi model to analyze the performance of IEEE 802.11e (EDCA), using the different AIFSN of Access Categories (ACs) parameter set and virtual collision. The analysis has also been performed under saturation conditions. Saturation condition is relaxed by Engelstad and Østerbø [21]. Engelstad and Østerbø provide a non-saturation analysis model for IEEE 802.11e, using a modified Markov chain. Hung and Marsic [35] provide analysis of performance in the presence of the hidden station effect for the IEEE 802.11. However, heterogeneous traffic is not discussed in [21] and

[35]. A remarkable improvement on the Markov chain analytical model is still wanted so that non-saturation Markov is able to compute performance of wireless networks with heterogeneous traffic. The stations in real wireless networks have heterogeneous traffic.

The summary of our contribution versus the previous research conclusion is briefed in Table 1-1.

Video application, transmitted over IEEE 802.11 wireless networks, has a successful boom in the 2000s. And video over a convergence of infrastructures of IEEE802.11 and of mobile systems will also be regarded as the next step in mobile/wireless broadband evolution. Hence, evaluating the video quality over IEEE 802.11 wireless networks has been needed by engineers and has drawn much attention. Khan et. al. [39] try to provide quality prediction for various video content types over wireless networks. They use cluster analysis to classify video content into three specific content types. Then, their automatic content classification predicts video quality with optimization of bandwidth allocation for specific content the bandwidth. Other researchers([5], [9] and [13]) provide methods to estimate the distortion caused by packet losses in wireless video communication. Their methods to evaluate video quality over IEEE 802.11 wireless networks are measured with video measurement instrument in wireless network test beds.

Distortion of video over IEEE 802.11 wireless networks is one interesting research area. It is a fundamental need to evaluate the quality distortion of video over IEEE 802.11 wireless networks. The main factor of distortion of video is packet loss over IEEE 802.11 wireless networks. It is good to have the measurement methods in previous researches([5], [9] and [13]). However, these methods are expensive and time consuming, and are not convenient to optimize parameters of IEEE 802.11. We lacked a theoretical calculation on video quality over wireless networks. Optimization of parameters of IEEE 802.11 to minimize the distortion of video becomes difficult without the theoretical tools. It is necessary to seek an innovative computable formula to evaluate objective video quality.

In the dissertation, our research investigates a transition from parameters of IEEE 802.11 to an objective video quality metric and provides a theoretical calculation on the inherent distortion of video quality. The research on the inherent distortion has considerable room for improvement. According to IEEE 802.11 protocols, a frame retry limit is defined. The frame retry limit results in a consequence that a packet will be discarded due to exceeding the maximum frame retry limit. As a result, this packet loss brings in an inherent distortion of video quality, even if the networks operate in an ideal physical environment, i.e. no frame errors. Generally, we can combat other packet losses and thus improve video quality. But the packet losses brought by MAC schemes are inherent.

The inherent distortion may be serious with some parameters of IEEE 802.11 wireless networks, and may force us to give up some methods to send videos, which have no higher layer retransmission guaranty. Unfortunately, the research on the inherent distortion remains poor and there is considerable room for improvement. In chapter 3, our research is more focused on the inherent distortion of video quality.

The enhancement of video quality over IEEE 802.11 wireless networks also has become a popular topic. Jrad, et. al. [38], present a context-aware mechanism to improve video quality over wireless networks. Lee, et.al [48] consider forward-error correction code of each layer to maximize the overall video quality. Optimal cross-layer strategies for enhancing the robustness and efficiency of video over the IEEE 802.11 networks are discussed in [22] and [61]. Tian, et. al. [72] develop an optimal scheduling framework to minimize the expected distortion by first estimating the receiving status. Hady et. al. [30] present a generic framework solution for minimizing video distortion of all multiple video streams transmitted over IEEE 802.11e wireless networks.

Following the enhancement of video quality over IEEE 802.11 wireless networks, we discuss an optimization of setting parameters of IEEE 802.11 to improve received video quality. We find that it is

important to choose the network settings so that they maximize the end-user quality. Numerical results will show how the setting parameters affect the video quality. As another example, we apply the equation of video quality in wireless networks where some IEEE 802.11 wireless nodes manipulate their backoff. We prove quantitatively in chapter 3 that the video quality of manipulating nodes is enhanced.

The capacity of IEEE 802.11 channel has significant shortcomings, especially when compared with wire line networks. One of the reasons is that only one omni-directional antenna node may transmit to a neighboring node or receive from a neighboring node at one time and this limits the system's performance. The directional antenna systems have better spatial multiplexing, and reduced interference as by directing the radio beam towards a desired direction; this spatial multiplexing and reduced interference will increase the capacity of wireless systems.

The potential use of directional antennas has been attracting the attention of researchers recently, from proposing new MAC protocols suitable for wireless networks equipped with directional antennas, to evaluating, testing, enhancing its performance, and even addressing the shortcomings of directional antennas. There are two categories of directional antenna systems which are discussed in current research literature on wireless networks. In the first category, the wireless station's transceiver has only one antenna at the physical layer, but the antenna radiates greater power in one or more directions allowing for increased performance on transmit and receive and reduced interference from unwanted sources. The second category is referred to as a directional antenna (array); where the wireless station transceiver has multi-antennas and can simultaneously serve many user terminals. In this dissertation, the second category is discussed.

In [17], [34], [42], [43], [46], [55] and [60], a directional Medium Access Control (MAC) protocol using directional antennas is designed, summarized, and compared.. During the same period, the fundamental issues arising from the deployment of directional antennas are discussed in ([17], [24], [37],

[43], [55] and [69]. These issues include increased occurrences of deafness and directional hidden terminal problem ([17], [24], [43] and [69]), in scenarios of wireless multihop networks. Current D-MAC does not provide a scheme to discover and track its neighbors in the presence of mobility ([37] and [55]).

Some authors prefer to focus on developing a method to evaluate performance of D-MAC. Evaluation of the capacity of D-MAC can be found [6], [16], [32], [45], [59], [68], [70], and [74]. For example, Choudhury and Vaidya [16] address the impact of directional antennas on the performance of routing protocols. Spyropoulos and Raghavendra [68] calculate interference-based capacity bounds and analyze how gain and bandwidth affect these bounds. Hsu and Rubin [32] obtain mathematical equations and characterize the throughput performance of a directional-ALOHA by using a collision channel analytical interference model and a SINR interference model. Lal and others [45] introduce a method for analytical performance of multiple-beam antenna nodes. Sundaresan and Sivakumar [70] present a unified representation of the PHY layer capabilities of the different types of smart antennas.

Table 1-1, Summary of the analyses of IEEE 802.11 in this thesis

	saturation	non-saturation	hidden stations	non-saturation &Video quality	hidden& Video quality	Greedy behavior & Video quality	D-MAC
Bianchi [7]	○						
Huang [33]	○						
Engelstad[21]	○	○					
Hung[35]	○		○				
proposed work	○	○	○	○	○	○	○

Unlike previous research papers, we propose a new Markov chain to calculate the throughput and delay of a directional MAC in chapter 4.

The distributed coordination function (DCF) of the IEEE 802.11 protocol is designed under the assumption that all nodes would obey the protocols honestly. Using DCF fairly requires that all wireless nodes shall use a binary exponential backoff scheme to access the medium. A good-behavior node with

a packet to transmit selects a random back-off value from a contention window; if the node has a collision, it doubles the contention window and selects a random back-off value again from the new contention window. However, in some case, greedy nodes will deviate from the fair binary exponential backoff scheme to greedily obtain a higher throughput than the other nodes. They manipulate the backoff value to maximize their own bandwidth.

Detection of greedy nodes has attracted much attention in the academic literature. The recent achievements to detection research are found in [11], [26], [27], [28], [56], [58], [61], [62] and [65]. Some authors decide whether a node is acting selfishly or not based on an observed behavior ([11], [26], [62] and [65]), and others propose to modify the MAC protocol to avoid greedy behavior ([27], [28], [56], [61] and [62]). Detecting greedy nodes effectively is a most challenging task. A single detecting algorithm might not be suitable for all complex circumstances.

Some greedy strategies in the MAC layer employ a single strategy during its manipulation of backoff. Others will combine different strategies during whole period in order to avoid being detected. There are four common greedy strategies found in recent research. We summarize them as follows:

- Strategy 1: randomly select a small value from a fixed contention window $\{0, w_0 - 1\}$; nodes do not double the contention window after a collision, ([25] [44],[61]);
- Strategy 2: select a random backoff value from a smaller contention window, $\{0, w_j/A\}$, where A is larger than one ([24] [25] [63]);
- Strategy 3: always select a fixed backoff counter value during whole period ([25]);
- Strategy 4: select a backoff of zero L-1 times and select a value above $w_0/4$ as the Lth backoff ([11]).

A performance analysis of MAC layer in the presence of greedy behaviors, under single-hop saturation conditions, is provided in [12] and [28]. Another relative analysis, under single-hop non-saturations

condition, is presented in [51]. Those three papers have analyzed Greedy Strategy 2, "selecting a random backoff value from a smaller range of backoff value"; however, they do not expand to other greedy strategies, or multihop networks. Neither do they expand to a network with a hidden node, or nodes with different arrival rates, or other more complex topologies.

In chapter 5, we focus on analysis of performance characteristic in the presence of combined greedy behavior strategies, such as delay and throughput, which may help to detect misbehavior in future research. Each node's expected throughput and delay, including greedy nodes, are calculated with the help of three bi-dimensional Markov Chain Models. Our analysis covers more general scenarios of non-saturation conditions, as well as different packet arriving rates. In practical networks, this is significant because each node often has different applications in various scenarios.

2. Markov Chain Analytical Models in IEEE802.11

2.1. Overview of IEEE 802.11

2.1.1. IEEE 802.11 family and CSMA/CA

The IEEE 802.11 family consists of a series of over-the-air physical layer techniques that use the same Carrier Sense Multiple Access with Collision Avoidance(CSMA/CA) protocol at MAC layer. IEEE 802.11b was the first widely accepted one, followed by amendments IEEE 802.11a, IEEE 802.11g and IEEE 802.11n.

IEEE 802.11b has a maximum raw data rate of 11 Mbit/s and uses CSMA/CA media access protocol. IEEE 802.11a standard operates in the 5 GHz band with a maximum data rate of 54 Mbit/s with an OFDM based air interface (physical layer). IEEE 802.11g was ratified in 2003, and works in the 2.4 GHz band (like IEEE 802.11b), but has the same OFDM as IEEE 802.11a. IEEE 802.11g operates at a maximum physical layer bit rate of 54 Mbit/s. IEEE 802.11g hardware is fully backwards compatible with IEEE 802.11b hardware.

IEEE 802.11 current version is IEEE 802.11-2007, rolling up many of the amendments to the 1999 version of the IEEE 802.11 standard. The merged eight amendments (IEEE 802.11a, b, d, e, g, h, i, j) was named to IEEE 802.11-2007 after the merged amendments were approved on March 8, 2007.

A newer amendment is published in October 2009. It is called IEEE 802.11n, which has a new multiple-input multiple-output antenna (MIMO). MIMO allows a significant increase in the maximum raw data rate from 54 Mbit/s to 600 Mbit/s at a channel width of 40 MHz.

CSMA/CA is used in IEEE 802.11 wireless LANs as media access protocol. CSMA/CA protocol, defined in the original IEEE 802.11-1997, includes a carrier sensing scheme. The protocol requires that a node wishing to transmit data has to listen to the channel to determine whether or not another node is transmitting on the channel within its wireless coverage range. If the channel is sensed "idle," then the

node is permitted to begin the transmission process. If the channel is sensed as "busy," the node defers its transmission for a random period of time.

CSMA/CA is able to improve the performance of Carrier Sense Multiple Access (CSMA) by not allowing wireless transmission if a node is transmitting, thus reducing the probability of collision due to the use of a random binary exponential backoff time. CSMA is a probabilistic Media Access Control (MAC) protocol in which a node verifies the absence of other traffic before transmitting on a shared transmission medium, such as an electrical bus, or a band of the electromagnetic spectrum.

CSMA/CA can optionally be supplemented by the exchange of a Request to Send (RTS) frame sent by the sender S, and a Clear to Send (CTS) frame sent by the intended receiver R. The RTS/CTS alerts all nodes within range of the sender and receiver to hold off transmission while the requesting station transmits. This is known as the IEEE 802.11 RTS/CTS handshake. RTS/CTS handshake helps to solve the hidden terminal problem that is often found in wireless LANs. A station sends a RTS frame as the first step. A station will respond to the RTS frame with a CTS frame. The mechanism provides clearance for the requesting station to send a data frame.

2.1.2. MAC architecture of IEEE 802.11

The MAC architecture of IEEE 802.11 is described in Figure 2-1 as providing the point coordinator function (PCF) through the services of the distributed coordination function (DCF). DCF, running CSMA/CA protocol, is a fundamental access method of the IEEE 802.11 MAC.

On the other hand, the PCF operation provides a contention-free (CF) access, with the point coordinator (PC) performing the role of the polling master. The PCF is an optional access method, which is only usable on infrastructure network configurations.

The CSMA/CA protocol is implemented in all stations (STAs). When a PC is operating in a basic service set, a contention-free period and a contention period will alternate. The DCF and the PCF operate concurrently within the same basic service set.

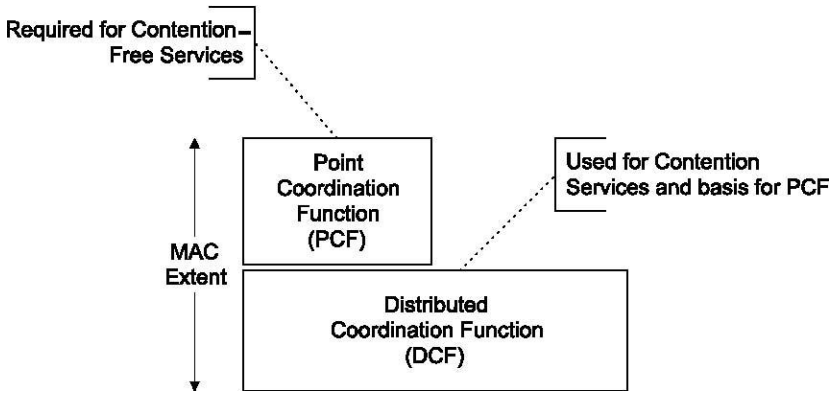

Figure 2-1: MAC architecture

2.1.3. DCF access procedure

The CSMA/CA protocol is the foundation of the DCF. Operation of CSMA/CA requires that a station shall sense the medium to determine if another station is transmitting when the station attempts to transmit. A transmitting station shall ensure that the medium is idle for a required duration before attempting to transmit. If the medium is determined to not be busy, the transmission may proceed. If the medium is determined to be busy, the station shall defer until the end of the current transmission. After deferral, or prior to attempting to transmit again immediately after a successful transmission, the station shall select a random backoff interval and shall decrement the backoff interval counter while the medium is idle.

A station performing the backoff procedure shall use the carrier-sense mechanism to determine whether there is activity during each backoff slot. If no medium activity is indicated for the duration of a particular backoff slot, then the backoff procedure shall decrease its backoff time by a SlotTime. If the medium is determined to be busy at any time during a backoff slot, then the backoff procedure is suspended; that is, the backoff timer[1] shall not decrease for that slot. The medium shall be determined to be idle for the duration of a distributed interframe space (DIFS) period, before the backoff procedure is allowed to resume. Transmission commences whenever the backoff timer reaches zero.

[1] backoff counter times timeslot

A backoff procedure shall be performed immediately after the end of every transmission, even if no additional transmissions are currently queued. If the transmission is successful, the contention window value reverts to a CWmin(minimum contention window) before the random backoff interval is chosen.

An ACK is immediately transmitted by the destination station to signal the successful packet reception, after a period of time called short inter-frame space (SIFS). If the transmitting station does not receive the ACK within a specified ACK_Timeout, or it detects the transmission of a different packet on the channel, it reschedules the packet transmission according to the given backoff rules.

A. Basic mechanism

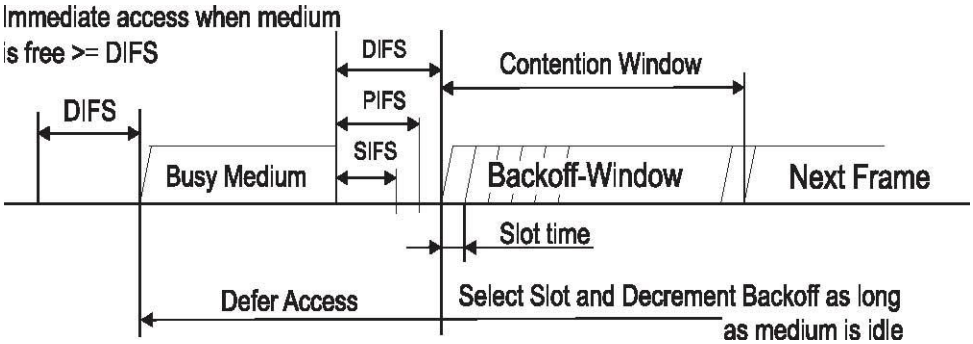

Figure 2-2: Basic access method

Basic mechanism refers to the default mechanism which a station uses to determine whether it may transmit when the station determines that the medium is idle for greater than or equal to a DIFS period. After transmitting, it is required that stations having an associated acknowledgment before a dwell time boundary. The basic access mechanism is illustrated in Figure 2-2. It is characterized by the immediate transmission of a positive acknowledgement (ACK) by the destination station, upon successful reception of a packet transmitted by the sender station. The scheme is called as a two-way handshaking technique. If the medium is determined to be busy when a station desires to initiate the initial frame, the random exponential backoff algorithm shall be followed.

B. RTS/CTS mechanism

In addition to the basic mechanism, DCF has an optional request-to-send /clear-to-send (RTS/CTS) mechanism to transmit packets. RTS/CTS is a four way handshaking technique.

A station operating in RTS/CTS mode “reserves” the channel by sending a RTS frame before transmitting a data frame. First it waits until the channel is sensed idle for a DIFS, follows the backoff procedure, and then preliminarily transmits a RTS frame. Then after transmitting an RTS frame, the station shall wait for a CTS Timeout interval. The station that addresses an RTS frame acknowledges the receipt of an RTS frame by sending back a CTS frame. The transmitting station is allowed to transmit its data packet only if the CTS frame is correctly received. Any listening station also updates the network allocation vector(NAV) to indicate busy until the end of ACK. Therefore, any listening station can suitably delay further transmission, and thus avoid collision of a hidden station.

Since collision may occur only on the RTS frame, and it is detected by the lack of CTS response, the RTS/CTS mechanism allows to increase the system performance by reducing the duration of a collision when long messages are transmitted. The RTS/CTS mechanism is very effective in terms of system performance.

2.1.4. Evolution of Markov chain analytical models in IEEE802.11

Performance of IEEE 802.11 is a very important issue. Analyzing the basic issue has attracted lots of researchers and will last as long as the performances of IEEE 802.11 need to be improved.

Bianchi's Markov chain analysis model is an important milestone in the performance analysis of IEEE 802.11, a representative theoretical approach. After simplifying the realistic MAC access, Bianchi model, a Markov chain analysis model, is able to solve the throughput of IEEE 802.11. The model focuses on predicting the throughput, mean delay of the medium access under saturation conditions. It has been cited by 4343 papers [80] since it was published in 2000. However the Bianchi's Markov chain analysis model is only applied to a situation under an assumption that all stations have the same packet arriving rate. This model has vulnerability to determine the performance of stations which have different packet

arriving rates. Without a modification, Bianchi's Markov chain analysis model cannot implement determining the performance of stations with different packet arrival rates.

Malone, et al [54] made an attempt to extend Bianchi's model to a situation where users have heterogeneous arrival rates. Malone gave their equation (11) as a key step to determine the performance of stations with different packet arriving rates. However the expression has a contradiction; the formula would not become one under the saturation condition. They define q_l as "the probability of at least one packet waiting transmission at the start of counter decrement", and "taking $q_l \to 1$ models a saturated station". When we check the equation with $q_l \to 1$, we find it has a contradiction. Saturation condition will equivalently mean $Th_l \le \lambda_l \le \infty$, where Th_l is throughput of node l and λ_l is an arrival rate of the node l. For all values of $\lambda_l (Th_l \le \lambda_l \le \infty)$, it is difficult to prove Equation (11) in [54] become one. A probability of at least one awaiting packet would not become 1 easily if we use their formula under the saturation condition. The probability of at least one awaiting packet should be 1 under saturation conditions.

Malone's method has other two weakness. First, if the arrival rate λ_l is a rate on demand by the node l, and $\lambda_l > Th_l$, the demanded rate may not be satisfied totally by channel. For example, higher layer application claims λ_l =200 Mbps. So that it is dangerous to substitute this λ_l into equation (11) directly. If the arrival rate λ_l is a rate supported by the node l, it is a unknown variable and $\lambda_l \le Th_l$.

Second, the expansion of $\sum_{r=2}^{n} \sum_{1 \le k_1 < k_2 \cdots < k_r \le n} P_{c\, k_1 k_2 \cdots k_r}$ in Equation (11) is very cumbersome. It is very hard to expand the term $\sum_{r=2}^{n} \sum_{1 \le k_1 < k_2 \cdots < k_r \le n} P_{c\, k_1 k_2 \cdots k_r}$. If the number of nodes is more than 50, it is very hard to expand the term.

To solve Malone's trouble, and determine the performance of heterogeneous stations under a non-saturation Markov model, we provide a simpler method to determine q_l instead of Equation (11) in [54]. Our approach is able to approach unity as the station's arrival rate approaches infinity. The approach

uses the ratio of packet arrival rate to the packet service rate. This approach averts some difficulties in [54]. We also provide the degree of non-saturation, or the ratio of packet arrival rate to the packet service rate in advance of calculation; the ratio will not be provided until calculating if Malone's method is used. We later apply the non-saturation property-formula of IEEE 802.11 to every station, and provide individual throughput and delay for each station with different packet arriving rates. Heterogeneous traffic is discussed in section 2.3 and section 5.2.

2.2. Markov chain analysis model for IEEE 802.11 under saturation condition

A Markov chain is a special Markov process, where the mathematical system can occupy a finite or countable infinite number of states; once it is in a given state, the future evolution of the process depends only on the present state and not on how it arrived at that state. In an one-dimensional Markov chain, the transition probability from state i to state j in n time steps is denoted as $p_{i,j}^{(n)} = Pr(X_n = j|X_0 = i)$. If the discrete distribution states are stationary distribution, or time-independent, the Markov chain is a time-homogeneous Markov chain. The single-step transition of time-homogeneous Markov chain is denoted as $p_{i,j} = Pr(X_{k+1} = j|X_k = i)$. Markov chain can be equivalently represented as a graphical model in a chainlike manner, which has finite states and transition probabilities changing states from one state i to another state j.

Bianchi [7] has introduced a two-dimensional Markov chain to analyze the performance of IEEE 802.11 wireless networks. The two-dimensional Markov chain is shown in Figure 2-3. The analysis model first chooses randomly a station among IEEE 802.11stations, then the time is slotted in the analysis performance, using the state machines to describe the behavior of the station, and obtaining the stationary probability that the station transmits a packet in a randomly chosen slot time. The random station's state machine is represented in the discrete-time two-dimensional Markov chain shown in Figure 2-3. The two-dimensional Markov chain has two state parameters, the backoff stage j and the

backoff counter k. The backoff time counter k is decremented as long as the channel is sensed idle, "frozen" when a transmission is detected on the channel, and reactivated when the channel is sensed idle again for more than a DIFS. The station transmits when the backoff time counter k reaches zero. When time immediately following an idle DIFS is slotted, a station is required to transmit only at the beginning of each slot time. The slot time size σ is set equal to the time needed at any station to detect the transmission of a packet from any other station.

This discrete-time state chain fit well what has been mentioned earlier in section 2.1.3. A station with a new packet to transmit shall sense the channel activity. If the channel is idle for a period of time equal to a DIFS, the station is allowed to transmit. Otherwise, if the channel is sensed busy, the station shall persist to monitor the channel until the channel is measured idle for a DIFS. At this point, the station generates a random backoff interval before transmitting to minimize the probability of collision with packets transmitted by other stations. In addition, the station shall wait a random backoff time between two consecutive new packet transmissions, even if the medium is sensed idle in the DIFS time.

Following the exponential backoff scheme of IEEE 802.11, the backoff time counter k is uniformly chosen in the range $(0, w_j - 1)$, where the value w_j is the contention window size at backoff stage j, and depends on the number of transmissions failed for the packet. At the first transmission attempt, w_j is set equal to a value w_0 called minimum contention window. After each unsuccessful transmission, is doubled, up to a maximum value $w_{max} = 2^m w_0$. After each unsuccessful transmission attempt, j will increase by one while the contention window doubles until the maximum frame retry limit L, or the maximum contention window w_m, is reached.

In Markov chain depicted in Figure 2-3, we define $b_{j,k}$ as the stationary distribution probability of being in state (j, k), where $j \in (0, L)$ is the backoff stage, and $k \in (0, w_j - 1)$ is the backoff counter.

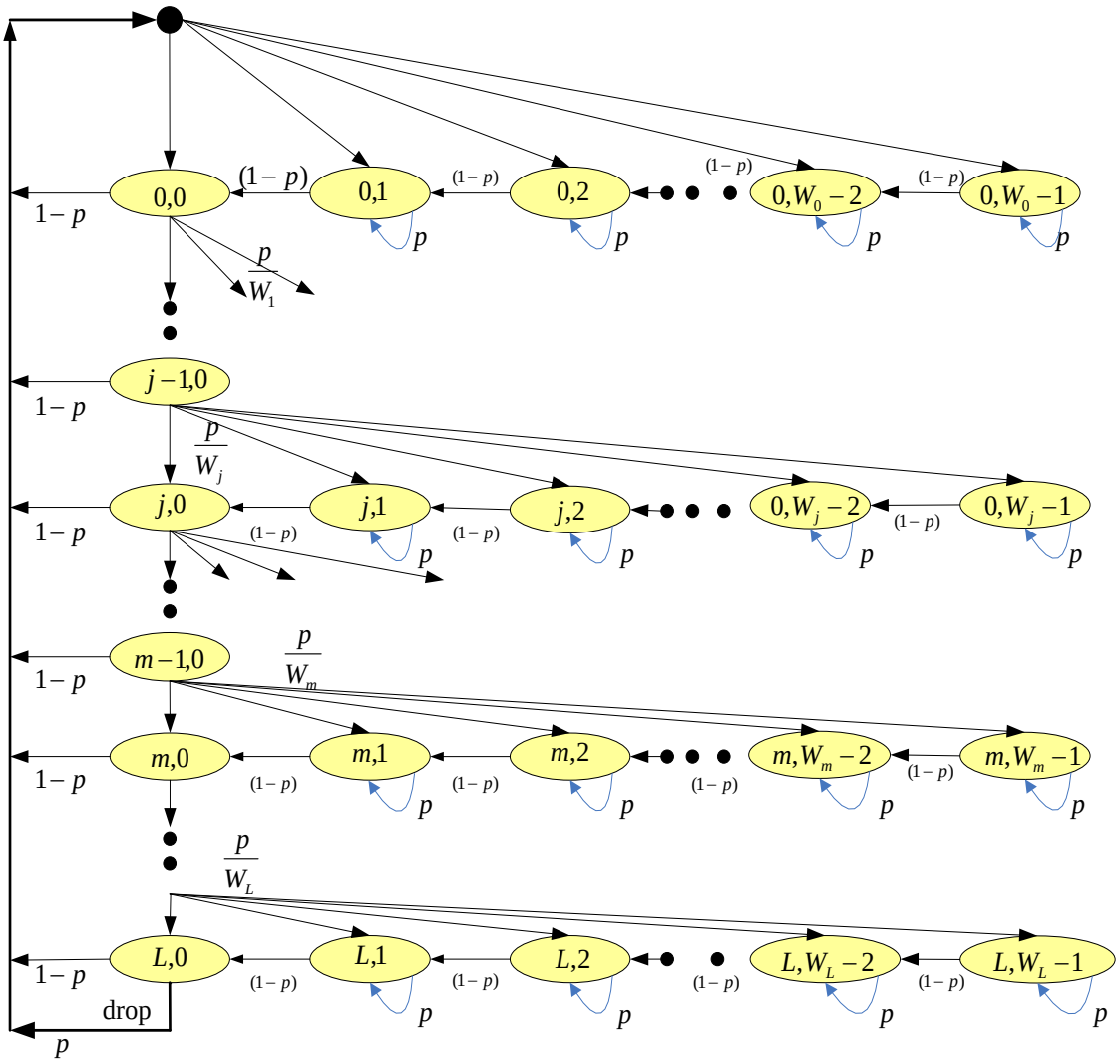

Figure 2-3: Markov Chain analysis model

Looking at the rows in the Markov chain in Figure 2-3, contention windows double as $w_j = \begin{cases} 2^j w_0 & j \le m \\ 2^m w_0 & m < j \le L \end{cases}$ (exponential backoff) after each unsuccessful transmission. The backoff counter k is "decremented" when the channel is sensed "idle", "frozen" when a transmission is detected on the channel, and "reactivated" when the channel is sensed "idle" again for more than the DIFS. The station can transmit one packet when the backoff time counter k reaches zero, and starts a new backoff procedure, shown in Figure 2-3. We define $L = m + f$, where m is the maximum times that the

contention window may be doubled; f is the number of times the contention window will not be doubled after it exceeds m.

In Figure 2-3, p is the channel busy probability that a node senses channel busy when it attempts to transmit a packet in a random slot. An assumption is that the probability p is approximated to be constant and independent regardless of the backoff stage the node is already going through. There are other assumptions with this Markov chain, (a) the wireless networks operated in an ideal physical environment, i.e. no frame error or capture effect; (b) the collision probability is equal to the probability that a backoff is sensing the channel busy; and (d) the number of stations which transmit a packet under saturation condition is fixed.

Under saturation condition, each station always has a packet available for transmission. In other words, the transmission queue of each station is assumed to be always nonempty. With the Markov chain shown in fig. 2-3, we now are able to list the single-step transition relationships of probabilities as following:

$$Prob\{j,k|j,k+1\} = 1-p \qquad j \in (0,\ L)\ \ k \in \left(0,\ w_j - 2\right) \tag{2-1a}$$

$$Prob\{0,k|j,0\} = \frac{(1-p)}{w_j} \qquad j \in (0,\ L-1)\ \ k \in \left(0,\ w_j - 1\right) \tag{2-1b}$$

$$Prob\{j,k|j-1,0\} = \frac{p}{w_j} \qquad j \in (0,\ L)\ \ k \in \left(0,\ w_j - 1\right) \tag{2-1c}$$

$$Prob\{0,k|L,0\} = \frac{(1-p+p)}{w_0} \qquad k \in (0,\ w_0 - 1) \tag{2-1d}$$

The first equation (2-1a) accounts for the fact that, at the beginning of each slot time, the backoff time is decremented with probability $(1-p)$. The second equation (2-1b) accounts for the fact that a new backoff starts with backoff stage 0 following a successful packet transmission, and thus the backoff is initially uniformly chosen in the range $(0, w_0 - 1)$. In the third equation (2-1c), when an unsuccessful

transmission occurs at backoff stage $j-1$, the backoff stage increases, and the new initial backoff value is uniformly chosen in the range $(0, w_j - 1)$ with probability $\frac{p}{w_j}$. When $j = L$, in the fourth equation (2-1d), probability of unsuccessful transmission and the successful transmission is $\frac{(1-p+p)}{w_0}$, and k is uniformly chosen in the range $(0, w_0 - 1)$.

We now move to obtain a closed-form solution for this Markov chain. The kernel rule is that the birth rate of a state will be equal to its death rate when the Markov chain becomes a stationary distribution of the chain. With this discipline, we will obtain an analysis solution for this Markov chain. As a first step, we analyze transitions of states in the first row, where the previous transmission is completed and has a new arriving packet in the queue. We assume the node is counting down backoff value. In the first row, the state $(0, w_0 - 1)$ has the distribution probability b_{0,w_0-1} during an arbitration time slot. It undertakes a countdown at probability $1-p$ to moves to its adjacent state $(0,\ w_0 - 2)$. On the other hand, its birth probability is $\frac{a}{w_0}$, where we define $a = p \times b_{L,0} + \sum_{j=0}^{L}(1-p)b_{j,0}$, we get the first birth-death equation. $\frac{a}{w_0} = (1-p)b_{0,w_0-1}$. The states continue transiting to its adjacent state until the state$(0,0)$. At the state$(0,0)$, the countdown has completed. It senses channel idle, transmits and moves to a new state $(0,k)$ at probability $(1-p)$ $k \in (0, w_0 - 1)$. Otherwise, it performs a new backoff at $\frac{p}{w_1}$ probability, and moves to next row $j = 1$.

We continue to analyze transitions of states in the other rows. If the transmission does not succeed, the backoff procedure doubles the contention window and goes into the next row backoff. If the transmission succeeds at the time a transmission is completed, the backoff procedure resets its contention window and goes into first row backoff again. Once the backoff stage reaches the max retry value *L*, the stage j does not increase again after the current retransmission. Backoff procedure drops the packet if it fails again and resets its contention window then goes into first row backoff.

Hence, by working recursively through the chain from first state $(0, w_0 - 1)$ to the last state$(L, 0)$, we have correlative birth-death equations for the distribution probabilities, and obtain following

$$b_{0,k} = \frac{(w_0 - k)a}{w_0} \quad k \in (1, \quad w_0 - 1) \tag{2-2}$$

$$b_{j,0} = pb_{j-1,0} \qquad j = 1, 2, \dots, L \tag{2-3}$$

$$b_{j,k} = \frac{(w_j - k)pb_{j-1,0}}{w_j} \quad k \in \left(1, \quad w_j - 1\right), j = 1, 2, \dots, L \tag{2-4}$$

From equations (2-2,2-3,2-4), we obtain $b_{j,0} = p^j b_{0,0}$ and $b_{j,k} = \frac{(w_j - k)}{w_j} p^j b_{0,0}$. Substitute equations (2-2,2-3,2-4), and apply a normalization requirement, $1 = \sum_{j=0}^{L} \sum_{k=0}^{w_j - 1} b_{j,k}$, and $w_j = \begin{cases} 2^j w_0 & j \le m \\ 2^m w_0 & m < j \le L \end{cases}$ (normal binary exponential backoff) , we obtain

$$1 = \sum_{j=0}^{L} \sum_{k=0}^{w_j - 1} b_{j,k} = \left\{ \frac{1 - 2p^{L+1}}{2(1-p)} - \frac{p - p^{L+1}}{2(1-p)(1-p)} + \frac{w_0}{2(1-p)} \left[1 + \frac{2p - (2p)^{m+1}}{(1-2p)} + \frac{2^m (p^{m+1} - p^{L+1})}{1-p} \right] \right\} b_{0,0} \tag{2-5}$$

We finally have

$$\frac{1}{b_{0,0}} = \frac{1 - 2p^{L+1}}{2(1-p)} - \frac{p - p^{L+1}}{2(1-p)(1-p)} + \frac{w_0}{2(1-p)} \left[1 + \frac{2p - (2p)^{m+1}}{(1-2p)} + \frac{2^m (p^{m+1} - p^{L+1})}{1-p} \right] \tag{2-6}$$

If the packet has not been successfully transmitted after L times attempting, the packet is dropped. Hence, the frame dropping probability can be estimated as: $p_{drop} = p^{L+1}$ (collision $L + 1$ times before dropping).

We denote τ the transmission probability that a node attempts to transmit a packet in a randomly chosen slot time. Knowing that any transmission occurs when the backoff time counter equals to zero, we will have Equation (2-7).

$$\tau = \sum_{j=0}^{L} b_{j,0} = \frac{1 - p^{L+1}}{1-p} \times b_{0,0} \tag{2-7}$$

Substitute equations (2-6) into (2-7), obtain

$$\tau = \frac{1-p^{L+1}}{(1-p)\left\{\frac{1-2p^{L+1}}{2(1-p)} - \frac{p-p^{L+1}}{2(1-p)(1-p)} + \frac{w_0}{2(1-p)}\left[1+\frac{2p-(2p)^{m+1}}{(1-2p)} + \frac{2^m(p^{m+1}-p^{L+1})}{1-p}\right]\right\}} \quad (2\text{-}8)$$

Equation (2-8) is defined as property formula of IEEE 802.11 under saturation condition. The set of variables of (p, τ) in equation (2-8) will be regarded as the attributes of a transmission of an IEEE 802.11-based station under saturation. p and τ are unknown. But p depends on the transmission status of its neighbors. We are able to write an equation of p in terms of its neighbor stations' transmission probability τ. With the new equation and equation (2-8), the two unknowns τ and , then can be solved using numerical techniques.

2.3. Markov chain analysis model with heterogeneous traffic

Bianchi's Markov model [7] is a milestone in the performance analysis of MAC layer of IEEE 802.11. However the Bianchi's Markov model is only applied to a situation under an assumption that all stations have the same packet arriving rate under saturation.

Clearly each user may have different applications and as a result, users have different arrival rates. In order to meet the practical requirement, we extend Bianchi's model here to a case where users have different arrival rates under non-saturation. We provide a simpler method to determine q_l instead of Equation (11) in [54]. We denote q_l as q. q is a probability of at least one packet waiting in the transmission queue. Our method defines the ratio of packet arrival rate to the packet service rate in advance of calculation. And this averts some difficulties in [54] as mentioned earlier.

After we apply the non-saturation property-formula of IEEE 802.11 to every station, we provide individual throughput and delay for each station with different packet arriving rates. Our method is a general approach to compute performance of wireless networks. It is able to be applied to various topologies of wireless networks.

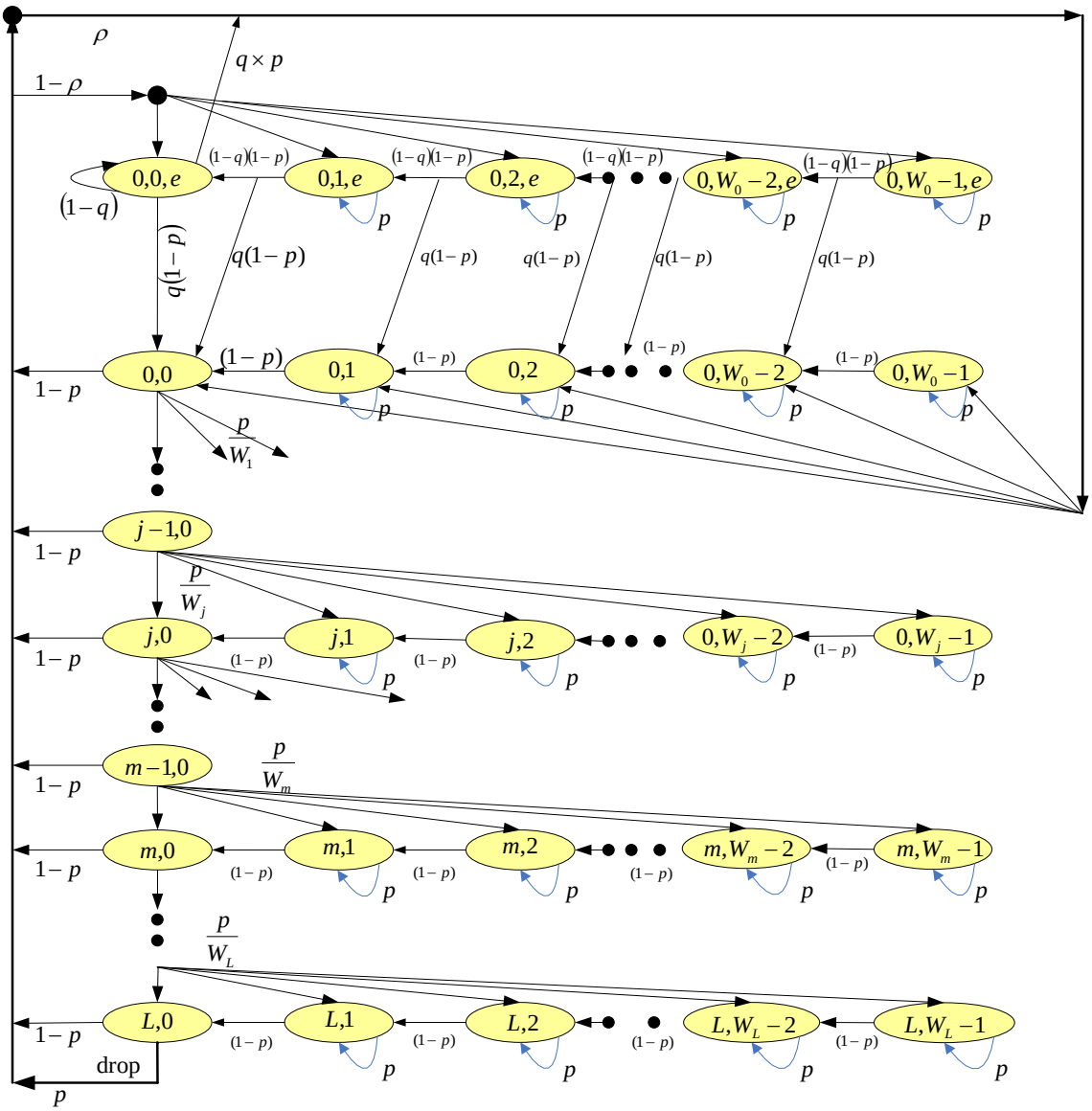

Figure 2-4: Markov Chain model for non-saturation

Following previous section, in a discrete-time non-saturation two-dimensional Markov chain shown in Figure 2-4, under non-saturation condition, we introduce empty states (0, k, e), $k \in (0,\ w_0 - 1)$, the upper row to represent states when a transmission is completed, but has no packet waiting in the station's transmission queue at a random time slot([21],[33], [35]). We define $b_{0,k,e}$ as the probability of being in stationary distribution state $(0, k, e)$, $k \in (0, w_0 - 1)$. We denote by $(1 - \rho)$ the probability that there is no packet waiting in the transmission queue at the time when a transmission is completed. Hence, ρ is

the probability that there is at least one packet waiting in the transmission queue at the time when a transmission is completed.

We define $b_{j,k}$ as the stationary distribution probability of being in state (j, k), where $j \in (0, L)$ is the backoff stage, and $k \in (0, w_j - 1)$ is the backoff counter and w_j is the contention window size at backoff stage j.

If the queue has at least an arriving packet, the queue is non-empty and the backoff state enters the second row states $(0, k)$ in Figure 2-4, where at least one packet waiting for transmission, $k \in (0, w_0 - 1)$. State (0, k) is a state which its stage $= 0$, backoff counter is k, $k \in (0, w_0 - 1)$ and stationary distribution probability is $b_{0,k}$. We denote by q the probability, entering the second row states $(0, k)$ from the upper row states (0, k, e) while the queue has at least an arrival packet and is thus non-empty.

The non-saturation Markov chain, expressed equivalently with a finite set of transition probabilities, is able to be summarized with equations. Before we obtain a closed-form solution for this non-saturation Markov chain, we summarize the one-step transition relationships of states as following:

$$Prob\{0,k|0,0,e\} = \frac{q \times p}{w_0} \qquad k \in (0, w_0 - 1) \tag{2-9a}$$

$$Prob\{0,0|0,0,e\} = q \times (1-p) \tag{2-9b}$$

$$Prob\{0,0,e|0,0,e\} = 1 - q \tag{2-9c}$$

$$Prob\{0,k|0,k+1,e\} = q(1-p) \qquad k \in (0, w_0 - 2) \tag{2-9d}$$

$$Prob\{0,k,e|0,k+1,e\} = (1-q)(1-p) \qquad k \in (0, w_0 - 2) \tag{2-9e}$$

$$Prob\{j,k|j,k+1\} = 1 - p \qquad j \in (0, L) \;\; k \in (0, w_j - 2) \tag{2-9f}$$

$$Prob\{j,k|j-1,0\} = \frac{p}{w_j} \qquad j \in (0, L) \;\; k \in (0, w_j - 1) \tag{2-9g}$$

$$Prob\{0,k|j,0\} = \frac{\rho(1-p)}{w_j} \qquad j \in (0,\ L-1)\ \ k \in (0,\ w_0-1) \tag{2-9h}$$

$$Prob\{0,k,e|j,0\} = \frac{(1-\rho)(1-p)}{w_0} \quad j \in (0,\ L-1),\ k \in (0,\ w_0-1) \tag{2-9i}$$

$$Prob\{0,k|L,0\} = \frac{\rho(1-p+p)}{w_0} \qquad k \in (0,\ w_0-1) \tag{2-9j}$$

$$Prob\{0,k,e|L,0\} = \frac{(1-\rho)(1-p+p)}{w_0} \qquad k \in (0,\ w_0-1) \tag{2-9k}$$

The equation (2-9a) accounts for the fact that, in the state (0, 0, e), the backoff has completed and is only waiting for a packet to arrive in the queue. If assuming queue receives a packet during a timeslot at a probability q and senses the channel busy at a probability p, it moves to a new state in the second row at a probability qp . Otherwise, equation (2-9b) it moves to state (0, 0) to do a transmission attempt at a probability $q \times (1-p)$, since a packet is now ready to be sent.

With the equation (2-9c), state will stay in the states (0, k, e) at a probability $1-q$ if it does not receive a packet during a timeslot. The equation (2-9d) accounts for the fact that it moves to a corresponding state in the second row with a packet waiting for transmission. The equation (2-9e) accounts for the fact that it remains in the first row with no packets waiting for transmission. The equation (2-9f) accounts for the fact that, at the beginning of each slot time, the backoff time is decremented with probability $(1-p)$, when the channel idle and the station is counting down backoff slots from its pervious state { j, k+1} to { j, k}. In the equation (2-9g), when an unsuccessful transmission occurs at backoff stage $j-1$, the backoff stage increases, and the new initial backoff value is uniformly chosen in the range $(0, w_j - 1)$ with probability $\frac{p}{w_j}$. The equation (2-9h) accounts for the fact that a new backoff starts following a successful packet transmission at backoff stage j, and thus the backoff is initially uniformly chosen in the range $(0, w_0 - 1)$. Equation (2-9i) accounts for the fact that if the transmission does succeeds and no packet waiting in the transmission queue at the time a

transmission is completed, queue reset its contention window and goes into first row empty states (0, k, e), backoff counter k uniformly chooses in the range $(0, w_0 - 1)$ at probability $\frac{(1-\rho)(1-p)}{w_0}$.

Finally, the equation (2-9j) models the fact that once the backoff stage reaches the max retry value $j = L$, stage is not increased in subsequent packet transmissions , but reset its contention window and goes into second row backoff if a new packet waiting in the transmission queue at the time a transmission is completed at probability $\frac{\rho(1-p+p)}{w_0}$. The equation (2-9k) accounts for the fact when $j = L$ and queue does not receive a packet, new backoff starts re-entry empty states (0, k, e), k uniformly chosen in the range $(0, w_0 - 1)$ at probability $\frac{(1-\rho)(1-p+p)}{w_0}$ (unsuccessful transmission and the successful transmission).

Similar to the analysis under saturation condition, the kernel rule of Markov chain is that the birth rate of a state will be equal to its death rate when the Markov chain becomes a stationary distribution. The stationary distribution states are also called steady states. With this principle, we will obtain an analytical solution for the non- saturation Markov chain. In fig 2-4, p is the probability that the station senses the channel busy in a random slot. Let $a = p \times b_{L,0} + \sum_{j=0}^{L}(1-p)b_{j,0}$ and $= \rho\left[b_{L,0} + \sum_{j=0}^{L-1}(1-p)b_{j,0}\right] + q \times p \times b_{0,0,e}$.

We assume the node is still able to counting down backoff value when the queue is empty. In the first row, the transmission queue is empty and waits for arriving packet at the time when a transmission is completed. The first state $(0, w_0 - 1, e)$ has the distribution probability $b_{0,w_0-1,e}$ during an arbitration time slot. It undertakes a countdown at probability $(1-q)(1-p)$ to moves to its adjacent state$(0,\ w_0 - 2, e)$, and moves to a corresponding state $(0,\ w_0 - 2)$ in the second row at a probability $\mathrm{q}(1-\mathrm{p})$. On the other hand, the birth probability of state $(0, w_0 - 1, e)$ is $a \times \frac{1-\rho}{w_0}$. Hence, we have the

first birth-death equation. $\frac{a(1-\rho)}{w_0} = (1-p)b_{0,w_0-1}$. At the state$(0,0,e)$, the countdown has completed and is waiting for a packet to arrive in its transmission queue. It senses channel idle and moves to a new state $(0,0)$ at probability $q(1-p)$ when it receives a packet. Otherwise, it performs a new backoff, at $q \times p$ probability, and moves to $j = 0$ row.

If the transmission does not succeed, the backoff procedure doubles the contention window and goes into the next row backoff. If the transmission succeeds and a new received packet waits in the transmission queue at the time a transmission is completed, the backoff procedure resets its contention window and goes into second row backoff. If the transmission succeeds but no packet waits in the transmission queue at the time a transmission is completed, the backoff procedure resets its contention window and goes into first row backoff. Once the backoff stage reaches the max retry value L, the stage j does not increase again after the current retransmission. Backoff procedure drops the packet if it fails again and resets its contention window then goes into second row backoff if a new packet waits in the transmission queue. A node will reset its contention window and go into first row backoff if no packet waits in the transmission queue when a transmission is completed.

Finally, by working recursively through the non saturation Markov chain from first state $(0, \mathrm{w}_0 - 1, \mathrm{e})$ to the last state$(L, 0)$, we have its correlative birth-death equations for the distribution probabilities, and obtain following

$$b_{0,k,e} = \left[\frac{1-(1-q)^{w_0-k}}{q}\right]\frac{a(1-\rho)}{w_0(1-p)} \qquad k = (1,\ 2, 3, \dots\dots,\ w_0 - 1) \tag{2-10}$$

$$b_{0,0,e} = \left[\frac{1-(1-q)^{w_0}}{q}\right]\frac{a(1-\rho)}{q\times w_0} \tag{2-11}$$

$$b_{0,k} = q \times \sum_{n=k+1}^{w_0-1} b_{0,n,e} + \frac{(w_0-k)B}{w_0(1-p)} \quad k = (1,\ 2, 3, \dots\ w_0 - 2) \tag{2-12}$$

$$b_{0,k} = \frac{(w_0-k)B}{w_0(1-p)} \qquad k = \ w_0 - 1 \tag{2-13}$$

$$b_{0,0} = (1-p)q \times \sum_{k=0}^{w_0-1} b_{0,k,e} + \rho a + qpb_{0,0,e} \quad (2\text{-}14)$$

$$b_{j,0} = pb_{j-1,0} \qquad j = 1, 2, \dots, L \quad (2\text{-}15)$$

$$b_{j,k} = \frac{(w_j - k)pb_{j-1,0}}{w_j(1-p)} \qquad k = (1,\ 2, 3\ \ w_j - 1),\ j = 1, 2, \dots, L \quad (2\text{-}16)$$

Substituting equations (2-10) and (2-11) into equation (2-14), we have $b_{0,0} = a$. Using the normalization requirement, $1 = \sum_{j=0}^{L} \sum_{k=0}^{w_j-1} b_{j,k} + \sum_{k=0}^{w_0-1} b_{0,k,e}$, equations (2-10,2-11,2-12,2-13,2-14,2-15,2-16) and contention window size $w_j = \begin{cases} 2^j w_0 & j \le m \\ 2^m w_0 & m < j \le L \end{cases}$, we have

$$\frac{1}{b_{0,0}} = \frac{1-2p^{L+1}}{2(1-p)} - \frac{p-p^{L+1}}{2(1-p)(1-p)} + \frac{w_0}{2(1-p)}\left[1 + \frac{2p-(2p)^{m+1}}{(1-2p)} + \frac{2^m(p^{m+1}-p^{L+1})}{1-p}\right] + \frac{(1-\rho)}{w_0}\left[\frac{1-(1-q)^{w_0}}{q}\right]\left\{\frac{(w_0-1)p}{2(1-p)} + \frac{1}{q}\right\} \quad (2\text{-}17)$$

We know ρ represents the probability that there is a packet waiting in the transmission queue at the time a transmission is completed or a packet dropped. ρ balances the non-saturated situation with the saturated situation. When $\rho \to 1$, third term $\frac{(1-\rho)}{w_0}\left[\frac{1-(1-q)^{w_0}}{q}\right]\left\{\frac{(w_0-1)p}{2(1-p)} + \frac{1}{q}\right\}$ will become zero. In this special situation, the non-saturation equation becomes saturation equation, and it is simplified by

$$\frac{1}{b_{0,0}} = \frac{1-2p^{L+1}}{2(1-p)} - \frac{p-p^{L+1}}{2(1-p)(1-p)} + \frac{w_0}{2(1-p)}\left[1 + \frac{2p-(2p)^{m+1}}{(1-2p)} + \frac{2^m(p^{m+1}-p^{L+1})}{1-p}\right] \quad (2\text{-}18)$$

Equation (2-18) is the same one we can obtain under saturation condition directly, equation (2-6).

We denote by τ the transmission probability that a station transmits a packet in a random slot time. Knowing that a transmission occurs when the backoff time counter equals to zero, we will have

$$\tau = \sum_{j=0}^{L} b_{j,0} = \frac{1-p^{L+1}}{1-p} \times b_{0,0} \quad (2\text{-}19)$$

Substituting equation (2-17) into equation (2-19), we obtain equation (2-20). Equation (2-20) is defined as the IEEE 802.11 station property formula under non-saturation since it represents a binary

exponential backoff scheme to access to the medium. It determines the station's transmission probability in terms of the channel busy probability p as well as the network configuration parameters (ρ, L, m, w_0) .

$$\tau = \frac{1-p^{L+1}}{(1-p)\left\{\frac{1-2p^{L+1}}{2(1-p)}-\frac{p-p^{L+1}}{2(1-p)(1-p)}+\frac{w_0}{2(1-p)}\left[1+\frac{2p-(2p)^{m+1}}{(1-2p)}+\frac{2^m(p^{m+1}-p^{L+1})}{1-p}\right]+\frac{(1-\rho)}{w_0}\left[\frac{1-(1-q)^{w_0}}{q}\right]\left\{\frac{(w_0-1)p}{2(1-p)}+\frac{1}{q}\right\}\right\}} \quad (2\text{-}20)$$

We assume we analyze a network which has N stations. Every station i, $i \in (1,2,\dots N)$, will have its own $\{p, \tau\}$ and (ρ, L, m, w_0). We apply the non-saturation property-formula of IEEE 802.11 to every station. Thus we can analyze the performance of stations with different packet arriving rates λ_i. We attach the station's serial number i to $\{p, \tau\}$ and formula (2-20) becomes (2-21).

$$\tau_i = \frac{1-p_i^{L+1}}{(1-p_i)\left\{\frac{1-2p_i^{L+1}}{2(1-p_i)}-\frac{p_i-p_i^{L+1}}{2(1-p_i)(1-p_i)}+\frac{w_0}{2(1-p_i)}\left[1+\frac{2p_i-(2p_i)^{m+1}}{(1-2p_i)}+\frac{2^m(p_i^{m+1}-p_i^{L+1})}{1-p_i}\right]+\frac{(1-\rho_i)}{w_0}\left[\frac{1-(1-q_i)^{w_0}}{q_i}\right]\left\{\frac{(w_0-1)p_i}{2(1-p_i)}+\frac{1}{q_i}\right\}\right\}} \quad (2\text{-}21)$$

On the other side, each collision $p_i$depends on the transmission status of its neighbors stations. We are able to write an equation of p_i in terms of its neighbor stations' transmission probability τ_u, where u is a set of serial numbers of station i's neighbors.

$$p_i = 1 - \prod_{u=all\ i's\ neighbors}(1-\tau_u) \quad (2\text{-}22)$$

Using numerical solution technology, we should be able to solve equation (2-21) and (2-22). Hence, for a given network topology, we can apply equation (2-22) for every station. Recalling that τ_i is the transmission probability that station i attempts to transmit in a random time slot, we can obtain its throughput and delay. The details are given in equations (2-31) and (3-13).

There are two notes to equations (2-21). First, we can attach the node's serial number to (L, m, w_0), which means we can set different L, m, w_0 for each node. Second, we have attached the node's serial number i to ρ_i, q_i , which means we are able to analyze the performance for nodes with different arrival rates.

Now we determine ρ and q. Assuming the packets are Poisson arrival traffic, we denote the traffic arrival rate and packet service rate of a station as λ and μ packets per second respectively. The station is under non-saturation condition if $\lambda < \mu$. According to the $M/M/1$ queue under steady-state conditions, the probability that there are x packets waiting in the transmission queue is

$$P_x = \left(1 - \frac{\lambda}{\mu}\right)\left(\frac{\lambda}{\mu}\right)^x \tag{2-23}$$

Hence the probability that there is no packet waiting in the transmission queue is $P_0 = \left(1 - \frac{\lambda}{\mu}\right)$. The probability that there is at least one packet waiting in the transmission queue will is given by

$$P(x > 0) = \sum_{x=1}^{\infty} P_x = \frac{\lambda}{\mu} \tag{2-24}$$

As mentioned before, ρ is defined as the probability that there is at least one packet waiting in the transmission queue at the time when a transmission is completed. However under steady-state conditions, we have

$$\rho = P(x > 0) = \frac{\lambda}{\mu} \tag{2-25}$$

We are able to obtain the packet service rate μ with the station's throughput (packets per second). The retransmission probabilities are $p, p^2, \ldots, p^L$, and if the wireless networks operate in an ideal physical environment, the average number for each successful packet is $(1-p) + \sum_{i=1}^{L}(i+1)p^i$, thus, $\mu = throughput \times \left[(1-p) + \sum_{i=1}^{L}(i+1)p^i\right]$.

As mentioned earlier, we define q as the probability entering the second row states from the upper row states while the transmission queue has at least an arrival packet and thus is non-empty. Since under steady state, no matter when, the probability that there is at least one packet waiting in the transmission

queue is ρ. So that the probability, q, that the queue enters the second row states $(0, \mathrm{k})$ (non-empty states) equals to ρ.

$$q = \rho \tag{2-26}$$

Hence, for Poisson arrival traffic $\rho = \frac{\lambda}{\mu}$, the probability q while the backoff is started by entering the second row states $(0, k)$ equals to $\frac{\lambda}{\mu}$.

$$q = \frac{\lambda}{\mu} \tag{2-27}$$

To determine the performance of stations which have different packet arriving rates λ_i, we first choose a ρ_i because λ_i is reflected in ρ_i.

Then, the left task is to obtain the throughput. We define $P_{i,tr}$ as the probability that there is at least one transmission within station i's coverage area in a random time slot. We denote by $P_{i,success}$ the probability that station i successfully transmits its packet to its neighbors, which equals the probability that exactly only one station transmits on the channel covered by station i in a given time slot, and no hidden station transmits either. Hence the formulas for $P_{i,tr}$ and $P_{i,success}$ are given by

$$P_{i,tr} = 1 - (1 - \tau_i) \prod_{u=all\ i's\ neighbors} (1 - \tau_u) \tag{2-28}$$

$$P_{i,success} = \tau_i \prod_{u=all\ i's\ neighbors} (1 - \tau_u) \prod_{v=\ i's\ hidden\ station} (1 - \tau_v) \tag{2-29}$$

Let $throughput_i$ be the normalized capacity of station i, Let$E[length]$ be the average length of a slotted time and $E[payload]$ be the average packet payload size. The average amount of payload information successfully transmitted in a time slot is $P_{i,success} E[payload]$. $E[length]$ will be $(1 - P_{i,tr})\sigma + P_{i,success} T_S + [P_{i,tr} - P_{i,success}] T_C$. σ is the duration of a time slot. Here the term $(1 - P_{i,tr})\sigma$ accounts for an idle time slot with probability $1 - P_{i,tr}$; the term $P_{i,success} T_S$ stands for successful

transmissions of station i with successful probability $P_{i,success}$; and the term $[P_{i,tr} - P_{i,success}]T_C$ deals with the collision duration. T_S is the average time for a successful transmission, and T_C is the average time duration for the collision. T_C and T_S can be derived for both the basic and the RTS/CTS access mechanisms. We obtain (2-30a, 2-30b) for the basic access mechanism and (2-30c,2-30d) for the RTS/CTS access mechanism.

$$T_{S,bas} = \left[t_{phy} + t_{MAC} + E[packet]\right] + SIFS + \delta + \left[t_{phy} + ACK\right] + DIFS + \delta \quad (2\text{-}30a)$$

$$T_{C,bas} = \left[t_{phy} + t_{MAC} + E[packet]\right] + \delta + DIFS \quad (2\text{-}30b)$$

$$T_{S,rts} = \left[t_{phy} + RTS\right] + SIFS + \delta + \left[t_{phy} + CTS\right] + SIFS + \delta + \left[t_{phy} + t_{MAC} + E[packet]\right] + SIFS + \delta + \left[t_{phy} + ACK\right] + DIFS + \delta \quad (2\text{-}30c)$$

$$T_{C,rts} = \left[t_{phy} + RTS\right] + DIFS + \delta \quad (2\text{-}30d)$$

As in the Bianchi model [7], we have the throughput of each station which have different packet arriving rates λ_i, $throughput_i$:

$$throughput_i = \frac{P_{i,success}E[P]}{(1-P_{i,tr})\sigma + P_{i,success}T_S + [P_{i,tr}-P_{i,success}]T_C} \quad (2\text{-}31)$$

Here is summary about how to get the performance of a network which has different packet arriving rates. We assume we analyze a network which has N stations. Every station i, $i \in (1,2,\dots N)$, will have its own $\{p, \tau\}$ and (ρ, L, m, w_0). We apply the non-saturation property-formula of IEEE 802.11 to every station. We have (2-21). Each collision p_i in (2-21) depends on the transmission status of its neighbors stations. We are able to have (2-22). We have $q_i = \rho_i$. If give each ρ_i, then we are able to obtain the τ_i and p_i in (2-21) and (2-22) with a numerical technology. From (2-23), we will have $throughput_i$. Then have μ_i with $\mu = throughput \times \left[(1-p) + \sum_{i=1}^{L}(i+1)p^i\right]$. Then have λ_i with $\rho = \frac{\lambda}{\mu}$.

3. Markov Chain Analysis of Video Quality in IEEE802.11 Wireless Networks

Investigating a theoretical prediction of the video quality over wireless network becomes more and more important for network and application designers when the video application has shown a very huge market. For example, people want to know the quality of video when they plan to deliver multiple HD streams to several receivers, or to display stored digital contents from media servers to display devices, or to browse contents in distributed devices through big screen TVs at home network. Their neighbors also have wireless networks, and their neighbors' computers maybe become the hidden stations of their computers. Analyses of performance in present of hidden station can help planer to get quality of video.

3.1. Quality of Experience of ITU-T recommendation G.1070

Video quality can be evaluated by subjective and objective measurements. Subjective quality is the user's perception of service quality, proposed by ITU and Video Quality Experts Group. The determination of subjective quality is Mean Opinion Score (MOS). Objective video evaluations are mathematical models that approximate results of subjective quality assessment. Objective video evaluations are based on criteria that can be measured objectively and automatically by a computer program.

The most traditional ways of evaluating objective video quality are the peak signal-to-noise ratio (PSNR). PSNR is expressed by the Mean Squared Error (MSE) between an original frame and the distorted frame. Typical values of the PSNR in lossy image or video compression are between 30 dB and 50 dB, where higher PSNR value provides a higher image quality. Acceptable values of PSNR in wireless transmission quality loss are considered to be about 20 dB to 25 dB([3] and [4]). PSNR is evaluation to distortion of video quality in more general situations. But evaluation to the distortion bought by loss of video packets, ITU-T G.1070 has an opinion model as alterative measurement.

Quality of Experience (QoE), is a measurement to grade perceptual quality which is able to map subjective quality to PNSR's rankings. It has been chosen in ITU-T G.1070. QoE is simple enough to be calculated at the receiver side. The opinion model is able to eventually map the packet loss ratio of the transmission channel to the quality degradation. The opinion model demonstrates calculations of objective video quality with its subjective video quality. It predicts the video quality and maintains the user's specific level satisfaction and provides planners QoE to help ensure that users will be satisfied with end-to-end service quality. Hence, QoE will allow us to obtain an analytical estimation of video quality with the setting parameters of IEEE 802.11 networks. With a Markov Chain Model [7], we can obtain an analytical dropping rate for packets; after we substitute the analytical dropping rate into a formula in ITU-T G.1070, we obtain an analytical expression of the inherent distortion of video quality in IEEE 802.11 wireless networks. Thus, we are able to predict video quality using setting parameters of IEEE802.11. The prediction can be used for application and network planning and provides a required level of customer satisfaction.

In ITU-T G.1070, video quality parameters are introduced, such as video delay (including jitter-buffer delay), T_v [ms], video packet-loss rate, P_{plV} [%] and key-frame interval. These parameters affect video quality when video is transmitted over wireless networks. The video packet-loss rate, delay and jitter in terminals, are extremely important. For high quality video streaming services, according to ITU-T J.241, T_v must be less than hundreds milliseconds and a jitter less than tens milliseconds may be tolerated. Video packet-loss rate (P_{plV}) refers to end-to-end packet-loss rate in video and should be less than 10 [%].

According to the ITU-T G.1070, objective measurement of video quality, V_q, is able to be calculated by equation (3-1):

$$V_q = 1 + I_{coding} exp\left(-\frac{P_{plV}}{D_{PplV}}\right) \quad (3\text{-}1)$$

where D_{PplV} is degree of video quality robustness against packet loss; P_{plv} is video packet-loss rate; I_{coding} is objective measurement of basic video quality accounting for coding distortion. I_{coding} represents the basic video quality affected by the coding distortion under a combination of video bit rate and video packet rate.

Table 3-1: Coefficients of I_coding and D_PplV for a video

	I_{coding}	D_{PplV}
value	3.655	0.0037

Every video content has its own video quality robustness D_{PplV}, and its own objective measurement of basic video quality accounting for coding distortion, I_{coding}. These two values are able to be derived by applying the method described in ITU-T G.1070. We only cite some measurements from [75], and list them in Table 3-1(to simply the discussion, we assume D_{PplV} is constant under different P_{plv} and I_{coding} is constant with different video bit rate and video packet rate). Thus, in this paper, we only focus on obtaining video packet-loss rate, P_{plv}, which we are able to obtain from the Markov chain analytical model. The details will be discussed in next section.

3.2. Analytical video quality in IEEE 802.11 wireless networks

If we know the topology of a network, we are able to use a two-dimensional saturation Markov chain models(Fig.2-3) or a two-dimensional non-saturation Markov chain models(Fig 2-4) to analyze p , where p is the probability that a node senses the channel busy in a random slot and has been obtained in previous section. As mentioned earlier, if the packet has not been successfully transmitted after packet retry limit L times attempting, the packet is dropped. Hence, the packet dropping probability can be estimated as: $p_{drop} = p^{L+1}$ (collision $L + 1$ times before dropping). If the traffic is video, (assuming IP and TCP/UDP does not change packet-loss rate) then the video packet-loss rate, P_{plv} in equation (3-1), is obtained by

$$P_{plv} = p^{L+1} \tag{3-2}$$

As an example, we demonstrate the steps to obtain objective measurement of video quality, V_q in a non saturation wireless network here, where there are N nodes and all N nodes are able to cover within single hop. Noticing that every node i will have its own $\{p, \tau\}$, we have attached the node's serial number to $\{p, \tau\}$ and formulae, and have equations (2-21), where i=1,2,… N;

$$\tau_i = \frac{1-{p_i}^{L+1}}{(1-p_i)\left\{\frac{1-2p_i{}^{L+1}}{2(1-p_i)} - \frac{p_i-p_i{}^{L+1}}{2(1-p_i)(1-p_i)} + \frac{w_0}{2(1-p_i)}\left[1+\frac{2p_i-(2p_i)^{m+1}}{(1-2p_i)} + \frac{2^m(p_i{}^{m+1}-p_i{}^{L+1})}{1-p_i}\right] + \frac{(1-\rho_i)}{w_0}\left[\frac{1-(1-q_i)^{w_0}}{q_i}\right]\left\{\frac{(w_0-1)p_i}{2(1-p_i)} + \frac{1}{q_i}\right\}\right\}} \tag{2-21}$$

In equation (2-21), probability, p_i that a node senses the channel busy in a random slot, depends on the transmission status of its neighbors nodes and varies from one node to the other. If given a network topology, we can obtain the other equation for every node i's p_i . Hence, if all N nodes are able to cover within single hop, we will have

$$p_i = 1 - \prod_{u\neq i}^{u=1,2,\ldots,N}(1-\tau_u) \tag{3-3}$$

For Poisson arrival traffic, we have $q_i = \rho_i$. If giving each node's ρ_i, then using numerical solution technology, we are able to solve equation (3-3) and (2-21) , and ultimately obtain every node's objective measurement of video quality, V_q by equation (3-2) and (3-1). If all $\rho_i = 1$, the network becomes saturated situation from non-saturated situation. Then $p_i = p$ and $\tau_i = \tau$.

In order to check if video delay T_v is less than hundreds milliseconds and if a jitter is less than tens milliseconds, in this section, we discuss the delay and jitter of video packets.

The packet delay is defined as the time interval between the packet's first backoff attempt and its successful transmission if the packet is not dropped. The total packet delay D is able to be divided into four sub-delays: packet propagation delay, $D_{propagation}$, successful packet transmission delay,

$D_{successful}$, delay in queue[2], $D_{in\ queue}$ and packet access delay, D_{access}. Packet propagation delay, $D_{propagation}$, is the time spent during propagation. A successful packet transmission delay, $D_{successful}$, is the time consumed during the successful transmissions, which equals to T_s, gained from formula (2-30a) for basic mechanism and (2-30c) for RTS/CTS mechanism.

We know that the station shall generate a random backoff period for an additional deferral time before retrying if the medium is determined to be busy. We refer to the backoff deferral time as packet access delay, D_{access}.

In order to find D_{access}, we let $Backoff(j)$ denote backoff counters before a transmission attempt at current stage, $j \in (0, L)$. $Backoff(j)$ is a random variable uniformly distributed in $(0, w_j - 1)$. Each value of $Backoff(j)$ at current stage j has a probability, $\frac{1}{w_j}$. The expectation of $Backoff(j)$ can be expressed by $[Backoff(j)] = \sum_{k=0}^{w_j-1} \frac{k}{w_j} = \frac{w_j-1}{2}$. Let $X(j)$ be a total backoff counter when a successful transmission happens after j retries. (a summary of average $Backoff(j)$).

$$X(j) = \sum_{v=0}^{j} E[Backoff(j)] = \sum_{v=0}^{j} \frac{w_v-1}{2} \tag{3-4}$$

Because stage j may be a random value from $j = 0$ to $j = L$, while performing a backoff procedure and having a successful transmission. Each stage j will have a probability, $\frac{(1-p)p^j}{1-p^{L+1}}$. (normalization) Hence the expectation of $X(j)$ can be expressed by

$$E[X(j)\ ] = \sum_{j=0}^{L} X(j)\ \frac{(1-p)p^j}{1-p^{L+1}} = \sum_{j=0}^{L} \left[\frac{(1-p)p^j}{1-p^{L+1}} \sum_{v=0}^{j} \frac{w_v-1}{2}\right] \tag{3-5a}$$

Similar, each $X^2(j)$ will have a probability $\frac{(1-p)p^j}{1-p^{L+1}}$. $E[X^2]$, the expectation of X^2 can be expressed by

$$E[X^2] = \sum_{j=0}^{L} X^2 \frac{(1-p)p^j}{1-p^{L+1}} = \sum_{j=0}^{L} \left(\sum_{v=0}^{j} \frac{w_v-1}{2}\right)^2 \frac{(1-p)p^j}{1-p^{L+1}} \tag{3-5b}$$

[2] For the even traffic arrival, delete $Delay_{in\ queue}$

By equation (3-5a-d), we can obtain $E[X_{norm}]$ and $E\left[X_{norm}{}^2\right]$ for normal node, $E[X_s]$ and $E\left[X_s{}^2\right]$ for manipulating node (details will be found in chapter 5.2).

$$E[X_s(j)] = \sum_{j=0}^{L} X_s(j) \frac{(1-p_s)p_s{}^j}{1-p_s{}^{L+1}} = \sum_{j=0}^{L} \left[\frac{(1-p_s)p_s{}^j}{1-p_s{}^{L+1}} \sum_{v=0}^{j} \frac{w_v-1}{2}\right] \quad (3\text{-}5c)$$

$$E\left[X_s{}^2\right] = \sum_{j=0}^{L} X_s{}^2 \frac{(1-p_s)p_s{}^j}{1-p_s{}^{L+1}} = \sum_{j=0}^{L} \left(\sum_{v=0}^{j} \frac{w_v-1}{2}\right)^2 \frac{(1-p_s)p_s{}^j}{1-p_s{}^{L+1}} \quad (3\text{-}5d)$$

Let $E[slot]$ be the average time a station defers in a successful backoff counter decrement.

$$E[slot] = (1 - P_{tr})\sigma + P_S T_s + (P_{tr} - P_s)T_c. \quad (3\text{-}6)$$

where T_s is the average time of a successful transmission , and T_c is the average time of a collision. σ is a slot time. P_{tr} is probability that there is at least one transmission in normal node′s coverage area in a random time slot; P_s is probability that node successfully transmits its packet to its neighbors. By equation (3-6), we obtain similar for manipulating node.

$$E[slot_s] = (1 - P_{s.tr})\sigma + P_{s.S} T_s + (P_{s.tr} - P_{s.s})T_c. \quad (3\text{-}6a)$$

P_{tr}, $P_{s.tr}$, P_s and $P_{s.S}$ can be obtained from equations (3-24) to (3-27) if the network is single hop wireless network. The access delay, a total time spent in the backoff procedure, can be expressed by

$$D_{access}(j) = E[slot] \times X(j) \quad (3\text{-}7)$$

The expectation of $D_{access}(j)$ is obtained by

$$E[D_{access}(j)] = E[slot] \times E[X(j)] = E[slot] \times \sum_{j=0}^{L} \left[\frac{(1-p)p^j}{1-p^{L+1}} \sum_{v=0}^{j} \frac{w_v-1}{2}\right] \quad (3\text{-}8)$$

Thus we obtain packet delay by

$$D(j) = Delay_{in\ queue} + D_{access}(j) + D_{successful} + D_{propagation} \quad (3\text{-}9)$$

$$E[D(j)] = E\left[D_{in\ queue} + D_{access}(j) + D_{successful} + D_{propagation}\right] = D_{in\ queue} + E[slot] \times$$

$$\sum_{j=0}^{L} \left[\frac{(1-p)p^j}{1-p^{L+1}} \sum_{v=0}^{j} \frac{w_v-1}{2}\right] + T_s + D_{propagation} \quad (3\text{-}10)$$

For normal behavior nodes, $w_j = \begin{cases} 2^j w_0 & j \le m \\ 2^m w_0 & m < j \le L \end{cases}$, we obtain normal behavior node's average packet delay and average total backoff counter of a successful transmission by

$$E[X_{norm}(j)\,] = \frac{(1-p)}{1-p^{L+1}}\left\{\frac{\left(1-(2p)^{m+1}\right)w_0}{1-2p} + \frac{w_0}{2(1-p)}\left\{p^{L+1} - 1 + 2^m\left[\frac{p^{m+1}-p^{L+1}}{1-p} - Lp^{L+1} + mp^{L+1} + 2(p^{m+1} - p^{L+1})\right]\right\} - \frac{1}{2(1-p)}\left[\frac{1-p^{L+1}}{(1-p)} - (L+1)p^{L+1}\right]\right\} \quad (3\text{-}11)$$

$$E[D_{norm}(j)] = D_{in\ queue} + E[slot] \times \left\{\frac{(1-p)}{1-p^{L+1}}\left\{\frac{\left(1-(2p)^{m+1}\right)w_0}{1-2p} + \frac{w_0}{2(1-p)}\left\{p^{L+1} - 1 + 2^m\left[\frac{p^{m+1}-p^{L+1}}{1-p} - Lp^{L+1} + mp^{L+1} + 2(p^{m+1} - p^{L+1})\right]\right\} - \frac{1}{2(1-p)}\left[\frac{1-p^{L+1}}{(1-p)} - (L+1)p^{L+1}\right]\right\}\right\} + T_s + D_{propagation} \quad (3\text{-}12)$$

For manipulation nodes, $w_j = \begin{cases} w_{0,s} & j \le m \\ w_{0,s} & m < j \le L \end{cases}$, we obtain their average packet delay by

$$E[X_s(j)\,] = \frac{w_{0,s}-1}{2(1-{p_s}^{L+1})}\left[\frac{p_s-{p_s}^{L+1}}{(1-p_s)} - L{p_s}^{L+1}\right] + \frac{w_{0,s}-1}{2} \quad (3\text{-}13)$$

$$E[D_s(j)] = D_{in\ queue,s} + E[slot_s]\left[\frac{w_{0,s}-1}{2(1-{p_s}^{L+1})}\left[\frac{p_s-{p_s}^{L+1}}{(1-p_s)} - L{p_s}^{L+1}\right] + \frac{w_{0,s}-1}{2}\right] + T_s + D_{propagation} \quad (3\text{-}14)$$

Taking standard deviation of $D(j)$, we obtain the $Jitter = \sqrt{var[D(j)]}$, where

$$var[D(j)] = var\left[D_{in\ queue} + E[slot] \times X(j) + T_s + D_{propagation}\,\right] \cong var\left[X \times E[slot]\right] = \{E[X^2] - (E[X])^2\,\}(E[slot])^2 \quad (3\text{-}15)$$

$$Jitter = \sqrt{var[D(j)]} = E[slot]\sqrt{(E[X^2] - (E[X])^2)} \quad (3\text{-}16)$$

Then we obtain $Jitter_{norm} = \sqrt{var[D_{norm}(j)]}$ and $Jitter_s = \sqrt{var[D_s(j)]}$.

3.3. Optimization of objective video quality under saturation condition

In this section, we discuss optimal setting parameters for video quality in single hop IEEE 802.11 wireless network. Assuming a wireless network has *N* normal nodes; all nodes are in a single hop coverage area. Hence we obtain

$$p = 1 - (1-\tau)^{N-1} \quad (3\text{-}17)$$

First, we discuss about optimization under saturation condition. Under saturation condition, equation (2-8) is list here

$$\tau = \frac{1-p^{L+1}}{(1-p)\left\{\frac{1-2p^{L+1}}{2(1-p)} - \frac{p-p^{L+1}}{2(1-p)(1-p)} + \frac{w_0}{2(1-p)}\left[1+\frac{2p-(2p)^{m+1}}{(1-2p)} + \frac{2^m(p^{m+1}-p^{L+1})}{1-p}\right]\right\}} \quad (2\text{-}8)$$

We can solve equations (2-8) and (3-22) numerically. The parameters L, m, w_0, N will determine p, then affect V_q. If parameters L, m, w_0, N change, V_q will change; we will compare our numerical calculations for IEEE 802.11a/b/g in Table 3-2. When parameters L, m, w_0, N do not change, V_q will not change; however, we can change throughput by changing data packets lengths, or access mechanism (basic access mechanism, or RTS/CTS access mechanism). Hence, we will challenge the idea which says higher bandwidth will support higher video quality.

Table 3-2: System default parameters /configuration

	802.11a	802.11b	802.11g
CWmin	15	31	15
CWmax	1023	1023	1023
L	6	5	6
M	6	5	6

3.4. Analytical video quality and enhancement at manipulation nodes under Non-saturation

For video application over wireless networks, limited bandwidth may be one of main issues. In order to improve video quality, we will apply a strategy that allows nodes randomly select a small value from a fixed contention window $\{0, w_0 - 1\}$; these nodes do not double the contention window size after a collision as normal binary exponential backoff. These manipulation nodes are able to grasp bandwidth greedily([11],[24],[26],[61],[63]).

We derive a similar analytical formula to computer $V_{s.q}$ at manipulation node. According to the strategy, nodes randomly select a backoff value from contention window $\{0, w_0 - 1\}$; and do not double

the contention window size if they have collisions. Thus, the contention window size becomes $w_j = \begin{cases} w_0 & j \le m \\ w_0 & m < j \le L \end{cases}$, where $j \in (0, L)$. We will have a similar Markov chain (depicted in Figure 2-4) for manipulation nodes. By working recursively through the Markov chain, using the normalization requirement, $1 = \sum_{j=0}^{L} \sum_{k=0}^{w_j - 1} b_{j,k} + \sum_{k=0}^{w_0 - 1} b_{0,k,e}$, and $w_j = \begin{cases} w_0 & j \le m \\ w_0 & m < j \le L \end{cases}$, we obtain

$$1 = \mathrm{b}_{0,0}\left\{\frac{1-2\mathrm{p}^{\mathrm{L}+1}}{2(1-\mathrm{p})} - \frac{\mathrm{p}-\mathrm{p}^{\mathrm{L}+1}}{2(1-\mathrm{p})^2} + \frac{(\mathrm{w}_0)}{2(1-\mathrm{p})}\left[1 + \frac{\mathrm{p}-\mathrm{p}^{\mathrm{L}+1}}{1-\mathrm{p}}\right] + \frac{(1-\rho)}{\mathrm{w}_0}\frac{1-(1-\mathrm{q})^{\mathrm{w}_{0,s1}}}{\mathrm{q}}\left[\frac{(\mathrm{w}_0-1)\mathrm{p}}{2(1-\mathrm{p})} + \frac{1}{\mathrm{q}}\right]\right\}$$

Adding subscripts to represent the backoff manipulation strategy, we finally obtain

$$\frac{1}{b_{0,0,s}} = \frac{1-2{p_s}^{L+1}}{2(1-p_s)} - \frac{p_s-{p_s}^{L+1}}{2(1-p_s)^2} + \frac{(w_{0,s})}{2(1-p_s)}\left[1 + \frac{p_s-{p_s}^{L+1}}{1-p_s}\right] + \frac{(1-\rho_s)}{w_{0,s}}\frac{1-(1-q_s)^{w_{0,s}}}{q_s}\left[\frac{(w_{0,s}-1)p_s}{2(1-p_s)} + \frac{1}{q_s}\right] \quad (3\text{-}18)$$

We denote τ_s the transmission probability that a manipulation node attempts to transmit a packet in a randomly chosen slot time. τ_s given by

$$\tau_s = \frac{1-{p_s}^{L+1}}{1-p_s} \times b_{0,0,s} \quad (3\text{-}19)$$

Substituting equations (3-18) into equation (3-19) furthermore, we obtain equations (3-20), the manipulation node's transmission probabilities τ_s .

$$\tau_s = \frac{1-(p_s)^{L+1}}{(1-p_s)\left\{\frac{1-2{p_s}^{L+1}}{2(1-p_s)} - \frac{p_s-{p_s}^{L+1}}{2(1-p_s)^2} + \frac{(w_{0,s})}{2(1-p_s)}\left[1+\frac{p_s-{p_s}^{L+1}}{1-p_s}\right] + \frac{(1-\rho_s)1-(1-q_s)^{w_{0,s}}}{w_{0,s}\quad q_s}\left[\frac{(w_{0,s}-1)p_s}{2(1-p_s)} + \frac{1}{q_s}\right]\right\}} \quad (3\text{-}20)$$

Equations (3-20) are called the IEEE 802.11 manipulation node property. Noticing that every manipulation node w will have its own $\{p_s, \tau_s\}$, formulae (3-20) become equations (3-21), where w=1,2,…N_s; N_s is numbers of manipulation nodes in the network.

$$\tau_{w,s} = \frac{1-(p_{w,s})^{L+1}}{(1-p_{w,s})\left\{\frac{1-2p_{w,s}{}^{L+1}}{2(1-p_{w,s})} - \frac{p_{w,s}-p_{w,s}{}^{L+1}}{2(1-p_{w,s})^2} + \frac{(w_{0,w,s})}{2(1-p_{w,s})}\left[1+\frac{p_{w,s}-p_{w,s}{}^{L+1}}{1-p_{w,s}}\right] + \frac{(1-\rho_{w,s})1-(1-q_{w,s})^{w_{0,w,s}}}{w_{0,w,s}\quad q_{w,s}}\left[\frac{(w_{0,w,s}-1)p_{w,s}}{2(1-p_{w,s})} + \frac{1}{q_{w,s}}\right]\right\}} \quad (3\text{-}21)$$

Adding subscripts to equations (3-1), (3-2) to represent the backoff manipulation strategy,

$$V_{w,s.q} = 1 + I_{coding} exp\left(-\frac{P_{s.plV}}{D_{PplV}}\right) \quad (3\text{-}1a)$$

$$p_{w,s.plv} = p_{w,s.}^{L+1} \tag{3-2a}$$

Using a similar method in section 3.2, if given a network topology, we can obtain the numerical solution technology of every normal node i's p_i and every manipulated node w's $p_{w,s}$. and ultimately obtain every node's delay by equations (3-12), (3-14), jitter by equation (3-16), and objective measurement of video quality, V_q and $V_{w,s.q}$by equation (3-1) and (3-1a).

Assuming a wireless network has N normal behavior nodes, N_s manipulating nodes; all nodes are in a single hop coverage area. Hence we obtain

$$p_i = 1 - \prod_{v=1,v\neq i}^{N}(1-\tau_v)\prod_{v=1}^{N_s}(1-\tau_{v,s}) \tag{3-22}$$

$$p_{w,s} = 1 - \prod_{v=1}^{N}(1-\tau_v)\prod_{v=1,v\neq w}^{N_s}(1-\tau_{v,s}) \tag{3-23}$$

We can solve equations (2-21), (3-20), (3-22) and (3-23) numerically. After we get p_i and $p_{w,s}$, we will obtain $V_{i.q}$ and $V_{w,s.q}$. After we get τ_i and $\tau_{i,s}$, we will also obtain

$$P_{i,tr} = 1 - \prod_{v=1}^{N}(1-\tau_v)\prod_{v=1}^{N_s}(1-\tau_{v,s}) \tag{3-24}$$

$$P_{i,tr,s} = P_{i,tr} \tag{3-25}$$

$$P_{i,success} = \tau_i \prod_{v=1,v\neq i}^{N}(1-\tau_v)\prod_{v=1}^{N_s}(1-\tau_{v,s}) \tag{3-26}$$

$$P_{i,success,s} = \tau_{i,s} \prod_{v=1}^{N}(1-\tau_v)\prod_{v=1,v\neq i}^{N_s}(1-\tau_{v,s}) \tag{3-27}$$

3.5. Video quality in the presence of hidden nodes

A network in the presence of hidden station becomes a very common scenario when consumers use wireless router at home in urban. In this section, we discuss the video quality V_q in the presence of a hidden station. Assuming a wireless network has N normal nodes in area C, depicted in figure 3-1, Node A and hidden Node B are located depicted in figure 3-1. All N nodes are in a single hop coverage area C. Noticing that equation (2-8) is property formula under saturation and every node will have its own

argument (p,τ) in equation (2-8), we now attach the node serial number to (p,τ) . Hence we obtain following equations under saturation condition,

$$\tau_A = \frac{1-{p_A}^{L+1}}{(1-p_A)\left\{\frac{1-2p_A{}^{L+1}}{2(1-p_A)}-\frac{p_A-p_A{}^{L+1}}{2(1-p_A)(1-p_A)}+\frac{w_0}{2(1-p_A)}\left[1+\frac{2p_A-(2p_A)^{m+1}}{(1-2p_A)}+\frac{2^m(p_A{}^{m+1}-p_A{}^{L+1})}{1-p_A}\right]\right\}} \quad (3\text{-}28a)$$

$$\tau_B = \frac{1-{p_B}^{L+1}}{(1-p_B)\left\{\frac{1-2p_B{}^{L+1}}{2(1-p_B)}-\frac{p_B-p_B{}^{L+1}}{2(1-p_B)(1-p_B)}+\frac{w_0}{2(1-p_B)}\left[1+\frac{2p_B-(2p_B)^{m+1}}{(1-2p_B)}+\frac{2^m(p_B{}^{m+1}-p_B{}^{L+1})}{1-p_B}\right]\right\}} \quad (3\text{-}28b)$$

$$\tau_C = \frac{1-{p_C}^{L+1}}{(1-p_C)\left\{\frac{1-2p_C{}^{L+1}}{2(1-p_C)}-\frac{p_C-p_C{}^{L+1}}{2(1-p_C)(1-p_C)}+\frac{w_0}{2(1-p_C)}\left[1+\frac{2p_C-(2p_C)^{m+1}}{(1-2p_C)}+\frac{2^m(p_C{}^{m+1}-p_C{}^{L+1})}{1-p_C}\right]\right\}} \quad (3\text{-}28c)$$

According to the topology of the network depictured in Fig 3-1, we have

$$p_A = 1-(1-\tau_C)^N(1-\tau_B) \quad (3\text{-}28d)$$

$$p_B = 1-(1-\tau_A) \quad (3\text{-}28e)$$

$$p_C = 1-(1-\tau_C)^{N-1}(1-\tau_A) \quad (3\text{-}28f)$$

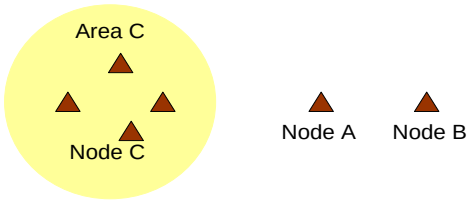

Figure 3-1 :There are N nodes in area C

We can solve equations (3-28a,b,c,d,e,f) numerically. Substitute the results of p_A, p_B, p_C into equation (3-2), (3-2), then we have $V_{q,A,B,C}$ for all the nodes in fig. 3-1. The result of $V_{q,A,B,C}$ will be discussed later.

3.6. Numerical results of video quality

We choose the default configures of IEEE 802.11a/b/g in our numerical calculations. We have IEEE 802.11 default parameters here to compute the delay and jitter of nodes: MAC header =272bits; PHY header =192 bits (including preamble 144bits and PLCP header 48 bits); ACK length =112bit +PHY header; RTS length =160bit +PHY header; CTS length =112bit +PHY header; other parameters are

summarized in Table 3-3. To simplify the presentation of the results of the delay and jitter of nodes, we have assumed that all data packets have the same length (1024 bytes) and each packet fits perfectly into one Transmit Opportunity.

Table 3-3: System default parameters /configuration

	802.11a	802.11b	802.11g	Manipulation backof
data rate	54 Mbits/s	11 Mbits/s	54 Mbits/s	11 Mbits/s
Slot time	9 µs	20 µs	9 /20 µs	20 µs
SIFS	16 µs	10 µs	16 /10 µs	10 µs
DIFS	34 µs	50 µs	34 /50 µs	50 µs
CWmin	15	31	15	31
CWmax	1023	1023	1023	31
L	6	5	6	5
M	6	5	6	5

In order to find the optimal setting parameters for video quality, we change the packet retry limit, L, minimum contending windows, w_0, the number of nodes, N, and the degree of saturation, ρ. We also let $m = L$. We find the packet retry limit has the significant effect than the minimum contending windows, w_0, in figure 3-2. When the $L = 5$, the V_q changes at more moderate pace when increase the number of node; which means, more nodes may have higher V_q when $L = 5$. Otherwise, when $L = 2$, V_q decline rapidly with the increase in the number of nodes; if we want to keep $V_q > 4$,we can only have 2 nodes in a network. When the degree of saturation, ρ, changes from 1.0 to 0.5, the curves almost overlap. (the blue lines($\rho = 0.5$) almost overlap red lines($\rho = 1.0$)). Figure 3-3.

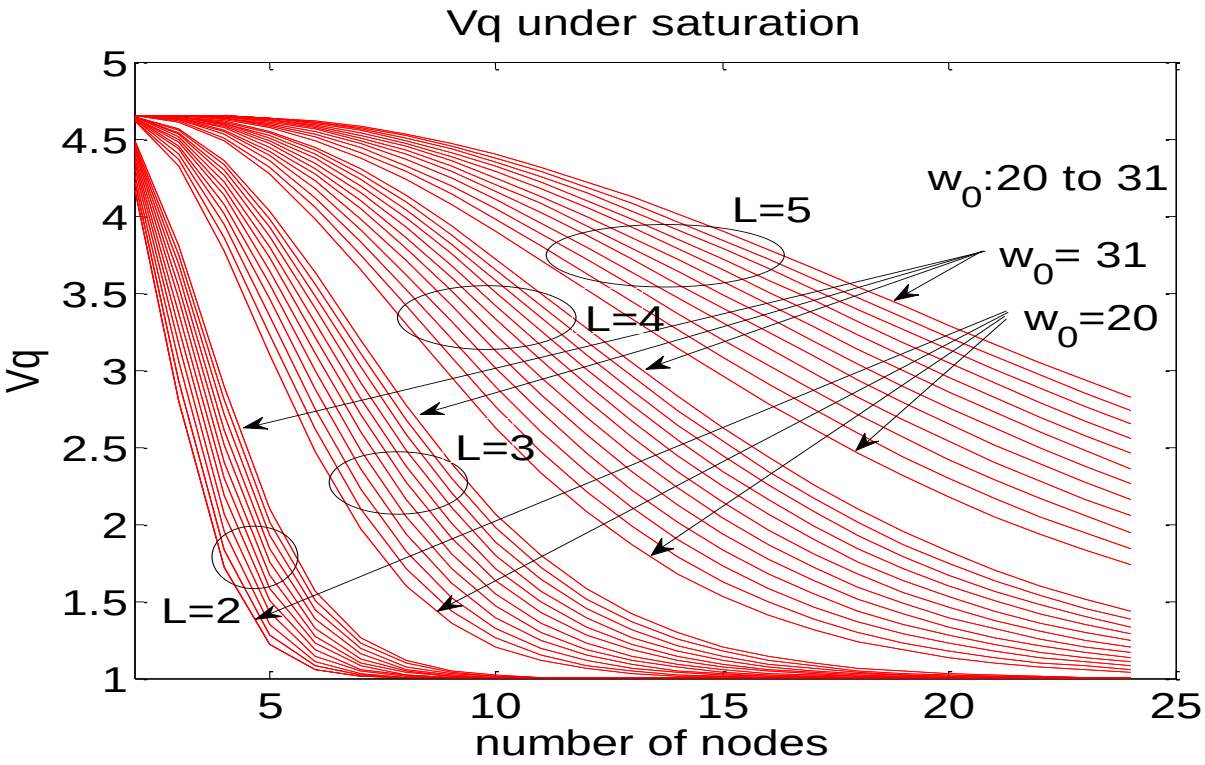

Figure 3-2: Optimal setting parameter for video quality V_q. change L and w_0

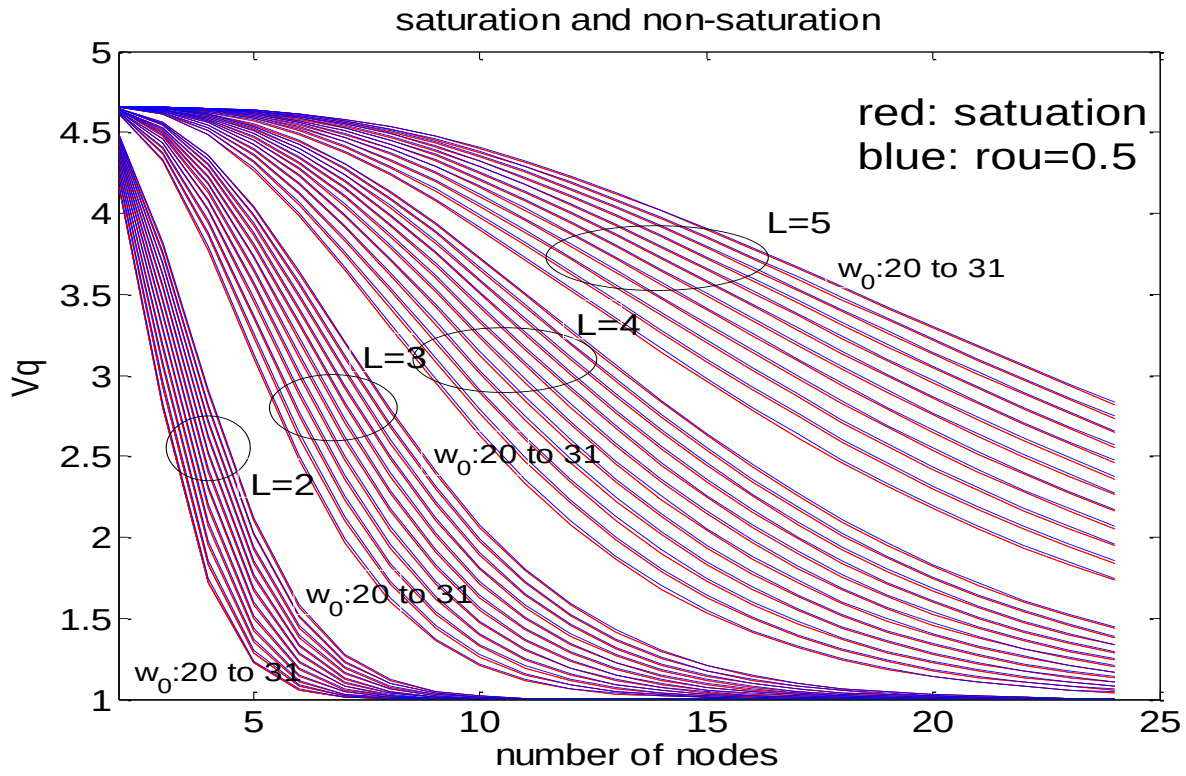

Figure 3-3: Optimal setting parameter for video quality V_q, change ρ

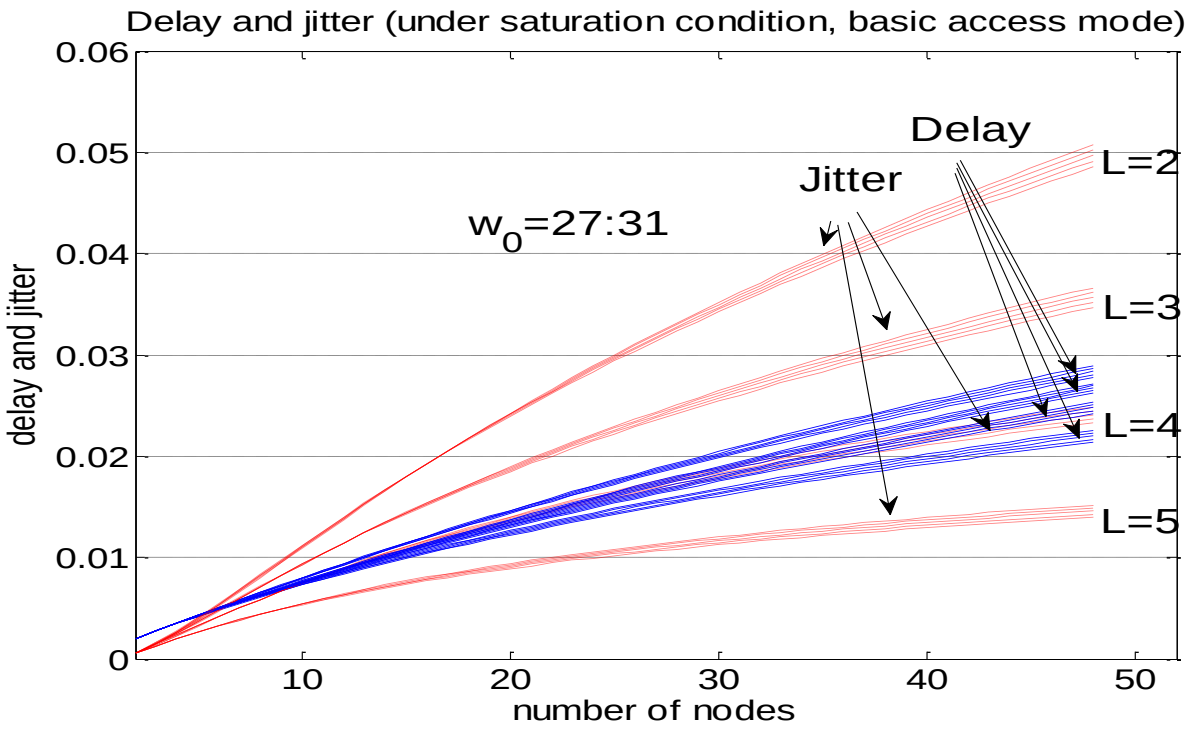

Figure 3-4: Delay and jitter of nodes node(under saturation condition and basic access mechanism)

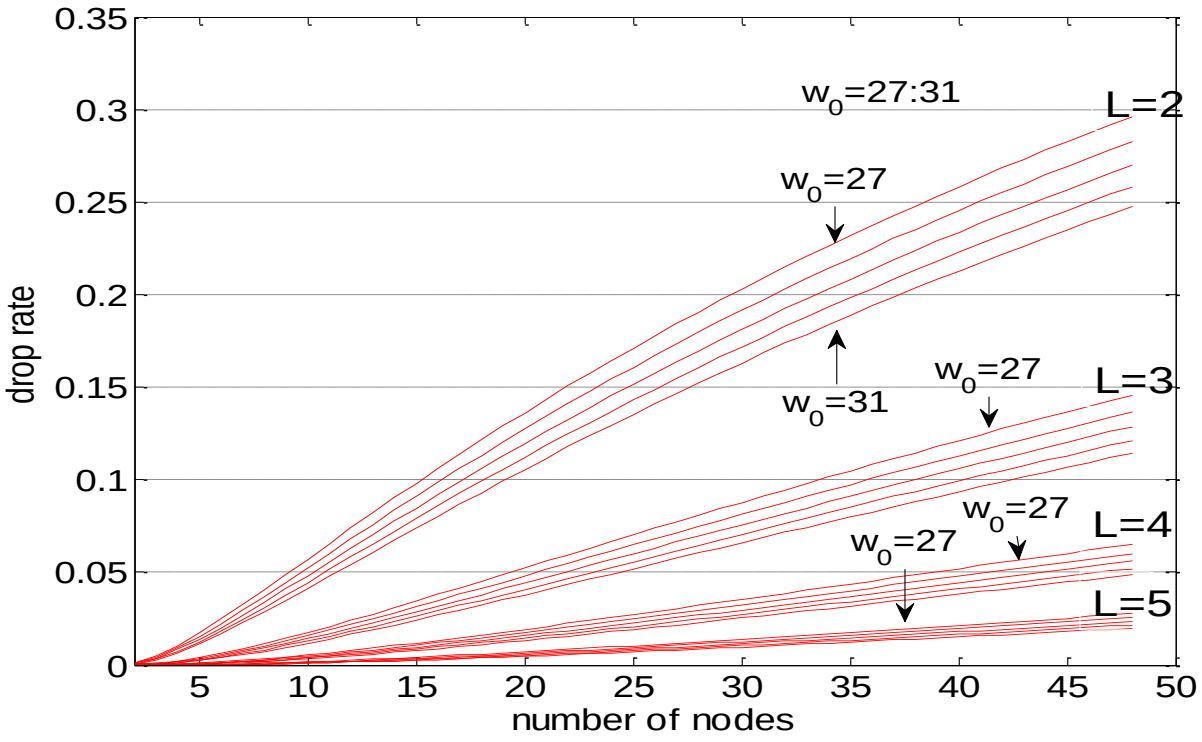

Figure 3-5: Video packet-loss rate(under saturation condition and basic access mechanism)

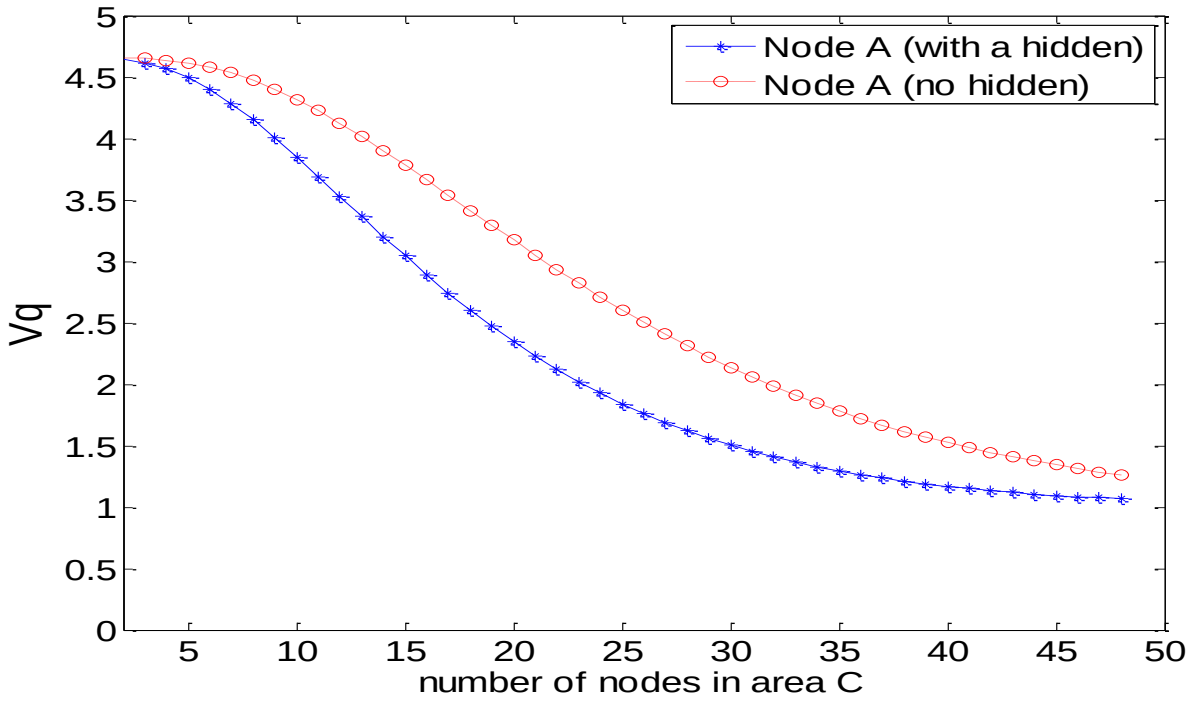

Figure 3-6: Compare the V_q at Node A, hidden vs no hidden

Compare the V_q at Node A, hidden vs no hidden

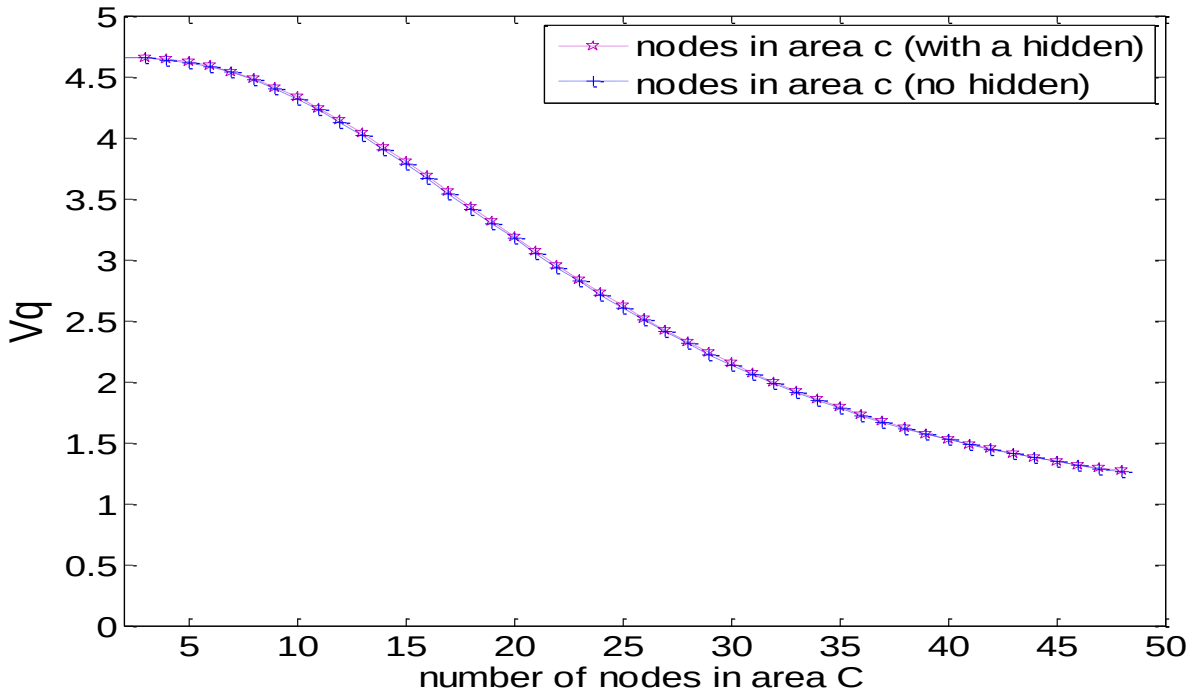

Figure 3-7: V_q at nodes C: in the presence of a hidden station vs no hidden station

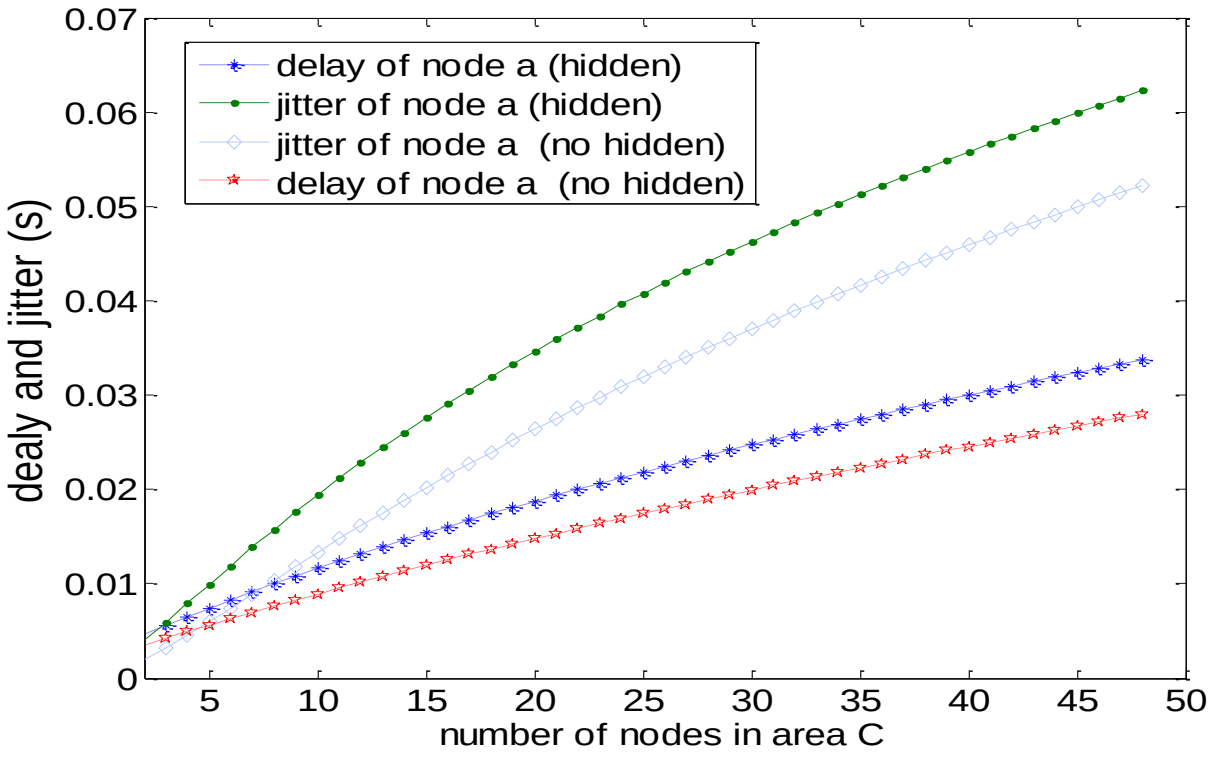

Figure 3-8: Delay and jitter at node A, one hidden station vs no hidden station

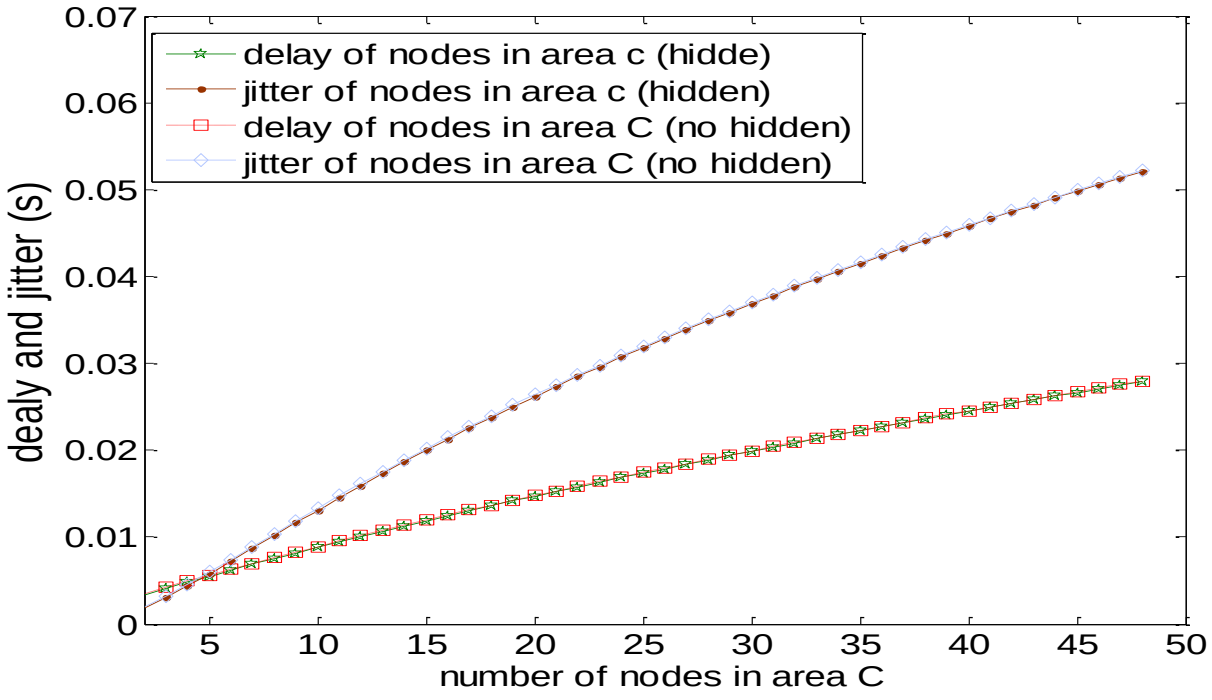

Figure 3-9: Jitter and delay at nodes C: in the presence of a hidden station vs no hidden station

Compare the requirement of in ITU-T G.1070 and ITU-T J.241, values of T_v should be less than few hundreds milliseconds and a jitter less than tens milliseconds; numerical results show that delay and jitter are less 80 milliseconds in Figure 3-4 ($L = 2,3,4,5.\ w_0 \in (15,31)$). So that, the delay and jitter of nodes are able to meet the requirement of ITU-T G.1070 and ITU-T J.241. However, in some cases, video packet-loss rate (P_{plV}) in video is more than 10 [%] in Figure 3-5 ($L = 2,.w_0 \in (27,31)$, $N \in (20,48)$). This does not meet the requirement of ITU-T G.1070 and ITU-T J.241.

The optimal setting should choose large L and large w_0 to get large V_q and acceptable delay and jitter for more nodes. Otherwise the loss rate will be higher, and V_q will decline quickly; and it may force us to give up some methods of delivering videos, which have no retransmission mechanism in a higher layer, for example, using UDP, or broadcasting, or multicasting video to more than 20 nodes.

The effect of the presence of a hidden station is obvious at node A. But it is not obvious at nodes C. Compares in the presence of a hidden station with no hidden station are shown in Figures 3-7,3-8, 3-9, 3-10 and 3-11. The V_q of node A change due the hidden station. The delay, jitter and drop rate of node A also changes due the presence of a hidden station. Node A is affected by hidden node directly. On the other side, the V_q, delay, jitter and drop rate of node C does not changes due to the presence of a hidden station. (The curves of node C almost overlay.)

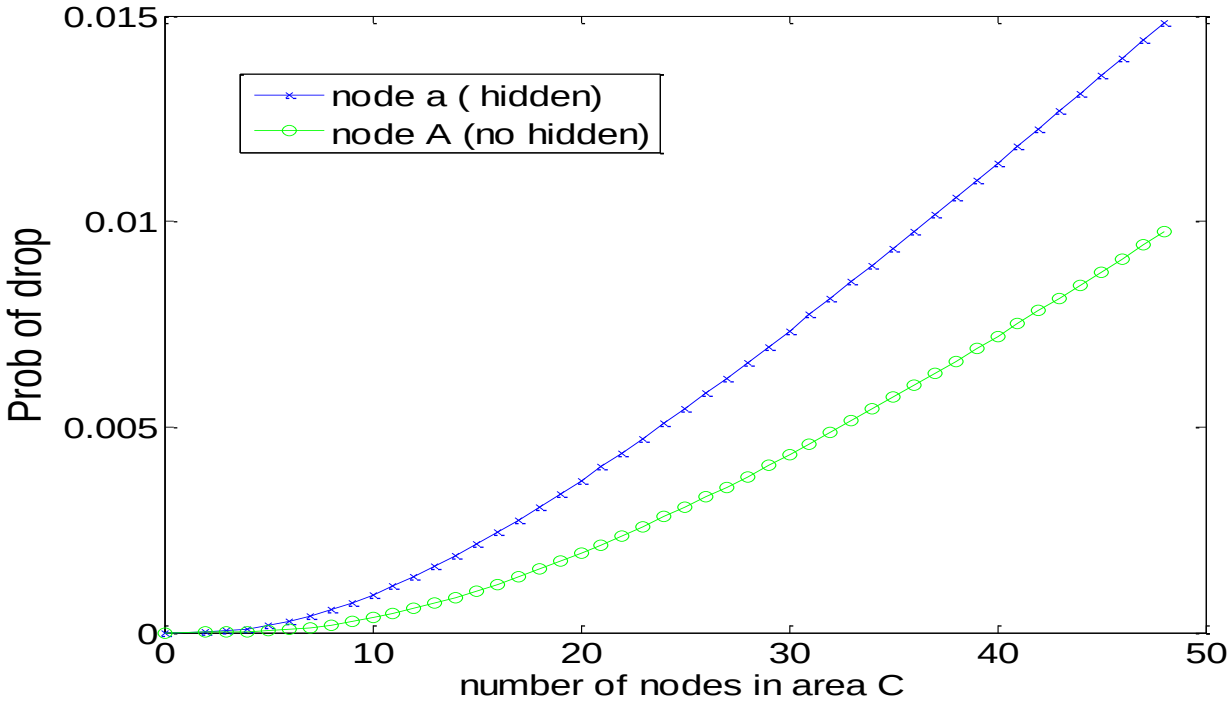

Figure 3-10: Compare the drop rate in the presence of a hidden station with no hidden station

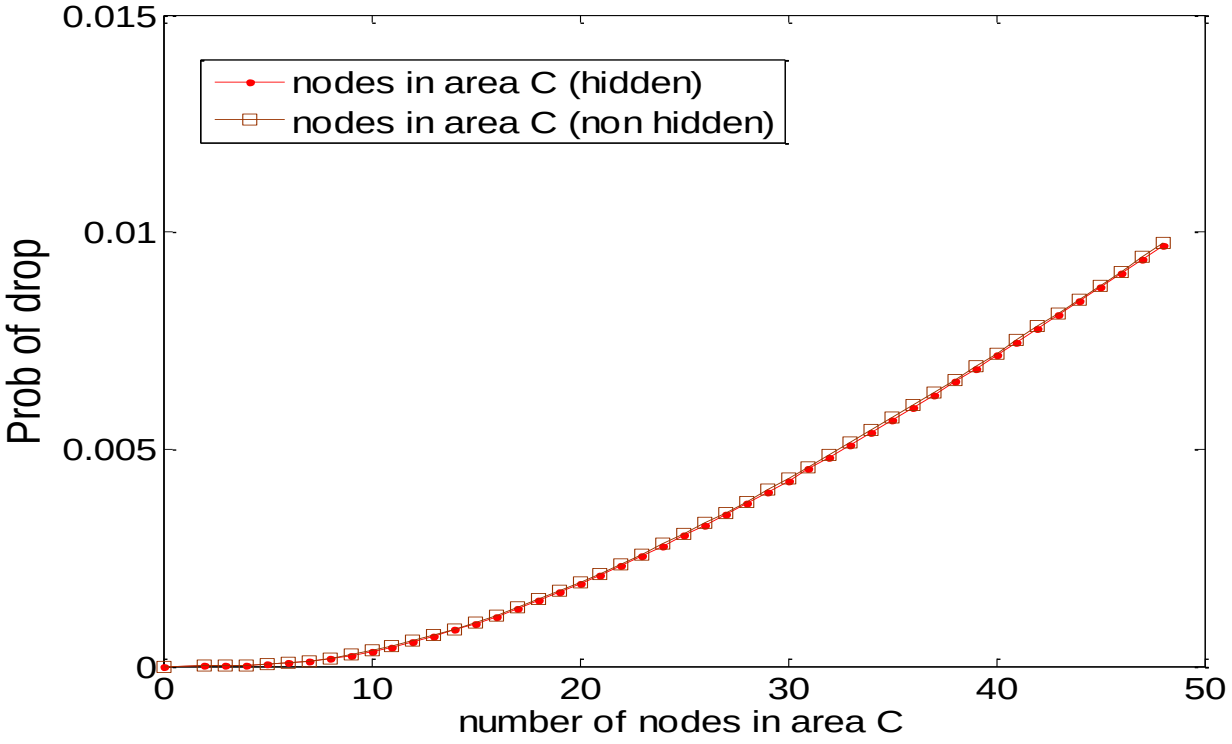

Figure 3-11: Compare the drop rate in the presence of a hidden station with no hidden station

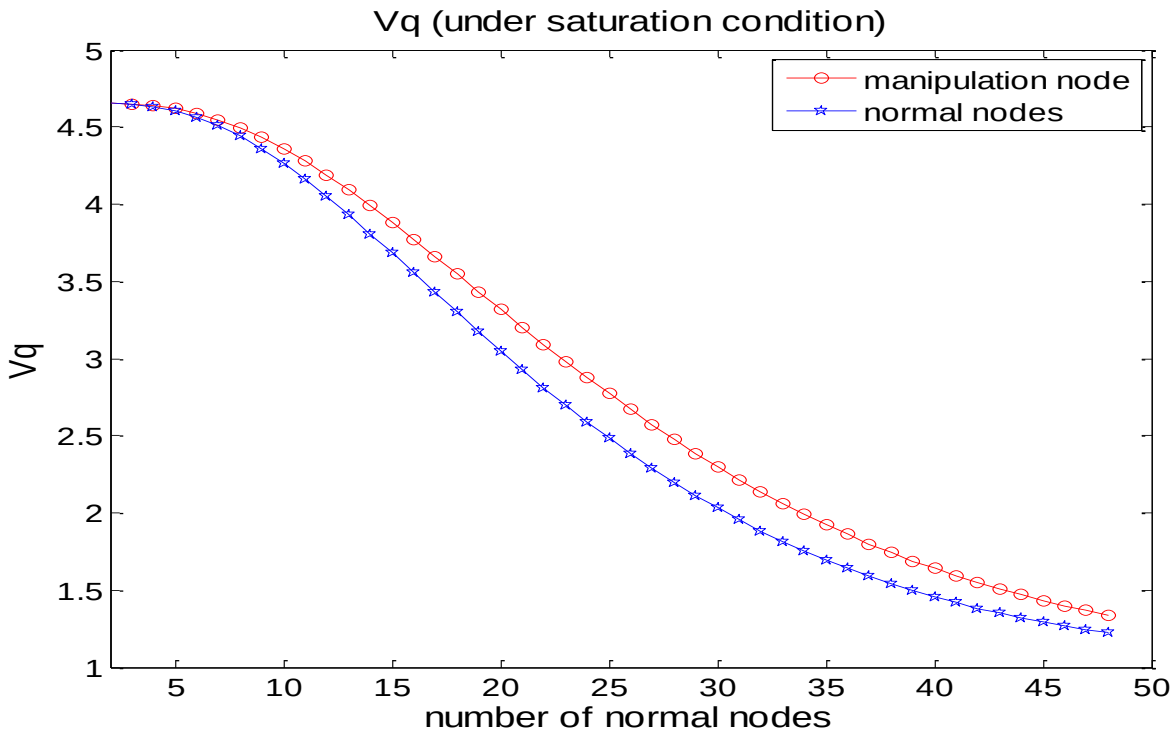

Figure 3-12: Video quality, V_q, of normal nodes and a manipulation node (under saturation condition)

In section 3.3, we discuss video quality enhancement with backoff manipulation. We study an example scenario in which there is one manipulation node and N normal nodes, in the single hop wireless networks, where $N \in (2,48)$. Figure 3-12 shows that the manipulation node has higher video quality V_q than the normal nodes have, because the probability that manipulation nodes sense the channel busy in a random slot is lower than normal nodes' (the probability is depicted in figure 3-18). Figures 3-12, 3-13, 3-16,3-17 and 3-18 are computed under saturation condition. For non-saturation condition, we repeat the calculation of V_q, setting $N = 24$, and $N = 38$. The results are depicted in Figures 3-14 and 3-15. We prove quantitatively that the video quality of the manipulating node is enhanced, having higher V_q. Delay and jitter of normal nodes and a manipulation node(under saturation condition and basic access mechanism, and $L = 5, w_0 = 31$) is shown in Figures 3-16 and 3-17. The manipulation node's delay is better than normal nodes'. However, the manipulation node's $(E[X^2] - (E[X])^2)$ may be larger, then its jitter will be larger than normal nodes' jitter.

We also compare V_q, delay and jitter of normal node and manipulation node with different settings $L = 3$ and $L = 5$. The V_q will decline more quickly at $L = 3$ than $L = 5$ (in Figure 3-13.) The delay and jitter are in the range required by ITU-T.

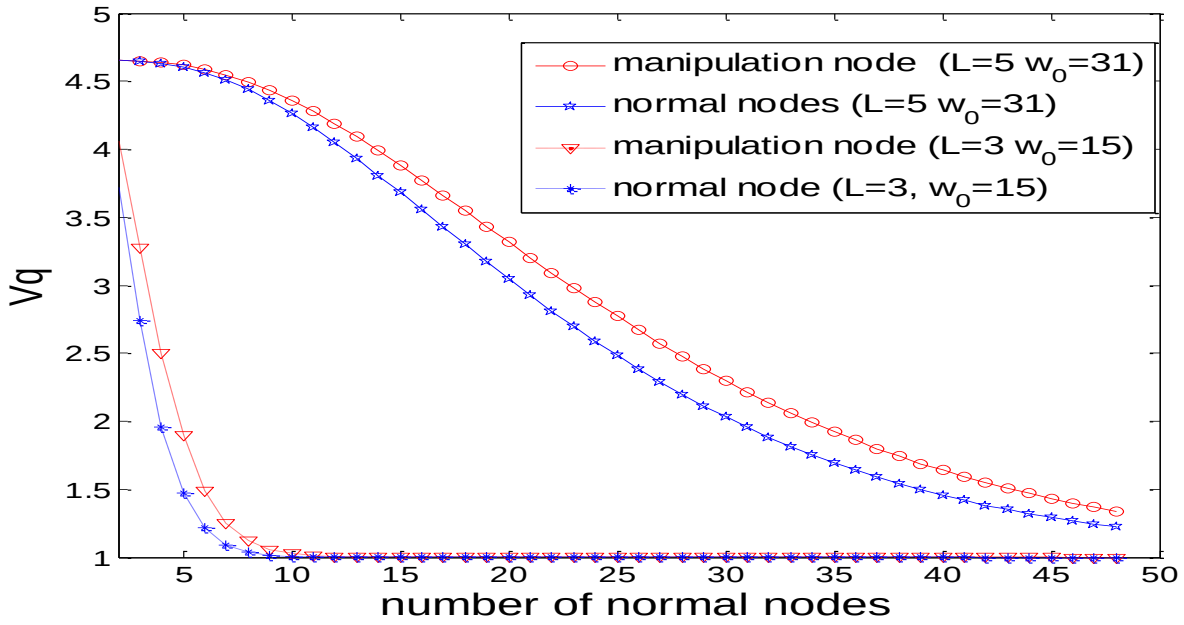

Figure 3-13: Video quality, V_q, of normal nodes and a manipulation node (under saturation condition)

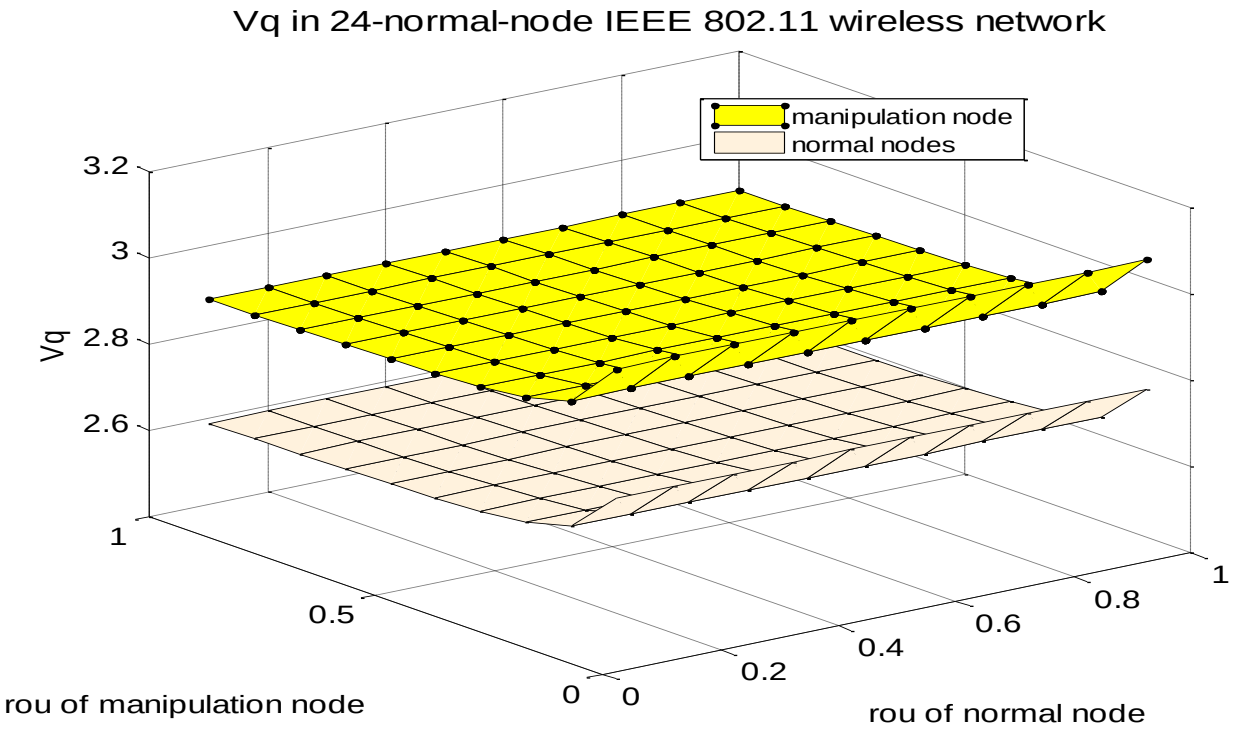

Figure 3-14: Video quality, V_q, of 24-normal nodes and a manipulation node (under non-saturation condition)

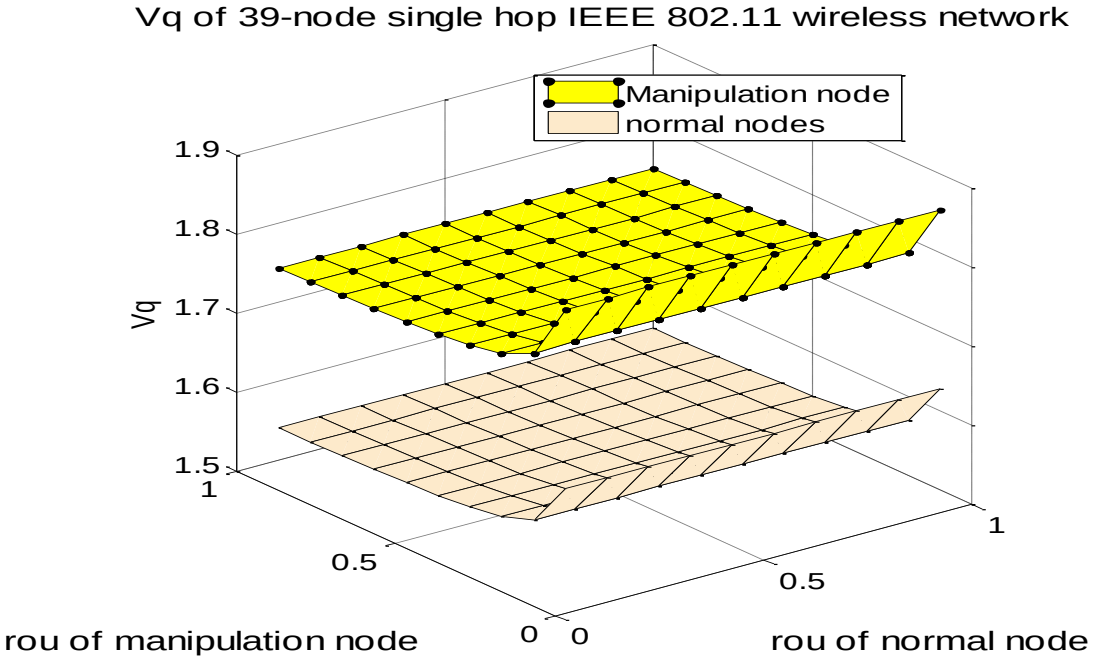

Figure 3-15: Video quality, V_q, of 38-normal nodes and a manipulation node (non-saturation)

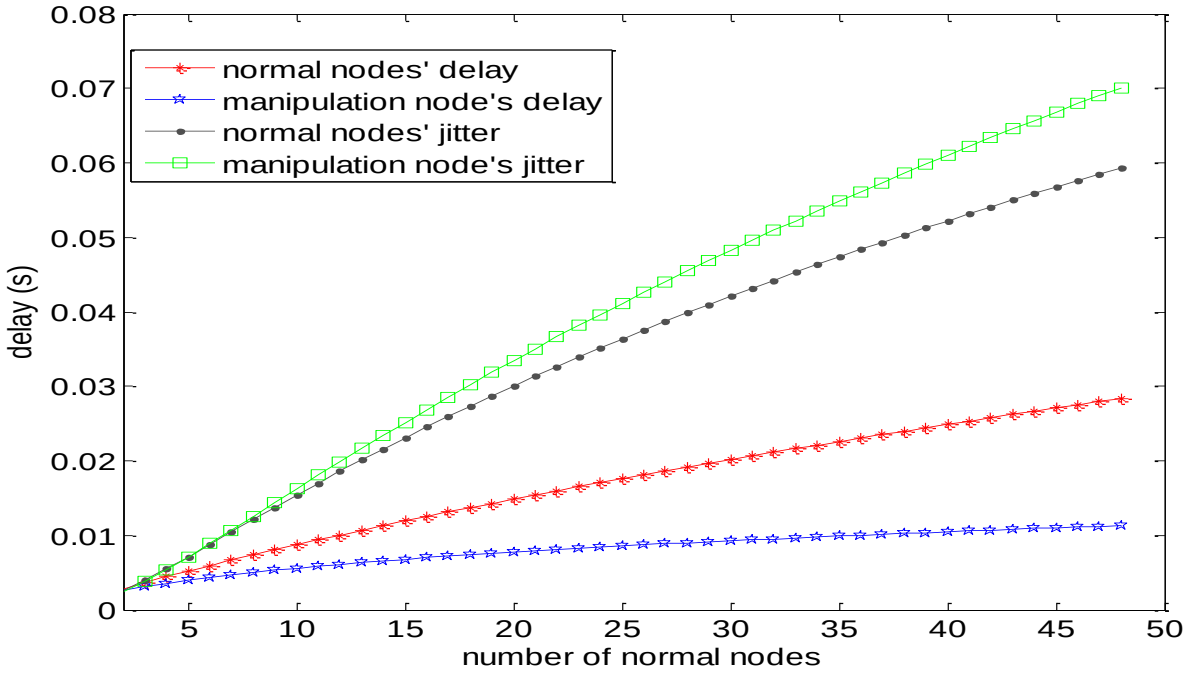

Figure 3-16: Delay and jitter of normal nodes and a manipulation node(saturation and basic access)

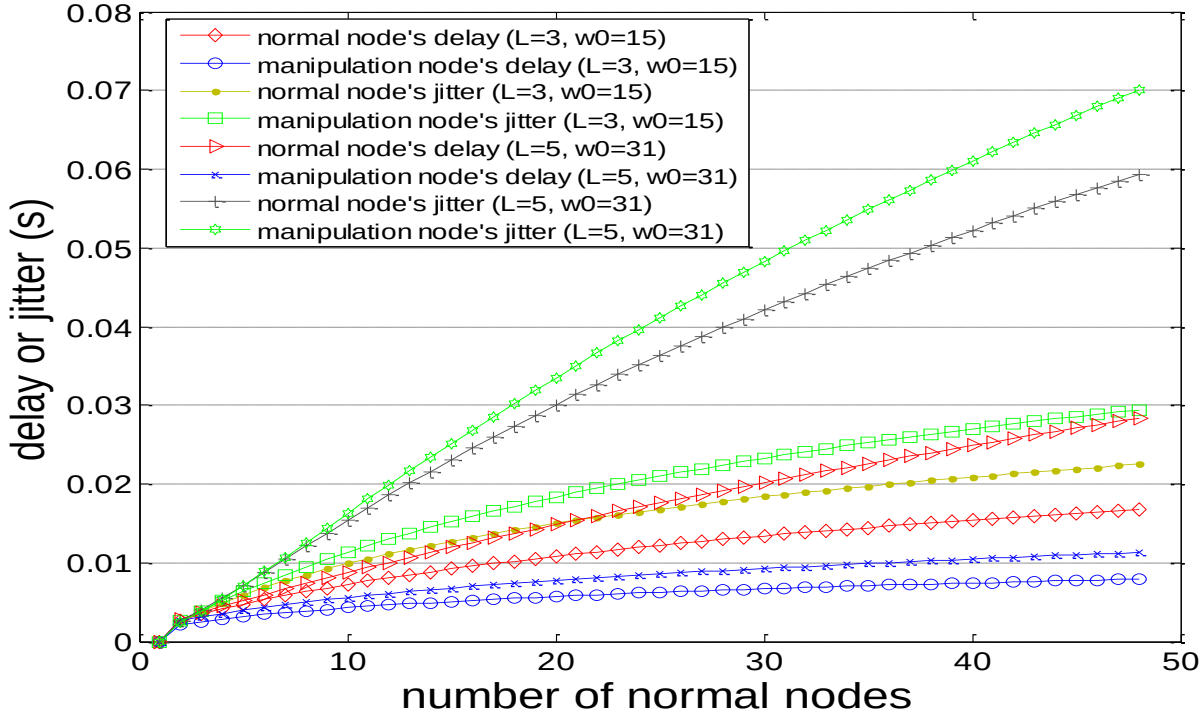

Figure 3-17: Delay and jitter of normal nodes and a manipulation node(saturation and basic access)

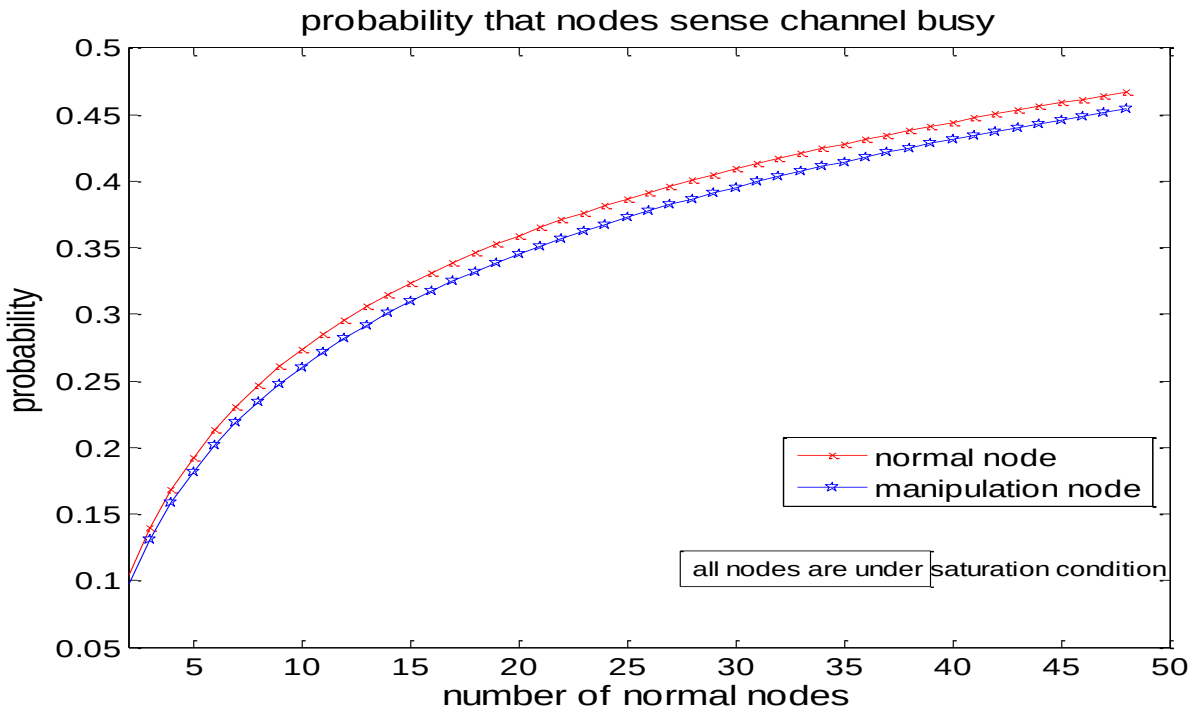

Figure 3-18: Probability that nodes sense the channel busy in a random slot (saturation)

3.7. Summary

As one of the last-mile infrastructures for video application, IEEE 802.11 wireless networks have attained maturity for years. It is well known that a packet will be discarded due to exceeding maximum retry failures in IEEE 802.11 protocol. This packet loss results in an inherent distortion of video quality in IEEE 802.11 wireless networks, even if the networks operate in an ideal physical environment, i.e. no packet errors. However, there is not much research that discusses the inherent distortion of video quality analytically. As a result, we are blind to this inherent distortion and we are not able to find the quantitative inherent distortion of video quality in IEEE 802.11 wireless networks.

In this chapter, we propose an integral approach to compute the inherent distortion of video quality in IEEE 802.11 wireless networks. It may be called an integrated approach. With a two-dimensional non-saturation Markov chain analysis model and ITU-T Recommendation G.1070, we obtain an analytical expression of the inherent distortion of video quality in IEEE 802.11 wireless networks. In this chapter,

we also discuss an optimization of setting parameters of IEEE 802.11 to minimize the distortion. The optimal setting suggestion says that we should choose large L and large w_0 to get large V_q and acceptable delay and jitter. Otherwise the loss rate will be higher, and the video application becomes un-acceptable, and it may force us give up some methods to send videos, which have no higher layer retransmission guarantee, for example, using UDP or broadcast, or multicast to deliver video to more than 20 wireless nodes.

In this chapter, the effect of the presence of a hidden station is obvious. The V_q, delay, jitter and drop rate of Node A, which is affected by hidden node directly, change due the presence of a hidden station. On the other side, the V_q, delay, jitter and drop rate of node C, which is not affected by hidden node directly, does not changes due the presence of a hidden station. We also expand the expressions to scenarios where some IEEE 802.11 wireless nodes manipulate their backoff schemes. We prove quantitatively that the video quality of those manipulating nodes is enhanced. As a conclusion, in this chapter we show how to predict a quantitative video quality with setting parameters of IEEE802.11, so that video planners are able to maintain users' specific level satisfaction with the setting parameters.

We notice that basic access and RTS/CTS access have the same packet-loss rate in a wireless network, we then have the same V_q; however, the two accesses have different throughputs. Higher throughputs do not always imply higher video quality. The size of packets also affects the throughput, but the size does not affect the packet-loss rate and the V_q .

4. Markov Chain Analysis of Directional MAC

4.1. Overview of directional MAC protocols

Directional Medium Access Control (D-MAC) Protocols for wireless networks built with directional antennas are first discussed in [43]; although directional antennas have emerged much earlier. Unlike IEEE 802.11, D-MAC protocols still is not an official standard so far.

In this chapter, we propose a new Markov chain to evaluate of the throughput of a directional MAC wireless network and compare performances of different versions of D-MAC protocols. We focus analyze the transmission collision probability of D-MAC layer, where wireless nodes have a transmitter with multiple transmitting antennas and a receiver with multiple receiving antennas. After that, we calculate the throughput and delay of MAC layer based on the collision probability.

We introduce some notations which will be used in our analysis and list them in Table 4-1.

Table 4-1: Notations used in this chapter

N	a number of nodes in a wireless network equipped with directional antennas
N_{tx}	a number of transmitting antenna elements of each node's.
N_{rx}	a number of each node's receiving antenna elements.
δ	serial number of transmitting antenna element $\delta \in \{1,2,\dots,N_{tx}\}$
x, y, z	when $N_{tx} = 3$, we use subscript x, y and z instead of δ. for example $b_{x,j,k}$, $b_{x,locked,j,0}$,$a_{x,j}$, $p_{x,j}$, $\bar{p}_x$
j	backoff stage(frame retry) value, j ∈ $(0, \mathrm{L}_\delta)$.
L_δ	a maximum value of backoff stage (frame retry) in transmitting antenna element δ;
m_δ	a maximum backoff stage(frame retry) when contention windows will not double again in antenna element δ;
k	backoff counter value. k is uniformly chosen in the range$(0, w_{\delta,j} - 1)$.
$w_{\delta,0}$	minimum contention window value of direction δ
$w_{\delta,j}$	contention window value of direction δ when stage is j.
$b_{\delta,j,k}$	a distribution probability that a node stays in a state when backoff stage(frame retry) is j , backoff counter is k and antenna element is δ .
$b_{\delta,locked,j,0}$	a distribution probabilities that a node stays in a locked state when backoff counter is $k = 0$ and other antenna element is transmitting.
$a_{\delta,j}$	a probability that a state of antenna element δ jumps to a locked state when this state's backoff reaches zero at stage j in a random slottime.

Table 4-1: Notations used in this chapter (continue)

$p_{\delta,j}$	a probability that a node senses the channel in direction δ and the channel is busy when it attempts to transmit a packet; at this moment, its backoff stage is j in direction δ at a random slot time.
$\bar{p}_{\delta}$	an average channel busy probability that a node senses channel busy in a random slot when it attempts to transmit a packet in direction δ, which is simply referred to as the average channel busy probability in direction δ.
τ_{δ}	a transmission probability in antenna element δ that a node attempts to transmit a packet in a randomly chosen slot time
$P\{\delta,j,k\|\delta,j,k+1\}$	state transition probabilities, from state $(\delta,j,k+1)$ to state (δ,j,k).
$\mathfrak{D}_{\delta}(i)$	a set of nodes which are destination nodes of node i in direction δ. we can use a program to search the set.
$\mathfrak{S}_{\delta}(i)$	set of nodes which transmits in direction δ and be sensed by node i . These nodes are contention nodes of node i in direction δ. $\mathfrak{S}_{\delta}(i)$, represent neighbors of node i in direction δ. We can use a program to find the set
$\mathfrak{W}_{\delta}(\varphi)$	a set which is formed from merging set of $\mathcal{H}_{\delta}(\varphi\|i)$ and $\mathfrak{S}_{\delta}(i)$;exclude node i if node i is element of $\mathcal{H}_{\delta}(\varphi\|i)$
$\mathcal{H}_{\delta}(\varphi\|i)$	the hidden node set of destination node φ; node φ is one of destination nodes of node i; $\varphi \in \mathfrak{D}_{\delta}(i)$; hidden nodes of destination node φ are nodes which affect it receive packet from node i.
$P_{i,success,\delta}$	a probability that node i successfully transmits its packet to its neighbors at transmitting antenna element δ.
$P_{i,tr,\delta}$	a probability that there is at least one transmission in node i's coverage area for a random slot time at transmitting antenna element δ.
$f(x,y)$	the distribution function of nodes in a two-dimension plan

Based on [17], [19], [34] and [43], we summarize D-MAC Protocols in section 4.1.1, section 4.1.2 and section 4.1.3.

4.1.1. Directional antenna model

Each node is equipped with a directional antenna (array) consisting of a transmitter with N_{tx} transmitting antennas and a receiver with N_{rx} receive antennas. The transmitting and receiving antennas have a fixed, even and non-overlapping angle. Depicted in Figure 4-1, each node has six transmitting antenna elements. We sometimes call transmitting and receiving antennas as transmitting antenna element and receiving antenna element. The antenna element will be referring to transmitting antenna element in the later of this paper if without special claim.

Each node’s upper layer knows its neighbors' location as well as its own location before it attempts to transmit a packet.

Transmitting antenna elements need to contend a common wireless channel in the same coverage area. Transmissions from one node to different directions are not allowed simultaneously. Transmitting antenna elements may be used as receiving antenna elements, or half-duplex mode.

Each transmitting antenna element senses channel directionally. (i.e., the medium is sensed only for an angular range before transmission in the particular direction.) Further, backoff or contention window is maintained independently for each transmitting antenna element and is managed in the same way as in IEEE 802.11 DCF.

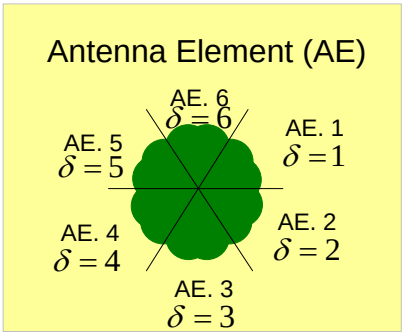

Figure 4-1: Directional Antenna Model, N_tx=N_rx=6

4.1.2. RTS/CTS access mechanism of D-MAC protocols

One D-MAC protocol, according to Dai and Ng [19], is referred to as pure request-to-send/clear-to-send access mechanism of Directional Medium Access Control (RTS/CTS D-MAC) protocols. The pure RTS/CTS D-MAC protocols are accommodated directional antennas based on RTS/CTS access mechanism of the IEEE 802.11.

In the directional RTS/CTS access mechanism, the sender and receiver nodes use directional[3] RTS/CTS frame to build up handshakes, instead of using an omni-directional antenna to transmit. Then, they estimate and use the antennas facing each other to transmit a DATA frame directionally. The receiver sends an ACK frame immediately and directionally after receiving the DATA frame. Idle nodes are assumed to listen to channels omnidirectionally.

The identical transmitting antenna element will be 'blocked' when the other nodes receive RTS/CTS packets whose owner is not themselves. The blocked antenna element will not be available to transmit anything until transmissions of other nodes in the same direction are completed. But the unblocked transmitting antenna elements of the node will be allowed to transmit. Directional Network Allocation Vector (D-NAV) Table is used to describe how to transfer status between blocked and unblocked for each transmitting antenna element, instead of Network Allocation Vector(NAV) in omnidirection. When a node hears an RTS or a CTS frame, it will set the D-NAV to defer itself from access the transmitting antenna element until a corresponding ACK frame is received.

If we refer to a sender node as node S and the receiver node as node R, according to description of Choudhury and Yang [17], we have more details of procedures in RTS/CTS/DATA/ACK four handshakes of D-MAC.

- RTS Transmission

The D-MAC layer at node S receives a packet from its upper layers, along with a direction requirement. Having received this, DMAC detects whether it is safe to transmit a RTS frame in the direction. If the channel is sensed idle, DMAC checks its DNAV to find out whether it must defer transmitting in the direction.

- CTS Transmission

[3] Dai and Ng [19] says "use omnidirectional RTS/CTS to build up the handshake". But we also find in [17] [35] and[44] "D-MAC scheme utilizes a directional antenna for sending the RTS packets in a particular direction, whereas CTS packets are transmitted in all directions. " We will discuss the performance of different protocols/schemes.

Node R listens to channels omnidirectionally and is able to receive the RTS frame from Node S. Having the RTS frame from node S, node R determines a direction to send a CTS frame in response. If the DNAV table at node R permits transmissions in the direction, then the node R replies the CTS frame in this direction after deferring for SIFS slot time. If the carrier is sensed busy during the SIFS period, the CTS frame transmission is canceled.

Nodes other than R receive the RTS, update their respective DNAV tables to be blocked status in the captured direction of arrival and defer all transmissions in the directions.

- DATA Transmission

The sender, node S, meanwhile, waits for the CTS frame. If the CTS frame does not come back within a CTS-timeout duration, then S schedules a retransmission of the RTS frame. If S receives the CTS frame, it initiates the transmission of a DATA frame.

- ACK Transmission

Node R, on receiving the DATA successfully, transmits an ACK frame.

Nodes, other than S and R, that receive the RTS frame, CTS frame, DATA frame or ACK frame, will update their DNAV table with the respective direction of arrival. The blocked direction of arrival an ACK frame will become unblocked the update, if the ACK frame arrives within an ACK-timeout duration.

4.1.3. Basic access mechanism of D-MAC protocols

In basic access mechanism of D-MAC protocols, the basic access mechanism only has DATA/ACK handshakes directionally and does not need RTS/CTS handshake. Basic access mechanism has fewer throughputs than pure-RTS/CTS mode. Both modes' performances are given in section 4.3.

In the rest of this thesis, the pure-RTS/CTS D-MAC protocols and basic access D-MAC protocol will be referred as D-MAC in this paper if without special claim.

4.2. A new Markov chain analytical model for DMAC protocols

In this section, we propose a Markov chain analytical model to describe the behavior of D-MAC. With the help of the new Markov chain analytical model, or state transition diagram, we demonstrate an approach to compute the throughput of an arbitrary topology wireless network in which nodes are equipped with directional antenna system.

4.2.1. Equivalently describe the behavior of D-MAC with a Markov chain

If each node has N_{tx} antenna elements, we mark each transmitting antenna element with a serial number, 1st, 2nd, …, N_{tx}th. We assume that a transmitting antenna element of nodes faces an identical and fixed direction. Thus, transmitting antenna element X, in figure 4-2 for example, should share the channel in direction X with other nodes.

From the summary of D-MAC protocols in previous section, we know that each antenna element is required to detect directionally whether the medium is idle when it attempts to transmit a packet in the identical transmitting antenna element. This behavior, contending a directional wireless channel with other nodes, is the same behavior that each omni directional node does. In other words, this behavior is the same behavior that is defined in IEEE 802.11 standard for omnidirecrional node. Bianchi introduces an effective two-dimension Markov chain to analyze the behavior of omnidirecrional nodes which support IEEE 802.11 standard in [7]. Hence, we propose to analyze each transmitting antenna element with Markov chain. Thus, each transmitting antenna element of nodes will be represented with an independent two-dimension Markov chain, depicted in Figure 4-3, similar to Bianchi's Markov Chain diagram. We refer to the discrete-time Markov chain for each transmitting antenna element as a branch chain of transmitting antenna element (BC) in the main Markov Chain. Our Markov chain analytical model differs from that of Bianchi's mode in two aspects; first there are N_{tx} BCs for N_{tx} transmitting antenna elements, second locked states are introduced in BCs.

Considering there are N_{tx} transmitting antenna elements in every node, we need N_{tx} Markov chains to simulate the backoff procedures of D-MAC in every direction, as shown in Figure 4-4.

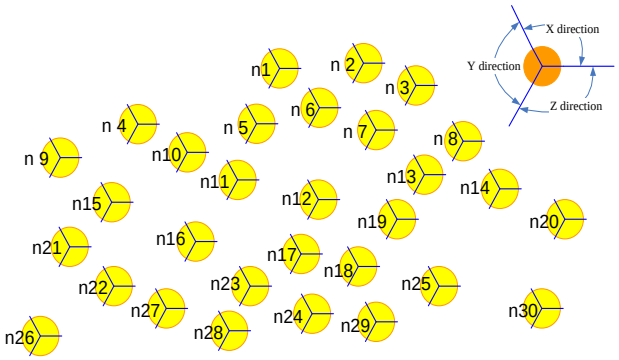

Figure 4-2: An arbitrary topology which each node has three transmitting antenna elements

In the branch chain shown in Figure 4-3, we define the state parameters $b_{\delta,j,k}$ as the stationary distribution probability being in state (δ, j, k), where $j \in (0, L_\delta)$ is the backoff stage. k is the backoff counter on direction δ. Because of an exponential backoff scheme, each backoff counter k is uniformly chosen in the range $(0, w_{\delta,j} - 1)$. $w_{\delta,j}$ is called contention window when backoff procedure of transmitting antenna element δ is in stage j. δ is serial number of transmitting antenna element. After each unsuccessful transmission attempt, j will increase by one while the contention window doubles until the maximum frame retry limit L, or the maximum contention window $w_{\delta,m}$, is reached. We define $L_\delta = m_\delta + f_\delta$, where m_δ is the maximum times that the contention window may be doubled; f_δ is the times that the contention window will not be doubled after it exceeds m_δ. The backoff counter k is "decremented" when the channel is sensed "idle" on direction δ, or "frozen" when a transmission is detected on the channel(direction) δ, and "reactivated" when the channel is sensed "idle" again for more than the distributed interframe space (DIFS). The station can transmit one packet when the backoff time reaches zero.

According to D-MAC protocols, each one of N_{tx} transmitting antenna elements will maintain their backoff procedures independently unless the transmitting antenna elements attempt to transmit

simultaneously; the transmitting antenna elements manage the procedures in the same way as in IEEE 802.11. At the beginning of each slot time, the BC's backoff counter is decremented. Backoff counter k is counted down at every slottime if the channel is idle.

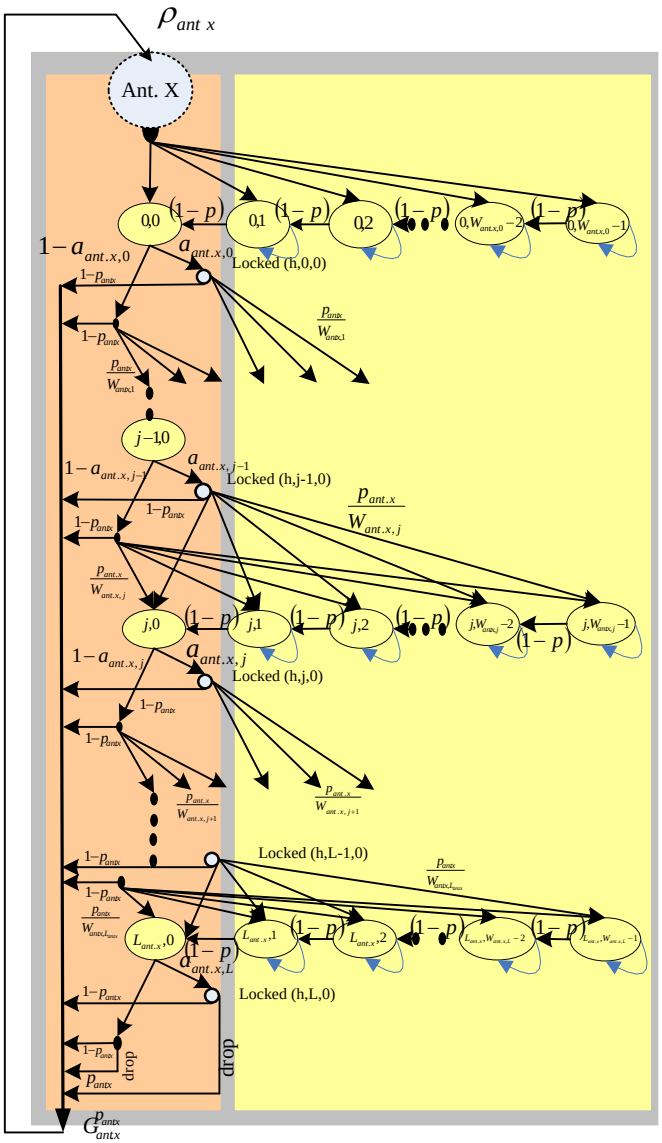

Figure 4-3: State transition diagram, one branch chain

When the channel is idle, each BC in the main Markov Chain in the Fig. 4-3a is counting down the backoff of transmitting antenna element δ from its pervious state$(\delta, j, k+1)$ to (δ, j, k). The packet in a waiting queue of transmitting antenna element δ is sent when the backoff counter becomes zero

regardless of its backoff stage, if there is no other transmitting antenna element transmitting a packet. The transmission of state $(\delta, j, 0)$ succeeds at a probability $b_{\delta,j,0}(1 - a_{\delta,j})(1 - \bar{p}_{\delta})$. Otherwise, it moves to locked state $(\delta, h, j, 0)$ to defer the transmission attempt at a probability $b_{\delta,j,0}a_{\delta,j}$, where $a_{\delta,j}$ is a probability that a backoff state of antenna element δ jumps to a locked state when its backoff reaches zero at stage j in a random slottime, but its other antenna is transmitting. $\bar{p}_{\delta}$ is an average channel busy probability that a node senses channel busy in a random slot when it attempts to transmit a packet in direction δ, which is simply referred to as the average channel busy probability in direction δ. If the transmission does not succeed, queue doubles the contention window and goes into the next row backoff. After the locked state $(\delta, h, j, 0)$ is released, the transmitting antenna element continues the transmission attempt, successfully with probability $b_{\delta,locked,j,0}(1 - \bar{p}_{\delta})$ or unsuccessfully with probability $b_{\delta,locked,j,0}\bar{p}_{\delta}$. If the transmission is successful and a new received packet is waiting in the transmission queue at the time when a transmission is completed, the queue resets its contention window; if it is not successful it goes into the second row backoff.

At the first transmission attempt, $w_{\delta,j}$ is set equal to a value $w_{\delta,0}$. $w_{\delta,0}$ is called minimum contention window. After each unsuccessful transmission in transmitting antenna element δ, contention window is doubled, up to a maximum value $w_{\delta,m_{\delta}}$ and $w_{\delta,j} = \begin{cases} 2^{j}w_{\delta,0} & j \leq m_{\delta} \\ 2^{m_x}w_{\delta,0} & m_{\delta} < j \leq L_{\delta} \end{cases}$. As mentioned earlier, where m_{δ} is the maximum retry that the contention window may be doubled, L_{δ} is a maximum value of backoff stage in transmitting antenna element δ.

Now let us discuss why we add locked state for BCs. Although each backoff procedure of N_{tx} BCs is independently handled, their transmissions interfere with each other while D-MAC requires that different transmitting antenna elements are not allowed to transmit simultaneously. In other words, an antenna element will be required to defer its transmission when its backoff reaches zero if any other

direction is transmitting. Considering "Transmissions by a node to different directions are not allowed simultaneously", we introduce locked state in our BCs. We refer to this situation as "locked state in a BC". We mark the different locked states of BC during different backoff stage j. We introduce $b_{\delta,locked,j,0}$ to represent a distribution probabilities, in random slottime, that a node stays in a locked situation when backoff stage is , backoff counter is $k = 0$ and antenna element is δ. Those BCs with locked states are shown in Figures 4-3 and 3-4.

All state transition probabilities for a BC in the proposed Markov model are listed as follows:

when $j = 0$

$$\begin{cases} P\{\delta,0,k|\delta,0,k+1\} = 1-p_\delta & k \in (0, w_{\delta,0}-2) \\ P\{\delta,h,0,0|\delta,0,0\} = a_{\delta,0} & \\ P\{\delta,1,k|\delta,h,0,0\} = \frac{p_\delta}{w_{\delta,1}} & k \in (0, w_{\delta,1}-1) \\ P\{\delta,1,k|\delta,0,0\} = \frac{(1-a_{\delta,0})p_\delta}{w_{\delta,1}} & k \in (0, w_{\delta,1}-1) \\ P\{\delta,0,k|\delta,0,0\} = \frac{(1-p_\delta)(1-a_{\delta,0})}{w_{\delta,0}} & k \in (0, w_{\delta,0}-1) \\ P\{\delta,0,k|\delta,h,0,0\} = \frac{(1-p_\delta)a_{\delta,0}}{w_{\delta,0}} & k \in (0, w_{\delta,0}-1) \end{cases} \quad (4\text{-}1a)$$

when $j \in (1, L_\delta - 1)$

$$\begin{cases} P\{\delta,j,k|\delta,j,k+1\} = 1-p_\delta & k \in (0, w_{\delta,j}-2) \\ P\{\delta,h,j,0|\delta,j,0\} = a_{\delta,j} & \\ P\{\delta,j+1,k|\delta,h,j,0\} = \frac{p_\delta}{w_{\delta,j+1}} & k \in (0, w_{\delta,1}-1) \\ P\{\delta,j+1,k|\delta,j,0\} = \frac{(1-a_{\delta,j})p_\delta}{w_{\delta,j+1}} & k \in (0, w_{\delta,j+1}-1) \\ P\{\delta,0,k|\delta,j,0\} = \frac{(1-p_\delta)(1-a_{\delta,j})}{w_{\delta,0}} & k \in (0, w_{\delta,0}-1) \\ P\{\delta,0,k|\delta,h,j,0\} = \frac{(1-p_\delta)a_{\delta,j}}{w_{\delta,0}} & k \in (0, w_{\delta,0}-1) \end{cases} \quad (4\text{-}1b)$$

when $j = L_\delta$

$$\begin{cases} P\{\delta, L_\delta, k|\delta, L_\delta, k+1\} = 1 - p_\delta \quad k \in (0, w_{\delta,j} - 2) \\ P\{\delta, h, L_\delta, 0|\delta, L_\delta, 0\} = a_{\delta,L_\delta} \\ P\{\delta, 0, k|\delta, L_\delta, 0\} = \frac{(1-a_{\delta,L_\delta})p_\delta + (1-a_{\delta,L_\delta})(1-p_\delta)}{w_{\delta,0}} \quad k \in (0, w_{\delta,0} - 1) \\ P\{\delta, 0, k|\delta, h, L_\delta, 0\} = \frac{1-p_\delta+p_\delta}{w_{\delta,0}} \quad k \in (0, w_{\delta,1} - 1) \end{cases} \tag{4-1c}$$

The first equation in (4-1a) accounts for the fact that, at the backoff stage $j = 0$ of the BC δ, the backoff counter is decreased by one with probability 1-p_δ. The second equation says that the backoff counter becomes zero, but encounter a locked state because the node's other transmitting antenna element is transmitting a frame. Its state transition probability is $a_{\delta,0}$. After the locked state ends, nodes continue to attempt to transmit a packet. The third and sixth equations account for attempting successfully with probability $\frac{(1-p_\delta)a_{\delta,0}}{w_{\delta,0}}$; or attempting not successfully and jumping into stage $j = 1$ with probability $\frac{p_\delta}{w_{\delta,1}}$. The fourth and fifth equations account for transition starting from a normal state, the backoff counter becomes zero and does not run into locked states. Equations in (4-1b) and (4-1c) account for similar state transitions starting from different stage j, $j \in (1, L_\delta - 1)$, or $j = L_\delta$.

In this chapter, we concentrate on the saturation conditions. Under saturation conditions, each station always has a packet available for transmission in every transmitting antenna element, or the transmission queue in every transmitting antenna element of each station is assumed to always have a packet waiting for transmission. In saturation conditions, each station has immediately a packet available for transmission after a completion of each successful transmission. According to the conditions, we can infer that if a transmission is completed in transmitting antenna element δ_1, also called BC in direction δ_1, a new backoff will be reset and its new state will return to BC in direction δ_1 again and will not enter other BCs in direction, for example δ_2 or δ_3, or δ_B. If it would be able to go to other BCs in direction δ_2 or δ_3, or δ_B at the moment, it will mean there is no packet in the queue of direction δ_2 or δ_3, or δ_B at the

moment. This will contravene the previous assumption. So we have fifth and sixth equations in (4-1a) and (4-1b), third and fourth equations in (4-1c).

As an example, we let $N_{tx} = 3$, and use subscript x, y and z to refer the three transmitting antenna elements. Three BCs are depicted in Figure 4-4 representing three transmitting antenna elements in a node.

4.2.2. Transmission probability of transmitting antenna element at a random slottime

In the performance analysis, we make the two assumptions. One is the same assumption in section 2.2, assuming that the wireless networks operate in an ideal physical environment, i.e. no frame error or capture effect. The other is that $p_{\delta,j}$ (at every backoff stage j) can be approximated to be the average of $p_{\delta,j}$, referred as average channel busy probability $\bar{p}_{\delta}$. $p_{\delta,j}$ is referred to as a probability that a node senses the channel in direction δ is busy when it attempts to transmit a packet at backoff stage j in direction δ. $p_{\delta,j}$ relates with the surrounding nodes' packet transmission probabilities.

This probability $p_{\delta,j}$ in Bianchi's model, and under the assumption of large number of nodes, is approximated to be constant and independent regardless of the backoff stages the node is already going though. Considering that the number of nodes surrounding a considered node may be smaller than ten in the periphery region of wireless networks, we need to introduce the new parameter $\bar{p}_{\delta}$ to relax the limit in a Bianchi's model. $\bar{p}_{\delta}$ is the average channel busy probability that a node senses channel in direction δ busy in a random slot when it attempts to transmit a packet in direction δ, which is simply referred to as the average channel busy probability in direction δ. As defined earlier, $\bar{p}_{\delta}$ is the average channel busy probability that a node senses channel busy when it attempts to transmit a packet in a random slot. It will be $\bar{p}_{\delta} = \frac{1}{1+L_{\delta}} lim_{t\to\infty} \sum_{j=0}^{L_{\delta}} p_{\delta,j}$, where L_{δ} is the maximum frame retry limit in direction δ. We use an average channel busy probability $\bar{p}_{\delta}$ to approximate probability $p_{\delta,j}$ at each backoff stage j when a node attempts to transmit a packet and finds the channel busy. In other words,

probability $p_{\delta,j}$ is approximated to be $\bar{p}_\delta$ at each backoff stage j when a node attempts to transmit a packet and finds the channel busy, and $\bar{p}_\delta$ approximates to be constant and independent regardless of the backoff stages already the node is going though.

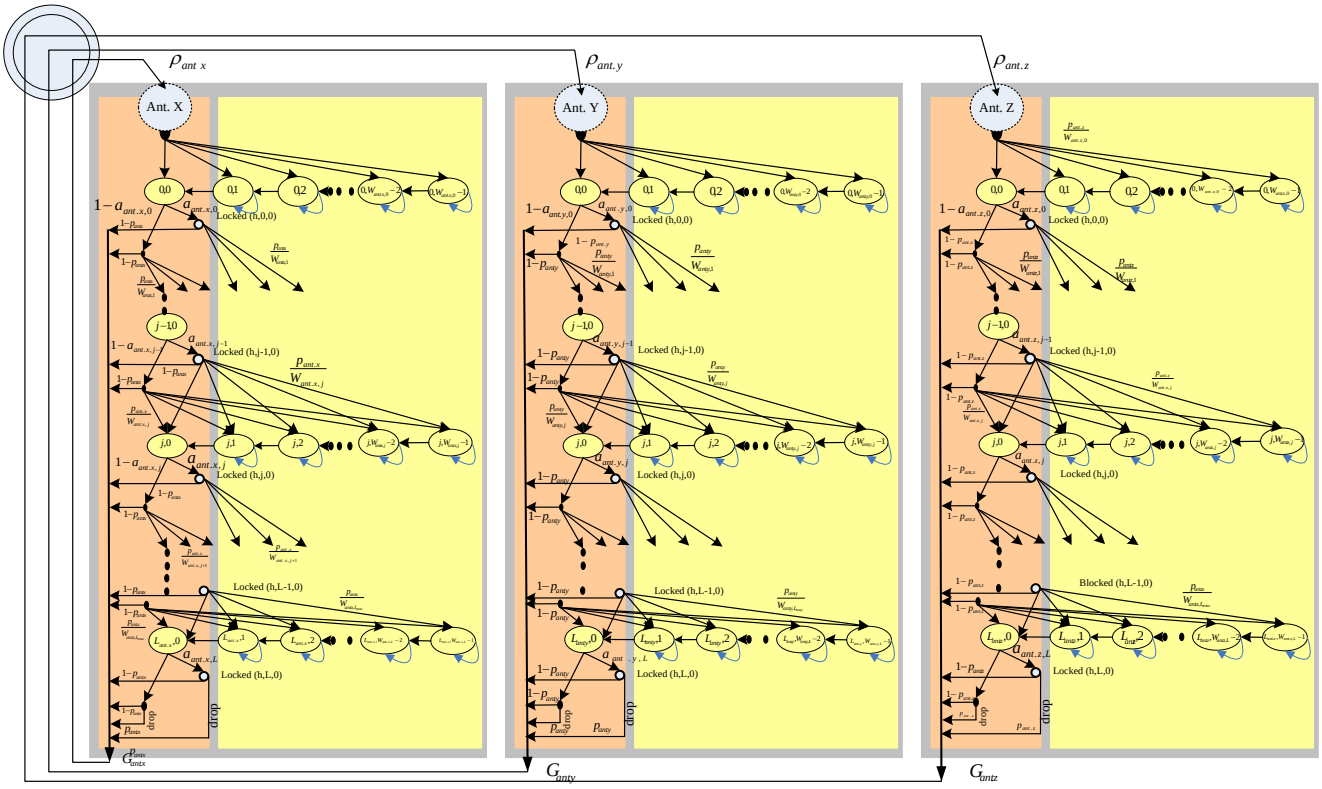

Figure 4-4: State transition diagram with three branch of Markov chain for directional antenna

As an example, we let $N_{tx} = 3$, and use subscript x, y and z to represent the three directions. All possible states and transition probabilities have their notations in its BC respectively, in the state transition diagram, Figure 4-4.

As mentioned earlier, we define state parameters b_{x,j,k_x} as the stationary distribution probability of being in state (j, k_x) in direction x in a random slot, $b_{x,locked,j,0}$ as the stationary distribution probability of being in locked state at stage j in direction x in a random slot, where j is backoff stage value; $j \in (0, L_x)$. L_x is a maximum value of backoff stage in antenna element x. k_x is backoff time value,

uniformly chosen in the range $k_x \in (0, w_{x,j} - 1)$. k_x is counted down at every slottime. After each unsuccessful transmission attempt, j will increase by one and the contention window is doubled until the maximum is reached. Locked state at stage j is a state in which its transmission is held when backoff in direction x reaches zero and other directions is transmitting.

With a D-MAC's equivalent diagram and BCs in main Markov Chain, Figure 3-4, we can proceed to find the stationary distribution probability b_{x,j,k_x} and b_{x,h,j,k_x}. First, according to the BC in direction x, and formulas (4-1a-c), first relationships, which relates the state probability $b_{x,j,k}$ and locked state probability $b_{x,h,j,0}$, will be

$$b_{x,h,j,0} = a_{x,j} b_{x,j,k_x} \tag{4-2}$$

Define $\rho_x = \sum_{j=0}^{L_x} (1 - \bar{p}_x)\left[(1 - a_{x,j}) b_{x,j,k_x} + b_{x,h,j,0}\right] + \left[(1 - a_{x,j}) b_{x,L_x,0} + b_{x,h,L_x,0}\right]\bar{p}_x$; ρ_x accounts for the aggregation probability that all states $(x, j, 0)$ or $(x, h, j, 0)$ complete a successful transmission. $a_{x,j}$is probability encountering locked states from state $(x, j, 0)$ to $(x, h, j, 0)$ state. From (4-2), we get

$$\rho_x = \sum_{j=0}^{L_x} (1 - \bar{p}_x)\left[(1 - a_{x,j}) b_{x,j,k_x} + b_{x,h,j,0}\right] + \left[(1 - a_{x,L_x}) b_{x,L_x,0} + b_{x,h,L_x,0}\right]\bar{p}_x = \sum_{j=0}^{L_x} (1 - \bar{p}_x) b_{x,j,k_x} + b_{x,L_x,0}\bar{p}_x \tag{4-3}$$

After having equation (4-2), we move on to find the second relationships about b_{x,j,k_x}. Using the Markov Chain regularities, we will have the following formulas for $b_{x,j,k}$:

$$b_{x,0,k_x} = \frac{(w_{x,0} - k_x) b_{x,0,0}}{w_{x,0}} \quad \text{where } k_x = 1,2,3, \dots, w_{x,0} - 1 \tag{4-4}$$

$$b_{x,j,k_x} = \frac{\bar{p}_x (w_{x,j} - k_x) b_{x,j-1,0}}{w_{x,j}} \text{ where } k_x = 1,2,3, \dots, w_{x,j} - 1 \; j = 1,2,3, \dots, L_x - 1, L_x \tag{4-5}$$

$$b_{x,0,0} = \rho_x \tag{4-6}$$

$$b_{x,j,0} = \bar{p}_x b_{x,j-1,0} \tag{4-7}$$

From (4-7), we get

$$b_{x,j,0} = (\bar{p}_x)^j \times b_{x,0,0} \quad (4\text{-}8)$$

From (4-5) and (4-8), we have

$$b_{x,j,k_x} = \frac{(w_{x,j}-k_x)(\bar{p}_x)^j \times b_{x,0,0}}{w_{x,j}} \text{ where } k_x = 1,2,3,\dots,w_{x,j}-1 \quad (4\text{-}9)$$

Each BC handles its own backoff procedure independently. If a directional antenna (array) has a transmitter with N_{tx} transmitting antennas, there are N_{tx} backoff procedures; the N_{tx} BCs will coexist and are independent. That means a total state probabilities in each BC should also be normalized respectively (normalization in each BCs and we have N_{tx} normalized equations.) As an example, we give one for BC of x

$$1 = \sum_{j=0}^{L_x} \sum_{k_x=0}^{w_{x,j}-1} b_{x,j,k_x} + \sum_{j=0}^{L_x} b_{x,h,j,0} \quad (4\text{-}10)$$

By substituting from (4-4), (4-5), (4-7), (4-8) and (4-9) and $w_{x,j} = \begin{cases} 2^j w_{x,0} & j \le m_x \\ 2^{m_x} w_{x,0} & m_x < j \le L_x \end{cases}$, normalization requirement, we obtain:

$$1 = b_{x,0,0}\left\{\frac{1-2(\bar{p}_x)^{L_x+1}}{1-\bar{p}_x} - \frac{\bar{p}_x-\bar{p}_x{}^{L+1}}{2(1-\bar{p}_x)(1-\bar{p}_x)} + \frac{w_{x,0}}{2(1-\bar{p}_x)}\left[1 + \frac{(2\bar{p}_x-(2\bar{p}_x)^{m_x+1})}{(1-2\bar{p}_x)} + 2^{m_x}\frac{(\bar{p}_x)^{m_x+1}-(\bar{p}_x)^{L_x+1}}{(1-\bar{p}_x)}\right]\right\} + \sum_{j=0}^{L_x} b_{x,h,j,0}$$

Defining $Hold_x = \sum_{j=0}^{L_x} b_{x,h,j,0}$ (it will be shown later that it represents the total probability of locked state), we obtain

$$1 = b_{x,0,0}\left\{\frac{1-2(\bar{p}_x)^{L_x+1}}{1-\bar{p}_x} - \frac{\bar{p}_x-\bar{p}_x{}^{L+1}}{2(1-\bar{p}_x)(1-\bar{p}_x)} + \frac{w_{x,0}}{2(1-\bar{p}_x)}\left[1 + \frac{(2\bar{p}_x-(2\bar{p}_x)^{m_x+1})}{(1-2\bar{p}_x)} + 2^{m_x}\frac{(\bar{p}_x)^{m_x+1}-(\bar{p}_x)^{L_x+1}}{(1-\bar{p}_x)}\right]\right\} + Hold_x \quad (4\text{-}11)$$

Similarly, defining $Hold_y = \sum_{j=0}^{L_y} b_{y,h,j,0}$ and $Hold_z = \sum_{j=0}^{L_z} b_{z,h,j,0}$, we have the following formulas for antenna elements y and z:

$$1 = b_{y,0,0}\left\{\frac{1-2(\bar{p}_y)^{L_y+1}}{1-\bar{p}_y} - \frac{\bar{p}_y-\bar{p}_y{}^{L+1}}{2(1-\bar{p}_y)(1-\bar{p}_y)} + \frac{w_{y,0}}{2(1-\bar{p}_y)}\left[1 + \frac{(2\bar{p}_y-(2\bar{p}_y)^{m_y+1})}{(1-2\bar{p}_y)} + 2^{m_y}\frac{(\bar{p}_y)^{m_y+1}-(\bar{p}_y)^{L_y+1}}{(1-\bar{p}_y)}\right]\right\} + Hold_y \quad (4\text{-}12)$$

$$1 = b_{z,0,0}\left\{\frac{1-2(\bar{p}_z)^{L_z+1}}{1-\bar{p}_z} - \frac{\bar{p}_z-\bar{p}_z{}^{L+1}}{2(1-\bar{p}_z)(1-\bar{p}_z)} + \frac{w_{z,0}}{2(1-\bar{p}_z)}\left[1 + \frac{(2\bar{p}_z-(2\bar{p}_z)^{m_z+1})}{(1-2\bar{p}_z)} + 2^{m_z}\frac{(\bar{p}_z)^{m_z+1}-(\bar{p}_z)^{L_z+1}}{(1-\bar{p}_z)}\right]\right\} + Hold_z \quad (4\text{-}13)$$

In D-MAC, transmitting antenna element is not always able to transmit when backoff counter k reaches zero; those probabilities are summed as $Hold_x$, $Hold_y$, $Hold_z$.

We denote τ_δ the transmission probability in direction δ that a node attempts to transmit a packet in a randomly chosen slottime. Knowing in Banich's model, an attempting transmission will occur when backoff counter k is counted down to zero. This principle is still true for BCs. And there is an additional transmission attempt in our BCs; the additional transmission attempt will occur after the locked states eliminate. Hence, we obtain the following equations with (4-2)

$$\tau_x = \sum_{j=0}^{L_x}\left[\left(1-a_{x,j}\right)b_{x,j,0} + b_{x,h,j,0}\right] = \sum_{j=0}^{L_x}(\bar{p}_x)^j \times b_{x,0,0} = \frac{1-(\bar{p}_x)^{L_x+1}}{1-\bar{p}_x} b_{x,0,0} \quad (4\text{-}14)$$

$$\tau_y = \sum_{j=0}^{L_y}\left[\left(1-a_{y,j}\right)b_{y,j,0} + b_{y,h,j,0}\right] = \frac{1-(\bar{p}_y)^{L_y+1}}{1-\bar{p}_y} b_{y,0,0} \quad (4\text{-}15)$$

$$\tau_z = \sum_{j=0}^{L_z}\left[\left(1-a_{z,j}\right)b_{z,j,0} + b_{z,h,j,0}\right] = \frac{1-(\bar{p}_z)^{L_z+1}}{1-\bar{p}_z} b_{z,0,0} \quad (4\text{-}16)$$

We notice that τ_δ , $\delta \in (x, y, z)$, in equations (4-14)-(4-16), do not have the obvious effects from locked states, however the effects from $Hold_x$, $Hold_y$ and $Hold_z$, have affected $b_{x,0,0}$, $b_{y,0,0}$ and $b_{z,0,0}$ in formula (4-9)-(4-11) , and deducted from τ_δ.

As mentioned earlier, the node stays in locked state when other antenna elements are transmitting. Hence, the locked state probabilities are given by:

$$Hold_x = 1 - \left(1-\tau_y\right)(1-\tau_z) \quad (4\text{-}17)$$

$$Hold_y = 1 - (1-\tau_x)(1-\tau_z) \quad (4\text{-}18)$$

$$Hold_z = 1 - (1-\tau_x)\left(1-\tau_y\right) \quad (4\text{-}19)$$

Thus far, we get the transmission probability $\tau_x\ \tau_y\ \tau_z$.

Generally, we can turn Equations (4-11)-(4-19) to a direction antenna array which has N_{tx} antenna elements, by using $\{\bar{p}_\delta, \tau_\delta\}$, $\delta \in (1,2,3, \dots\dots, N_{tx})$, instead of $\left\{\bar{p}_x, \tau_x, \bar{p}_y, \tau_y, \bar{p}_z, \tau_z\right\}$.

$$1 = b_{\delta,0,0}\left\{\frac{1-2(\bar{p}_\delta)^{L_\delta+1}}{1-\bar{p}_\delta} - \frac{\bar{p}_\delta - \bar{p}_\delta{}^{L+1}}{2(1-\bar{p}_\delta)(1-\bar{p}_\delta)} + \frac{w_{\delta,0}}{2(1-\bar{p}_\delta)}\left[1 + \frac{(2\bar{p}_\delta - (2\bar{p}_\delta)^{m_\delta+1})}{(1-2\bar{p}_\delta)} + 2^{m_\delta}\frac{(\bar{p}_\delta)^{m_\delta+1} - (\bar{p}_\delta)^{L_\delta+1}}{(1-\bar{p}_\delta)}\right]\right\} + Hold_\delta \quad (4\text{-}11a)$$

$$\tau_\delta = \frac{1-(\bar{p}_\delta)^{L_\delta+1}}{1-\bar{p}_\delta} b_{\delta,0,0} \quad (4\text{-}14a)$$

$$Hold_\delta = 1 - \prod_{\gamma=1;\gamma\neq\delta}^{N_{tx}}(1-\tau_\gamma) \quad (4\text{-}17a)$$

where $\delta \in (1,2,3,\ldots\ldots,N_{tx})$ and $i \in (1,2,3,\ldots\ldots,N)$.

Equations (11a),(14a) and (17a) are defined as node's property formula for D-MAC protocols because it determine the node's transmission probability τ_δ in terms of the average channel busy probability $\bar{p}_\delta$ as well as the network configure parameters $(L_\delta, m_\delta, w_{\delta,0})$. The relationship of variables of $\{\bar{p}_\delta, \tau_\delta\}$, $\delta \in (1,2,3,\ldots\ldots,N_{tx})$, described in equations (4-11a),(4-14a) and (4-17a), will be regarded as the attributes of a transmission of an D-MAC station under saturation condition. We can apply the relationship to each node equipped with directional antenna under saturation condition. We let i be the series of nodes, $i \in (1,2,3,\ldots\ldots,N)$. Using i as subscript and attaching the node's serial number to $\{\bar{p}_\delta, \tau_\delta\}$, we have $\{\bar{p}_{i,\delta}, \tau_{i,\delta}\}$, $\delta \in (1,2,3,\ldots\ldots,N_{tx})$, for each node,

$$1 = b_{i,\delta,0,0}\left\{\frac{1-2(\bar{p}_{i,\delta})^{L_{i,\delta}+1}}{1-\bar{p}_{i,\delta}} - \frac{\bar{p}_{i,\delta} - \bar{p}_{i,\delta}{}^{L+1}}{2(1-\bar{p}_{i,\delta})(1-\bar{p}_{i,\delta})} + \frac{w_{i,\delta,0}}{2(1-\bar{p}_\delta)}\left[1 + \frac{(2\bar{p}_{i,\delta} - (2\bar{p}_{i,\delta})^{m_{i,\delta}+1})}{(1-2\bar{p}_{i,\delta})} + 2^{m_{i,\delta}}\frac{(\bar{p}_{i,\delta})^{m_{i,\delta}+1} - (\bar{p}_{i,\delta})^{L_{i,\delta}+1}}{(1-\bar{p}_{i,\delta})}\right]\right\} + Hold_{i,\delta} \quad (4\text{-}11b)$$

$$\tau_{i,\delta} = \frac{1-(\bar{p}_{i,\delta})^{L_{i,\delta}+1}}{1-\bar{p}_{i,\delta}} b_{i,\delta,0,0} \quad (4\text{-}14b)$$

$$Hold_{i,\delta} = 1 - \prod_{\gamma=1;\gamma\neq\delta}^{N_{tx}}(1-\tau_{i,\gamma}) \quad (4\text{-}17b)$$

where $\delta \in (1,2,3,\ldots\ldots,N_{tx})$ and $i \in (1,2,3,\ldots\ldots,N)$.

If we know the geographical locations of nodes, we can determine who are neighbor nodes to every given node. Note that $\bar{p}_{i,\delta}$ in equations (4-11b) ,(4-14b) and (4-17b) depends on the transmission status of its neighbors nodes and varies from one node to the other; we can write equations of all $\bar{p}_{i,\delta}$ in terms of neighboring nodes transmission probability $\tau_{u,\delta}$, where u is serial number of node i's neighbors.

Using a given network topology and numerical solution technology, we should be able to solve equations (4-11b) ,(4-14b) and (4-17b) and obtain the network throughput and delay for every node.

If directional antenna come back and become omni direction antenna, the locked state is not necessary. With mathematics, we can have, $Hold_x = 0$ $Hold_y = 0$ and $Hold_z = 0$. Substitute $Hold_x = 0$ $Hold_y = 0$ and $Hold_z = 0$ into equations (4-11)-(4-19), and equations (4-11c)-(4-16c) are those formulas for omni-direction wireless networks, seeing equations (2-7), (2-7) and (2-8). And (4-17c)-(4-19c) do not need to exist for omni-direction wireless and can be neglected, or when we calculate τ_x , we do not need to care about τ_y and τ_z because they do not exist.

$$1 = b_{x,0,0}\left\{\frac{1-2(\bar{p}_x)^{Lx+1}}{1-\bar{p}_x} - \frac{\bar{p}_x - \bar{p}_x{}^{L+1}}{2(1-\bar{p}_x)(1-\bar{p}_x)} + \frac{w_{x,0}}{2(1-\bar{p}_x)}\left[1 + \frac{(2\bar{p}_x - (2\bar{p}_x)^{mx+1})}{(1-2\bar{p}_x)} + 2^{m_x}\frac{(\bar{p}_x)^{mx+1} - (\bar{p}_x)^{Lx+1}}{(1-\bar{p}_x)}\right]\right\} \quad (4\text{-}11c)$$

$$1 = b_{y,0,0}\left\{\frac{1-2\left(\bar{p}_y\right)^{Ly+1}}{1-\bar{p}_y} - \frac{\bar{p}_y - \bar{p}_y{}^{L+1}}{2\left(1-\bar{p}_y\right)\left(1-\bar{p}_y\right)} + \frac{w_{y,0}}{2\left(1-\bar{p}_y\right)}\left[1 + \frac{\left(2\bar{p}_y - \left(2\bar{p}_y\right)^{m_y+1}\right)}{\left(1-2\bar{p}_y\right)} + 2^{m_y}\frac{\left(\bar{p}_y\right)^{m_y+1} - \left(\bar{p}_y\right)^{Ly+1}}{\left(1-\bar{p}_y\right)}\right]\right\} \quad (4\text{-}12c)$$

$$1 = b_{z,0,0}\left\{\frac{1-2(\bar{p}_z)^{Lz+1}}{1-\bar{p}_z} - \frac{\bar{p}_z - \bar{p}_z{}^{L+1}}{2(1-\bar{p}_z)(1-\bar{p}_z)} + \frac{w_{z,0}}{2(1-\bar{p}_z)}\left[1 + \frac{(2\bar{p}_z - (2\bar{p}_z)^{mz+1})}{(1-2\bar{p}_z)} + 2^{m_z}\frac{(\bar{p}_z)^{mz+1} - (\bar{p}_z)^{Lz+1}}{(1-\bar{p}_z)}\right]\right\} \quad (4\text{-}13c)$$

$$\tau_x = \frac{1-(\bar{p}_x)^{Lx+1}}{1-\bar{p}_x} b_{x,0,0} \quad (4\text{-}14c)$$

$$\tau_y = \frac{1-(\bar{p}_y)^{Ly+1}}{1-\bar{p}_y} b_{y,0,0} \quad (4\text{-}15c)$$

$$\tau_z = \frac{1-(\bar{p}_z)^{Lz+1}}{1-\bar{p}_z} b_{z,0,0} \quad (4\text{-}16c)$$

$$0 = 1 - \left(1-\tau_y\right)(1-\tau_z) \quad (4\text{-}17c)$$

$$0 = 1 - (1-\tau_x)(1-\tau_z) \quad (4\text{-}18c)$$

$$0 = 1 - (1-\tau_x)\left(1-\tau_y\right) \quad (4\text{-}19c)$$

Generally, if knowing $f(x,y)$, the distribution function of nodes, we can find a node's surrounding nodes. This will help to find $\{\bar{p}_{i,\delta}, \tau_{i,\delta}\}$. All distribution of node in practical wireless networks are a

discrete distribution of nodes. That means $f(x,y) = \sum_{i=1,2,\dots N} \delta(\vec{r} - \vec{r}_i)$, where $\vec{r}_i$ is the locations of nodes. A 64-node network is show later.

4.3. Performance of DMAC wireless networks

To avoid additional complexity, we assume all nodes are static at first and the wireless networks operate in an ideal physical environment. We also take a further assumption that a source node randomly picks up a destination node from the nodes which the source node's directional antenna can reach when it attempts to send a packet. The direction of each transmitting antenna element is fixed. For example, in Figure 4-2, a 30-node network is depicted; each node has three antenna elements.

We will calculate the performance of an arbitrary topology wireless, which has N nodes and N_{tx} transmitting antenna elements. First, we summarize the equations used for each node as following,

$$1 = b_{i,\delta,0,0}\left\{\frac{1-2(\bar{p}_{i,\delta})^{L_{i,\delta}+1}}{1-\bar{p}_{i,\delta}} - \frac{\bar{p}_{i,\delta}-\bar{p}_{i,\delta}{}^{L+1}}{2(1-\bar{p}_{i,\delta})(1-\bar{p}_{i,\delta})} + \frac{w_{i,\delta,0}}{2(1-\bar{p}_{\delta})}\left[1 + \frac{\left(2\bar{p}_{i,\delta}-(2\bar{p}_{i,\delta})^{m_{i,\delta}+1}\right)}{(1-2\bar{p}_{i,\delta})} + 2^{m_{i,\delta}}\frac{(\bar{p}_{i,\delta})^{m_{i,\delta}+1}-(\bar{p}_{i,\delta})^{L_{i,\delta}+1}}{(1-\bar{p}_{i,\delta})}\right]\right\} + Hold_{i,\delta} \quad (4\text{-}11b)$$

$$\tau_{i,\delta} = \frac{1-(\bar{p}_{i,\delta})^{L_{i,\delta}+1}}{1-\bar{p}_{i,\delta}} b_{i,\delta,0,0} \quad (4\text{-}14b)$$

$$Hold_{i,\delta} = 1 - \prod_{\gamma=1;\gamma\neq\delta}^{N_{tx}}(1-\tau_{i,\gamma}) \quad (4\text{-}17b)$$

where $\delta \in (1,2,3,\dots\dots,N_{tx})$ and $i \in (1,2,3,\dots\dots,N)$.

Those peripheral nodes will not transmit packets if the peripheral nodes have no destination node to receive their data. Then, in this special situation, we will let their $\tau_{i,\delta} = 0$.

Note that $\bar{p}_{i,\delta}$ in equation (4-11b) and (4-14b) depends on the transmission status of its neighbors nodes which transmits in direction δ and contends for the media with node i. Those neighboring nodes vary from one node to the other. For a given network topology, we can use a program to find out neighbor nodes for node i, $i \in (1,2,3,\dots\dots,N)$. Let a set of nodes, $\mathfrak{S}_{\delta}(i)$, represent contention neighbors of node i in direction δ. If direction δ is fixed, only direction δ is the contention direction of

node i in direction δ; and we need only to consider direction δ of other nodes when we are finding neighboring nodes $\mathfrak{S}_\delta(i)$. Node i contend with the neighboring nodes for a channel in direction δ. (if the set $\mathfrak{S}_\delta(i)$ is an empty set, then the $\bar{p}_{i,\delta} = 0$, without collision when node i attempts to transmit.)

Now we are able to determine an equation (4-20) of $\bar{p}_{i,\delta}$ in terms of those nodes' transmission probability $\tau_{u,\delta}$, where u is one node of $\mathfrak{S}_\delta(i)$. $\mathfrak{S}_\delta(i)$ is node i's neighbors which are able to transmit in direction δ and be sensed by node i in direction δ . So, we can write the $\bar{p}_{i,\delta}$, sensing the direction δ busy, as following

$$\bar{p}_{i,\delta} = 1 - \prod_{u \in \mathfrak{S}_\delta(i)}\left(1 - \tau_{u,\delta}\right) \qquad i \in (1,2,\dots,N) \qquad \delta \in (1,2,\dots,N_{tx}) \tag{4-20}$$

Re-writing equations (4-11b), (4-14b), (4-17b) and (4-20) which are needed to find $\tau_{i,\delta}$ here as (4-21a-d):

$$1 = b_{i,1,0,0}\left\{\frac{1-2(\bar{p}_{i,1})^{L_{i,1}+1}}{1-\bar{p}_{i,1}} - \frac{\bar{p}_{i,1}-\bar{p}_{i,1}{}^{L+1}}{2(1-\bar{p}_{i,1})(1-\bar{p}_{i,1})} + \frac{w_{i,1,0}}{2(1-\bar{p}_1)}\left[1 + \frac{\left(2\bar{p}_{i,1}-(2\bar{p}_{i,1})^{m_{i,1}+1}\right)}{(1-2\bar{p}_{i,1})} + 2^{m_{i,1}}\frac{(\bar{p}_{i,1})^{m_{i,1}+1}-(\bar{p}_{i,1})^{L_{i,1}+1}}{(1-\bar{p}_{i,1})}\right]\right\} + Hold_{i,1} \tag{4-21a}$$

$$1 = b_{i,2,0,0}\left\{\frac{1-2(\bar{p}_{i,2})^{L_{i,2}+1}}{1-\bar{p}_{i,2}} - \frac{\bar{p}_{i,2}-\bar{p}_{i,2}{}^{L+1}}{2(1-\bar{p}_{i,2})(1-\bar{p}_{i,2})} + \frac{w_{i,2,0}}{2(1-\bar{p}_2)}\left[1 + \frac{\left(2\bar{p}_{i,2}-(2\bar{p}_{i,2})^{m_{i,2}+1}\right)}{(1-2\bar{p}_{i,2})} + 2^{m_{i,2}}\frac{(\bar{p}_{i,2})^{m_{i,2}+1}-(\bar{p}_{i,2})^{L_{i,2}+1}}{(1-\bar{p}_{i,2})}\right]\right\} + Hold_{i,2}$$

.....

$$1 = \frac{1-2\left(\bar{p}_{i,N_{tx}}\right)^{L_{i,N_{tx}}+1}}{1-\bar{p}_{i,N_{tx}}} b_{i,N_{tx},0,0} - \frac{\bar{p}_{i,N_{tx}}-\bar{p}_{i,N_{tx}}{}^{L+1}}{2\left(1-\bar{p}_{i,N_{tx}}\right)\left(1-\bar{p}_{i,N_{tx}}\right)} b_{i,N_{tx},0,0} + \frac{w_{i,N_{tx},0}}{2\left(1-\bar{p}_{i,N_{tx}}\right)} b_{i,N_{tx},0,0}\left[1 + \frac{\left(2\bar{p}_{i,N_{tx}}-\left(2\bar{p}_{i,N_{tx}}\right)^{m_{i,N_{tx}}+1}\right)}{\left(1-2\bar{p}_{i,N_{tx}}\right)} + 2^{m_{i,N_{tx}}}\frac{\left(\bar{p}_{i,N_{tx}}\right)^{m_{i,N_{tx}}+1}-\left(\bar{p}_{i,N_{tx}}\right)^{L_{i,N_{tx}}+1}}{\left(1-\bar{p}_{i,N_{tx}}\right)}\right] + Hold_{i,N_{tx}} \tag{4-21a}$$

$$\tau_{i,1} = \frac{1-(\bar{p}_{i,1})^{L_{i,1}+1}}{1-\bar{p}_{i,1}} b_{i,1,0,0} \tag{4-21b}$$

$$\tau_{i,2} = \frac{1-\left(\bar{p}_{i,2}\right)^{L_{i,2}+1}}{1-\bar{p}_{i,2}} b_{i,2,0,0}$$

.....

$$\tau_{i,N_{tx}} = \frac{1-(\bar{p}_{i,N_{tx}})^{L_{i,N_{tx}}+1}}{1-\bar{p}_{i,N_{tx}}} b_{i,N_{tx},0,0} \quad (4\text{-}21b)$$

$$Hold_{i,1} = 1 - \prod_{\gamma=2;\gamma\neq 1}^{N_{tx}} (1-\tau_{i,\gamma}) \quad (4\text{-}21c)$$

$$Hold_{i,2} = 1 - \prod_{\gamma=1;\gamma\neq 2}^{N_{tx}} (1-\tau_{i,\gamma})$$

.....

$$Hold_{i,N_{tx}} = 1 - \prod_{\gamma=1;\gamma\neq N_{tx}}^{N_{tx}} (1-\tau_{i,\gamma}) \quad (4\text{-}21c)$$

$$\bar{p}_{i,1} = 1 - \prod_{u\in \mathbb{S}_1(i)} (1-\tau_{u,1}) \quad (4\text{-}21d)$$

$$\bar{p}_{i,2} = 1 - \prod_{u\in \mathbb{S}_2(i)} (1-\tau_{u,2})$$

.....

$$\bar{p}_{i,N_{tx}} = 1 - \prod_{u\in \mathbb{S}_{N_{tx}}(i)} (1-\tau_{u,N_{tx}}) \quad (4\text{-}21d)$$

In equation (21a-d), $i \in (1,2,3,\dots\dots,N)$. Using numerical solution technology, we should be able to solve equations (4-21a)-(4-21d).

Recalling that $\tau_{i,\delta}$ is the transmission probability that node i attempts to transmit in a randomly chosen slot time, we will able to determine the network throughput and delay in section 4.3.1. and section 4.3.2. We also will evaluate performance according to different Directional MAC protocols.

4.3.1. Throughput of a DMAC wireless network at MAC layer

In order to obtain the nodes throughput, we need to define $P_{i,tr,\delta}$ as the probability that there is at least one transmission in node i's coverage area for a random slot time at the transmitting antenna element δ. And we let $P_{i,success,\delta}$ be the probability that node i successfully transmits its packet to its neighbors at transmitting antenna element δ.

Similar to the Bianchi model [7], let $Throughput_{i,\delta}$ be the normalized throughput of node i, defined as the fraction of time when the channel in the coverage area of node i is used to successfully transmit packets to its neighbors (including relay packets) in direction δ. We have $Throughput_{i,\delta} = \frac{E[payload\ succesfully\ transmitted\ in\ a\ slot\ time]}{E[length]}$, where $E[length]$ is the average length of a slotted time. E[payload] is the average packet payload size. The average amount of payload information successfully transmitted in a slot time is $P_{i,success,\delta}E[payload]$. Since a successful transmission occurs in a slot time with the probability $P_{i,success,\delta}$, $E[lenght]$ will be $(1-P_{i,tr,\delta})\sigma + P_{i,success,\delta}T_S + [P_{i,tr,\delta} - P_{i,success,\delta}]T_C$. The term $(1-P_{i,tr,\delta})\sigma$ accounts for an empty slot time with probability $1-P_{i,tr,\delta}$; the term $P_{i,success,\delta}T_S$ stands for successful transmissions of node i with successful probability $P_{i,success,\delta}$; and the term $[P_{i,tr,\delta} - P_{i,success,\delta}]T_C$ deals with the collision duration. T_S is the average time for a successful transmission, and T_C is the average time duration for the collision. σ is the duration of an empty slot time. T_C and T_S can be obtained for the basic mechanism with (2-30a-b) and for the RTS/CTS access mechanisms with (2-30c-d). And then we have $Throughput_{i,\delta}$, the throughput of each node in the direction δ:

$$Throughput_{i,\delta} = \frac{P_{i,success,\delta}E[P]}{(1-P_{i,tr,\delta})\sigma + P_{i,success,\delta}T_S + [P_{i,tr,\delta} - P_{i,success,\delta}]T_C} \quad (4\text{-}22)$$

where we still need to find $P_{i,success,\delta}$, successful transmission at node i in the transmitting antenna element δ and $P_{i,tr,\delta}$ the probability that there is at least one transmission in node i's coverage area for a given slot time at transmitting antenna element δ. $P_{i,tr,\delta}$ is given as following

$$P_{i,tr,\delta} = 1 - (1-\tau_{i,\delta})\prod_{u \in \Im_\delta(i)}(1-\tau_{u,\delta}) \quad (4\text{-}23)$$

To determine $P_{i,success,\delta}$, successful transmission probability at Node i, we need find which node will affect a successful transmission at a random slottime and which node should keep silent when node i has a successful transmission.

First, those nodes, $\mathfrak{S}_\delta(i)$, should be silent and should not transmit. Because they contend with node i in direction δ. Second, each destination node's hidden node also should not transmit. We will define a new set of node to notate it. We have node i's peripheral nodes, $\mathfrak{S}_\delta(i)$, in direction δ. We let a set of destination nodes of node i be $\mathfrak{D}_\delta(i)$ in direction δ. φ is one of destination nodes. We call the hidden node set of destination node φ, $\mathcal{H}_\delta(\varphi|i)$. We may notice that different destination φ will have different hidden nodes. (We need find out which is node φ's receiver antenna element first, then we find which nodes are hidden node. We can use a program to do this task.) We merge the two sets $\mathfrak{S}_\delta(i)$ and $\mathcal{H}_\delta(\varphi|i)$ and get rid repeating nodes and transmitting node i from the merged set.

$$\mathfrak{W}_\delta(\varphi|i) = \mathcal{H}_\delta(\varphi|i) \cup \mathfrak{S}_\delta(i) \qquad \text{(exclude node } i\text{)} \tag{4-24}$$

So nodes belonging to $\mathfrak{W}_\delta(\varphi|i)$should not transmit to grantee node i transmit to node φ successfully. After we need pick a destination φ from destination nodes set, $\mathfrak{D}_\delta(i)$, we are able to get $P_{(i,success,\delta|\varphi)}$ probability that node i successfully transmits its packet to one of its destination node φ at transmitting antenna element δ. Substitute equation (4-22, 4-23), we will have:

$$throughput_{(i,\delta|\varphi)} = \frac{P_{(i,success,\delta|\varphi)}E[P]}{(1-P_{i,tr,\delta})\sigma+P_{(i,success,\delta|\varphi)}T_S+[P_{i,tr,\delta}-P_{(i,success,\delta|\varphi)}]T_C}$$

Because node i pick up its destination for each transmission randomly, we will have an average throughput of node .

$$Throughput_{i,\delta} = \frac{\sum_{\varphi\in\mathfrak{D}_\delta(i)} throughput_{(i,\delta|\varphi)}}{number\ of\ \mathfrak{D}_\delta(i)} \tag{4-25}$$

Now we discuss how to determine the successful transmission probability $P_{(i,success,\delta|\varphi)}$ according to D-MAC protocols. D-MAC propose several ways to transmit RTS/CTS.

A. Sending RTS/CTS directionally while transmitting antenna elements are not used as receive antenna element

If the transmitting antenna elements are not used as receiving antenna elements and they send and receive RTS/CTS frame directionally and Rx/Tx are able to transmit simultaneously, then the successful transmission at node i takes place when nodes of set $\mathfrak{W}_{\delta}(\varphi|i)$ does not transmit,

$$P_{(i,success,\delta|\varphi)} = \tau_{i,\delta} \prod_{\beta\neq\delta} \left(1-\tau_{i,\beta}\right) \prod_{u\in\mathfrak{W}_{\delta}(\varphi|i)} \left(1-\tau_{u,\delta}\right) \quad (4\text{-}26)$$

B. Sending RTS/CTS directionally while transmitting antenna elements are used as receive antenna element

If the transmitting antenna elements are used as receiving antenna elements and they send and receive RTS/CTS frame directionally but are not able to transmit or receive simultaneously, then the successful transmission at Node i takes place when nodes in set $\mathfrak{W}_{\delta}(\varphi|i)$ does not transmit, and receiving antenna element of destination should not transmit.

$$P_{(i,success,\delta|\varphi)} = \tau_{i,\delta}\left(1-\tau_{destination,receiv\ direction}\right) \prod_{\beta\neq\delta} \left(1-\tau_{i,\beta}\right) \prod_{u\ \mathfrak{W}_{\delta}(\varphi|i)} \left(1-\tau_{u,\delta}\right) \quad (4\text{-}27)$$

The difference among the performances Case A and Case B is $\left(1-\tau_{destination,receiv\ direction}\right)$. The later numerical results will show $\tau_{destination,receiv\ direction}$ is very small. (0-0.056). so, not to build independent receive antenna element is good choice for engineering. (Making half-duplex antenna system is cheaper and full- duplex almost does not increase performance. In fact, each of current IEEE 802.11 device is equipped with one half-duplex transceiver. [67])

C. Sending RTS/CTS omni-directionally

Dai and Ng [19] says using omnidirectional RTS/CTS to build up the handshake. It means all other directions cannot transmit successfully during the RTS/CTS period, $T_{rts\ cts}$. We propose a quick deduction to modify our performance.

We know the number of successful transmissions. That means spend time in RTC/STC in node i will be $\sum_{v=0;v\neq i}^{N} \frac{Total\times Throughput_{v,\delta}}{E[lenght\ of\ packet]} \times T_{rts\ cts} + \sum_{\omega=1;\omega\neq\delta}^{N_{tx}} \sum_{v=0;v\neq i}^{N} \frac{Total\times Throughput_{v,\omega}}{E[lenght\ of\ packet]} \times T_{rts\ cts}$, so

$$\widetilde{Throughput}_{i,\delta} = Throughput_{i,\delta}\left[\frac{Total-\sum_{v=0;v\neq i}^{N}\frac{Total\times Throughput_{v,\delta}}{E[lenght\ of\ packet]}\times T_{rts\ cts}-\sum_{\omega=1;\omega\neq\delta}^{N_{tx}}\sum_{v=0;v\neq i}^{N}\frac{Total\times Throughput_{v,\omega}}{E[lenght\ of\ packet]}\times T_{rts\ cts}}{Total}\right] =$$

$$Throughput_{i,\delta}\left[1-\sum_{v=0;v\neq i}^{N}\frac{Throughput_{v,\delta}}{E[lenght\ of\ packet]}\times T_{rts\ cts}-\sum_{\omega=1;\omega\neq\delta}^{N_{tx}}\sum_{v=0;v\neq i}^{N}\frac{Throughput_{v,\omega}}{E[lenght\ of\ packet]}\times T_{rts\ cts}\right] \quad (4\text{-}28)$$

where $\frac{Throughput_{i,\delta}}{E[lenght\ of\ packet]}\times T_{rts\ cts} = \frac{\sum_{\varphi\in\mathfrak{D}_\delta(i)}\frac{throughput_{(i,\delta|\varphi)}}{E[lenght\ of\ packet]}}{number\ of\ \mathfrak{D}_\delta(i)}\times T_{rts\ cts}$. The second term $\sum_{v=0;v\neq i}^{N}\frac{Throughput_{v,\delta}}{E[lenght\ of\ packet]}\times T_{rts\ cts}$ accounts for the occur time of direction δ, the $\sum_{\omega=1;\omega\neq\delta}^{N_{tx}}\sum_{v=0;v\neq i}^{N}\frac{Throughput_{v,\omega}}{E[lenght\ of\ packet]}\times T_{rts\ cts}$ is the spending time of other direction.

4.3.2. Delay of a DMAC wireless network at MAC layer

Similar to previous section 3.2, frame delay is defined as the time interval between the frame's first backoff and its successful transmission if the frame is not dropped. The total frame delay D_δ is divided into three sub-delays: frame access delay ${D_\delta}^{access}(j)$, a successful frame transmission delay ${D_\delta}^{successful}(j)$ and frame propagation delay ${D_\delta}^{propagation}$. A successful frame transmission delay is the time consumed during the successful transmissions, it is equal to T_s, gained from formula (2-30a) and (2-30c). Frame propagation delay is the time spending during propagation.

At first we neglect retransmissions because of error recovery (etc. no acknowledgment frame error), and only focus on performing the backoff procedure and the contention process. we know that the station shall then generate a random backoff period for an additional deferral time before retrying if the medium is determined to be busy. We refer backoff deferral time as expectation of frame access delay.

Let $Backoff_\delta(j)$, $j\in(0,L_\delta)$, the aggregation of backoff counter when transmitting antenna element δ try a transmission attempt during j-th backoff stage for transmitting antenna element δ before a transmission attempt. As it is uniformly distributed in $(0,w_{\delta,j}-1)$, for each stage j, the average of $Backoff_\delta(j)$ can be expressed by $Backoff_\delta(j)=\sum_{v=0}^{j}\frac{w_{\delta,v}-1}{2}$. The $Backoff_\delta(j)$ will be derived as following:

$$E[Backoff_\delta(j)] = \sum_{v=0}^{j} \sum_{k=0}^{w_{\delta,v}-1} \frac{k}{w_{\delta,v}} = \sum_{v=0}^{j} \frac{w_{\delta,v}-1}{2}. \quad (4\text{-}29)$$

Because stage j may be a random value from $j = 0$ to $j = L_\delta$ while performing a backoff procedure and having a successful transmission, we need to an expectation of the aggregation of $Backoff_\delta(j)$. It should be $E[Backoff_\delta(j)]$

$$D_\delta{}^{access} = slottime \times E[Backoff_\delta(j)] = solttime \times \sum_{j=0}^{L_\delta} \left[(\bar{p}_\delta)^j \sum_{v=0}^{j} \frac{w_{\delta,v}-1}{2} \right] \quad (4\text{-}30)$$

$(\bar{p}_\delta)^j$is the probability that a node retry backoff j^{th} times because the medium is determined to be busy. $\bar{p}_\delta$ is an average channel busy probability that a node senses channel busy.

$$D_\delta = D_\delta{}^{access}(j) + D_\delta{}^{successful}(j) + D_\delta{}^{propagation} = solttime \times \sum_{j=0}^{L_\delta} \left[(\bar{p}_\delta)^j \sum_{v=0}^{j} \frac{w_{\delta,v}-1}{2} \right] + T_s + D_\delta{}^{propagation} \quad (4\text{-}31)$$

Apply to each node,

$$D_{i,\delta} = solttime \sum_{j=0}^{L_{i,\delta}} \left[(\bar{p}_{i,\delta})^j \sum_{v=0}^{j} \frac{w_{i,\delta,v}-1}{2} \right] + T_s + D_{i,\delta}{}^{propagation} \; i \in (1,2,3, \dots \dots, N) \quad (4\text{-}32)$$

Now, if we do not neglect error recovery and assume a packet is transmitted successfully after it is re-transmitted $(N_{retry} - 1)$ times. So we can know it experienced N_{retry} times of backoff procedure and $(N_{retry} - 1)$ times of error. Each error spends an ACK time-out, T_{out}. If ACK error probability is p_{err}. The total expectation of retransmission delay

$$D_\delta = E\left[D_\delta{}^{retrans}(N_{retry})\right] + T_s + D_\delta{}^{propagation}$$

$$= \sum_{r=0}^{N_{retry}} [p_{err}]^r \{T_c(N_{retry} - 1) + N_{retry} E[D_\delta{}^{access}(j)]\} + T_s + D_\delta{}^{propagation} \quad (4\text{-}33)$$

4.4. Numerical results of performance in DMAC networks

To simplify the presentation of the results, we have assumed that all data packets have the same lengths (1024 bytes) and each packet fits perfectly into one Transmit Opportunity. We have IEEE 802.11 default parameters here: MAC header=272bits; PHY header=192 bits (including preamble

144bits and PLCP header 48 bits); ACK length=112bit + PHY header; RTS length=160bit + PHY header; CTS length=112bit + PHY header; other parameters are summarized in Table 3-2.

We choose the same parameters from IEEE 802.11b for each transmitting antenna element in our numerical calculations. That means we have slot time=20 μs; SIFS= 10 μs; DIFS=50 μs; L=5; M=5; $w_0 = 31$. The channel data rate is 11 Mbits/s. We set nodes be within one-hop and their positions are listed in Table 3. Using (2-21a-d), we will have $T_{C,bas} = 835.2\,\mu s$, $T_{S,bas} = 871.15\,\mu s$; $T_{C,rts} = 80.3\,\mu s$, $T_{S,rts} = 947.4\,\mu s$.

Table 4-2: Nodes' locations of a 64-node wireless network

(-86.8m,49.3m); (-7.8m,74.3m); (102.2m,5.4m); (53.8m,64.2m); (20.7m,26.5m); (206.2m,10.6m); (-176.2m,5.2m); (-52.1m,-16.4m); (-0.2m,-36.7m); (54.7m,-24.1m); (116.1m,-57.6m); (135.3m,44.1m); (165.4m,-34.2m); (258.8m,31.6m); (306.1m,-22.8m); (-154.8m,-32.3m); (-79.4m,-73.2m); (-12.5m,-135.9m); (-26.8m,-77.1m); (64.6m,-140.4m); (102.7m,-108.8m); (118.2m,-156.3m); (174.2m,-83.6m); (155.9m,-124.7m); (221.1m,-97.3m); (221.6m,-165.9m); (281.2m,-110.6m); (-141.1m,-164.0m); (-95.7m,-121.0m); (-73.9m,-168.1m); (29.1m,-111.8m); (-14.6m,-199.0m); (-126.8m,139.3m); (-17.8m,174.3m); (122.4m,85.4m); (53.2m,164.2m); (220.2m,226.5m); (216.2m,199.6m); (-178.2m,59.2m); (-59.1m,-196.4m); (-9.2m,-156.7m); (59.7m,-134.1m); (196.1m,-59.6m); (195.3m,49.1m); (195.4m,-39.2m); (298.8m,39.6m); (126.1m,-29.8m); (-194.8m,-39.3m); (-179.4m,-79.2m); (-19.5m,-195.9m); (-99.8m,-177.1m); (69.6m,-140.4m); (192.7m,-188.8m); (198.2m,-169.3m); (194.2m,-89.6m); (195.9m,-194.7m); (291.1m,-397.3m); (292.0m,-115.9m); (291.2m,-190.6m); (-191.1m,-194.0m); (-120.7m,-191.0m); (-183.9m,-198.1m); (9.1m,-119.8m); (-4.6m,-191.2m);

Using equations (4-21a-d) with numerical solution techniques, we obtain the node capacities for the basic access mechanism and for the RTS/CTS access mechanism. We also obtain the delay of each node. We calculate the numerical values for each node in the 64-node wireless network. Nodes have transmitting antenna element from $N_{tx} = 1$ to $N_{tx} = 8$, $i \in (1,2,3,\ldots\ldots,64)$. As an example, $N_{tx} = 3$, $N = 64$, $i \in (1,2,3,\ldots\ldots,64)$, $\delta \in (1,2,3)$, the probability, $\bar{p}_{i,\delta}$, that a node senses the channel is used by other node's transmitting antenna element δ, can be written as follows,

$\bar{p}_{1,x} = 1 - \prod_{u \in \mathfrak{S}_x(1)}(1 - \tau_{u,x})$

$\bar{p}_{2,x} = 1 - \prod_{u \in \mathfrak{S}_x(2)}(1 - \tau_{u,x})$

.....

$\bar{p}_{64,x} = 1 - \prod_{u \in \mathfrak{S}_x(64)}(1 - \tau_{u,x})$

where the sets of completing neighbors

$\mathfrak{S}_x(1) = \{7,8,16,17,18,19,28,29,30,32,40,41,48,49,50,51,60,61,62,63,64\}$

$\mathfrak{S}_x(2) = \{1,7,8,9,16,17,18,19,20,22,28,29,30,31,32,39, 40,41,42,48,49,50,51,52,60,61,62,63,64\}$

.....

$\mathfrak{S}_x(64) = \{32,40,50,60,62\}$, obtained with a Matlab program,

First, we have the distribution in the 64-node networks and each node's contention nodes in direction x, y and z. They are depicted in Figures 4-5, 4-6,4-7.

Second, we have the transmission probability of each node in every direction, depicted in Figures 4-8, 4-9.

Third, we have the average throughput of each node in every direction, for basic access mechanism and RTC/CTS access mechanism. They depicted in Figures 4-10, 4-11.

Fourth, we have the delay of each node in direction x, y and z in a 64-nodes network, Figures 4-14, 4-15.

Fifth, the results of average throughput of each node, when the number of transmitting antenna elements, $N_{tx} = 2\ or\ 4,5,6,7,8$, are shown in from Figure 4-22 to Figure 4-27 (for RTS/CTS access mechanism) and in from Figure 4-28 to Figure 4-33 (for basic access mechanism). The results of transmission probability at each node, $N_{tx} = 2\ or\ 4,5,6,7,8$, are shown in from Figure 4-16 to Figure 4-21.

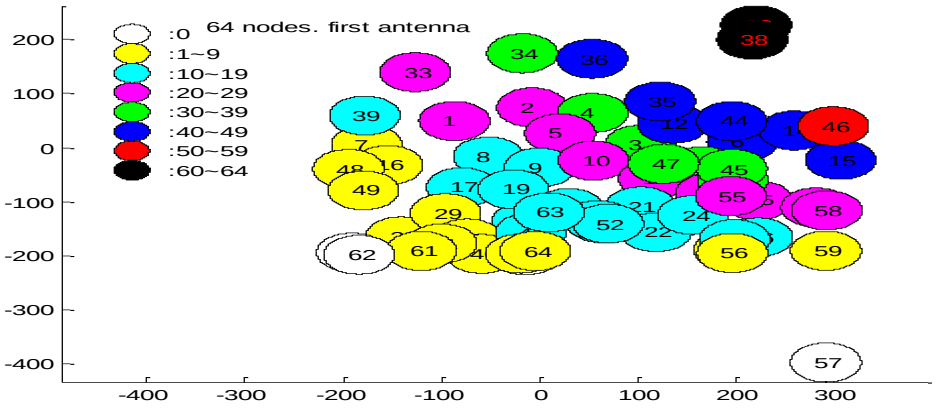

Figure 4-5: Each node's contention nodes in direction x

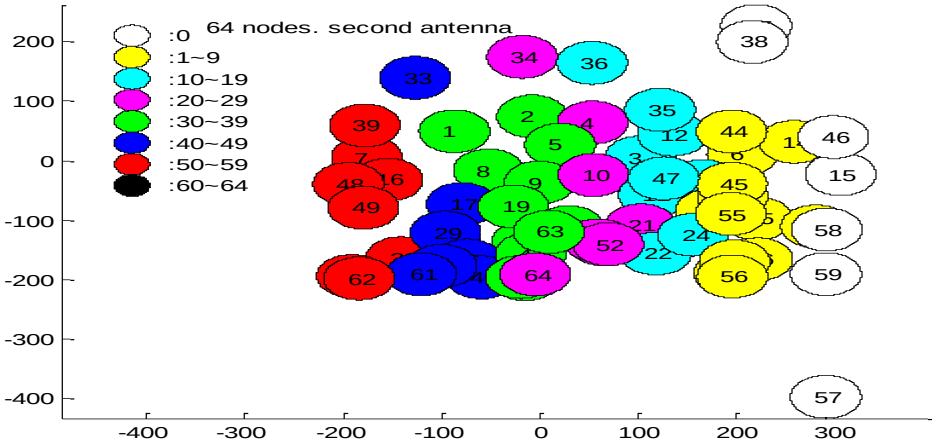

Figure 4-6: Each node's contention nodes in direction y

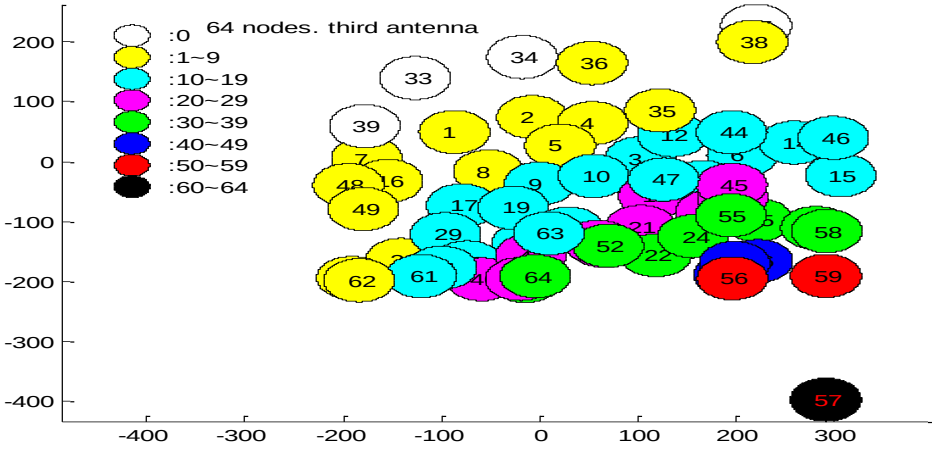

Figure 4-7: Each node's contention nodes in direction z

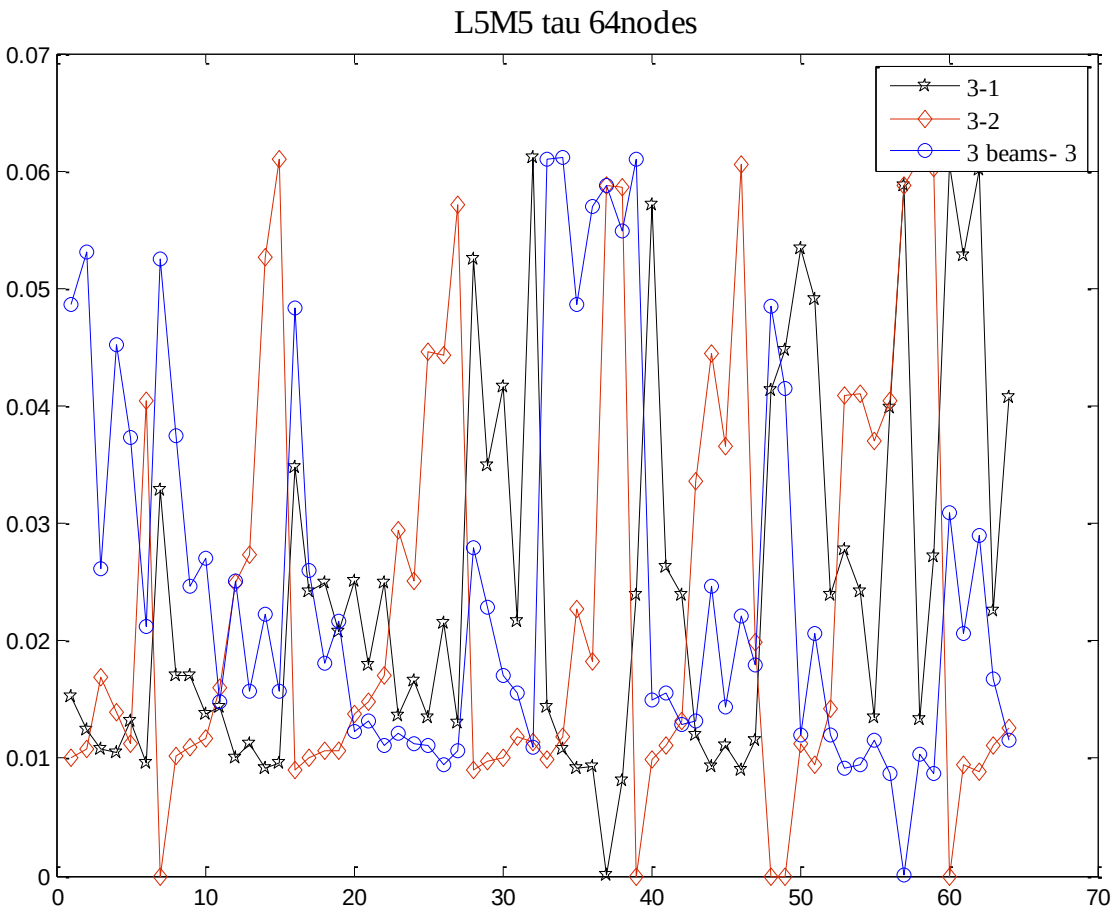

Figure 4-8: Transmission probability, τ_δ in direction x, y and z in a 64-nodes network

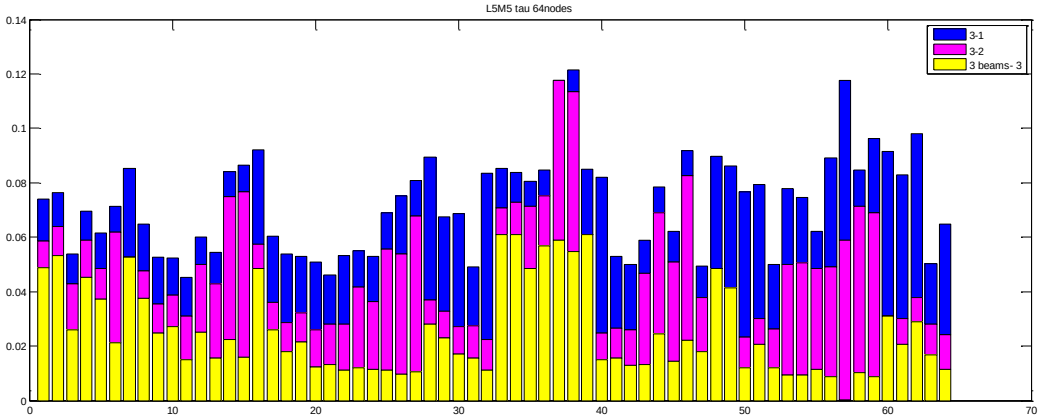

Figure 4-9: Transmission probability, τ_δ in direction x, y and z in a 64-nodes network

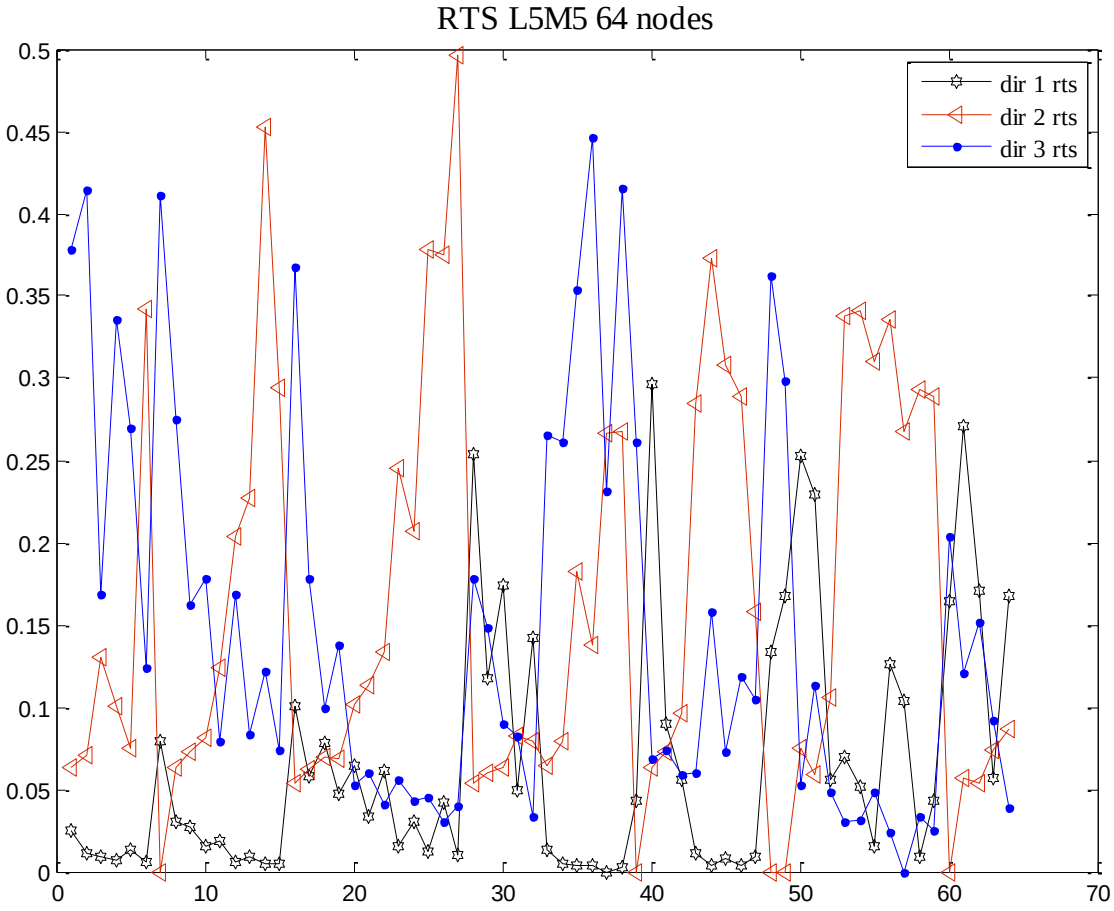

Figure 4-10: Average throughput(RTS/CTS), Throughput_(i,δ) in direction x, y and z in a 64-nodes network

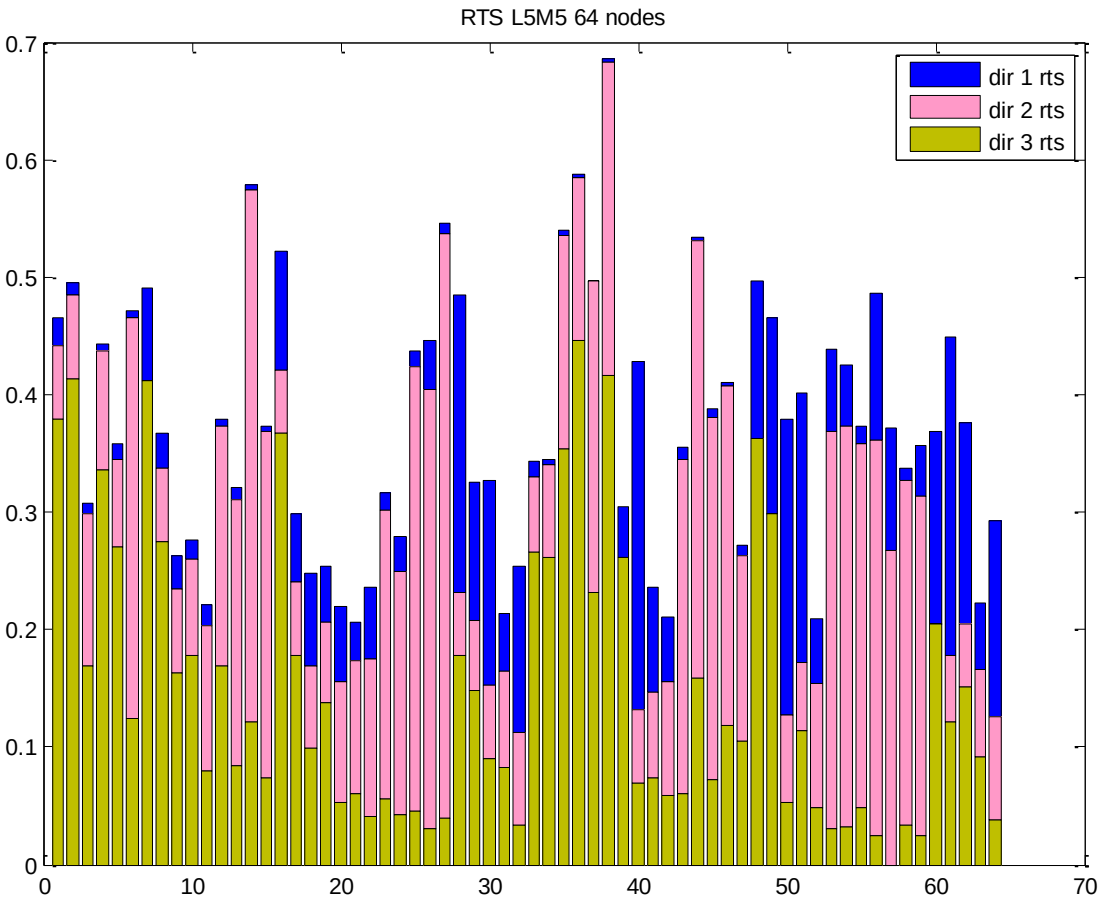

Figure 4-11: Average throughput(RTS/CTS), Throughput_(i,δ) in direction x, y and z in a 64-nodes network

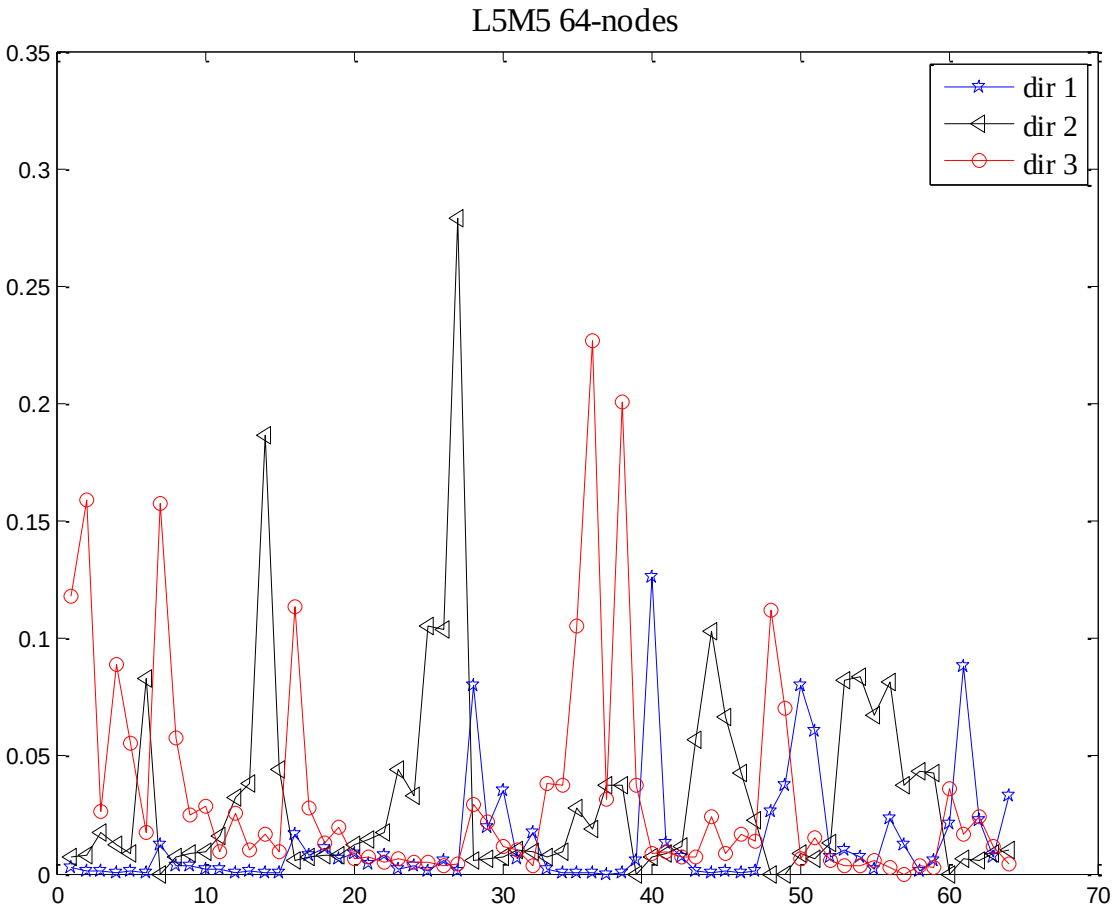

Figure 4-12: Average throughput(basic), Throughput_(i,δ) in direction x, y and z in a 64-nodes network

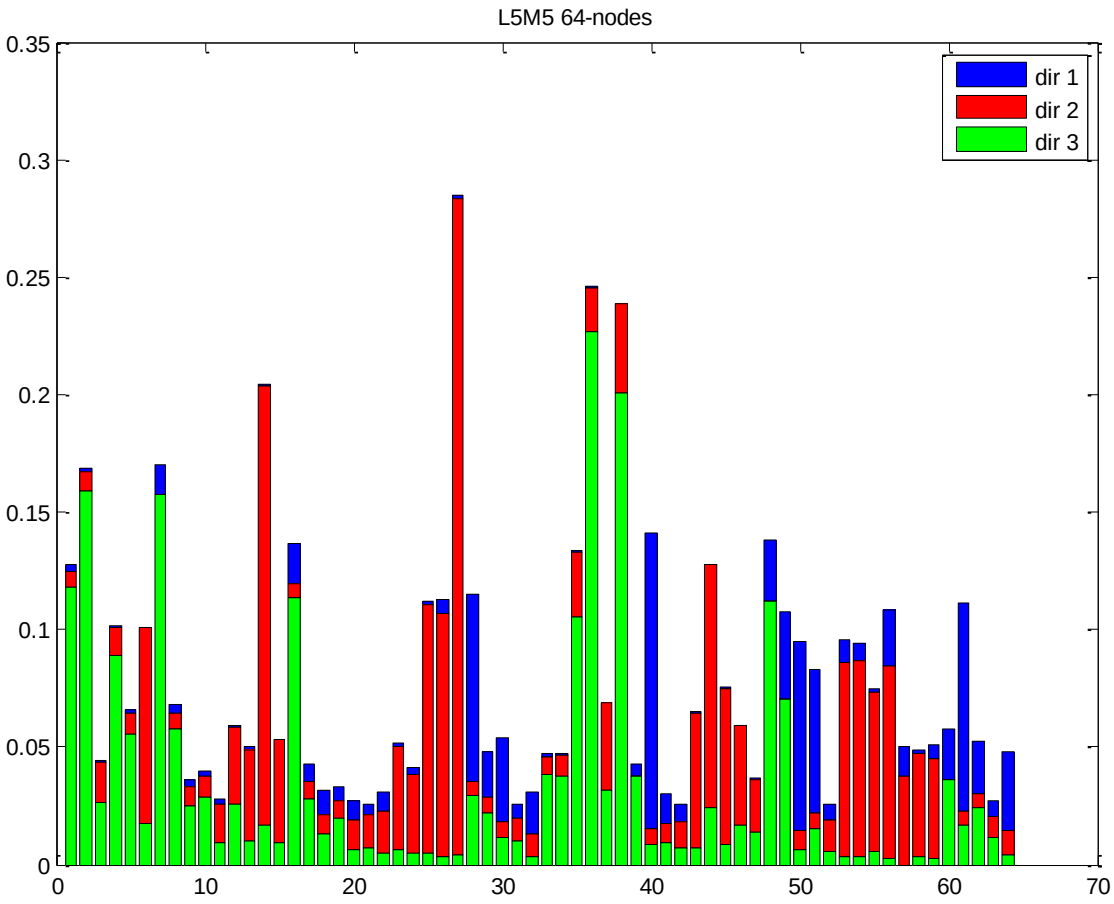

Figure 4-13: Average throughput(basic), Throughput_(i,δ) in direction x, y and z in a 64-nodes network

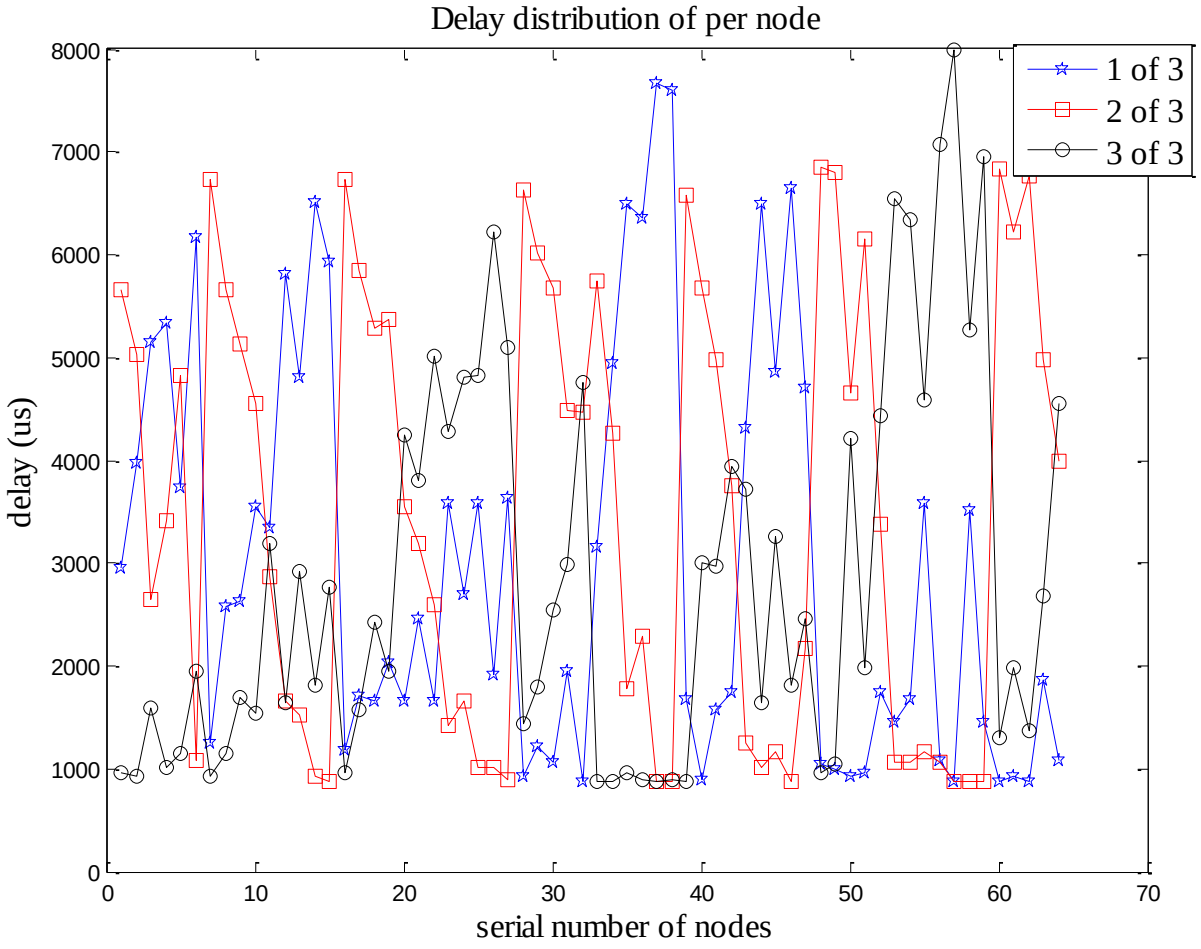

Figure 4-14:Average delay distribution of wireless network

So far, we have the numerical results from $N_{tx} = 1$ to $N_{tx} = 8$. It is useful to evaluate them when increase the N_{tx}. The average of direction aggregation transmission probability of per node and single direction average transmission probability of per node are shown in Figure 4-34. We notice that the single direction average transmission probability of per node almost does not change noticeably. They are 0.020157, 0.024208, 0.027249, 0.028939, 0.029541, 0.03034 and 0.029838.

Average throughput of per Node (RTS/CTS and basic access mechanism) is depicted in Figure 4-35. There are four scenarios, 32-node, 48-node, 56-node and 64-node wireless networks. RTS access mechanism has higher normalized throughput than Basic access mechanism. (since the ratio of the

average time for a successful transmission in RTS/CTS access mechanism to the average time duration for the collision is larger than the ratio in basic access mechanism, or $\frac{T_{s,rts}}{T_{C,rts}}$ is larger than $\frac{T_{s,bas}}{T_{C,bas}}$).

Average delay of per node decline which increase the number of transmitting antenna elements, they are in Table 4-3 and Figure 4-36.

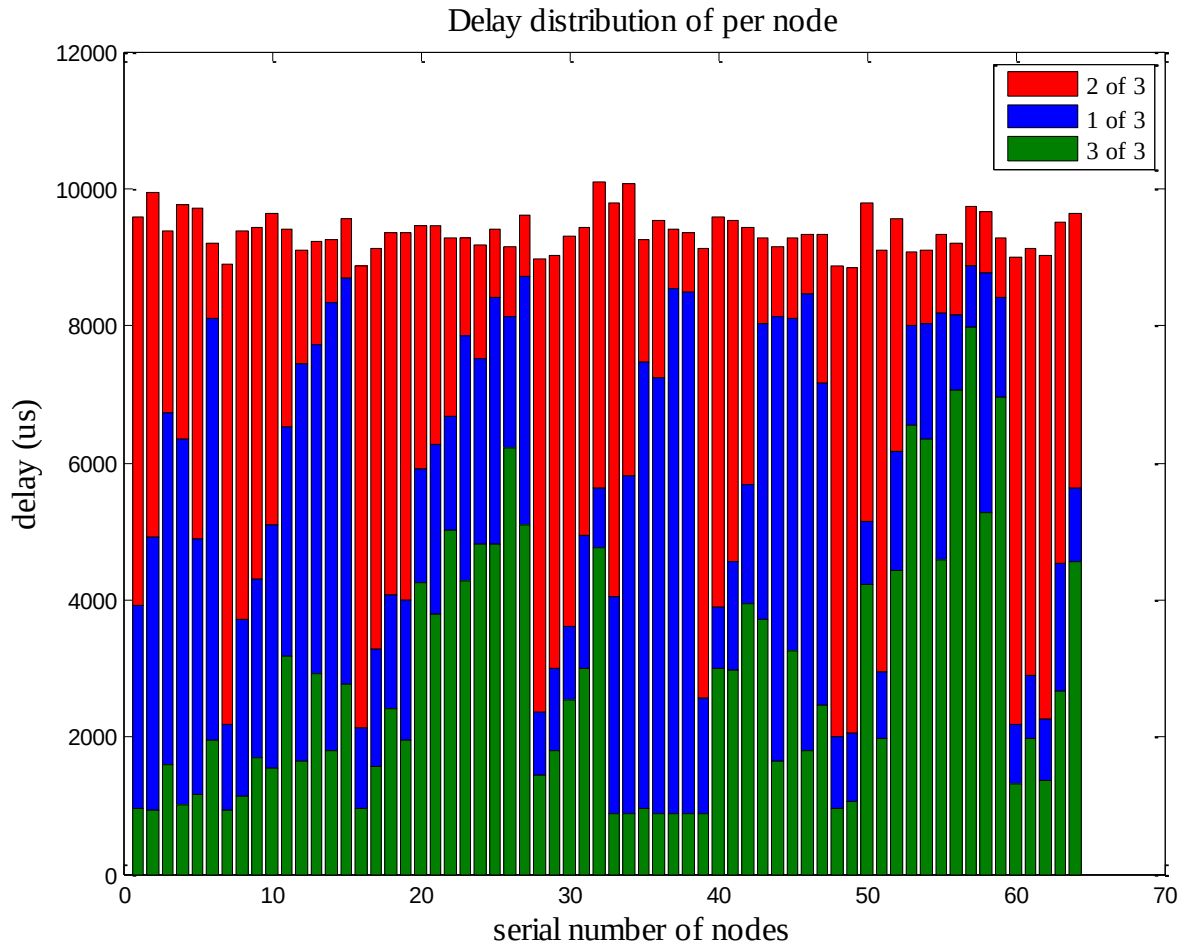

Figure 4-15:Average delay distribution of wireless network

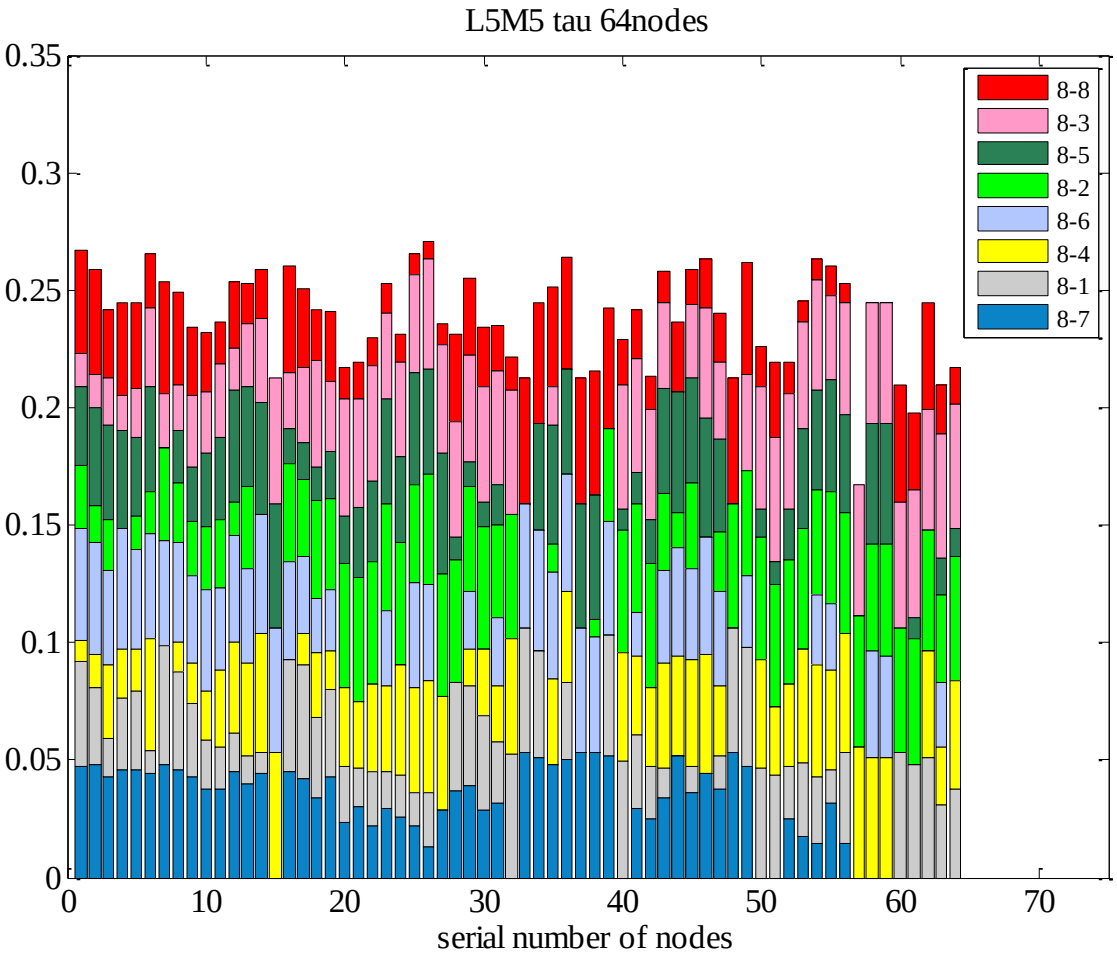

Figure 4-16: Transmission probability, τ_δ ,while N_tx=8 in a 64-nodes network

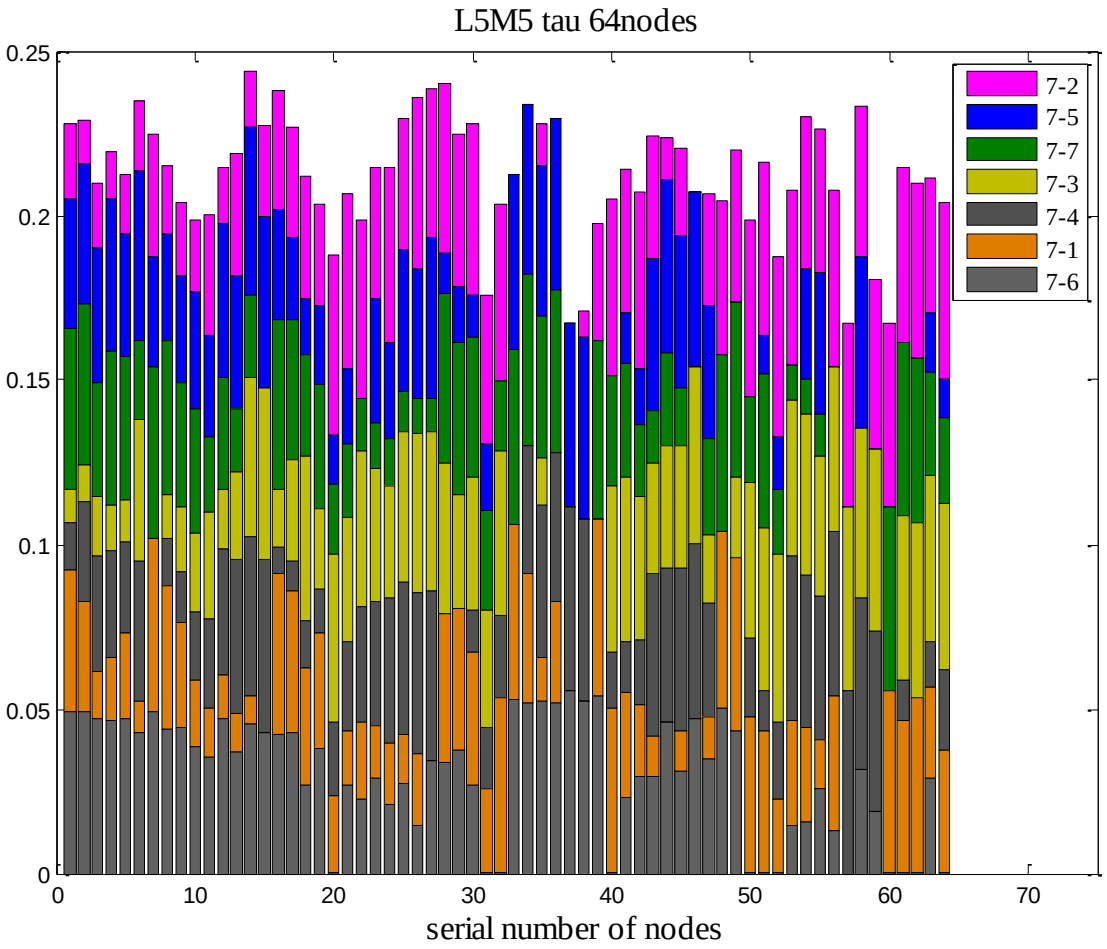

Figure 4-17: Transmission probability, τ_δ ,while N_tx=7 in a 64-nodes network

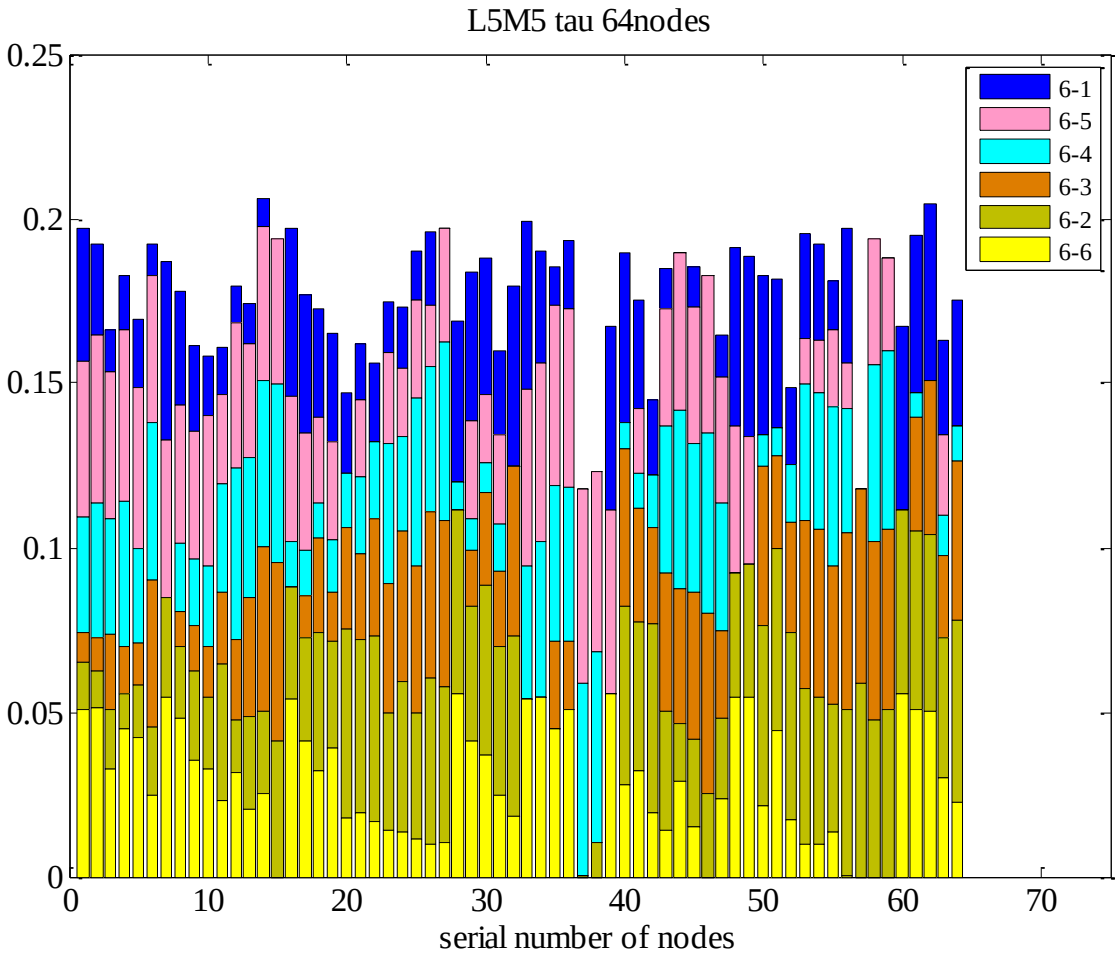

Figure 4-18: Transmission probability, τ_δ ,while N_tx=6 in a 64-nodes network

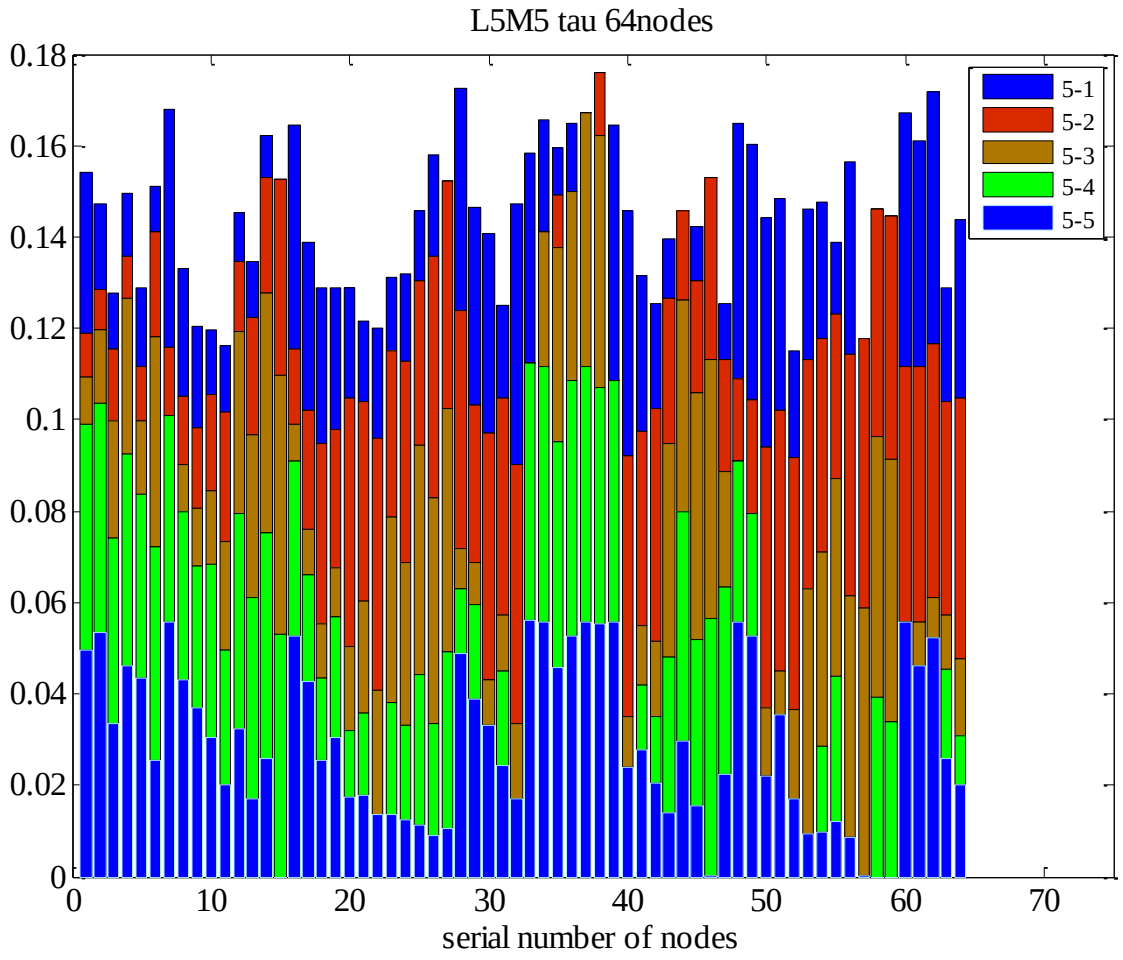

Figure 4-19: Transmission probability, τ_δ ,while N_tx=5 in a 64-nodes network

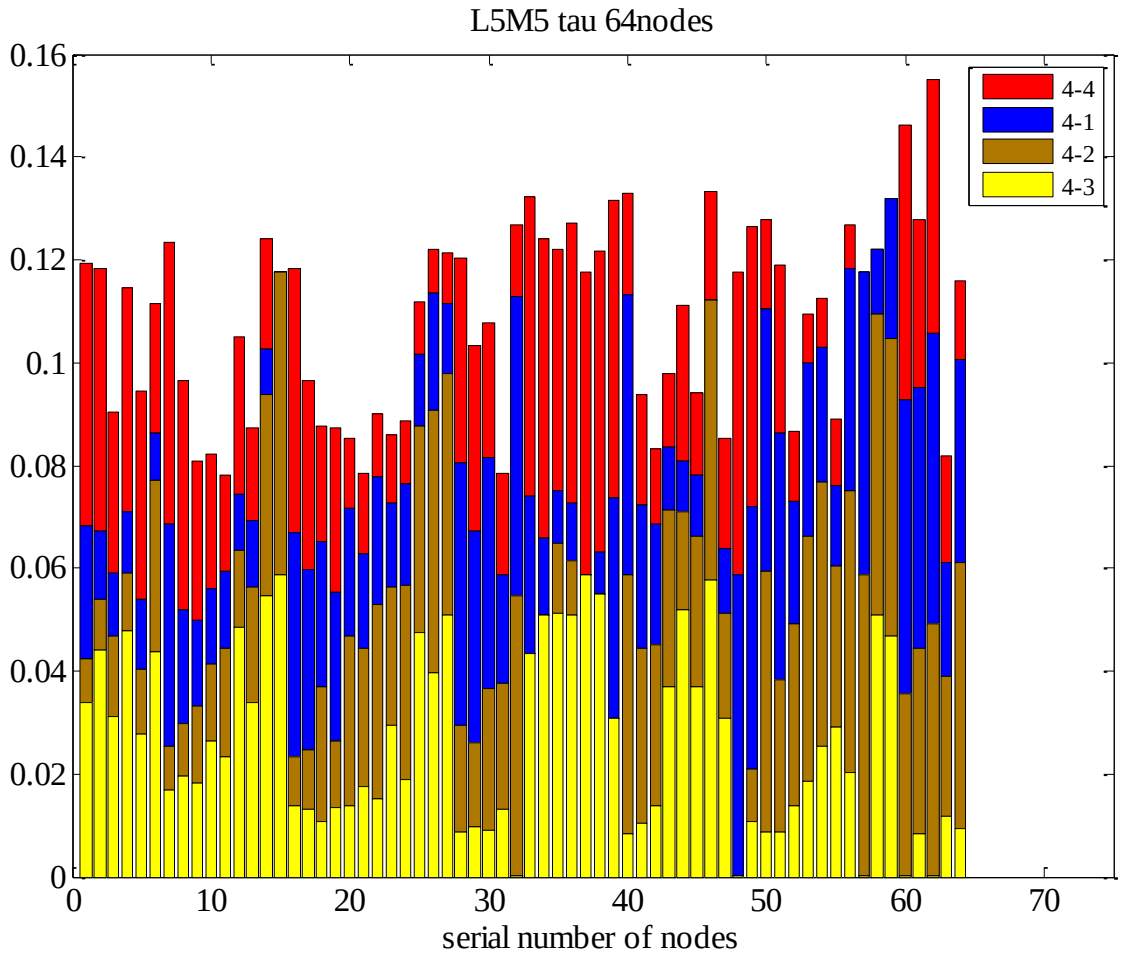

Figure 4-20: Transmission probability, τ_δ ,while N_tx=4 in a 64-nodes network

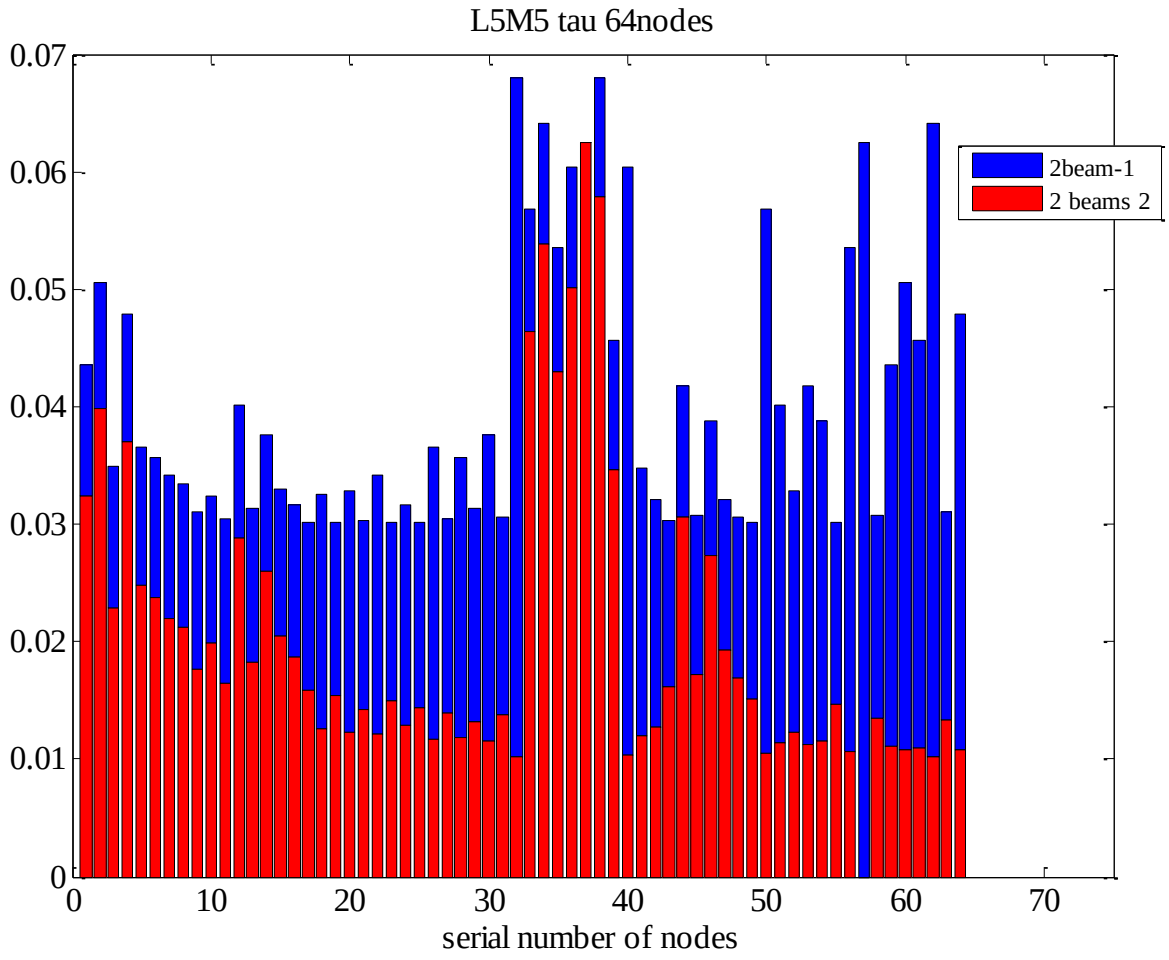

Figure 4-21: Transmission probability, τ_δ ,while N_tx=2 in a 64-nodes network

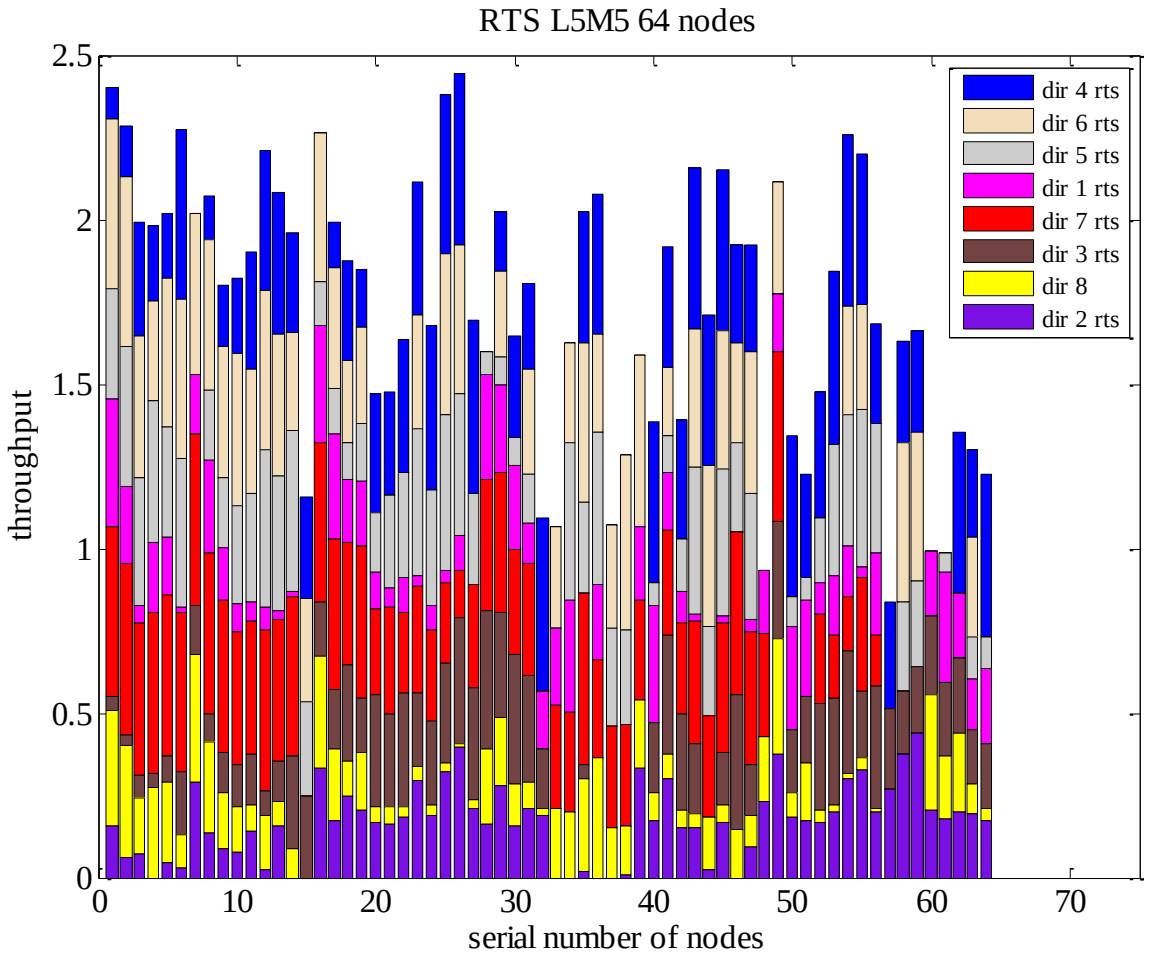

Figure 4-22: Average throughput(RTS/CTS), Throughput_(i,δ) , while N_tx=8 in a 64-nodes network

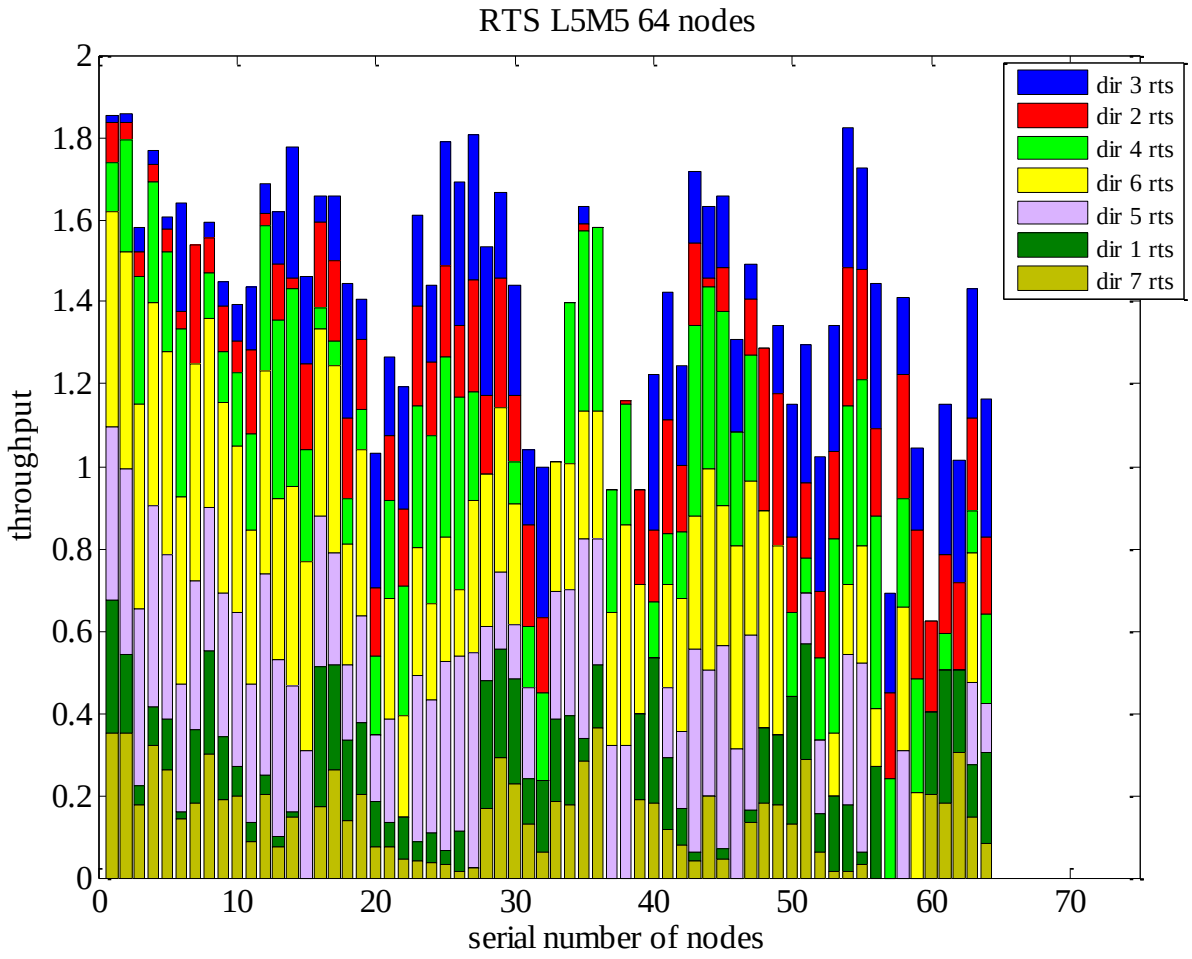

Figure 4-23: Average throughput(RTS/CTS), Throughput_(i,δ) , while N_tx=7 in a 64-nodes network

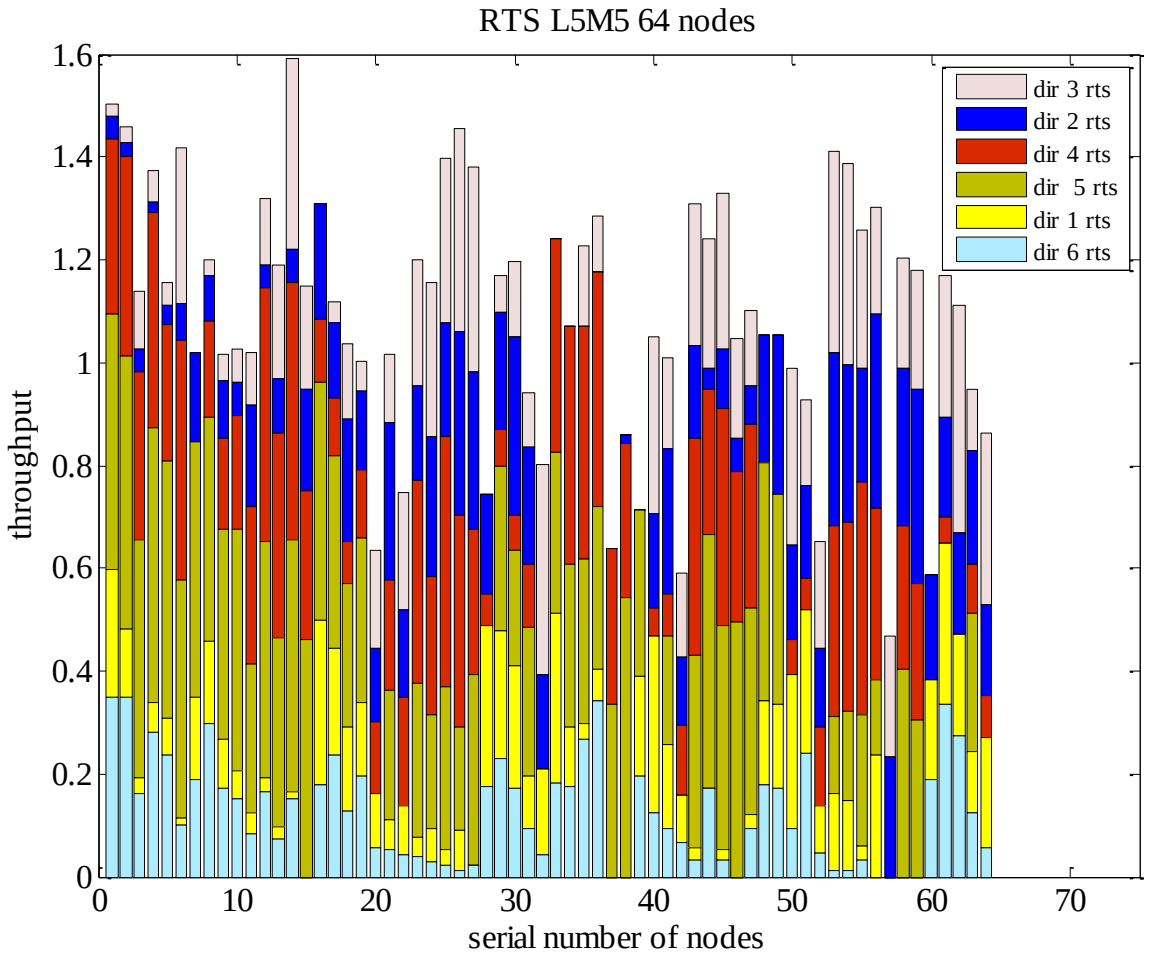

Figure 4-24: Average throughput(RTS/CTS), Throughput_(i,δ) , while N_tx=6 in a 64-nodes network

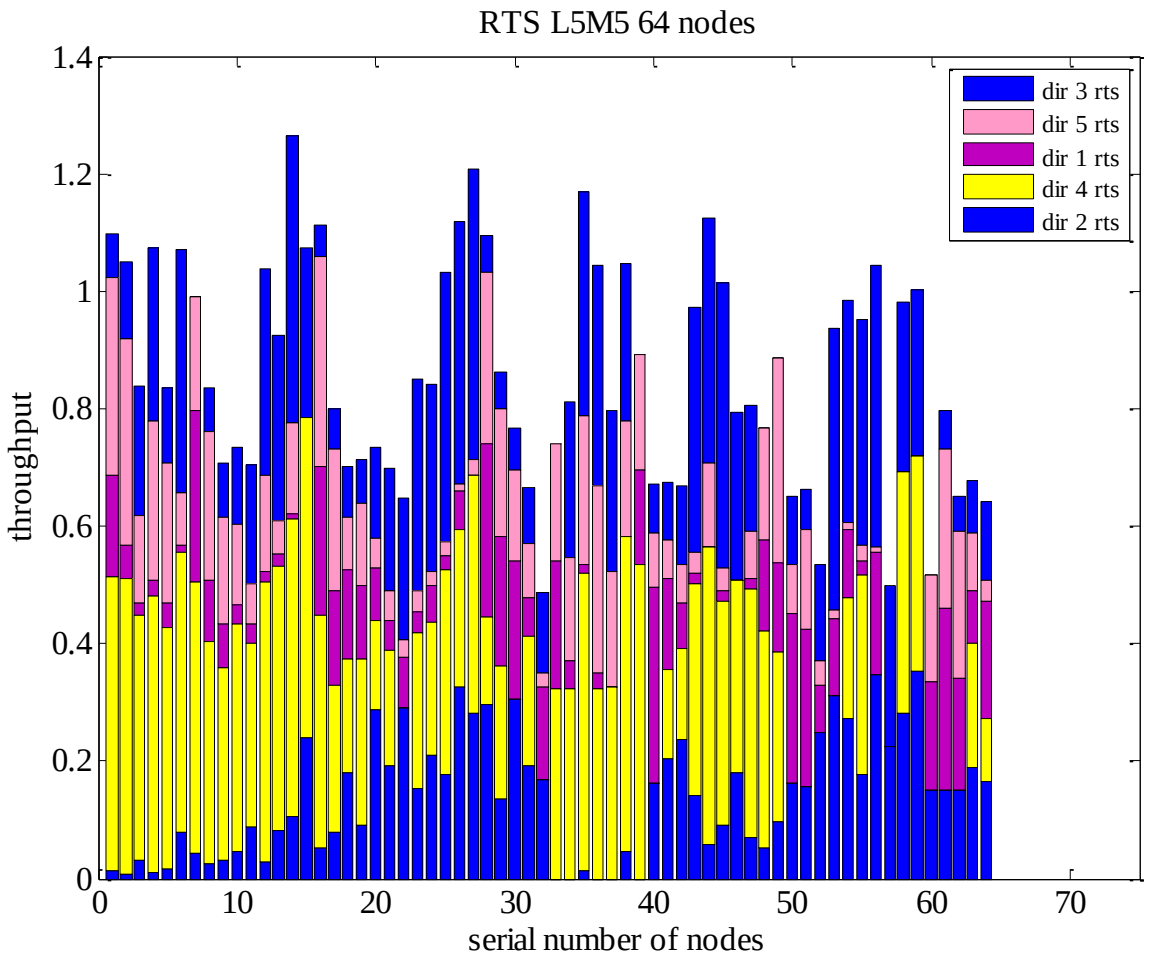

Figure 4-25: Average throughput(RTS/CTS), Throughput_(i,δ) , while N_tx=5 in a 64-nodes network

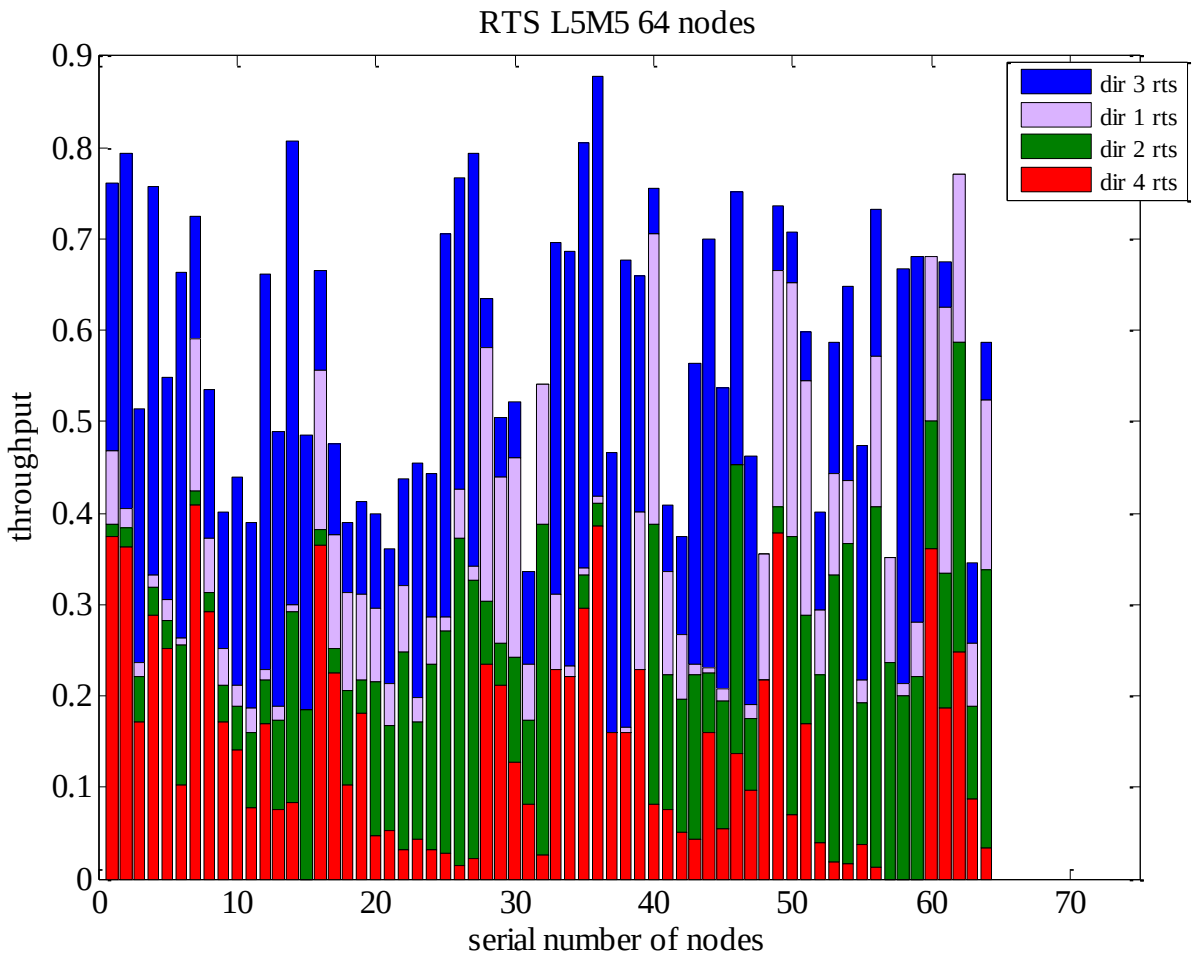

Figure 4-26: Average throughput(RTS/CTS), Throughput_(i,δ) , while N_tx=4 in a 64-nodes network

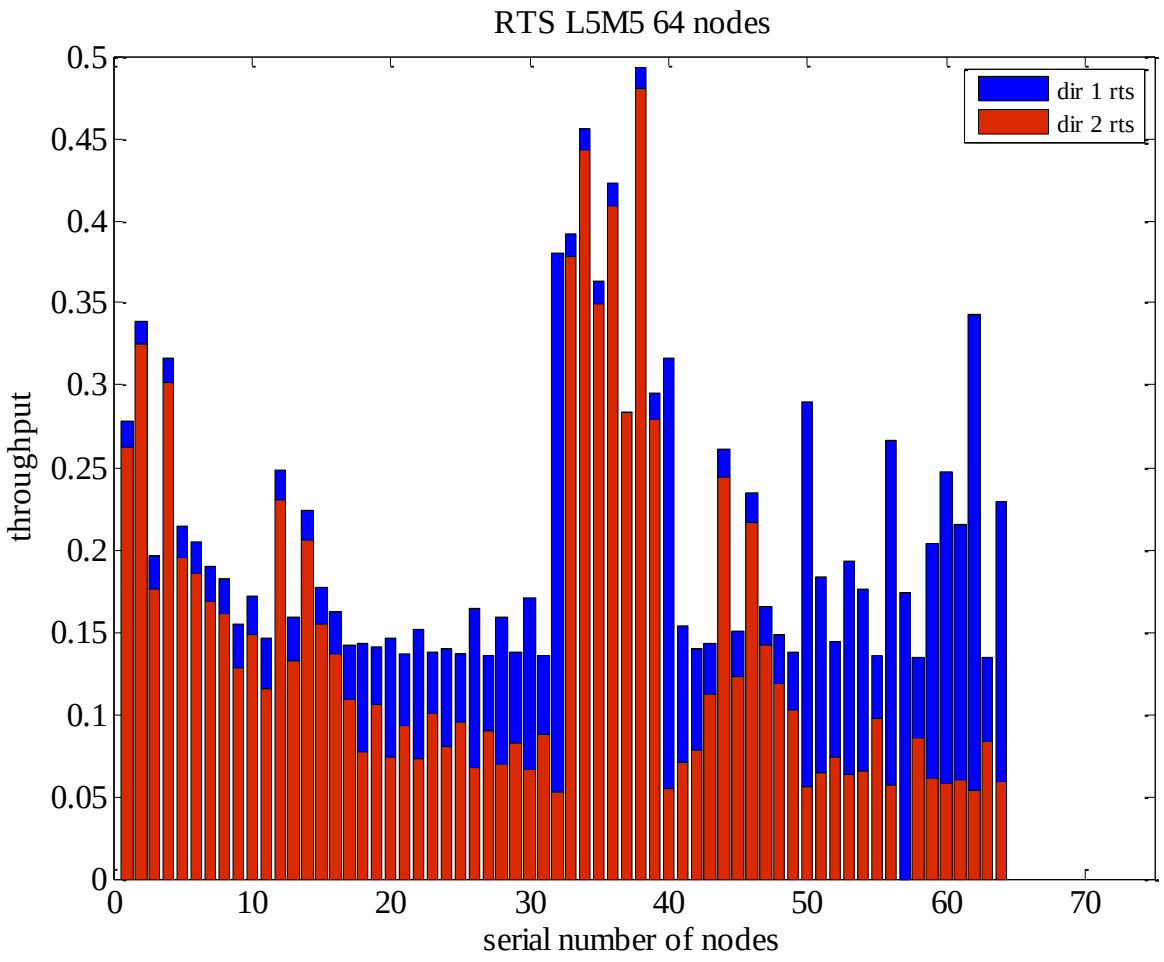

Figure 4-27: Average throughput(RTS/CTS), Throughput_(i,δ) , while N_tx=2 in a 64-nodes network

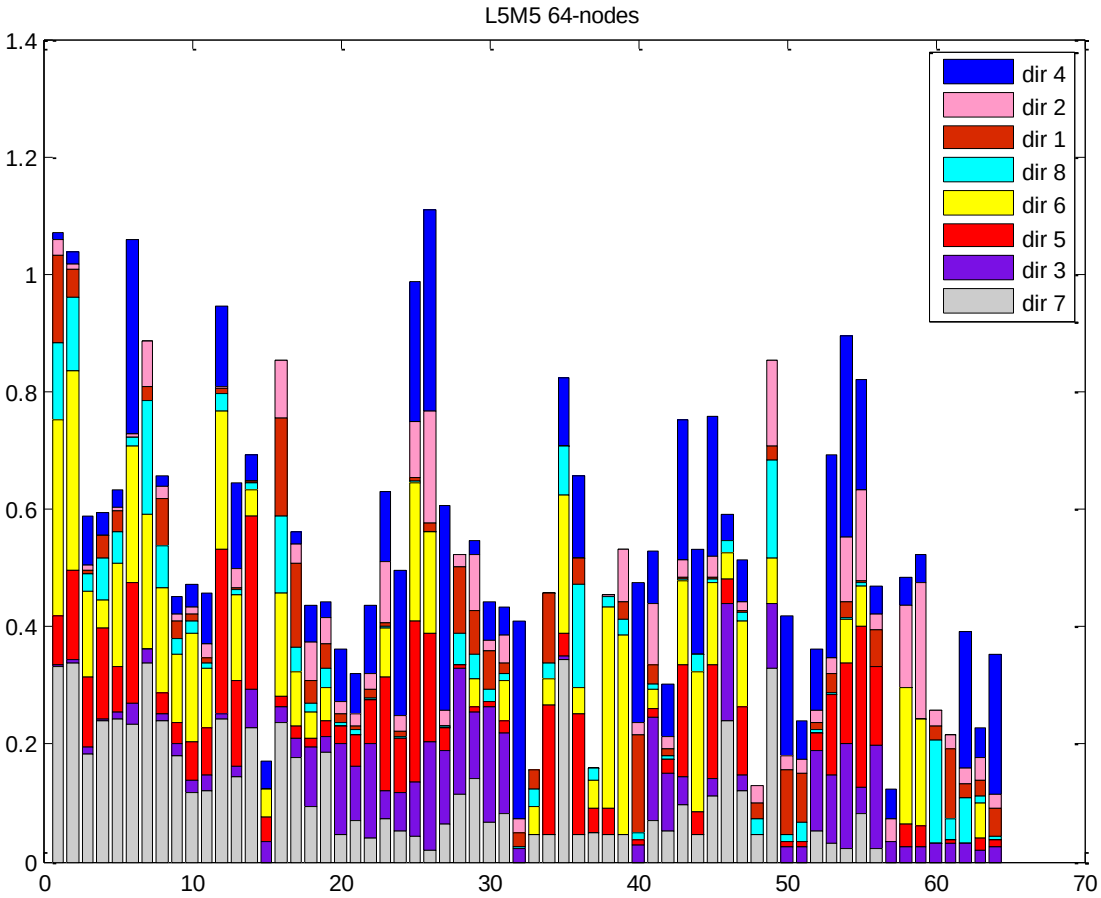

Figure 4-28: Average throughput(basic), Throughput_(i,δ) , while N_tx=8 in a 64-nodes network

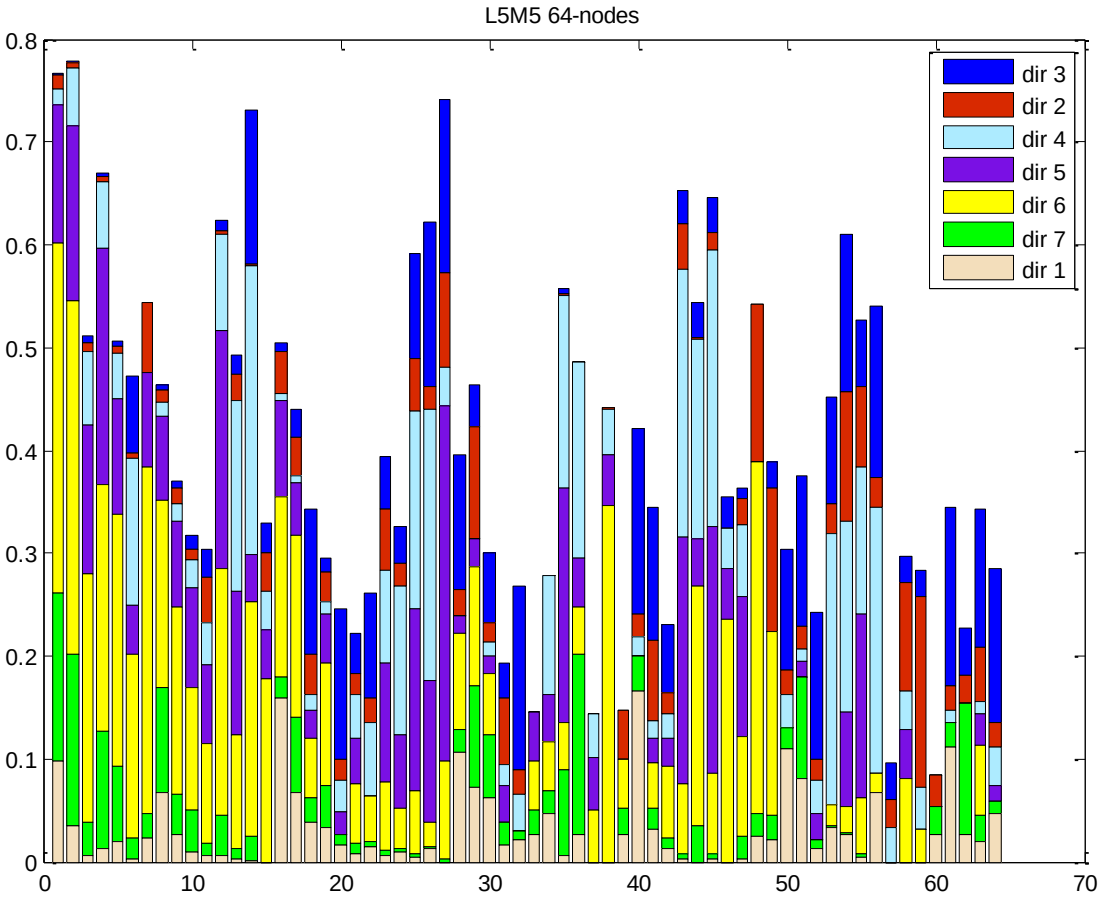

Figure 4-29: Average throughput(basic), Throughput_(i,δ) , while N_tx=7 in a 64-nodes network

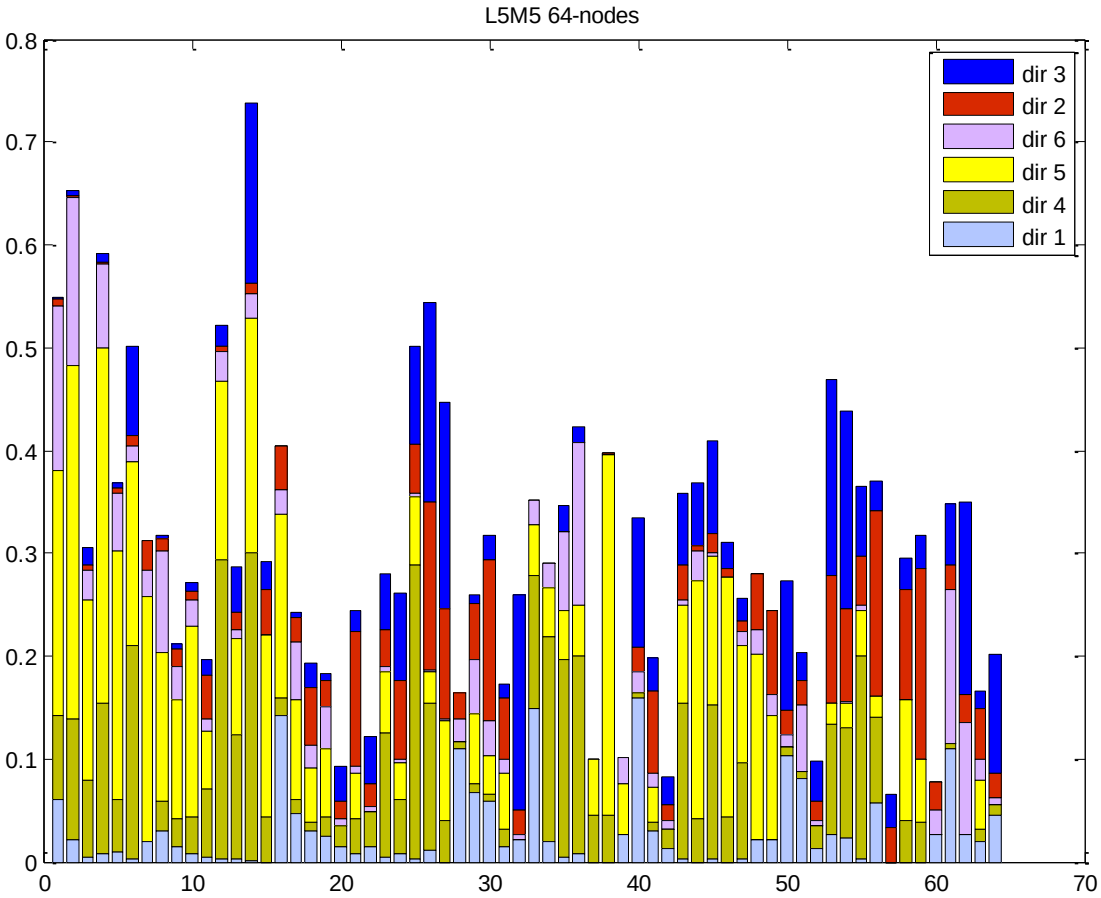

Figure 4-30: Average throughput(basic), Throughput_(i,δ) , while N_tx=6 in a 64-nodes network

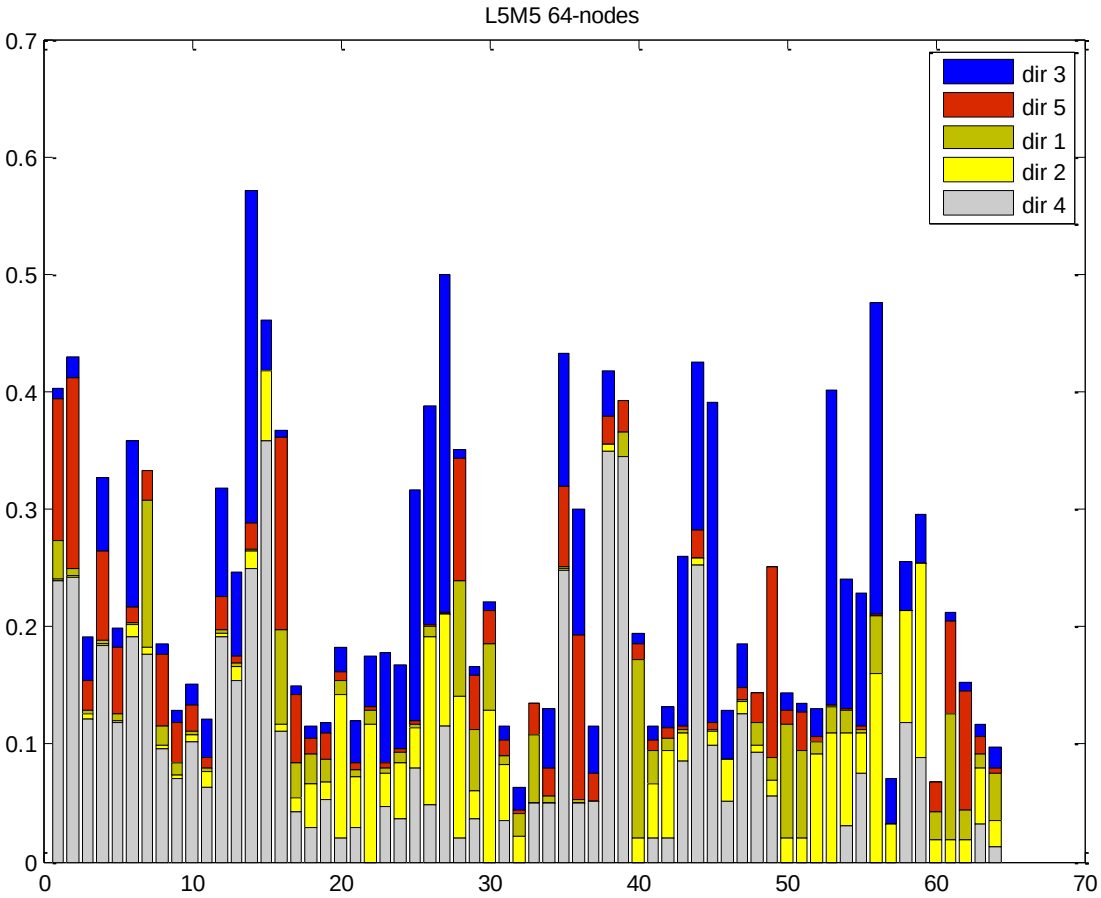

Figure 4-31: Average throughput(basic), Throughput_(i,δ) , while N_tx=5 in a 64-nodes network

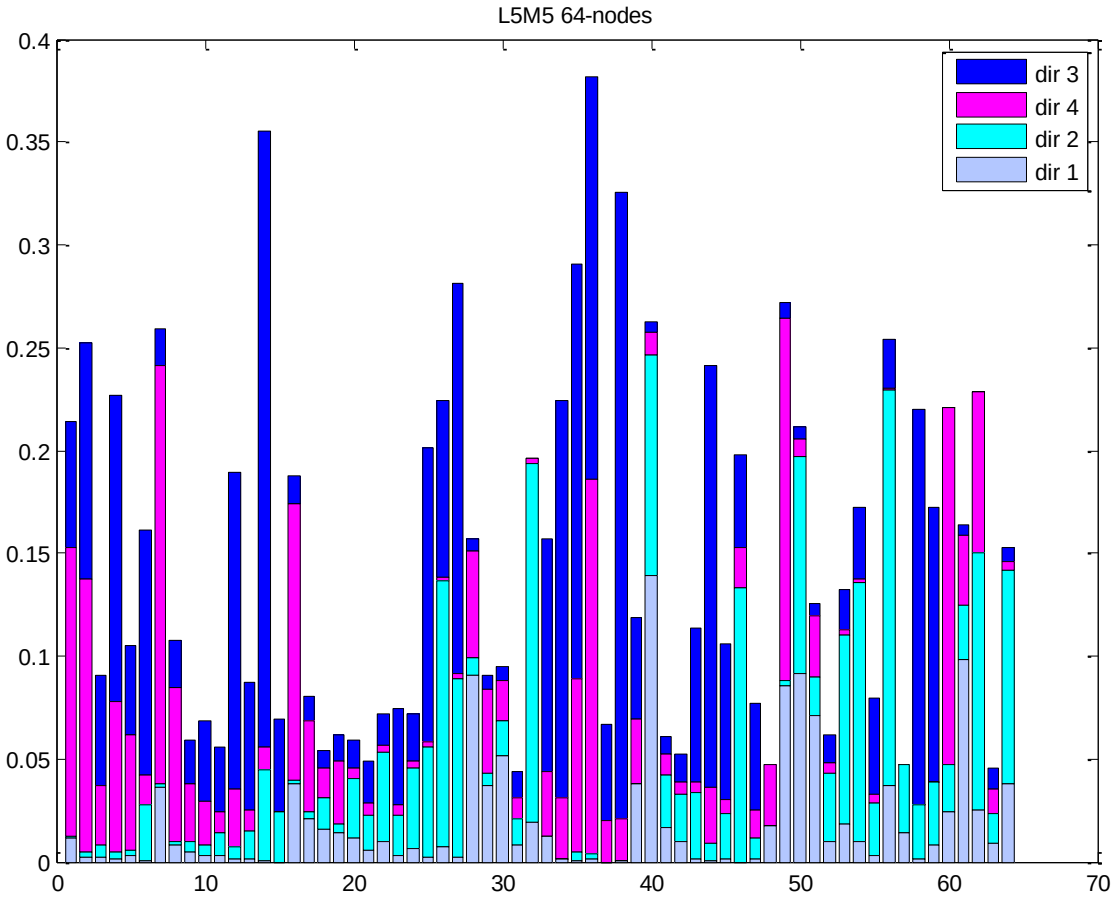

Figure 4-32: Average throughput(basic), Throughput_(i,δ) , while N_tx=4 in a 64-nodes network

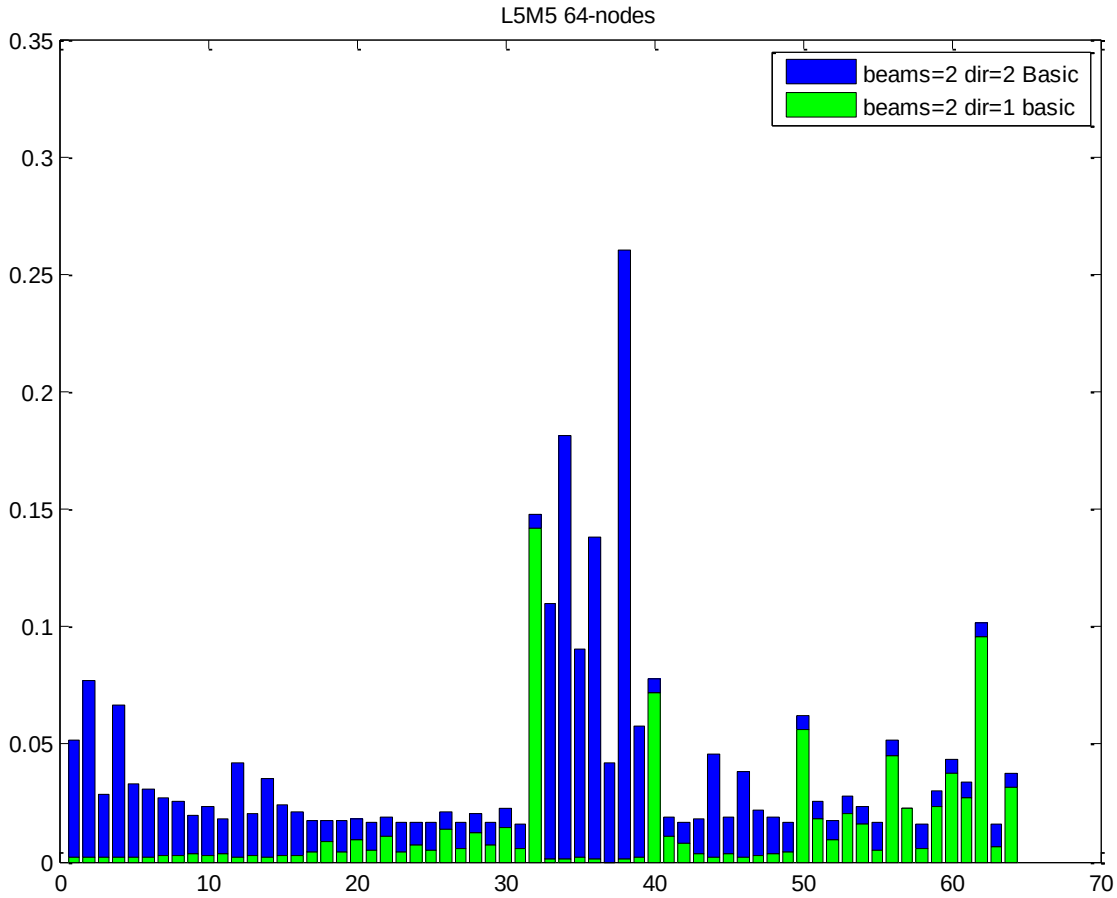

Figure 4-33:Average throughput(basic), Throughput_(i,δ) , while N_tx=2 in a 64-nodes network

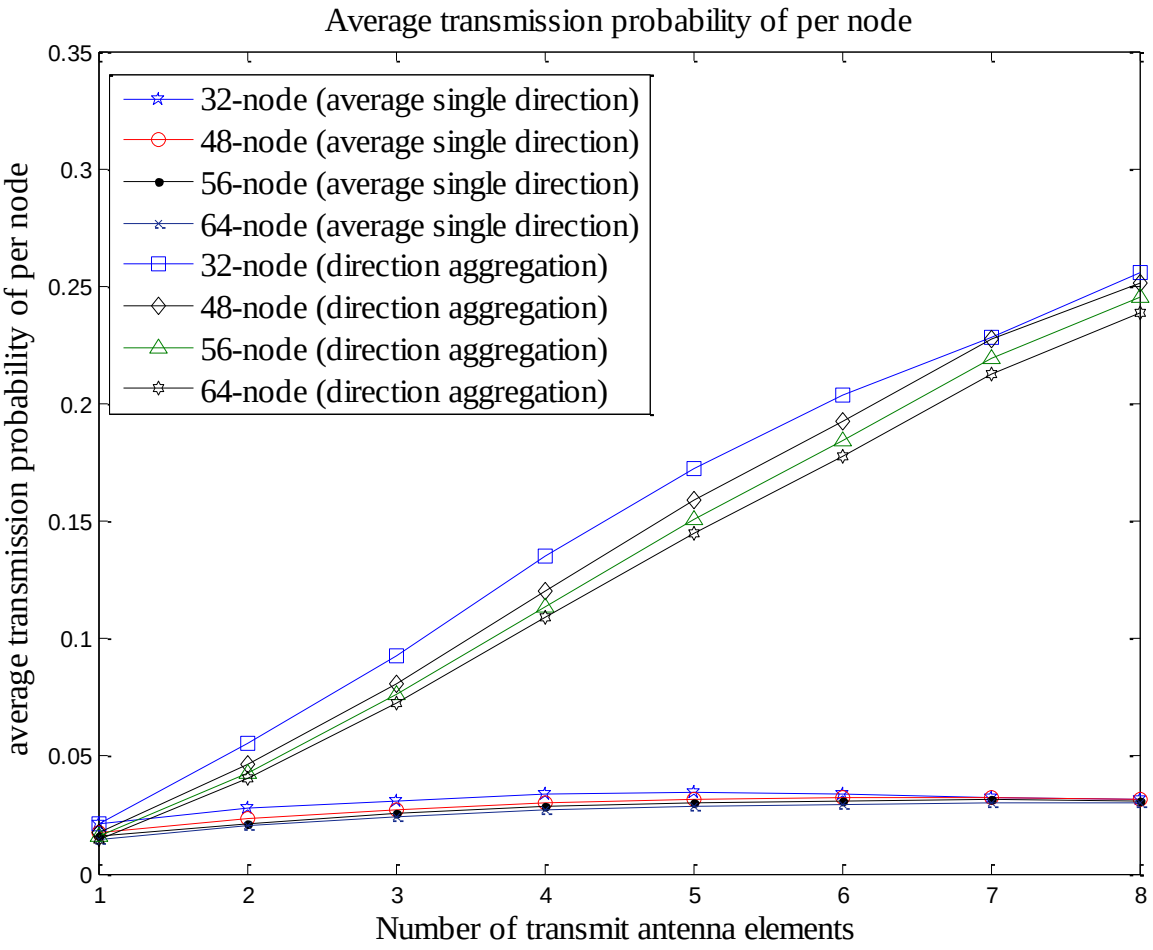

Figure 4-34： Average transmission probability of per node

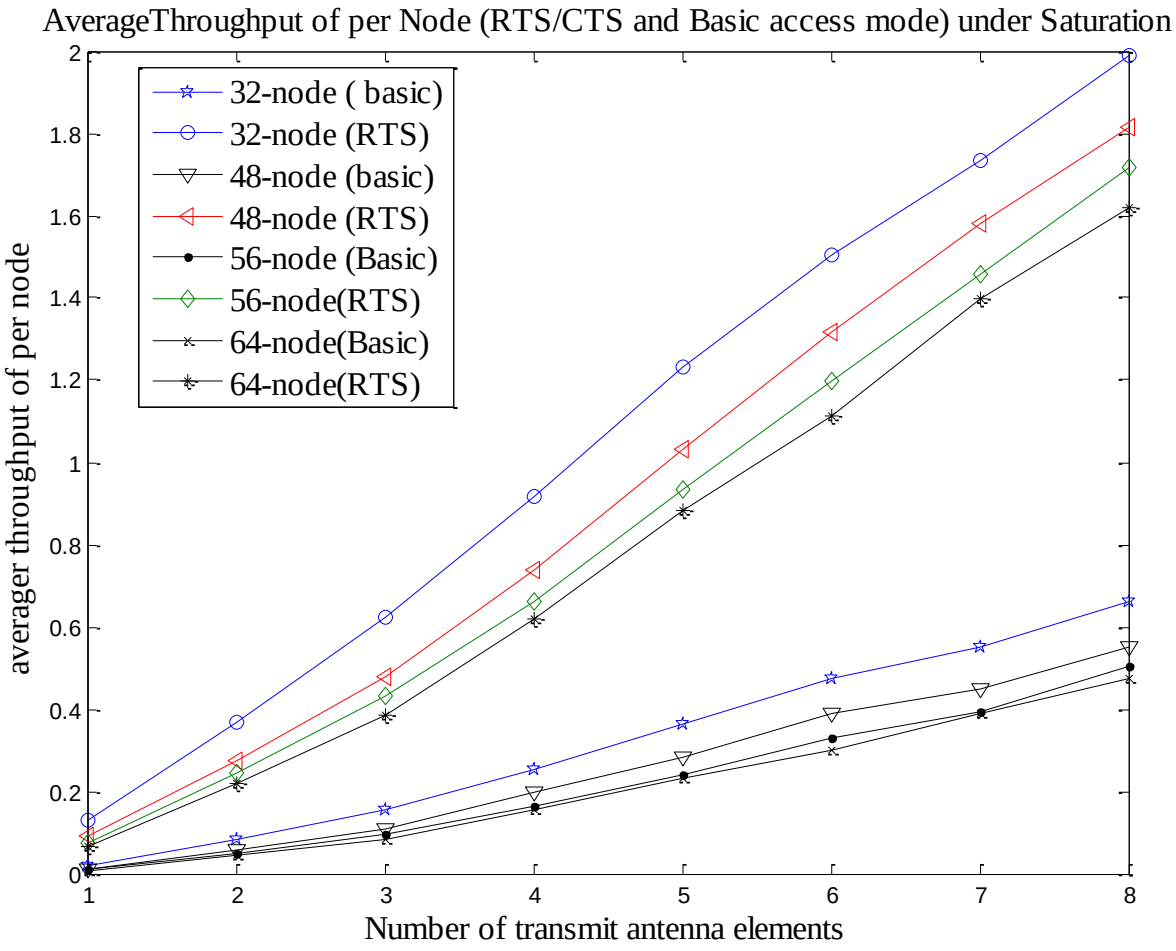

Figure 4-35：Average Throughput of per Node (RTS/CTS and Basic access mechanism) under Saturation

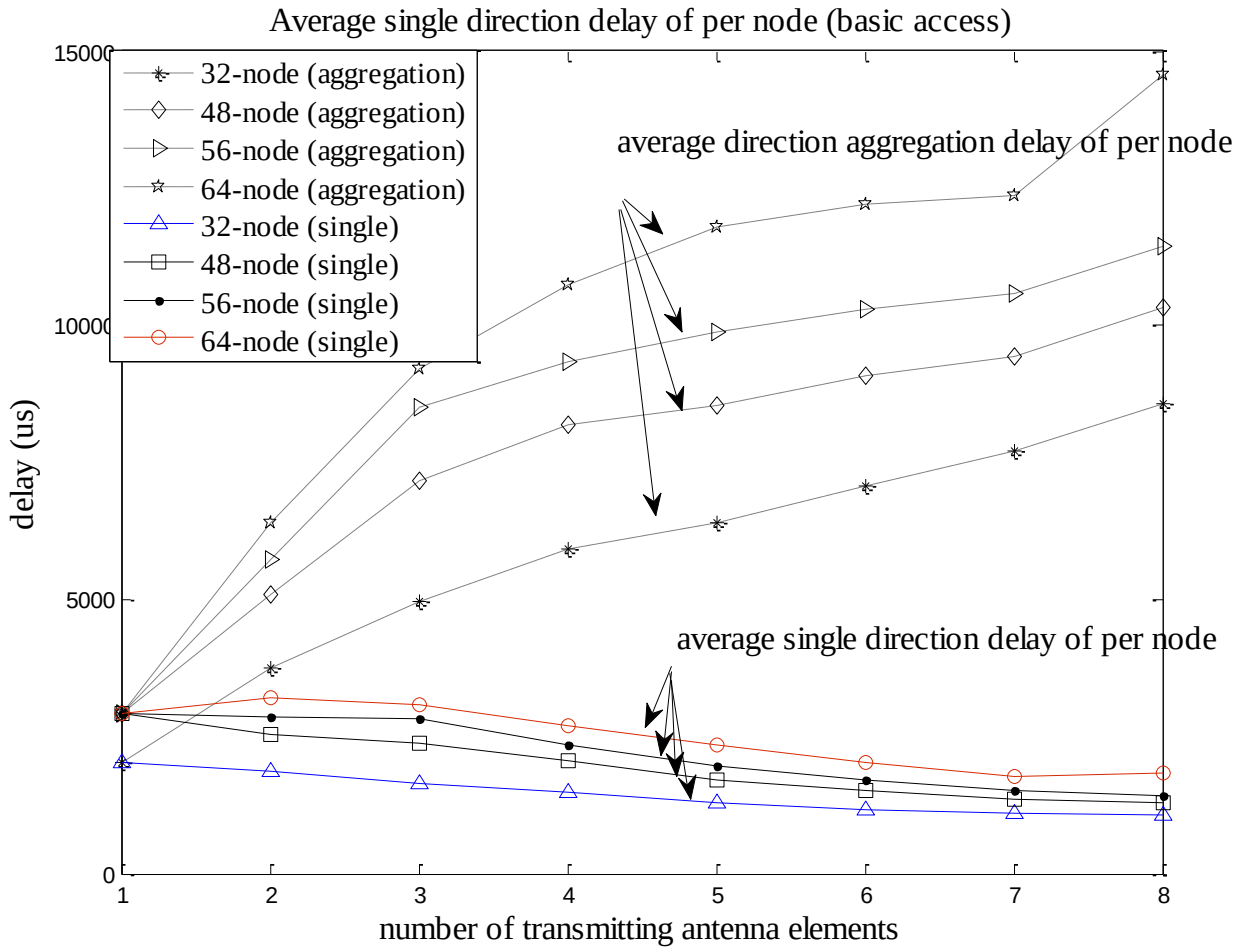

Figure 4-36：Average single direction delay of per node (basic access)

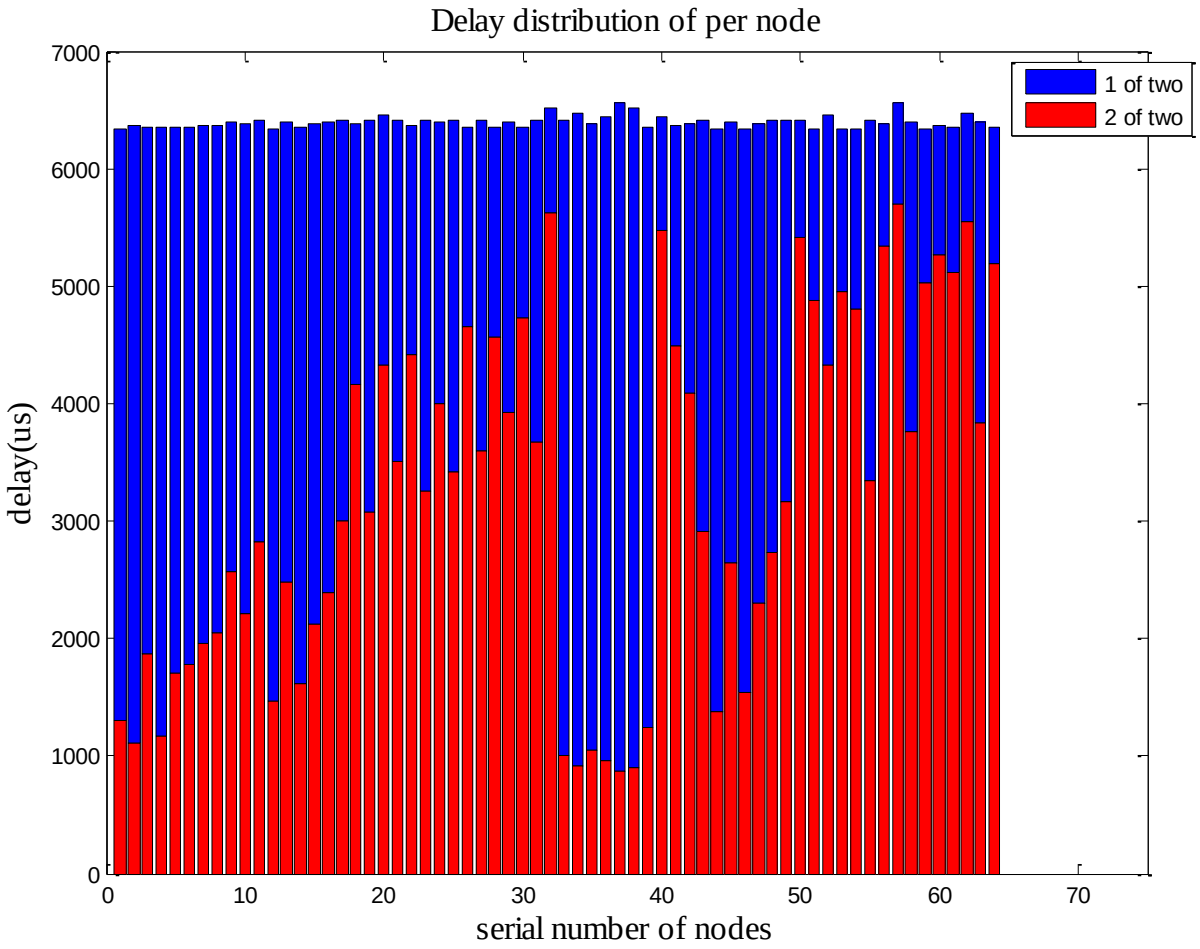

Figure 4-37：Average delay distribution of wireless network while N_tx=2 in a 64-node wireless

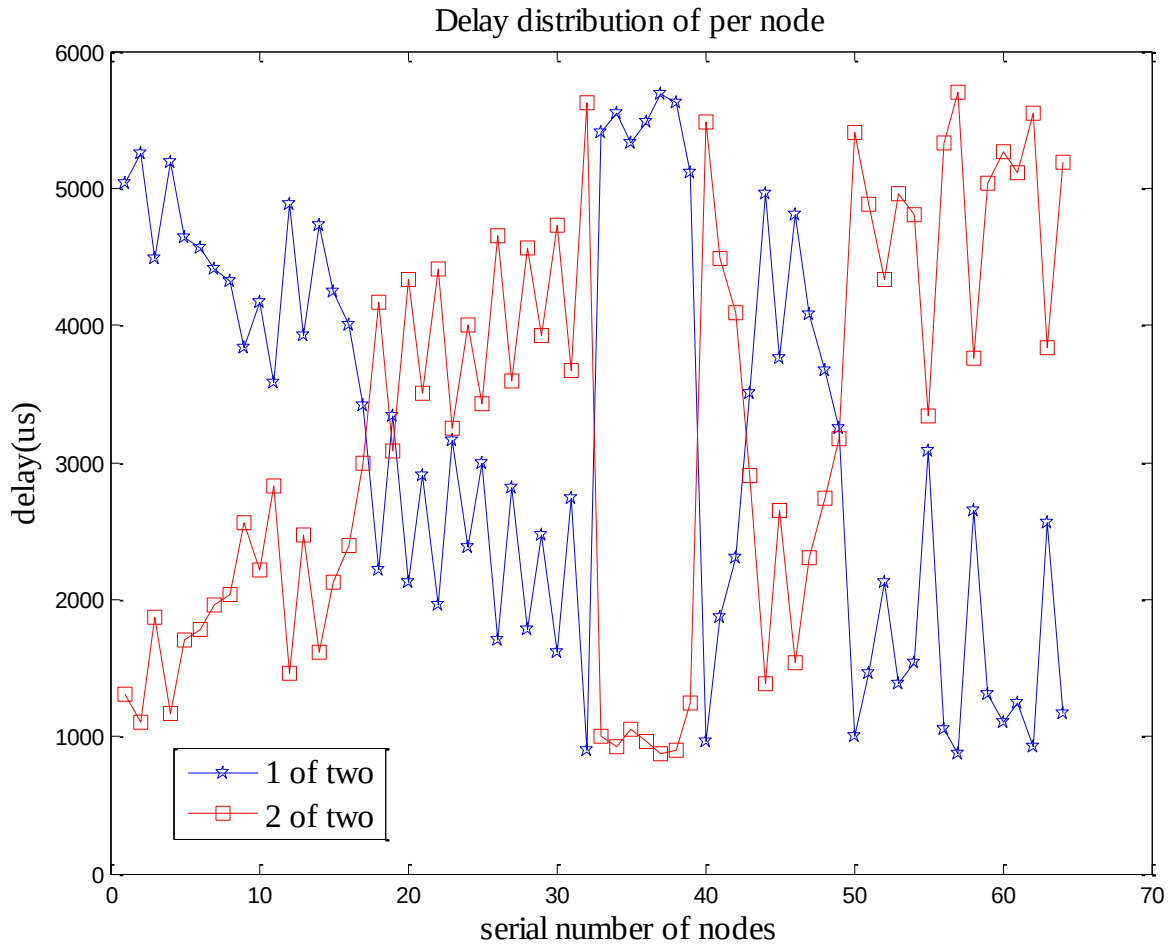

Figure 4-38：Average delay distribution of wireless network while N_tx=2 in a 64-node wireless

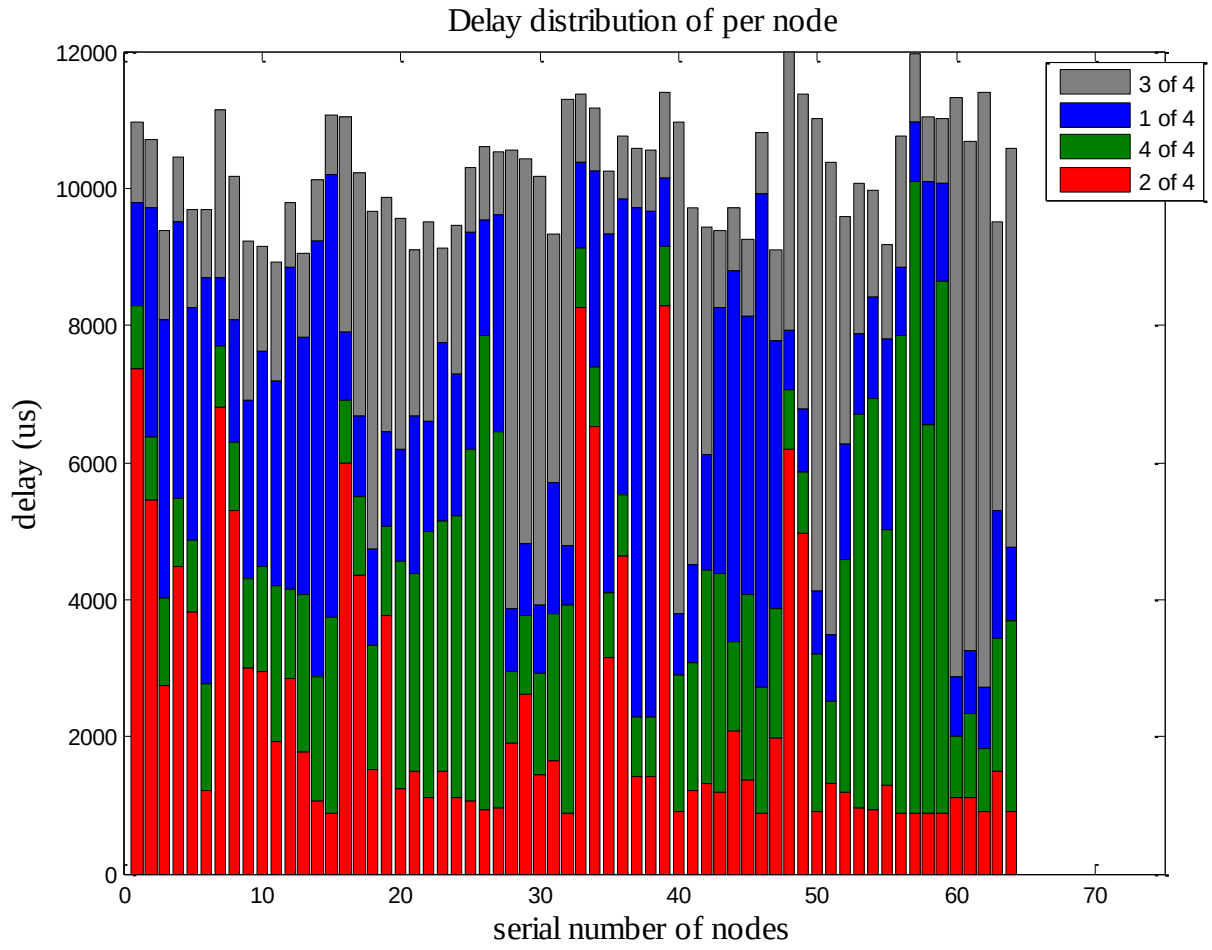

Figure 4-39: Average delay distribution of wireless network while N_tx=4 in a 64-node wireless

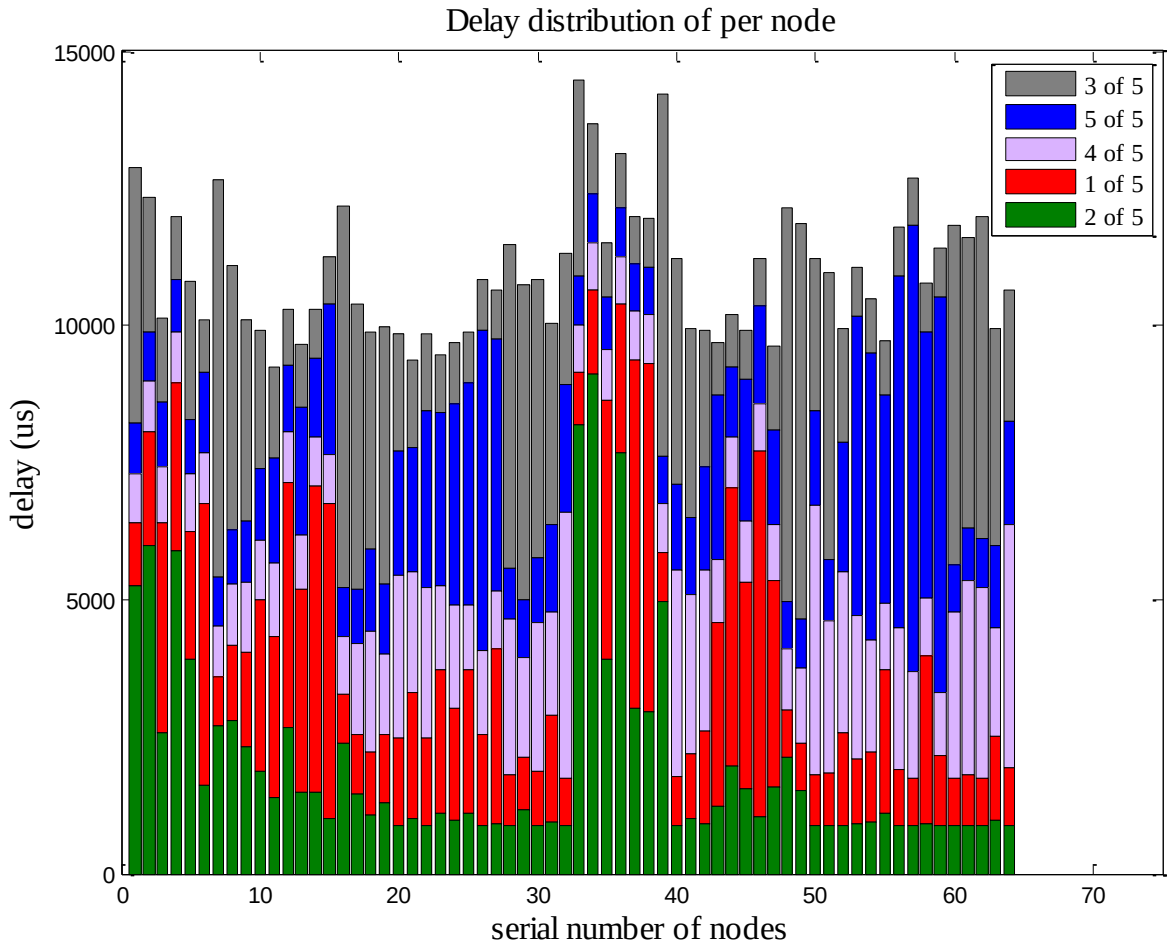

Figure 4-40： Average delay distribution of wireless network while N_tx=5 in a 64-node wireless

Table 4-3: Average delay of per node in single direction (base a 48-node network)

Number of antenna elements	1	2	3	4	5	6	7	8
Delay μs	2920	2540	2389	2046	1710	1514	1346	1291

4.5. Summary

The directional antenna systems have a better spatial multiplexing and a reduced interference as by directing the radio beam towards a desired direction; this spatial multiplexing and reduced interference will increase the capacity of wireless systems.

In this paper, we propose a Markov Chain to describe a directional MAC protocols equivalently. With the new Markov Chain, we obtain throughput and delay of each transmitting antenna element of each node in the wireless networks. As an example, our analytical approach is applied to several single-hop wireless networks where nodes are distributed randomly. We find by numerical results that the average throughput of a 64-node wireless network will increase at a faster pace for RTS/CTS access mechanism than Basic access mechanism; it has average increase of 0.2331 (normalization value) for RTS/CTS access mechanism and 0.0718 for Basic while transmitting antenna elements increase from one to eight. For a 48-node wireless network, we also calculate its average single direction delay of per node (basic access); the delay will decline from 2920.7 μs to 1291.4 μs when transmitting antenna elements are increased from one to eight. The direction average transmission probability of per node also change much (from 0.02016 to 0.03034) when the number of transmitting antenna elements is changed in the 64-node wireless network.

We will find the performance of MAC layer depends on the antenna system and its parameters as well as the topology and DMAC's requirements. The numerical results change in 32-node, 48-node, 56-node and 64-node wireless networks. 32-nodes has the lowest delay and 64-node has highest delay. With the results, we can know of whether directional antennas improve the performance straightforwardly; and evaluate their impact on network performance, and in proposing a protocol that attempts to maximize the benefits of directional antennas.

Some details of directional MAC protocols are discussed and their performances are compared in this paper. The difference of performances between half-duplex and full-duplex is $\left(1-\tau_{destination,receiv\ direction}\right)$. The numerical results will show $\tau_{destination,receiv\ direction}$ is very small, (0-0.056). So, not to build independent receive antenna element is good choice for engineering. (Making half-duplex antenna system is cheaper and full- duplex almost does not increase performance.

The throughputs difference between RTS/CTS sending Omni-directionally and RTS/CTS sending directionally is $\left[\sum_{v=0;v\neq i}^{N}\frac{Throughput_{v,\mu}}{E[lenght\ of\ packet]}\times T_{rts\ cts}+\sum_{\omega=1;\omega\neq\mu}^{N_{tx}}\sum_{v=0;v\neq i}^{N}\frac{Throughput_{v,\omega}}{E[lenght\ of\ packet]}\times T_{rts\ cts}\right]$.

5. Markov Chain Analysis of IEEE 802.11 Wireless Networks with Greedy behavior and Heterogeneous Traffic

In this chapter, we focus on analytical model in the presence of greedy behavior, extending the technology discussed in chapter 2 and chapter 3 to more scenarios. Each node's expected throughput and delay, including attacking nodes, are calculated with the help of three modified Markov Chain Models. The analysis covers scenarios of non-saturation conditions, different packet arriving rates. In practical networks, heterogeneous traffic is significant because that each node often has different applications in various scenarios. Previous research literature on analysis of greedy strategies does not include the combined situations and heterogeneous traffic.

5.1. Analysis models for greedy node with heterogeneous traffic

We use three two-dimensional non-saturation Markov chain models shown in Figures 2-4, 5-1 and 5-2 to analyze the performance of IEEE 802.11 in the presence of various types of greedy behavior nodes. In the performance analysis, we make the same assumptions mentioned in chapter 2. Analysis model for normal backoff nodes under non-saturation has discussed in section 2.3. So we only need to discuss analysis model for various greedy behavior strategies under non-saturation.

Table 5-1: Notations Used in the Analysis

$b_{0,0,s1}b_{0,0,s2}$ $b_{0,0,s3}b_{0,0,s4}$	greedy node's distribution probability, $j = 0$, backoff counter $k = 0$, playing strategy 1-4
$b_{0,k,e}$	distribution probability, when a transmission is completed, but has no packet waiting in transmission queue, its backoff stage is 0 , backoff counter is k ;
i	serial number of nodes
N	a number of normal nodes in a wireless network
$N_{s1}N_{s2}N_{s3}N_{s4}$	numbers of greedy nodes playing strategy 1, 2, 3 or 4
$P\{j,k\|j,k+1\}$	state transition probabilities, from state $(j,k+1)$ to state (j,k).
$p_{s1}p_{s2}p_{s3}p_{s4}$	probability that greedy nodes, with strategy 1- 4, senses the channel busy in a random slot
$P_{i,success,s1}P_{i,success,s2}$ $P_{i,success,s3}P_{i,success,s4}$	probability that greedy node i , playing strategy 1, 2, 3 or 4, successfully transmits its packet to its neighbors

Table 5-1: Notations Used in the Analysis (continue)

$P_{i,tr}$	probability that there is at least one transmission in normal node i's coverage area in a random time slot
$P_{i,tr,s1}P_{i,tr,s2}$ $P_{i,tr,s3}P_{i,tr,s4}$	probability that there is at least one transmission in greedy node i's coverage area in a random slot time, playing strategy 1, 2, 3 or 4
$q_{s1}q_{s2}q_{s3}q_{s4}$	probability that greedy nodes, playing strategy 1, 2, 3 or 4, receive packets and enter the second row states $(0, \mathrm{k})$ from the upper row states $(0, k+1, e)$
Th_i	throughput of normal node i
$Th_{i,s1}Th_{i,s2}Th_{i,s3}Th_{i,s4}$	throughput of greedy node i, playing strategy 1, 2, 3 and 4
$w_{0,s1}w_{0,s2}w_{0,s3}w_{0,s4}$	minimum contention window size in greedy nodes , playing strategy 1, 2, 3 or 4
$\rho_{s1}\rho_{s2}\rho_{s3}\rho_{s4}$	probability that there is a packet waiting in the transmission queue at the time when a transmission is completed or a packet dropped in greedy nodes , playing strategy 1, 2, 3 or 4
$\mu_{s1}\mu_{s2}\mu_{s3}\mu_{s4}$	packet service rate of a greedy node, playing strategy 1, 2, 3 or 4
$\lambda_{s1}\lambda_{s2}\lambda_{s3}\lambda_{s4}$	traffic arrival rate of a greedy node , with strategy 1, 2, 3 or 4
$\tau_{s1}\tau_{s2}\tau_{s3}\tau_{s4}$	transmission probability that a greedy node , playing with strategy 1, 2, 3 or 4, attempts to transmit a packet in a randomly chosen slot time

5.1.1. Greedy strategy 1: Node Randomly Selects a Backoff from Fixed Contention Window

Now we derive the analytical formula for a greedy node which plays greedy Strategy 1. According to the Strategy 1, nodes randomly select a backoff value from contention window $\{0, w_0 - 1\}$; and do not double the contention window size if they have collisions. Thus, the contention window size becomes $w_j = \begin{cases} w_0 & j \le m \\ w_0 & m < j \le L \end{cases}$, where $j \in (0, L)$. We will have a similar Markov chain (depicted in Figure 2-4, used for normal nodes) for greedy nodes playing strategy 1. By working recursively through the Markov Chain, we will have the same formulas (2-9) –(2-16)for $\mathrm{b_{j,k}}$. Using the normalization requirement, $1 = \sum_{j=0}^{L}\sum_{k=0}^{w_j-1} b_{j,k} + \sum_{k=0}^{w_0-1} b_{0,k,e}$, and $w_j = \begin{cases} w_0 & j \le m \\ w_0 & m < j \le L \end{cases}$, (the only difference is $w_j = w_0$), and adding subscripts to represent Strategy 1, we finally obtain

$$\frac{1}{b_{0,0,s1}} = \frac{1-2{p_{s1}}^{L+1}}{2(1-p_{s1})} - \frac{p_{s1}-{p_{s1}}^{L+1}}{2(1-p_{s1})^2} + \frac{(w_{0,s1})}{2(1-p_{s1})}\left[1 + \frac{p_{s1}-{p_{s1}}^{L+1}}{1-p_{s1}}\right] + \frac{(1-\rho_{s1})}{w_{0,s1}}\frac{1-(1-q_{s1})^{w_{0,s1}}}{q_{s1}}\left[\frac{(w_{0,s1}-1)p_{s1}}{2(1-p_{s1})} + \frac{1}{q_{s1}}\right] \quad (5\text{-}1)$$

5.1.2. Greedy strategy 2: Node Selects a Random Backoff from Contention Window $\{0, w_j/A\}$

Here, we derive an analytical formula for a greedy node which uses Strategy 2. According to the Strategy 2, nodes select a random backoff value from a smaller contention window, $\{0, w_j/A\}$, where A is larger than 1. Hence, we have its greedy contention window size $w_j = \frac{1}{A}\begin{cases} 2^j w_0 & j \le m \\ 2^m w_0 & m < j \le L \end{cases}$ where $j \in (0, L)$. We can use a similar Markov chain (depicted in Figure 2-4) again for greedy nodes playing Strategy 2. Using the Markov Chain regularities, we will have the same formulas (2-9) -(2-16) for $b_{j,k}$. Using the normalization requirement, $1 = \sum_{j=0}^{L}\sum_{k=0}^{w_j-1} b_{j,k} + \sum_{k=0}^{w_0-1} b_{0,k,e}$, and $w_j = \frac{1}{A}\begin{cases} 2^j w_0 & j \le m \\ 2^m w_0 & m < j \le L \end{cases}$ and adding subscripts to represent Strategy 2, we will obtain

$$\frac{1}{b_{0,0,s2}} = \frac{1-2p_{s2}{}^{L+1}}{2(1-p_{s2})} - \frac{p_{s2}-p_{s2}{}^{L+1}}{2(1-p_{s2})(1-p_{s2})} + \frac{w_{0,s2}}{2(1-p_{s2})}\left[1 + \frac{2p_{s2}-(2p_{s2})^{m+1}}{A(1-2p_{s2})} + \frac{2^m(p_{s2}{}^{m+1}-p_{s2}{}^{L+1})}{A(1-p_{s2})}\right] + \frac{1-(1-q_{s2})^{w_{0,s2}}}{q_{s2}}\frac{(1-\rho_{s2})}{w_{0,s2}}\left[\frac{1}{q_{s2}} + \frac{(w_{0,s2}-1)p_{s2}}{2(1-p_{s2})}\right] \quad (5\text{-}2)$$

5.1.3. Greedy strategy 3: Node Selects a Fixed Backoff Counter Value

According to Strategy 3, after every failure transmission, nodes always select a constant value of backoff counter. Hence, the greedy contention window size becomes $w_j = \begin{cases} w_0 & j \le m \\ w_0 & m < j \le L \end{cases}$, where $j \in (0, L)$. The non-saturation Markov Chain for strategy 3 will be depicted in Figure 5-1.

Define $a = p_{s3} \times b_{L,0} + \sum_{j=0}^{L}(1-p_{s3})b_{j,0}$ and let $B = \rho_{s3}\left[b_{L,0} + \sum_{j=0}^{L-1}(1-p_{s3})b_{j,0}\right] + q_{s3} \times p_{s3} \times b_{0,0,e}$. By working recursively through the chain, we have equations for the distribution probabilities

$$b_{0,k,e} = \left[\frac{1-(1-q_{s3})^{w_{0,s3}-k}}{q_{s3}}\right]\frac{a(1-\rho_{s3})}{w_{0,s3}} \quad k \in \left(1, \quad w_{0,s3}-1\right) \quad (5\text{-}3)$$

$$b_{0,0,e} = \left[\frac{1-(1-q_{s3})^{w_{0,s3}}}{q_{s3}}\right]\frac{a(1-\rho_{s3})}{q_{s3}\times w_{0,s3}} \quad (5\text{-}4)$$

$$b_{0,k} = \rho_{s3}a + q_{s3}p_{s3}b_{0,0,e} + q_{s3} \times \sum_{k=1}^{w_{0,s3}-1} b_{0,k,e} \quad k \in \left(1, \ w_{0,s3}-1\right) \quad (5\text{-}5)$$

$$b_{0,0} = \rho_{s3}a + q_{s3} \times \sum_{k=0}^{w_{0,s3}-1} b_{0,k,e} \quad (5\text{-}6)$$

$$b_{j,0} = p_{s3} b_{j-1,0} \qquad j = 1, 2, \dots, L \tag{5-7}$$

$$b_{j,k} = p_{s3} b_{j-1,0} \qquad k \in \left(1, \quad w_j - 1\right), j = 1, 2, \dots, L \tag{5-8}$$

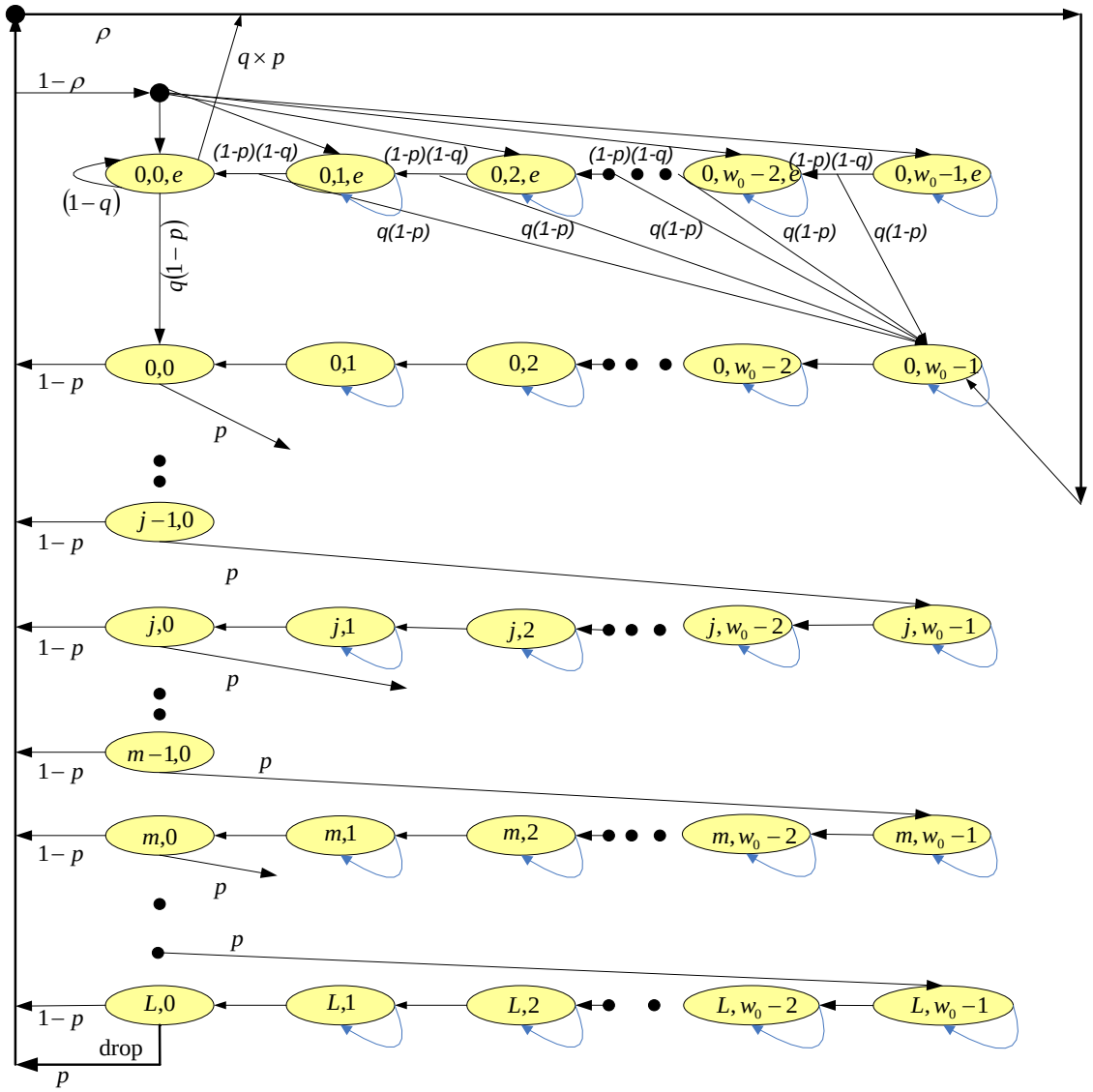

Figure 5-1: Markov Chain model for greedy nodes, playing Strategy 3, non-saturation

Substituting (5-7) into $a = p_{s3} \times b_{L,0} + \sum_{j=0}^{L}(1 - p_{s3}) b_{j,0}$, we obtain $a = b_{0,0}$. Using the normalization requirement, $1 = \sum_{j=0}^{L} \sum_{k=0}^{w_j - 1} b_{j,k} + \sum_{k=0}^{w_{0,s3} - 1} b_{0,k,e}$, and equations (5-3),- (5-8), and $w_j = \begin{cases} w_{0,s3} & j \le m \\ w_{0,s3} & m < j \le L \end{cases}$, and adding subscripts to represent Strategy 3, we finally have

$$\frac{1}{b_{0,0,s3}} = \frac{1-{p_{s3}}^{L+1}}{1-p_{s3}} + \frac{(w_{0,s3}-1)}{(1-p_{s3})}\left[\frac{1-{p_{s3}}^{L+1}}{1-p_{s3}}\right] + \frac{(1-\rho_{s3})}{q_{s3}(1-p_{s3})}\left(\frac{p_{s3}q_{s3}}{1-p_{s3}}+1\right) + \frac{(1-\rho_{s3})}{q_{s3}\times w_{0,s3}}\frac{1-(1-q_{s3})^{w_{0,s3}}}{q_{s3}(1-p_{s3})}\left[1-p_{s3}-w_{0,s3}-\frac{p_{s3}q_{s3}}{1-p_{s3}}\right] \quad (5\text{-}9)$$

5.1.4. Greedy strategy 4: Node Selects a Backoff of Zero L-1 Times and a Value above $w_0/4$ as the Lth Backoff.

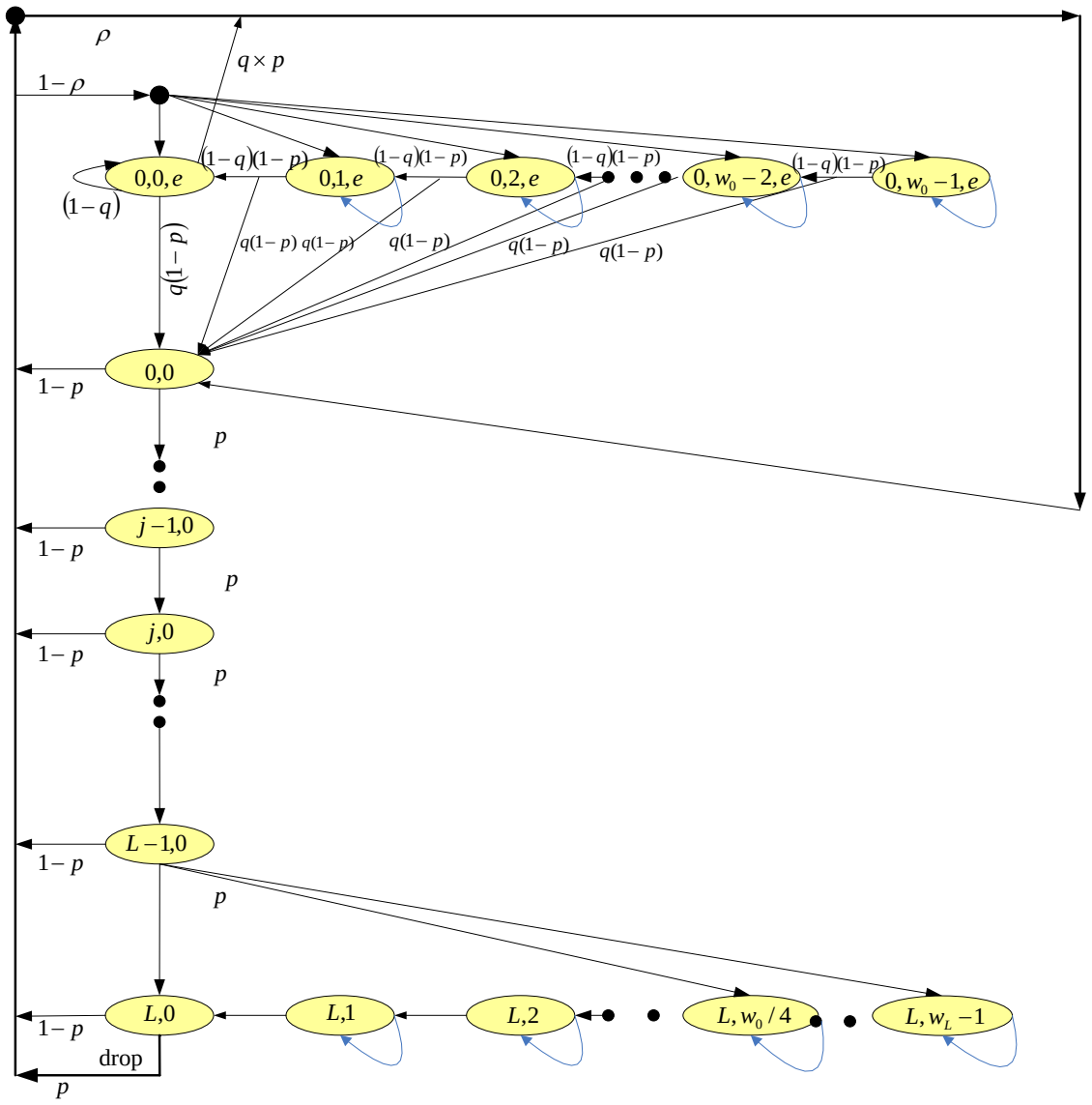

Figure 5-2: Markov Chain model for greedy nodes, Strategy 4, non-saturation

According to Strategy 4, nodes select a backoff of zero $L-1$ times and select a value above $w_0/4$ as the Lth backoff (we set it w_L, $w_L > w_0/4$). The non-saturation Markov Chain is depicted in figure 5-2.

Define $a = p_{s4} \times b_{L,0} + \sum_{j=0}^{L}(1-p_{s4})b_{j,0}$ and $= \rho_{s4}\left[b_{L,0} + \sum_{j=0}^{L-1}(1-p_{s4})b_{j,0}\right] + q_{s4} \times p_{s4} \times b_{0,0,e}$. By working recursively through the chain from state $(0, w_{0,s4}-1, e)$ to the last state $(L, 0)$, we have equations for the distribution probabilities

$$b_{0,k,e} = \left[\frac{1-(1-q_{s4})^{w_{0,s4}-k}}{q_{s4}}\right]\frac{a(1-\rho_{s4})}{w_{0,s4}} \quad k \in (1, \quad w_{0,s4}-1) \tag{5-10}$$

$$b_{0,0,e} = \left[\frac{1-(1-q_{s4})^{w_{0,s4}}}{q_{s4}}\right]\frac{a(1-\rho_{s4})}{q_{s4}\times w_{0,s4}} \tag{5-11}$$

$$b_{0,0} = \rho_{s4}a + q_{s4} \times \sum_{k=0}^{w_{0,s4}-1} b_{0,k,e} \tag{5-12}$$

$$b_{j,0} = p_{s4}b_{j-1,0} \qquad j = 1, 2, \dots, L \tag{5-13}$$

$$b_{L,k} = \frac{(w_L-k)p_{s4}b_{L-1,0}}{(w_L-w_0/4)w_L} \qquad k \in \left(\frac{w_0}{4}, \dots. \ w_L - 1\right) \tag{5-14}$$

$$b_{L,k} = b_{L,\frac{w_0}{4}} \qquad k \in \left(1,2,3, \dots, \frac{w_0}{4}-1\right), \tag{5-15}$$

From (5-13), we get $b_{j,0} = {p_{s4}}^{j} b_{0,0}$. From (5-14) , we get $b_{L,k} = \frac{(w_L-k)}{w_L}{p_{s4}}^{L} b_{0,0}$. Substituting (5-25) into $a = p_{s4} \times b_{L,0} + \sum_{j=0}^{L}(1-p_{s4})b_{j,0}$, we obtain $a = b_{0,0}$. Using the normalization requirement, $1 = \sum_{j=0}^{L}\sum_{k=0}^{w_j-1} b_{j,k} + \sum_{k=0}^{w_{0,s4}-1} b_{0,k,e}$, and equations (5-10)- (5-15) and $w_j = \begin{cases} 0 & j \le L-1 \\ w_L & j = L \end{cases}$, we obtain

$$1 = \sum_{j=0}^{L}\sum_{k=0}^{w_j-1} b_{j,k} + \sum_{k=0}^{w_{0,s4}-1} b_{0,k,e} = \frac{1-{p_{s4}}^{L+1}}{(1-p_{s4})} b_{0,0} + \frac{(w_{L,s4}-1)({p_{s4}})^{L}\times b_{0,0}}{2} + \frac{a(1-\rho_{s4})}{q_{s4}} \tag{5-16}$$

Simplifying and adding subscripts to represent Strategy 4, we finally have

$$\frac{1}{b_{0,0,s4}} = \frac{1-{p_{s4}}^{L+1}}{1-p_{s4}} + \frac{\left(w_{L,s4}+1+\frac{w_{0,s4}}{4}\right)}{2(1-p_{s4})}{p_{s4}}^{L} + \frac{(1-\rho_{s4})}{q_{s4}(1-p_{s4})}\left[1 - \frac{p_{s4}\left[1-(1-q_{s4})^{w_{0,s4}}\right]}{q_{s4}w_0}\right] \tag{5-17}$$

5.2. Throughput and delay of wireless networks with greedy behaviors and heterogeneous traffic

5.2.1. Throughput of each node

In section 2.3, we denote τ the transmission probability that a node attempts to transmit a packet in a randomly chosen slot time. Knowing that any transmission occurs when the backoff time counter equals to zero, we have equation (2-19)

$$\tau = \sum_{j=0}^{L} b_{j,0} = \frac{1-p^{L+1}}{1-p} \times b_{0,0} \quad (2\text{-}19)$$

Substituting equations (5-1), (5-2), (5-9) and (5-17) into equation (2-19) furthermore, we obtain equations (5-18), (5-19), (5-20) and (5-21) for the normal node's transmission probability τ and the greedy node's transmission probabilities τ_{s1} (playing strategy 1), τ_{s2} (playing strategy 2), τ_{s3} (playing strategy 3) and τ_{s4} (playing strategy 4).

Equations (5-18)-(5-21) are defined as the IEEE 802.11 normal/greedy node property formula since they determine the node's transmission probability in terms of the channel busy probability as well as the network configuration parameters $(L, m, \rho/\rho_{s1-s4}, q/q_{s1-s4}, w_0/w_{0,s1-s4})$. The pair of variables of $\{p, \tau\}$ in equations (5-18)-(5-21) will be regarded as the attributes of a transmission of an IEEE 802.11-based station with arbitrary traffic arrival rate. Noticing that every normal or greedy node i will have its own $\{p, \tau\}$, we now attach the node's serial number to $\{p, \tau\}$ and formulae (5-18)-(5-21) becomes (5-22)-(5-25), where i=1,2,… N or $N_{s1}, N_{s2}, N_{s3}, N_{s4}$; and N or $N_{s1}, N_{s2}, N_{s3}, N_{s4}$ are numbers of normal or greedy nodes in the network.

$$\tau_{s1} = \frac{1-(p_{s1})^{L+1}}{(1-p_{s1})\left\{\frac{1-2p_{s1}{}^{L+1}}{2(1-p_{s1})} - \frac{p_{s1}-p_{s1}{}^{L+1}}{2(1-p_{s1})^2} + \frac{(w_{0,s1})}{2(1-p_{s1})}\left[1+\frac{p_{s1}-p_{s1}{}^{L+1}}{1-p_{s1}}\right] + \frac{(1-\rho_{s1})1-(1-q_{s1})^{w_{0,s1}}}{w_{0,s1}\quad q_{s1}}\left[\frac{(w_{0,s1}-1)p_{s1}}{2(1-p_{s1})} + \frac{1}{q_{s1}}\right]\right\}} \quad (5\text{-}18)$$

$$\tau_{s2} = \frac{1-(p_{s2})^{L+1}}{(1-p_{s2})\left\{\frac{1-2p_{s2}{}^{L+1}}{2(1-p_{s2})} - \frac{p_{s2}-p_{s2}{}^{L+1}}{2(1-p_{s2})(1-p_{s2})} + \frac{w_{0,s2}}{2(1-p_{s2})}\left[1+\frac{2p_{s2}-(2p_{s2})^{m+1}}{A(1-2p_{s2})} + \frac{2^m(p_{s2}{}^{m+1}-p_{s2}{}^{L+1})}{A(1-p_{s2})}\right] + \frac{1-(1-q_{s2})^{w_{0,s2}}(1-\rho_{s2})}{q_{s2}\quad w_{0,s2}}\left[\frac{1}{q_{s2}} + \frac{(w_{0,s2}-1)p_{s2}}{2(1-p_{s2})}\right]\right\}} \quad (5\text{-}19)$$

$$\tau_{s3}=\frac{1-(p_{s3})^{L+1}}{(1-p_{s3})\left\{\frac{1-p_{s3}{}^{L+1}}{1-p_{s3}}+\frac{(w_{0,s3}-1)}{(1-p_{s3})}\left[\frac{1-p_{s3}{}^{L+1}}{1-p_{s3}}\right]+\frac{(1-\rho_{s3})}{q_{s3}(1-p_{s3})}\left(\frac{p_{s3}q_{s3}}{1-p_{s3}}+1\right)+\frac{(1-\rho_{s3})}{q_{s3}\times w_{0,s3}}\frac{1-(1-q_{s3})^{w_{0,s3}}}{q_{s3}(1-p_{s3})}\left[1-p_{s3}-w_{0,s3}-\frac{p_{s3}q_{s3}}{1-p_{s3}}\right]\right\}} \quad (5\text{-}20)$$

$$\tau_{s4}=\frac{1-(p_{s4})^{L+1}}{(1-p_{s4})\left\{\frac{1-p_{s4}{}^{L+1}}{1-p_{s4}}+\frac{\left(w_{L,s4}+1+\frac{w_{0,s4}}{4}\right)}{2(1-p_{s4})}p_{s4}{}^{L}+\frac{(1-\rho_{s4})}{q_{s4}(1-p_{s4})}\left[1-\frac{p_{s4}\left[1-(1-q_{s4})^{w_{0,s4}}\right]}{q_{s4}w_0}\right]\right\}} \quad (5\text{-}21)$$

$$\tau_{i,s1}=\frac{1-(p_{i,s1})^{L+1}}{(1-p_{i,s1})\left\{\frac{1-2p_{i,s1}{}^{L+1}}{2(1-p_{i,s1})}-\frac{p_{i,s1}-p_{i,s1}{}^{L+1}}{2(1-p_{i,s1})^{2}}+\frac{(w_{0,i,s1})}{2(1-p_{i,s1})}\left[1+\frac{p_{i,s1}-p_{i,s1}{}^{L+1}}{1-p_{i,s1}}\right]+\frac{(1-\rho_{i,s1})1-(1-q_{i,s1})^{w_{0,i,s1}}}{w_{0,i,s1}\quad q_{i,s1}}\left[\frac{(w_{0,i,s1}-1)p_{i,s1}}{2(1-p_{i,s1})}+\frac{1}{q_{i,s1}}\right]\right\}} \quad (5\text{-}22)$$

$$\tau_{i,s2}=\frac{1-(p_{i,s2})^{L+1}}{(1-p_{i,s2})\left\{\frac{1-2p_{i,s2}{}^{L+1}}{2(1-p_{i,s2})}-\frac{p_{i,s2}-p_{i,s2}{}^{L+1}}{2(1-p_{i,s2})(1-p_{i,s2})}+\frac{w_{0,i,s2}}{2(1-p_{i,s2})}\left[1+\frac{2p_{i,s2}-(2p_{i,s2})^{m+1}}{A(1-2p_{i,s2})}+\frac{2^{m}(p_{i,s2}{}^{m+1}-p_{i,s2}{}^{L+1})}{A(1-p_{i,s2})}\right]+\frac{1-(1-q_{i,s2})^{w_{0,i,s2}}(1-\rho_{i,s2})}{q_{i,s2}\quad w_{0,i,s2}}\left[\frac{1}{q_{i,s2}}+\frac{(w_{0,i,s2}-1)p_{i,s2}}{2(1-p_{i,s2})}\right]\right\}} \quad (5\text{-}23)$$

$$\tau_{i,s3}=\frac{1-(p_{i,s3})^{L+1}}{(1-p_{i,s3})\left\{\frac{1-p_{i,s3}{}^{L+1}}{1-p_{i,s3}}+\frac{(w_{0,i,s3}-1)}{(1-p_{i,s3})}\left[\frac{1-p_{i,s3}{}^{L+1}}{1-p_{i,s3}}\right]+\frac{(1-\rho_{s3})}{q_{s3}(1-p_{i,s3})}\left(\frac{p_{i,s3}q_{s3}}{1-p_{i,s3}}+1\right)+\frac{(1-\rho_{s3})}{q_{s3}\times w_{0,i,s3}}\frac{1-(1-q_{s3})^{w_{0,i,s3}}}{q_{s3}(1-p_{i,s3})}\left[1-p_{i,s3}-w_{0,i,s3}-\frac{p_{i,s3}q_{s3}}{1-p_{i,s3}}\right]\right\}} \quad (5\text{-}24)$$

$$\tau_{i,s4}=\frac{1-(p_{i,s4})^{L+1}}{(1-p_{i,s4})\left\{\frac{1-p_{i,s4}{}^{L+1}}{1-p_{i,s4}}+\frac{\left(w_{L,i,s4}+1+\frac{w_{0,i,s4}}{4}\right)}{2(1-p_{i,s4})}p_{i,s4}{}^{L}+\frac{(1-\rho_{i,s4})}{q_{i,s4}(1-p_{i,s4})}\left[1-\frac{p_{i,s4}\left[1-(1-q_{i,s4})^{w_{0,i,s4}}\right]}{q_{i,s4}w_0}\right]\right\}} \quad (5\text{-}25)$$

There are three notes to equations (5-22)- (5-25). First, we can attach the node's serial number to $(L,m,w_0/w_{0,s1-s4})$, which means we can set different $L,m,w_0/w_{0,s1-s4}$ for each node. Second, we have attached the node's serial number i to $\rho_i/\rho_{i,s1-s4},q_i/q_{i,s1-s4}$, which means we are able to analyze the performance for nodes with different arrival rates.

Third, p_i, $p_{i,s1},p_{i,s2},p_{i,s3}$ and $p_{i,s4}$ in equations (2-20),(5-22)- (5-25) depend on the transmission status of its neighbors nodes and varies from one node to the other. Hence for every node i, we can write an equation of p_i, $p_{i,s1},p_{i,s2},p_{i,s3}$ and $p_{i,s4}$ in terms of its neighboring nodes transmission probability τ_u, $\tau_{u,s1}$ $\tau_{u,s2}$, $\tau_{u,s3}$ and $\tau_{u,s4}$, where u,u_{s1},u_{s2},u_{s3} and u_{s4} are sets of serial number of node i's neighbors (including normal or greedy nodes with strategies 1,2,3,4). In other words, if given a network topology, we can obtain another equation for every node i's p_i, $p_{i,s1},p_{i,s2},p_{i,s3}$ and $p_{i,s4}$. Using numerical solution technology, we are able to solve equation (5-22)- (5-25) ultimately. Recalling that transmission probability τ_i, $\tau_{i,s1}$ $\tau_{i,s2}$, $\tau_{i,s3}$ and $\tau_{i,s4}$ are the transmission probability that node i

attempts to transmit in a randomly chosen time slot, we are able to obtain the network throughput and delay, similar to the section 2.3 and section 3.2.

We define similar variables for greedy notes, $P_{i,tr,s1}, P_{i,tr,s2}$, $P_{i,tr,s3}$ and $P_{i,tr,s4}$ as the probability that there is at least one transmission within greedy node i's coverage area for a given time slot. We also define $P_{i,success,s1}$, $P_{i,success,s2}$, $P_{i,success,s3}$ and $P_{i,success,s4}$ as the probability that greedy node i successfully transmits its packet to its neighbors, which equals to the probability that exactly only one station transmits on the channel covered by greedy node i in a given time slot. In presence of hidden station, the probability, $P_{i,success,s1}, P_{i,success,s2}, P_{i,success,s3}$ and $P_{i,success,s4}$ need the hidden nodes do not transmit. Similar to section 2.3, we show how to obtain$P_{i,tr,s1}$, $P_{i,tr,s2}$, $P_{i,tr,s3}$,$P_{i,tr,s4}$, $P_{i,success,s1}$, $P_{i,success,s2}$, $P_{i,success,s3}$ and $P_{i,success,s4}$.

Let Th_i, Th_{s1}, Th_{s2}, Th_{s3} and Th_{s14} be the normalized throughput of greedy node i, with a similar method, we obtain

$$Th_i = \frac{P_{i,success}E[P]}{(1-P_{i,tr,s1})\sigma+P_{i,success}T_S+[P_{i,tr,s1}-P_{i,success}]T_C} \quad (5\text{-}26)$$

$$Th_{i,s1} = \frac{P_{i,success,s1}E[P]}{(1-P_{i,tr})\sigma+P_{i,success,s1}T_S+[P_{i,tr}-P_{i,success,s1}]T_C} \quad (5\text{-}27)$$

$$Th_{i,s2} = \frac{P_{i,success,s2}E[P]}{(1-P_{i,tr})\sigma+P_{i,success,s2}T_S+[P_{i,tr}-P_{i,success,s2}]T_C} \quad (5\text{-}28)$$

$$Th_{i,s3} = \frac{P_{i,success,s3}E[P]}{(1-P_{i,tr})\sigma+P_{i,success,s3}T_S+[P_{i,tr}-P_{i,success,s3}]T_C} \quad (5\text{-}29)$$

$$Th_{i,s4} = \frac{P_{i,success,s4}E[P]}{(1-P_{i,tr})\sigma+P_{i,success,s4}T_S+[P_{i,tr}-P_{i,success,s4}]T_C} \quad (5\text{-}30)$$

T_C and T_S can be derived for both the basic and the RTS/CTS access mechanisms from (2-30a), (2-30b), (2-30c) and (2-30d).

5.2.2. Delay of nodes

As mentioned in section 3.2, the frame delay is defined as the time interval between the frame's first backoff attempt and its successful transmission if the frame is not dropped. The total frame delay D is divided into four sub-delays: delay in queue, $D_{in\ queue}$, frame access delay, $D_{access}(j)$, a successful frame transmission delay, $D_{successful}(j)$ and frame propagation delay, $D_{propagation}(j)$. A successful frame transmission delay, $D_{successful}(j)$, is the time consumed during the successful transmissions. Frame propagation delay, $D_{propagation}(j)$, is the time spent during propagation.

It is still true that the greedy station will then generate a random backoff period for an additional deferral time before retrying if the medium is determined to be busy. In section 3.2, we have shown the frame delay is given by

$$D = D_{in\ queue} + D_{access}(j) + D_{successful}(j) + D_{propagation} =$$

$$D_{in\ queue} + E[slot] \times \sum_{j=0}^{L} \left[\frac{(1-p)p^j}{1-p^{L+1}} \sum_{v=0}^{j} \frac{w_v - 1}{2} \right] + T_s + D_{propagation} \quad (3\text{-}10)^4$$

For normal nodes, $w_j = \begin{cases} 2^j w_0 & j \le m \\ 2^m w_0 & m < j \le L \end{cases}$,

$$D = D_{in\ queue} + E[slot] \times \frac{(1-p)}{1-p^{L+1}} \left\{ \frac{\left(1-(2p)^{m+1}\right)w_0}{1-2p} + \frac{w_0}{2(1-p)} \left\{ p^{L+1} - 1 + 2^m \left[\frac{p^{m+1} - p^{L+1}}{1-p} - Lp^{L+1} + \right. \right. \right.$$

$$mpL+1+2pm+1-pL+1-121-p1-pL+11-p-L+1pL+1+Ts+Dpropagation \quad (3\text{-}12)$$

For greedy nodes, playing strategy 1, $w_j = \begin{cases} w_{0,s1} & j \le m \\ w_{0,s1} & m < j \le L \end{cases}$,

$$D_{s1} = D_{in\ queue,s1} + E[slot] \frac{(1-p_{s1})}{1-{p_{s1}}^{L+1}} \times \frac{w_{0,s1}-1}{2(1-p_{s1})} \left[\frac{p_{s1} - (p_{s1})^{L+1}}{1-p_{s1}} - (L+1)(p_{s1})^{L+1} + 1 \right] + T_s +$$

$$D_{propagation} \quad (5\text{-}31)$$

For greedy nodes, playing strategy 2, $w_j = \frac{1}{A} \begin{cases} 2^j w_0 & j \le m \\ 2^m w_0 & m < j \le L \end{cases}$,

[4] For strategy 3, $\frac{w_v - 1}{2}$ should be change to $w_v - 1$

$$D_{s2} = D_{in\ queue,s2} + E[slot] \times \frac{(1-p_{s2})}{1-{p_{s2}}^{L+1}} \left\{ \frac{w_0}{A} \frac{1-(2p_{s2})^{m+1}}{1-2p_{s2}} + \frac{w_{0,s2}}{2A} \frac{1}{1-p_{s2}} \left[(p_{s2})^{L+1} - 1 + ((p_{s2})^{m+1} - (p_{s2})^{L+1}) 2^m [2-m] + \right. \right.$$

$$\left. \left. 2mps2m+1-ps2L+11-ps2-Lps2L+1+ps2L+1-1+mps2m+121-ps2-ps2-ps2m+121-ps21-ps2+Ts+Dpropagation \right] \right.$$

(5-32)

For greedy nodes, playing strategy 3, $w_j = \begin{cases} w_{0,s3} & j \le m \\ w_{0,s3} & m < j \le L' \end{cases}$

$$D_{s3} = D_{in\ queue,s3} + E[slot] \frac{(1-p_{s3})}{1-{p_{s3}}^{L+1}} \times \frac{w_{0,s3}-1}{(1-p_{s3})} \left[\frac{p_{s3}-(p_{s3})^{L+1}}{1-p_{s3}} - (L+1)(p_{s3})^{L+1} + 1 \right] + T_s +$$

$D_{propagation}$; (5-33)

For greedy nodes, playing 4, $w_j = \begin{cases} 0 & j \le L-1 \\ w_{0,s4} & j = L \end{cases}$

$$D_{s4} = D_{in\ queue,s4} + E[slot] \frac{(1-p_{s4})}{1-{p_{s4}}^{L+1}} \times (p_{s4})^L \frac{w_{L,s4}-1}{2} + T_s + D_{propagation} \quad (5\text{-}34)$$

5.2.3. Determinations of probabilities ρ_{s1-s4} and q_{s1-s4}

Assuming the packets at greedy nodes are Poisson arrival traffic, we denote the traffic arrival rate and packet service rate of a greedy node as λ_{s1-s4} and μ_{s1-s4} packets per second respectively. Greedy node is under non-saturation condition if $\lambda_{s1-s4} < \mu_{s1-s4}$. (which means the node still has some remained capacity to provide packet service). According to the $M/M/1/\infty$ queue[5] under steady-state conditions, the probability that there are x packets waiting in the transmission queue is

$$P_x = \left(1 - \frac{\lambda_{s1-s4}}{\mu_{s1-s4}}\right) \left(\frac{\lambda_{s1-s4}}{\mu_{s1-s4}}\right)^x$$

We can easily have the probability, $P_0 = \left(1 - \frac{\lambda_{s1-s4}}{\mu_{s1-s4}}\right)$, that there is no packet waiting in the transmission queue. We are interested in another probability that there is at least one packet waiting in the transmission queue as well. The probability will be obtained by

$$P(x > 0) = \sum_{x=1}^{\infty} P_x = 1 - P_0 = \frac{\lambda_{s1-s4}}{\mu_{s1-s4}} \quad (5\text{-}35)$$

[5] For $M/M/1/K$, $P_x = \frac{\left(1-\frac{\lambda}{\mu}\right)}{1-\left(\frac{\lambda}{\mu}\right)^{K+1}} \left(\frac{\lambda}{\mu}\right)^x$, $P(x>0) = \sum_{x=1}^{K} P_x = \frac{\frac{\lambda}{\mu} - \left(\frac{\lambda}{\mu}\right)^{K+1}}{1-\left(\frac{\lambda}{\mu}\right)^{K+1}}$

Under steady-state conditions, the probability that there is at least one packet waiting in the transmission queue is $\frac{\lambda_{s1-s4}}{\mu_{s1-s4}}$, either in per second or per time slot.

As mentioned before, ρ_{s1-s4} is defined as the probability that there is at least one packet waiting in the transmission queue when a transmission is completed. But under steady-state conditions, they are independent of time. This means the probability that there is at least one packet waiting in the transmission queue is equal to the probability that there is at least one packet waiting in the transmission queue at the time when a transmission is completed. Hence, we obtain an expression

$$\rho_{s1-s4} = \frac{\lambda_{s1-s4}}{\mu_{s1-s4}} \tag{5-36}$$

In order to obtain mean delay time in the queue , we obtain the expected of the number of packets in the transmission queue in steady state, $\overline{x} = E(x) = \sum_{x=0}^{\infty} xP_x = \frac{\lambda_{s1-s4}}{\mu_{s1-s4}-\lambda_{s1-s4}}$, thus, the mean delay time in the queue is

$$D_{in\ queue} = \frac{\overline{x}}{\lambda_{s1-s4}} = \frac{1}{\mu_{s1-s4}-\lambda_{s1-s4}} \tag{5-37}$$

The retransmission probabilities are p_{s1-s4}, ${p_{s1-s4}}^2$,..., ${p_{s1-s4}}^L$, and if the wireless networks operate in an ideal physical environment, the average times of packet service for each successful packet is $\sum_{i=0}^{L} {p_{s1-s4}}^i$, thus

$$\mu_{s1-s4} = Th_{s1-s4} \times \sum_{i=0}^{L} {p_{s1-s4}}^i = \frac{Th_{s1-s4}\left(1-{p_{s1-s4}}^{L+1}\right)}{1-p_{s1-s4}}. \tag{5-38}$$

Equation (5-38) shows how packet service rate μ_{s1-s4} links to the station's throughput. Substitute (95-38) into (5-36), we obtain

$$\rho_{s1-s4} = \frac{\lambda_{s1-s4}(1-p_{s1-s4})}{Th_{s1-s4}(1-{p_{s1-s4}}^{L+1})} \tag{5-39}$$

For greedy nodes, we have similar formulae.

$$\rho_{s1} = \frac{\lambda_{s1}(1-p_{s1})}{Th_{s1}(1-{p_{s1}}^{L+1})} \tag{5-39a}$$

$$\rho_{s2} = \frac{\lambda_{s2}(1-p_{s2})}{Th_{s2}(1-{p_{s2}}^{L+1})} \quad (5\text{-}39b)$$

$$\rho_{s3} = \frac{\lambda_{s3}(1-p_{s3})}{Th_{s3}(1-{p_{s3}}^{L+1})} \quad (5\text{-}39c)$$

$$\rho_{s4} = \frac{\lambda_{s4}(1-p_{s4})}{Th_{s4}(1-{p_{s4}}^{L+1})} \quad (5\text{-}39d)$$

In the later part of this paper, we will demonstrate how to gain the service rate μ_{s1-s4} and throughput.

As mentioned before, we define q_{s1-s4} as the probability entering the second row states, $(0,k)$, from the upper row state, $(0,k,e)$, while the transmission queue has at least one arrival packet and become non-empty. Look at the condition entering the second row from the upper row. We know the probability that the transmission queue will have at least one packet waiting in the transmission queue is ρ_{s1-s4}. Under steady state, this means that the probability, q_{s1-s4}, equals to ρ_{s1-s4}. For Poisson arrival traffic $\rho_{s1-s4} = \frac{\lambda_{s1-s4}}{\mu_{s1-s4}}$, the probability q_{s1-s4} while the backoff is started by entering the second row states $(0,\mathrm{k})$ equals to $\frac{\lambda_{s1-s4}}{\mu_{s1-s4}}$.

5.3. Example of various scenarios and numerical results of performances

To simplify the presentation of the results, we have assumed that all data packets have the same lengths (1024 bytes) and each packet fits perfectly into one Transmit Opportunity. We have IEEE 802.11 default parameters here: MAC header =272bits; PHY header =192 bits (including preamble 144bits and PLCP header 48 bits); ACK length =112bit +PHY header; RTS length =160bit +PHY header; CTS length =112bit +PHY header; other parameters are summarized in Table 3-3.

We choose the IEEE 802.11b in our numerical calculations. That means we have slot time =20 μs; SIFS = 10 μs; DIFS =50 μs; L=5; m=5; $w_0 = 31$. The channel data rate is 11 Mbits/s. Using Equation (2-30), we will have $T_{C,bas} = 835.2\ \mu s$, $T_{S,bas} = 871.15\ \mu s$; $T_{C,rts} = 80.3\ \mu s$, $T_{S,rts} = 947.4\ \mu s$.

5.3.1. Single hop wireless network with heterogonous traffic arrival rate

Assuming a single hop wireless network has N normal nodes, N_{s1} greedy nodes playing strategy 1, N_{s2} greedy nodes playing strategy 2, N_{s3} greedy nodes playing strategy 3, and N_{s4} greedy nodes playing strategy 4; all nodes are in a single hop coverage area. Hence we obtain

$$p_i = 1 - \prod_{v=1,v\neq i}^{N}(1-\tau_v)\prod_{v=1}^{N_{s1}}(1-\tau_{v,s1})\prod_{v=1}^{N_{s2}}(1-\tau_{v,s2})\prod_{v=1}^{N_{s3}}(1-\tau_{v,s3})\prod_{v=1}^{N_{s4}}(1-\tau_{v,s4}) \quad (5\text{-}40)$$

$$p_{i,s1} = 1 - \prod_{v=1}^{N}(1-\tau_v)\prod_{v=1,v\neq i}^{N_{s1}}(1-\tau_{v,s1})\prod_{v=1}^{N_{s2}}(1-\tau_{v,s2})\prod_{v=1}^{N_{s3}}(1-\tau_{v,s3})\prod_{v=1}^{N_{s4}}(1-\tau_{v,s4}) \quad (5\text{-}40)$$

$$p_{i,s2} = 1 - \prod_{v=1}^{N}(1-\tau_v)\prod_{v=1}^{N_{s1}}(1-\tau_{v,s1})\prod_{v=1,v\neq i}^{N_{s2}}(1-\tau_{v,s2})\prod_{v=1}^{N_{s3}}(1-\tau_{v,s3})\prod_{v=1}^{N_{s4}}(1-\tau_{v,s4}) \quad (5\text{-}40)$$

$$p_{i,s3} = 1 - \prod_{v=1}^{N}(1-\tau_v)\prod_{v=1}^{N_{s1}}(1-\tau_{v,s1})\prod_{v=1}^{N_{s2}}(1-\tau_{v,s2})\prod_{v=1,v\neq i}^{N_{s3}}(1-\tau_{v,s3})\prod_{v=1}^{N_{s4}}(1-\tau_{v,s4}) \quad (5\text{-}40)$$

$$p_{i,s4} = 1 - \prod_{v=1}^{N}(1-\tau_v)\prod_{v=1}^{N_{s1}}(1-\tau_{v,s1})\prod_{v=1}^{N_{s2}}(1-\tau_{v,s2})\prod_{v=1}^{N_{s3}}(1-\tau_{v,s3})\prod_{v=1,v\neq i}^{N_{s4}}(1-\tau_{v,s4}) \quad (5\text{-}40)$$

We solve equation (5-22)-(5-26) and (5-40) numerically. After we get τ_i and $\tau_{i,s1}$, $\tau_{i,s2}$ $\tau_{i,s3}$ and $\tau_{i,s4}$, we obtain

$$P_{i,tr} = 1 - \prod_{v=1}^{N}(1-\tau_v)\prod_{v=1}^{N_{s1}}(1-\tau_{v,s1})\prod_{v=1}^{N_{s2}}(1-\tau_{v,s2})\prod_{v=1}^{N_{s3}}(1-\tau_{v,s3})\prod_{v=1}^{N_{s3}}(1-\tau_{v,s4}) \quad (5\text{-}41)$$

$$P_{i,tr,s1} = P_{i,tr,s2} = P_{i,tr,s3} = P_{i,tr,s4} = P_{i,tr} \quad (5\text{-}41)$$

$$P_{i,success} = \tau_i \prod_{v=1,v\neq i}^{N}(1-\tau_v)\prod_{v=1}^{N_{s1}}(1-\tau_{v,s1})\prod_{v=1}^{N_{s2}}(1-\tau_{v,s2})\prod_{v=1}^{N_{s3}}(1-\tau_{v,s3})\prod_{v=1}^{N_{s4}}(1-\tau_{v,s4}) \quad (5\text{-}42)$$

$$P_{i,success,s1} = \tau_{i,s1} \prod_{v=1}^{N}(1-\tau_v)\prod_{v=1,v\neq i}^{N_{s1}}(1-\tau_{v,s1})\prod_{v=1}^{N_{s2}}(1-\tau_{v,s2})\prod_{v=1}^{N_{s3}}(1-\tau_{v,s3})\prod_{v=1}^{N_{s4}}(1-\tau_{v,s4}) \quad (5\text{-}42)$$

$$P_{i,success,s2} = \tau_{v,s2} \prod_{v=1}^{N}(1-\tau_v)\prod_{v=1}^{N_{s1}}(1-\tau_{v,s1})\prod_{v=1,v\neq i}^{N_{s2}}(1-\tau_{v,s2})\prod_{v=1}^{N_{s3}}(1-\tau_{v,s3})\prod_{v=1}^{N_{s4}}(1-\tau_{v,s4}) \quad (5\text{-}42)$$

$$P_{i,success,s3} = \tau_{i,s3} \prod_{v=1}^{N}(1-\tau_v)\prod_{v=1}^{N_{s1}}(1-\tau_{v,s1})\prod_{v=1}^{N_{s2}}(1-\tau_{v,s2})\prod_{v=1,v\neq i}^{N_{s3}}(1-\tau_{v,s3})\prod_{v=1}^{N_{s4}}(1-\tau_{v,s4}) \quad (5\text{-}42)$$

$$P_{i,success,s4} = \tau_{i,s4} \prod_{v=1}^{N}(1-\tau_v)\prod_{v=1}^{N_{s1}}(1-\tau_{v,s1})\prod_{v=1}^{N_{s2}}(1-\tau_{v,s2})\prod_{v=1}^{N_{s3}}(1-\tau_{v,s3})\prod_{v=1,v\neq i}^{N_{s4}}(1-\tau_{v,s4}) \quad (5\text{-}42)$$

Then, we have the throughput of normal nodes and attacking node in single hop network which nodes cheat with 4 strategies combined by equations (5-22)-(5-25).

In Figure 5-3, we show a 24-normal-node and two-greedy-node single hop wireless network, where $\rho = [0,1]$ and $\rho_{s1} = [0,1]$. Its two greedy nodes with Strategy 1 have much higher throughput than

normal nodes. Figure 5-4 shows the throughput of a 24-normal-node and one-greedy wireless network. Figure 5-5 shows the throughput of a 8-normal-node and two -greedy wireless network. Figure 5-6 show the throughput of a 8-normal-node and one-greedy wireless network.

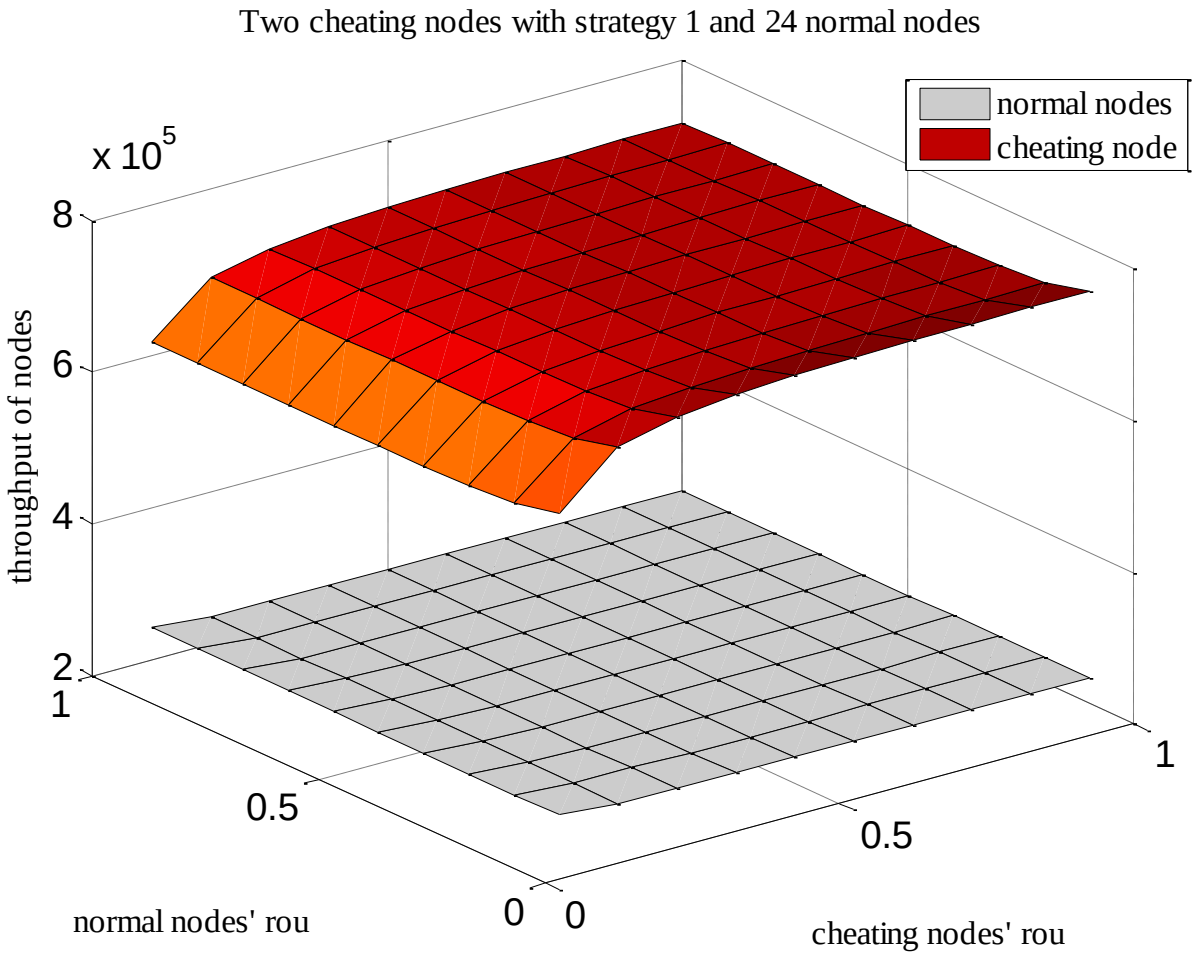

Figure 5-3: Throughput of a 24-normal-node and two-greedy-node single hop wireless (basic access)

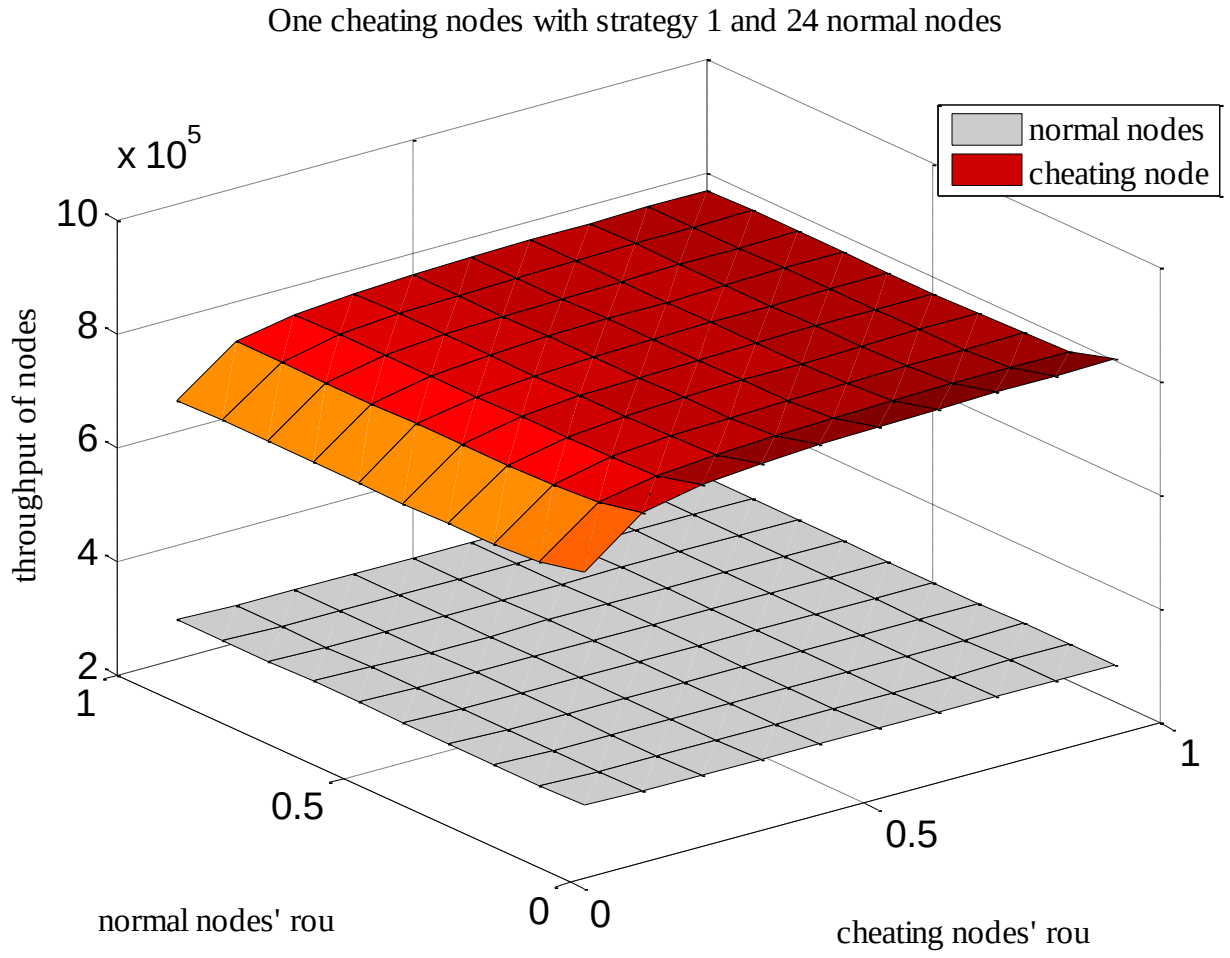

Figure 5-4: Throughput of a 24-normal-node and one-greedy-node single hop wireless (basic access)

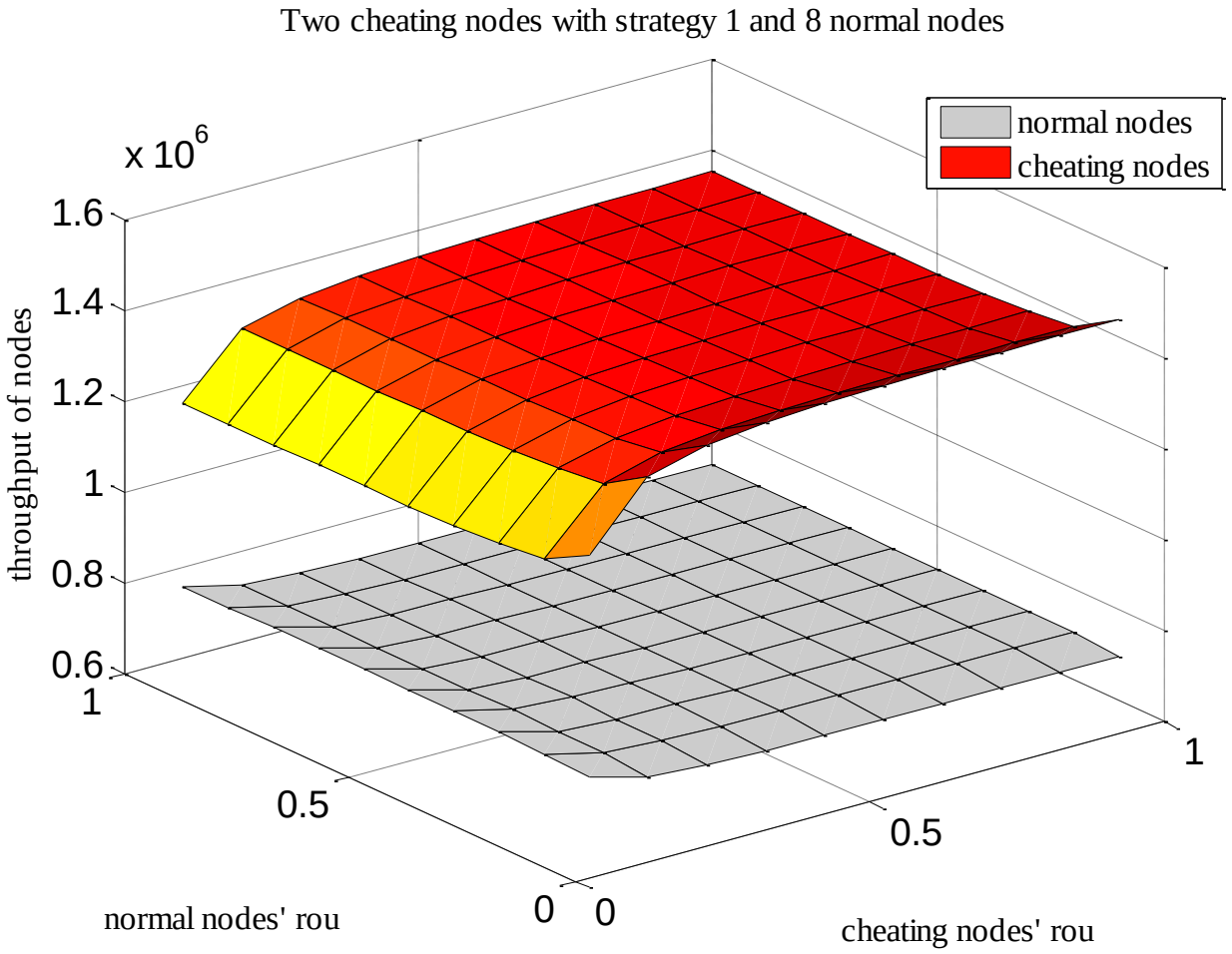

Figure 5-5: Throughput of a 8-normal-node and two-greedy-node single hop wireless (basic access)

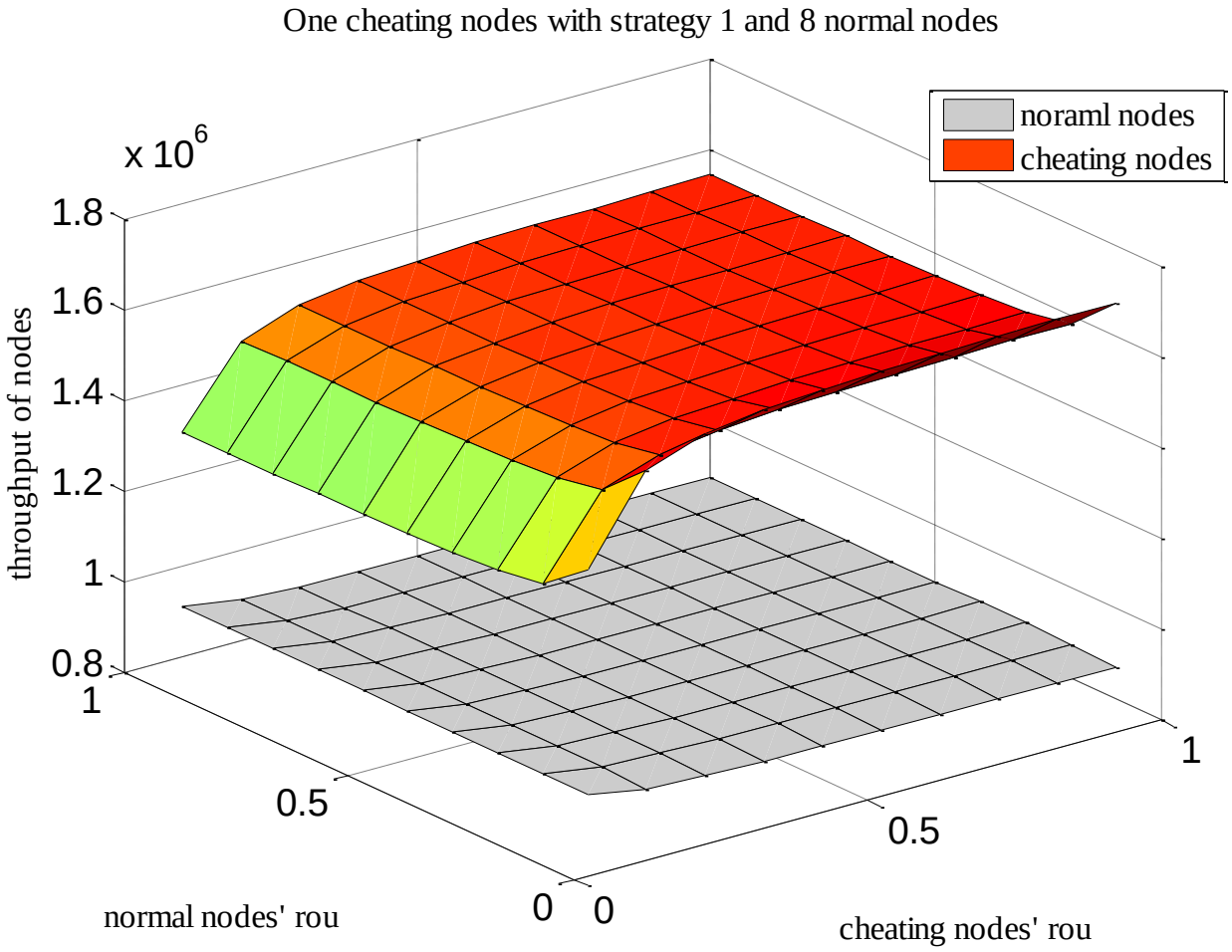

Figure 5-6 :Throughput of a 8-normal-node and one-greedy-node single hop wireless (basic access)

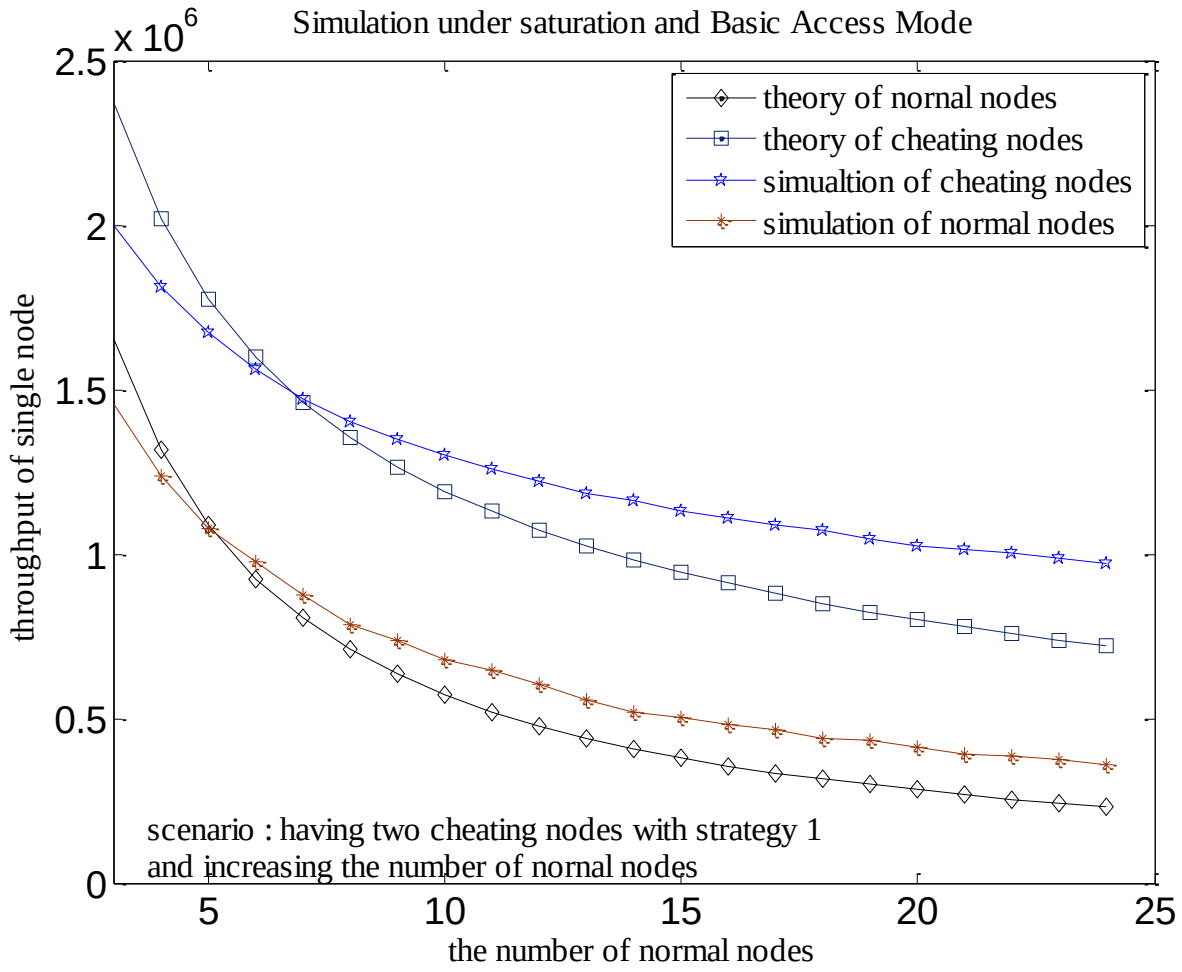

Figure 5-7: Throughput of a single hop wireless network(two greedy node playing strategy 1, under saturation and Basic Access mechanism)

OPNET is used as our simulation tools. In Figure 5-7, we compare theoretical and simulative throughput of a N -normal-node single hop and two-greedy wireless network, where greedy node applies Strategy 1, $\rho = 1$ and $\rho_{s1} = 1$. The theoretical throughput of normal node's is close to simulation throughput. The theoretical throughput of greedy node's is also close to its simulation throughput.

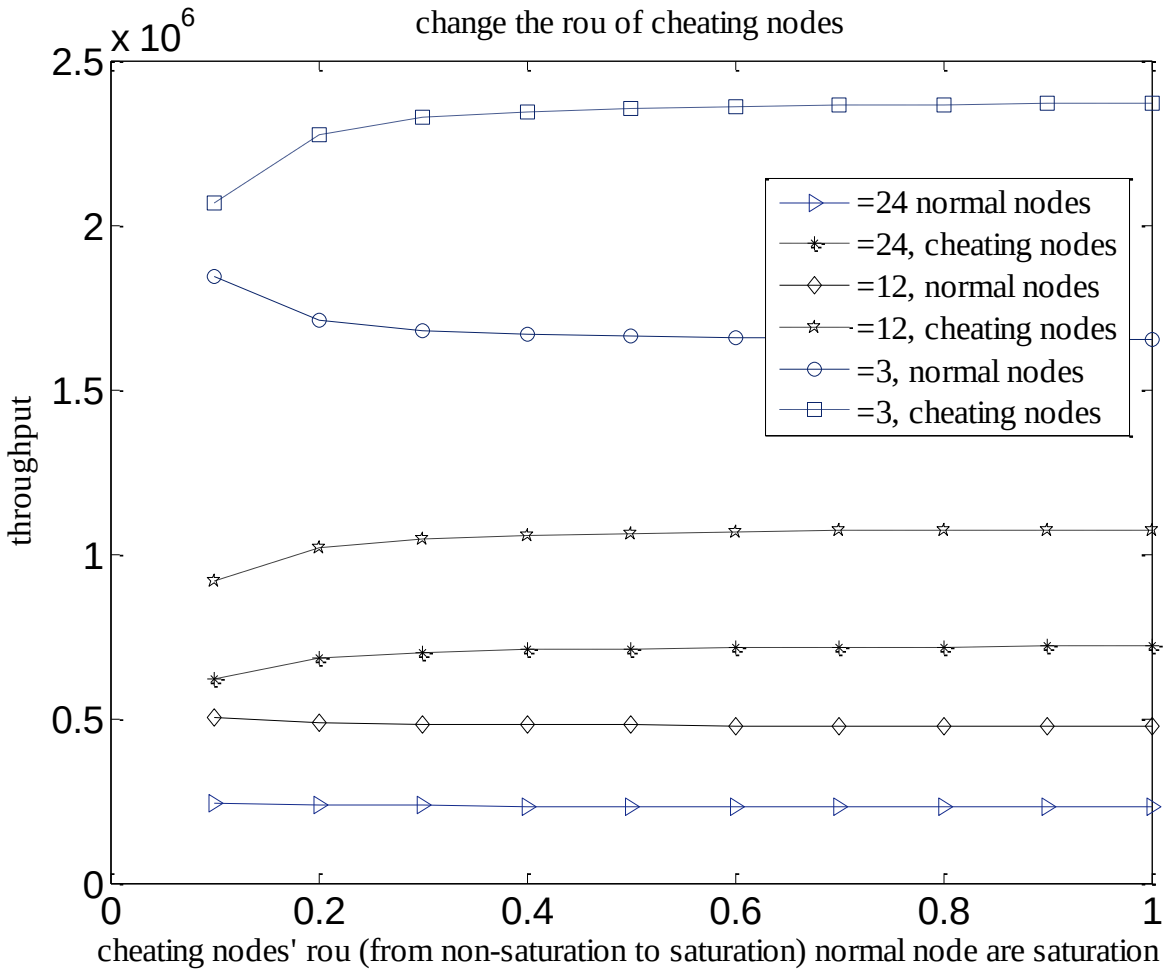

Figure 5-8: Change ρ_s1 of greedy nodes (from non-saturation to saturation) normal node are saturation

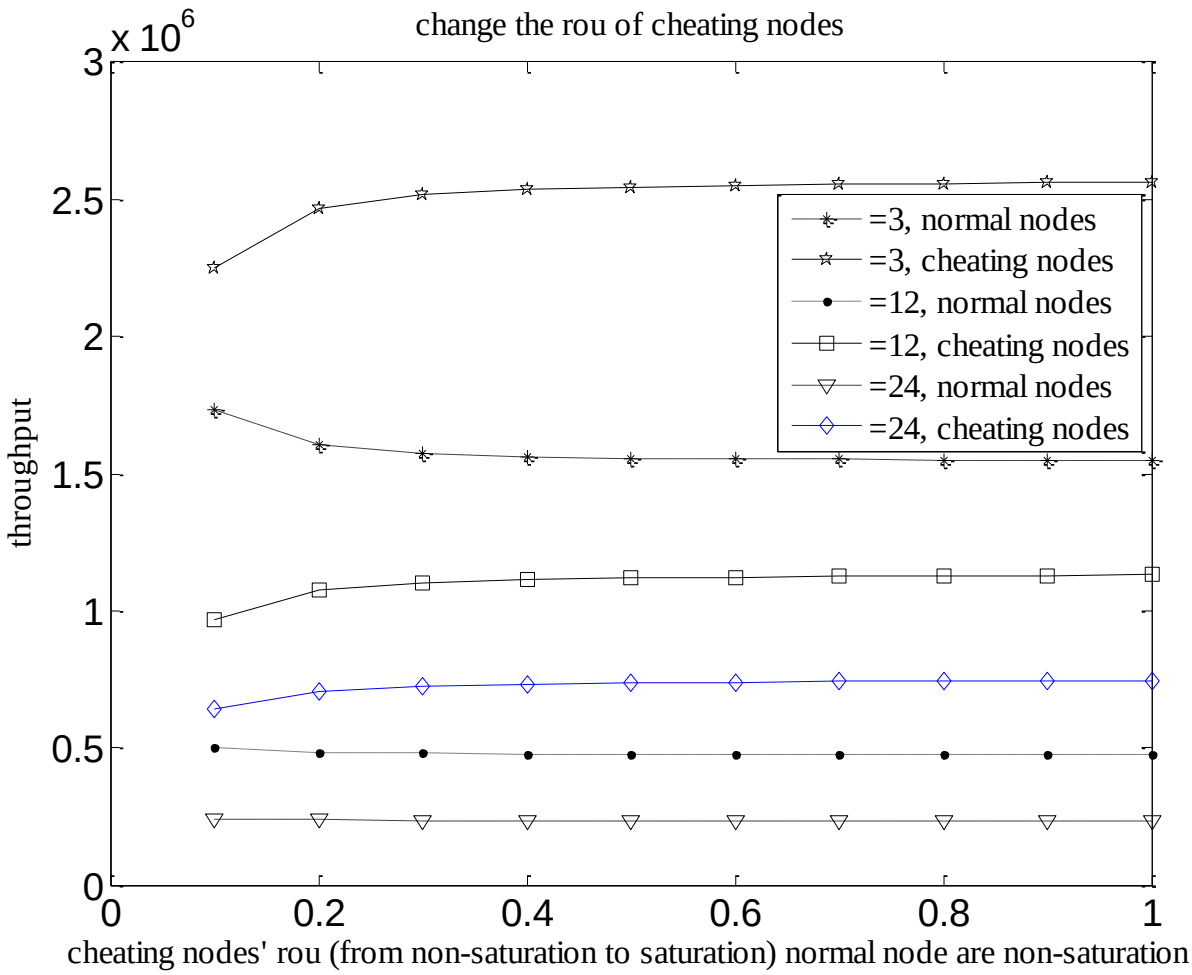

Figure 5-9: Change ρ_s1 of greedy nodes (from non-saturation to saturation) normal node are non-saturation

Figure 5-8 and figure 5-9 show the throughput of nodes when we change ρ_{s1} of greedy nodes, and keep same ρ normal node. Normal nodes are saturation in Figure 5-8 and are non-saturation in Figure 5-9. We can see the throughput of greedy node changes very gentle due to the change of ρ_{s1}. Unless the number of normal nodes is small, (3, for example, in figure 5-10). In a pair of curve, normal nodes are under non-saturation condition and in the other pair of curve, normal nodes are under saturation condition.

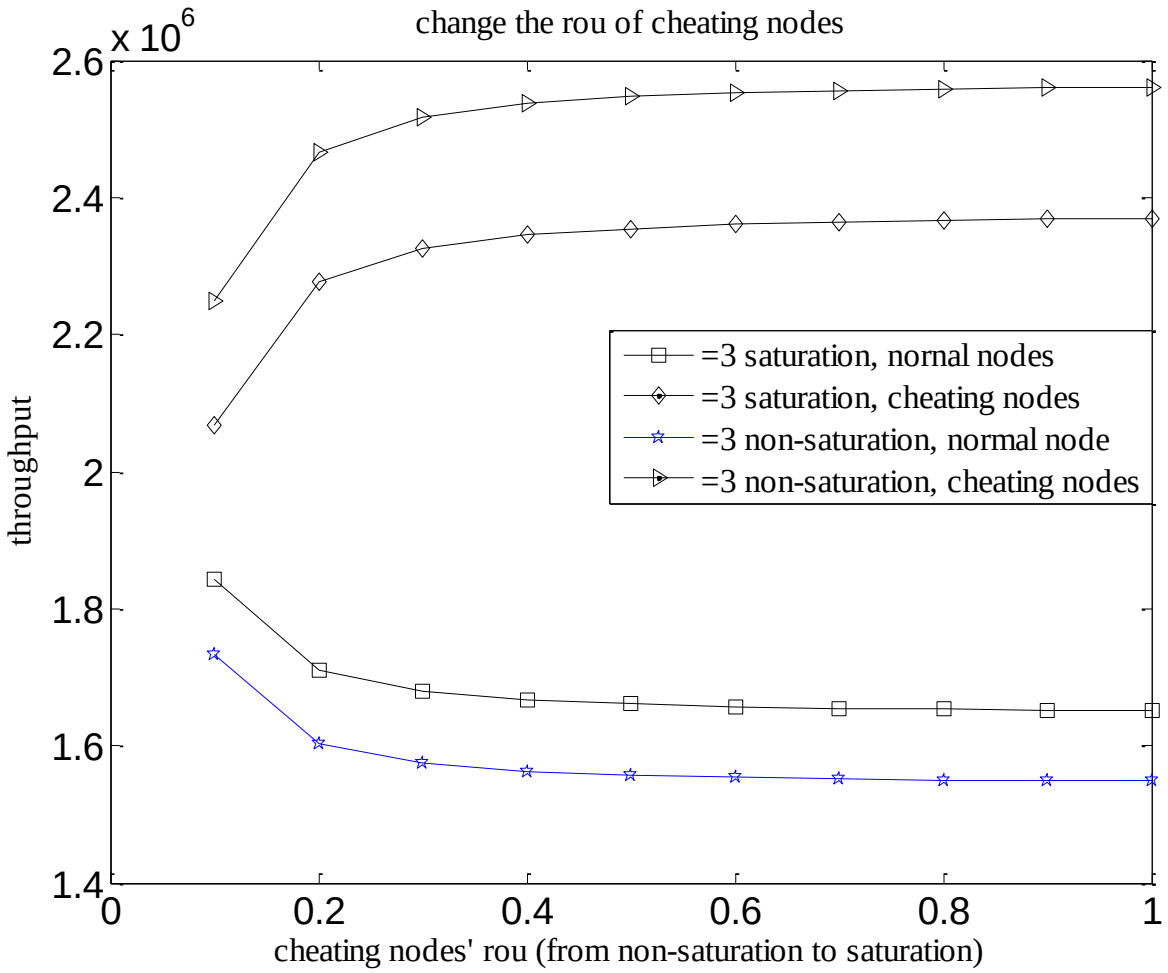

Figure 5-10: Change ρ_s1 of greedy nodes(from non-saturation to saturation). Normal node is saturation

5.3.2. Multihop wireless network with heterogonous traffic arrival rate

As a study scenario, depicted in Figure 5-11, all stations(dots) are randomly placed in three circles; the diameter of circles equals to a transmission range 912m. Yellow dots play normal backoff, red dots play greedy Strategy 1, blue dots play greedy Strategy 2; purple dots play greedy Strategy 3. All dots form a two-hop network.

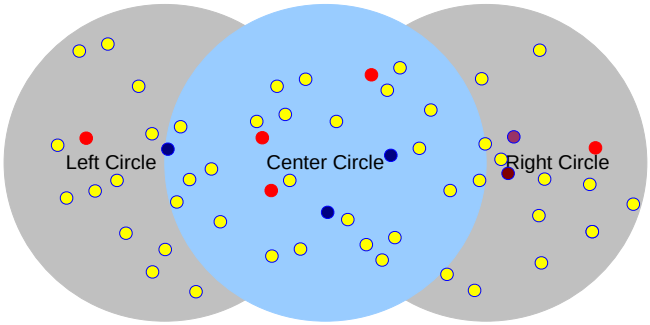

Figure 5-11: A two-hop ad hoc wireless network in presence greedy node

In the network, we have N yellow dots(good behaviors), N_{s1} red dots(playing strategy 1), N_{s2} blue dots(playing strategy 2) and N_{s3} purple dots(playing strategy 3). First we check the distance among dots. If the distance to dot i is less than 912 m, the dot will belong to neighbors' dots set of dot i, denoted by set v, v_{s1}, v_{s2} or v_{s3} relatively. Hence, we obtain

$$p_i = 1 - \prod_v (1-\tau_v) \prod_{v_{s1}} (1-\tau_{v,s1}) \prod_{v_{s2}} (1-\tau_{v,s2}) \prod_{v_{s3}} (1-\tau_{v,s3}) \quad (5\text{-}43)$$

$$p_{i,s1} = 1 - \prod_v (1-\tau_v) \prod_{v_{s1}} (1-\tau_{v,s1}) \prod_{v_{s2}} (1-\tau_{v,s2}) \prod_{v_{s3}} (1-\tau_{v,s3}) \quad (5\text{-}43)$$

$$p_{i,s2} = 1 - \prod_v (1-\tau_v) \prod_{v_{s1}} (1-\tau_{v,s1}) \prod_{v_{s2}} (1-\tau_{v,s2}) \prod_{v_{s3}} (1-\tau_{v,s3}) \quad (5\text{-}43)$$

$$p_{i,s3} = 1 - \prod_v (1-\tau_v) \prod_{v_{s1}} (1-\tau_{v,s1}) \prod_{v_{s2}} (1-\tau_{v,s2}) \prod_{v_{s3}} (1-\tau_{v,s3}) \quad (5\text{-}43)$$

Though the form of equation (5-46) are alike, the sets of yellow dots, red dots, blue dots and purple dots are different. We can solve equation (5-22)-(5-25) and (5-43) numerically again. After we get τ_i and $\tau_{i,s1}$, $\tau_{i,s2}$ and $\tau_{i,s3}$, we obtain

$$P_{i,tr} = 1 - (1-\tau_i) \prod_v (1-\tau_v) \prod_{v_{s1}} (1-\tau_{v,s1}) \prod_{v_{s2}} (1-\tau_{v,s2}) \prod_{v_{s3}} (1-\tau_{v,s3}) \quad (5\text{-}44)$$

$$P_{i,tr,s1} = 1 - (1-\tau_{i,s1}) \prod_v (1-\tau_v) \prod_{v_{s1}} (1-\tau_{v,s1}) \prod_{v_{s2}} (1-\tau_{v,s2}) \prod_{v_{s3}} (1-\tau_{v,s3}) \quad (5\text{-}44)$$

$$P_{i,tr,s2} = 1 - (1-\tau_{i,s2}) \prod_v (1-\tau_v) \prod_{v_{s1}} (1-\tau_{v,s1}) \prod_{v_{s2}} (1-\tau_{v,s2}) \prod_{v_{s3}} (1-\tau_{v,s3}) \quad (5\text{-}44)$$

$$P_{i,tr,s3} = 1 - (1-\tau_{i,s3}) \prod_v (1-\tau_v) \prod_{v_{s1}} (1-\tau_{v,s1}) \prod_{v_{s2}} (1-\tau_{v,s2}) \prod_{v_{s3}} (1-\tau_{v,s3}) \quad (5\text{-}44)$$

If the distance to a destination dot of dot i is less than 912m, the dots will belong to hidden dots set, denoted by hidden sets hv, hv_{s1}, hv_{s2} or hv_{s3}. Hence we obtain(if a dot belongs to neighbor set and hidden set, we only multiple $(1-\tau_v)$ once)

$$P_{i,success} = \tau_i \prod_v (1-\tau_v) \prod_{v_{s1}} (1-\tau_{v,s1}) \prod_{v_{s2}} (1-\tau_{v,s2}) \prod_{v_{s3}} (1-\tau_{v,s3}) \prod_{hv} (1-\tau_{hv}) \prod_{hv_{s1}} (1-\tau_{hv,s1}) \prod_{hv_{s2}} (1-\tau_{hv,s2}) \prod_{hv_{s3}} (1-\tau_{hv,s3}) \quad (5\text{-}45)$$

$$P_{i,success,s1} = \tau_{i,s1} \prod_v (1-\tau_v) \prod_{v_{s1}} (1-\tau_{v,s1}) \prod_{v_{s2}} (1-\tau_{v,s2}) \prod_{v_{s3}} (1-\tau_{v,s3}) \prod_{hv} (1-\tau_{hv}) \prod_{hv_{s1}} (1-\tau_{hv,s1}) \prod_{hv_{s2}} (1-\tau_{hv,s2}) \prod_{hv_{s3}} (1-\tau_{hv,s3}) \quad (5\text{-}45)$$

$$P_{i,success,s2} = \tau_{i,s2} \prod_v (1-\tau_v) \prod_{v_{s1}} (1-\tau_{v,s1}) \prod_{v_{s2}} (1-\tau_{v,s2}) \prod_{v_{s3}} (1-\tau_{v,s3}) \prod_{hv} (1-\tau_{hv}) \prod_{hv_{s1}} (1-\tau_{hv,s1}) \prod_{hv_{s2}} (1-\tau_{hv,s2}) \prod_{hv_{s3}} (1-\tau_{hv,s3}) \quad (5\text{-}45)$$

$$P_{i,success,s3} = \tau_{i,s3} \prod_v (1-\tau_v) \prod_{v_{s1}} (1-\tau_{v,s1}) \prod_{v_{s2}} (1-\tau_{v,s2}) \prod_{v_{s3}} (1-\tau_{v,s3}) \prod_{hv} (1-\tau_{hv}) \prod_{hv_{s1}} (1-\tau_{hv,s1}) \prod_{hv_{s2}} (1-\tau_{hv,s2}) \prod_{hv_{s3}} (1-\tau_{hv,s3}) \quad (5\text{-}45)$$

We may have multiple destination nodes of node i. So the $P_{i,success}$, $P_{i,success,s1}$, $P_{i,success,s2}$ and $P_{i,success,s3}$will have multiple values. Thus, we will have a summary of the throughputs. Assume every dot sends a packet to a destination randomly, then we add the multiple throughputs and obtain an average throughput of node .

We program and let a computer find the neighbor sets and hidden sets and obtain the average throughput and delay of the wireless network.

In Figure 5-12, we show a two-hop wireless network, where we have 3 red dots in Area A and 4 blue dots in Area C. Green dots is in Area B, increasing from 6 to 20. Two yellow dots are greedy node. We mark Node C1, Node C2 and Greedy Node 2 in figure 5-12. $\rho = 1$ and $\rho_{s1} = 1$. Its greedy node applies Strategy 1.

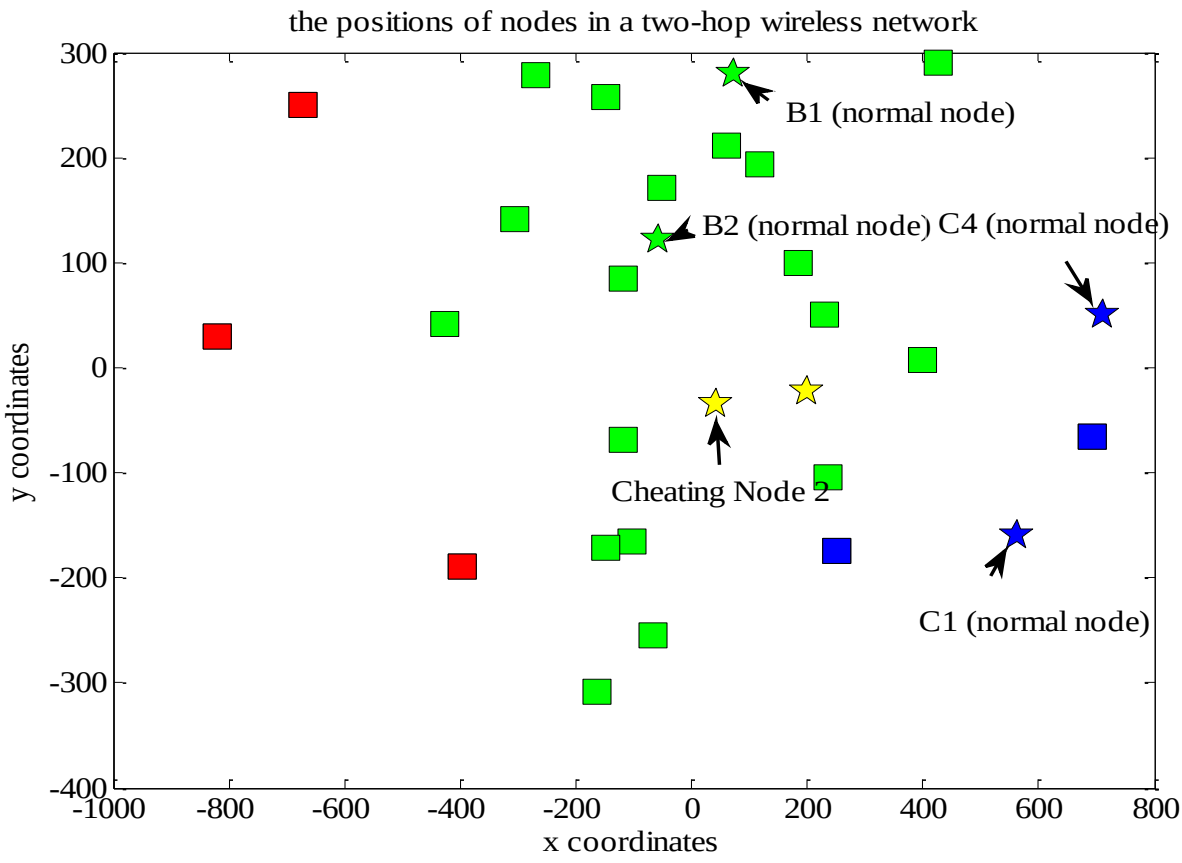

Figure 5-12: Location of each nodes

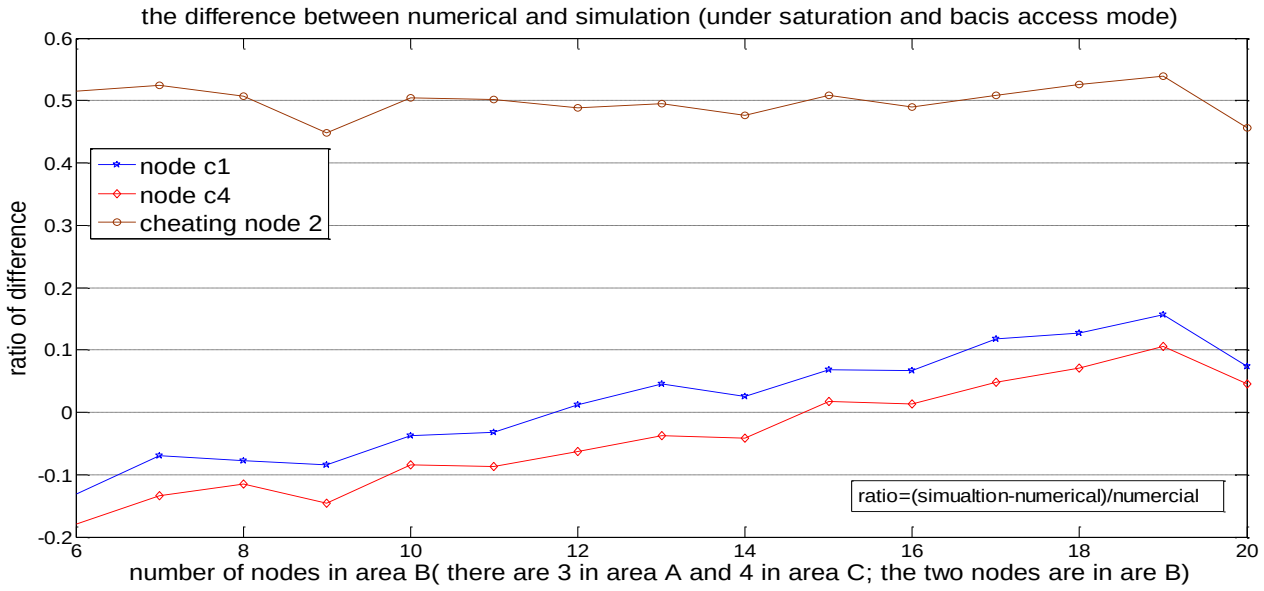

Figure 5-13: Ratio of throughput difference of the two-hop wireless network (under saturation and basic access mechanism)

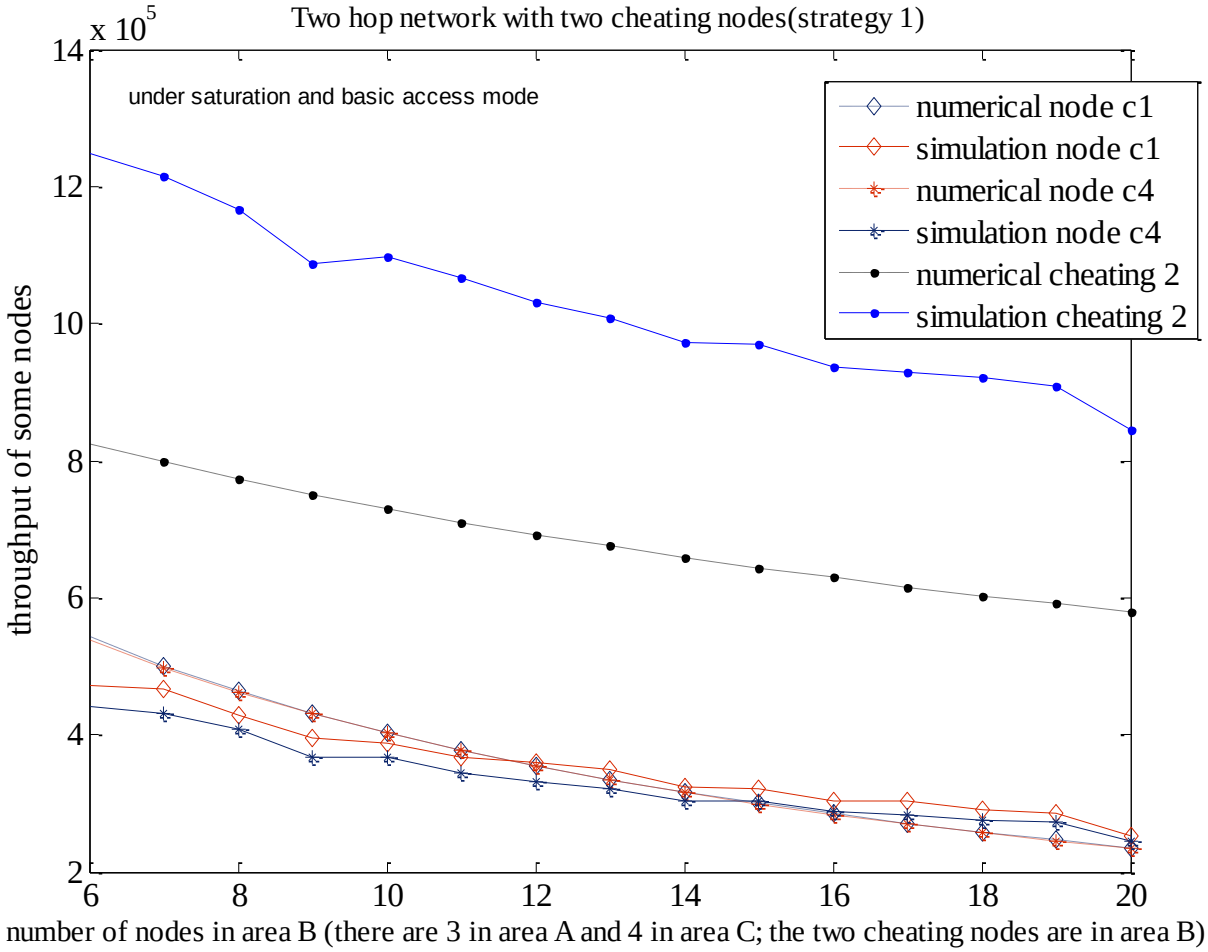

Figure 5-14: Throughputs of normal C1, C2 and Greedy 2 in the two-hop wireless network (under saturation and basic access mechanism, two greedy nodes playing strategy 1)

We compare throughputs of the two-hop wireless network. Figure 5-13 is the ratio of difference between theoretical and simulation throughput (under saturation and basic access mechanism). The theoretical throughputs of normal node C1 and C4(we choose the two objects randomly) are close to simulation throughput; most different are less than $\pm$10% when the number of nodes in area B increased from 6 to 20. The theoretical throughput of greedy node's has higher different ratio, 50%; we will discuss the reason latter. Figure 5-14. is the throughputs of normal Nodes C1 and C4 and Greedy Node 2 in a two hop network with two greedy nodes (strategy 1), under saturation and basic access mechanism. Figure 5-15. is throughputs of the normal Nodes B1 and B2 and Greedy node C2. The

curve for normal node match well and the curve of greedy node have a obvious different, however, their trends are the same.

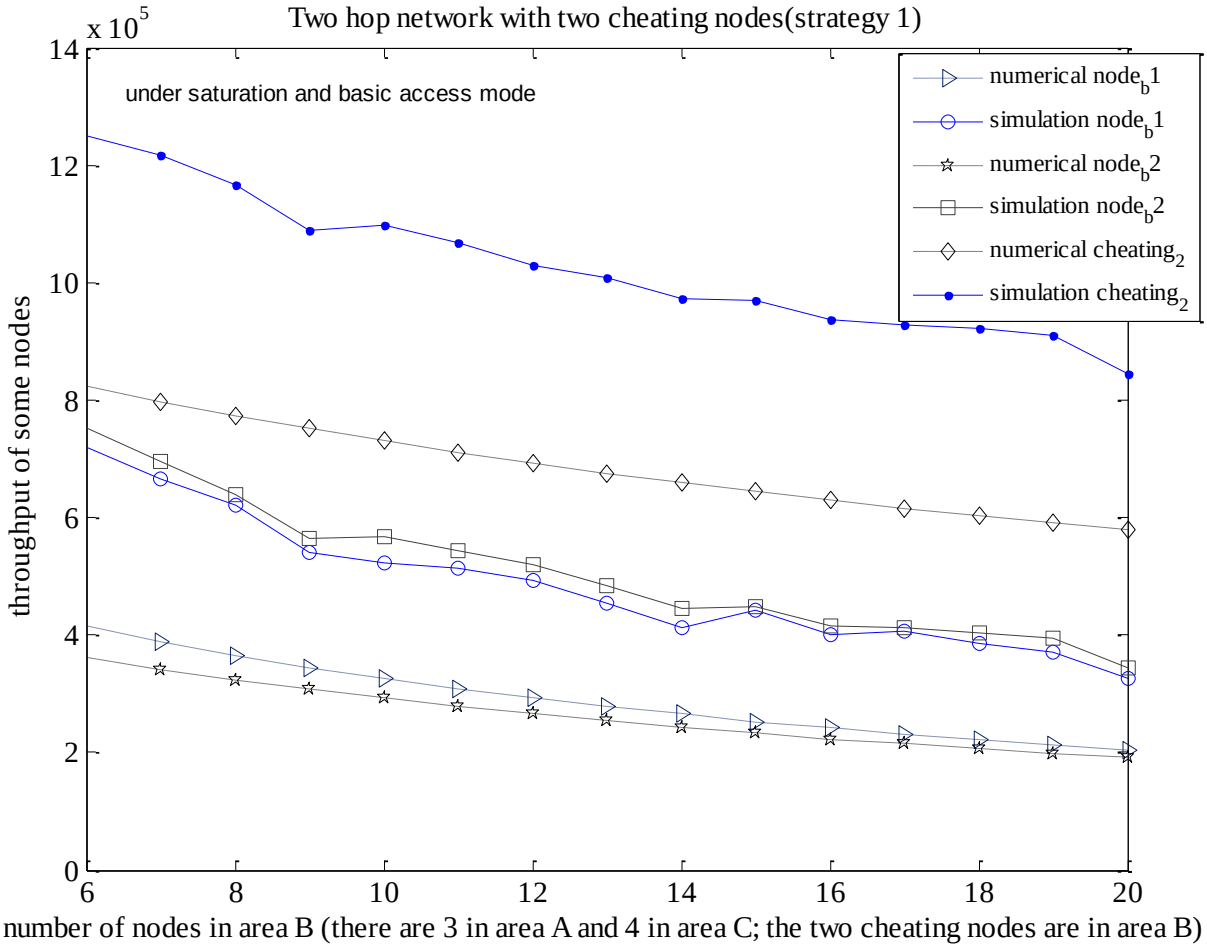

Figure 5-15: Throughputs of normal B1, B2 and Greedy 2 in the two-hop wireless network (under saturation and basic access mechanism, two greedy nodes playing strategy 1)

5.4. Summary

In this chapter, we investigate various greedy behavior strategies used in IEEE 802.11 wireless networks, and provide an analytical method to obtain the performance in the presence of various greedy behavior strategies. Our method is able to determine the performance of greedy nodes with different packet arriving rates. And our method is able to apply to different wireless network topology structures.

This is significant because each node often has different applications with different packet arriving rates in different topology networks.

Differently from previous papers, our improvement provides the performance parameters of greedy nodes with different arrival rates under non- saturation condition. It also provides an analytical performance of multi-hop networks, or networks with hidden nodes, or networks with multiple greedy strategies combined. Each node's expected throughput and delay of MAC layer in a complex network scenario, including attacking nodes, are calculated with three two-dimensional non-saturation Markov chain models.

The simulations are checked and prove that our analysis is validated in multiple greedy scenarios.

6. Conclusion

The goal of our research has been to discover and understand applications of the Markov chain analytical model. In this dissertation, we have investigated three focuses of current interest: the distortion of video quality, the performance of directional MAC (D-MAC) protocols, and the performances of IEEE 802.11 wireless networks with various greedy behavior and heterogeneous traffic. We have provided numerical solution to the three issues with the Markov chain analytical model. The major contributions are summarized as follows.

6.1. Contributions

In Chapter 2, we illustrate how to obtain the performances of IEEE 802.11 wireless networks with heterogeneous traffic. The applying of degree of ρ makes our approach simpler than previous research literature.

In Chapter 3, we propose an integral approach to compute the inherent distortion of video quality in IEEE 802.11 wireless networks. Our work is motivated by the increased needs of video services that have boomed through IEEE 802.11 wireless networks, the convergence of wireless/mobile, and other emerging networks. With a two-dimensional non-saturation Markov Chain model and ITU-T Recommendation G.1070, we obtain an analytical expression of the inherent distortion of video quality in IEEE 802.11 wireless networks. Then we employ the formulae to predict a quantitative video quality with setting parameters of IEEE802.11; so that video planners are able to maintain a user's specific level of satisfaction with the setting parameters. This provides flexibility for evaluating different topologies and parameter settings.

In this chapter, we further study optimization of setting parameters of IEEE 802.11 to minimize the distortion. The optimal setting suggestion tells us to choose a large frame retry and a large minimum contention window to get a large objective video quality, and acceptable delay and jitter. Otherwise the

loss rate will be higher, and the video application becomes unacceptable, and it may force us give up some methods to send videos, which have no higher layer retransmission guarantee, for example, using UDP or broadcast, or multicast to deliver video to more than 20 wireless nodes.

In this chapter, we also expand the expressions to scenarios where some IEEE 802.11 wireless nodes manipulate their backoff schemes. We prove quantitatively that the video quality of those manipulating nodes is enhanced.

In this chapter, we discuss the effect of the presence of a hidden station. The objective video quality, delay, jitter, and drop rate of Node A, which is affected by hidden nodes directly, change due to the presence of hidden stations. On the other hand, the objective video quality, delay, jitter, and drop rate of node C, which is not affected by hidden nodes directly, does not change much due to the presence of hidden stations.

We notice that basic access and RTS/CTS access have the same packet-loss rate in a wireless network, we then have the same objective video quality; however, the two accesses have different throughput. Higher throughput does not always imply higher video quality. The size of packets also affects the throughput, but the size does not affect the packet-loss rate and the objective video quality.

In Chapter 4, we propose a Markov Chain to equivalently describe a directional MAC protocols. With the new Markov Chain, we are able to presented transmission probabilities of each transmitting antenna element at a random slottime. Based on transmission probabilities, we obtain throughput and delay of a MAC layer of each transmitting antenna element of each node in the wireless network.

As an example, our analytical approach is applied to two single-hop wireless networks, which nodes are distributed randomly. Numerical results show that the average all-direction-aggregating throughput in a 64-node network will increase in a faster pace for RTS/CTS access mechanism than basic access mechanism; it has average increase of 0.2331 for RTS/CTS access mechanism and 0.0718 for Basic

access mechanism, while transmitting antenna elements increase from one to eight. The single direction average transmission probabilities of per node also change noticeably (0.02016-0.03034) when the number of transmitting antenna elements is changed in the 64-node wireless network. For a 48-node wireless network, its average single direction delay of per node (basic access) will decline from 2920.7 μs to 1291.4 μs when the transmitting antenna elements are increased from one to eight.

We find the performance of MAC layer depends on the antenna system and its parameters as well as the topology and DMAC's requirements. The numerical results change in 32-node, 48-node, 56-node and 64-node wireless networks. The 32-node network has the lowest delay and the 64-node network has highest delay. With the results, we can know that directional antennas improve the performance straightforwardly.

We also evaluate how protocols impact on network performance, and propose to maximize the benefits of directional antennas. Some details of directional MAC protocols are discussed and their performances are compared in this paper. The performance between half-duplex antenna system and full-duplex antenna system are $\left(1-\tau_{destination,receiv\ direction}\right)$. The numerical results will show $\tau_{destination,receiv\ direction}$ is very small, (0-0.056). Therefore, not to build independent receive antenna element is a good engineering choice. (Making half-duplex antenna system is cheaper and full- duplex antenna system does not increase performance. The throughputs difference between RTS/CTS sending Omni-directionally and RTS/CTS sending directionally is $\left[\sum_{v=0;v\neq i}^{N}\frac{Throughput_{v,\mu}}{E[lenght\ of\ packet]}\times T_{rts\ cts}+\sum_{\omega=1;\omega\neq\mu}^{N_{tx}}\sum_{v=0;v\neq i}^{N}\frac{Throughput_{v,\omega}}{E[lenght\ of\ packet]}\times T_{rts\ cts}\right]$.

In Chapter 5, we study some common greedy behavior strategies, and give analytical formulae for the performance of IEEE 802.11 wireless networks in the presence of various greedy nodes, such as throughput and delay. Theoretical and simulative results prove obviously that the greedy node has

higher throughput than a normal node no matter whether in single hop wireless network or multihop wireless networks.

Unlike previous research literature, we have shown that our analytical formulae are able to determine the performance with different packet arrival rates, and are able to apply to different wireless network topology structures, or networks with multiple greedy strategies combined. Each node's expected throughput and delay in a complex network scenario, including greedy nodes, are calculated with three two-dimensional non-saturation Markov chain analysis models. This is significant because each node often has different applications with different packet arriving rates in different topology networks.

The simulations are provided and prove that our analysis is validated in multiple greedy scenarios.

6.2. Future Directions

Objective video evaluations are mathematical models. This means we can develop an automatic program to predict quality of objective video. However, the QoE opinion model calculates objective video quality V_q, video quality robustness D_{PplV}, and objective measurement of basic video quality accounting for coding distortion, I_{coding}. These two values, D_{PplV} and I_{coding}, are derived with subjective video quality described in ITU-T G.1070. Getting I_{coding} and D_{PplV} is a subjective approach. It is not appropriate to be processed automatically using network parameters.

Video content has an impact on video quality under same network conditions, which means different video content has different I_{coding} and D_{PplV}, and then has different V_q under same network conditions. However, we do not investigate the effects of different content on the perceived video quality in this paper. We do not discuss the burst losses in video packets either.

Moreover, the QoE was proven to be inaccurate in terms of correlation with perceived visual quality in many cases [8]. The PSNR-mapped-to-MOS technique does not always match up with one another.

Therefore, based on PSNR, a new analytical expression of the inherent distortion of video quality in IEEE 802.11 wireless networks will be our future research.

Some simulations in OPNET 15.0 have checked the validity of the analytical model for greedy behavior. But simulation for DMAC and video quality has not been completed.

7. Bibliography

1. IEEE Std 802.11, 1999 Edition Part 11: Wireless LAN Medium Access Control (MAC) and Physical Layer (PHY) specifications.
2. IEEE 802.11e (2005) : Part 11: Wireless LAN Medium Access Control (MAC) and Physical Layer (PHY) Amendment 8: Medium Access Control (MAC) Quality of Service Enhancements.
3. ITU-T G.1070 "Opinion model for video-telephony applications".
4. ITU-T J.241 "Quality of service ranking and measurement methods for digital video services delivered over broadband IP networks ".
5. Babich, F. D'Orlando, M. and Vatta, F. "Video Quality Estimation in Wireless IP Networks: Algorithms and Applications" ACM Transactions on Multimedia Computing, Communications, and Applications (TOMCCAP) Volume 4, Issue 1 (January 2008) .
6. Bellofiore, S. Foutz, J. Govindarajula, R. Bahçeci, I. Balanis, C. Spanias, A. Capone, J. and Duman, T. Smart Antenna System Analysis, Integration and Performance for Mobile Ad-Hoc Networks, MOBICOM'02, Atlanta, Georgia, USA , September 23–28, 2002.
7. Bianchi, G.; Performance analysis of the IEEE 802.11 distributed coordination function. Selected Areas in Communications, IEEE Journal on Volume 18, Issue 3, March 2000 Page(s):535 – 547.
8. Bianchi, G. and Tinnirello, I. "Remarks on IEEE 802.11 DCF Performance Analysis" IEEE Communications Letters, Vol. 9, No. 8, AUGUST 2005 765.
9. Bouazizi, I. "Estimation of Packet Loss Effects on Video Quality", First International Symposium on Control, Communications and Signal Processing, 2004.
10. Calyam, P. Ekici, E. Lee, C. Haffner, M. Howes, N. ' A "GAP-Model" based Framework for Online VVoIP QoE Measurement', Journal of Communications and Networks, Vol. 9, No.4, Dec. 2007, pp. 446-56.

11. C´ardenas, A. Radosavac, S. and Baras, J “Detection and Prevention of MAC Layer Misbehavior in Ad Hoc Networks”, SASN’04, Washington, DC, USA, October 25, 2004.
12. Chen, L. and Leneutre, J. “Selfishness, Not Always A Nightmare Modeling Selfish MAC Behaviors in Wireless Mobile Ad Hoc Networks”,27th International Conference on Distributed Computing Systems (ICDCS'07).
13. Choi, L. Ivrlaˇc, M. Steinbach, E. and Nossek, J."Analysis of Distortion Due to Packet Loss in Streaming Video Transmission over Wireless Communication Links", Proceedings of the International Conference on Image Processing, vol. 1, pp. 189–192, September 2005.
14. Choudhury, R. Yang, X. Ramanathan, R. Vaidya, N. On designing MAC protocols for wireless networks using directional Antennas, MobiHoc’03, Annapolis, Maryland, USA, June 1–3, 2003.
15. Choudhury, R. Vaidya, N. Performance of ad hoc routing using directional antennas, IEEE Transactions on antennas and propagation, Vol. 50, No. 5, May 2002
16. Choudhury, R. and Vaidya, N. Deafness: A MAC problem in ad hoc networks when using directional antennas, MOBIHOC’02, EPFL, Lausanne, Switzerland, June 9-11, 2002.
17. Choudhury, R. Yang, X. Ramanathan R. and Vaidya, N. Using Directional Antennas for Medium Access Control in Ad Hoc Networks, IEEE Globecom 2005.
18. Cranley, N. “Video Frame differentiation for Streamed Multimedia over Heavily Loaded IEEE 802.11e WLAN” , IEEE 18th International Symposium on Personal, Indoor and Mobile Radio Communications, 2007. PIMRC 2007.
19. Dai, H. Ng , K. Wu, M. An Overview of MAC Protocols with Directional Antennas in Wireless ad hoc, IEEE Transactions on wireless communications, Vol. 6, No. 3, March 2007.
20. Duffy, K. Malone,D. and Leith, D."Modeling the 802.11 Distributed Coordination Function in Non-saturated Conditions," IEEE Comm. Letters. Vol. 9, No. 8, 715–717, Aug. 2005.

21. Engelstad, P.E. and Østerbø, O.N. Analysis of QoS in WLAN (this paper discuss about Analysis of Non-Saturation and Saturation Performance of IEEE 802.11 DCF), Telektronikk, Vol. 1, 2005.
22. Foh, C. Zhang, Y. , Ni, Z., Cai,J. and Ngan, K., "Optimized Cross-Layer Design for Scalable Video Transmission Over the IEEE 802.11e Networks", IEEE Transactions on Circuits and System for Video Technology, Vol. 17, No. 12, December 2007.
23. Goldsmith, A. Jafar, S. Jindal, N. Vishwanath, S. "Capacity Limits of MIMO Channels", IEEE Journal on Selected Areas in Communications, June 2003.
24. Gossain, H. Cordeiro, C. and Agrawal, D. MDA an efficient directional MAC scheme for wireless ad hoc networks, IEEE Journal on Selected Areas in Communications, Vol. 21, No. 5, June 2003
25. Guang, L. and Assi, C. "A Self-Adaptive Detection System for MAC Misbehavior in Ad Hoc Networks", ICC '06. IEEE International Conference on Communications, 2006.
26. Guang, L. Assi, C. and Benslimane, A. "Enhancing IEEE 802.11 Random Backoff in Selfish Environments", IEEE Transactions on Vehicular Technology, Vol. 57, No. 3, May 2008.
27. Guang, L. and Assi, C. "Vulnerabilities of ad hoc network routing protocols to MAC misbehavior", (WiMob'2005), IEEE International Conference on Wireless And Mobile Computing, Networking And Communications, 2005.
28. Guang, L., Assi, C. and Benslimane, A. "Enhancing IEEE 802.11 Random Backoff in Selfish Environments", IEEE Transactions on Vehicular Technology, Vol. 57, No. 3, MAY 2008
29. Gupta, P. "The capacity of wireless networks", IEEE Transactions on Information Theory, 2000.
30. Hady, M and Ward, R"A Framework for Evaluating Video Transmission over Wireless Ad Hoc Networks", IEEE Pacific Rim Conference on Communications, Computers and Signal Processing, 2007.

31. He, Z. and Xiong, H. "Transmission Distortion Analysis for Real-Time Video Encoding and Streaming Over Wireless Networks " IEEE Transactions on Circuits and System for Video Technology, Vol.. 16, No. 9, September 2006
32. Hsu, J. and Rubin, I. “Performance analysis of directional random access scheme for multiple access mobile ad-hoc wireless networks”, IEEE Transactions on Parallel and Distributed Systems, Vol. 15, No. 12, December 2004
33. Huang, C.L., Liao, W.; Throughput and delay performance of IEEE 802.11e enhanced distributed channel access (EDCA) under saturation condition. Wireless Communications, IEEE Transactions on Volume 6, Issue 1, Jan. 2007 Page(s):136 – 145.
34. Huang, Z. and Shen, C. “A comparison study of omnidirectional and directional MAC protocols for ad hoc network”, Global Telecommunications Conference, 2002. GLOBECOM '02.
35. Hung, F.-Y. and Marsic, I., Analysis of Non-Saturation and Saturation Performance of IEEE 802.11 DCF in the Presence of Hidden Stations, Proceedings of the IEEE 66th Vehicular Technology Conference (VTC-Fall-2007), Sept. 30 - Oct. 3, 2007.
36. Inaltekin, H. and Wicker,S. “The Analysis of a Game Theoretic MAC Protocol for Wireless Networks”, 3rd Annual IEEE Communications Society on Sensor and Ad Hoc Communications and Networks, 2006.
37. Jakllari, G. Luo, W. and Krishnamurthy, S. “An Integrated Neighbor Discovery and MAC Protocol for Ad Hoc Networks Using Directional Antennas”, IEEE Transactions on Wireless Communications, Volume: 6 Issue:3 March 2007.
38. Jrad, Z., Hammi, R. and Krief, F."Video Applications Quality Improvement in Wireless Systems: QoS Negotiation and Rate Control" , International Conference on Digital Telecommunications (ICDT'06).

39. Khan, A., Sun, L. and Ifeachor, E. , "Content-Based Video Quality Prediction for MPEG4 Video Streaming over Wireless Networks", Journal of Multimedia, Vol. 4, No. 4, August 2009
40. Konorski, J. A "Game-Theoretic Study of CSMA/CA Under a Backoff Attack", IEEE/ACM Transactions on NETWORKING, Vol. 14, No. 6, December 2006.
41. Konorski, J. "Solvability of a Markovian model of an IEEE 802.11 LAN under a backoff attack", Proceedings of the 13th IEEE International Symposium on Modeling, Analysis, and Simulation of Computer and Telecommunication Systems (MASCOTS'05).
42. Korakis, T. Jakllari, G. Tassiulas, L. CDR-MAC: A Protocol for Full Exploitation of Directional Antennas in Ad Hoc Wireless, Proceedings of the 12th IEEE International Conference on Network Protocols (ICNP'04).
43. Ko, Y. and Shankarkumar, V. and Vaidya, N. Medium access control protocols using directional antennas in Ad Hoc Networks, MobiHoc'04, May 24–26, 2004, Roppongi, Japan.
44. Kyasanur, P. and Vaidya, N. "selfish MAC layer misbehavior in wireless networks", IEEE Transactions on Mobile Computing, Vol. 4, No. 5, September/October 2005.
45. Lal, D. Jain, V. Zeng, Q. and Agrawal, D. "Performance evaluation of medium access control for multiple-beam antenna nodes in a wireless LAN", Ad Hoc Networks 3(2005).
46. Lal, D. Toshniwal, R. Radhakrishnan, R. Agrawal, D. and Caffery, J. "A novel MAC layer protocol for space division multiple access in wireless ad hoc networks", Eleventh International Conference on Computer Communications and Networks, 2002.
47. Lee, J. Tang,A. Huang,J. Chiang,M. and Calderbank,A. "Reverse-Engineering MAC A Non-Cooperative Game Model", IEEE Journal on Selected Areas in Communications, Vol. 25, No. 6, AUGUST 2007

48. Lee, T. Chan, S. Zhang, Q. Zhu, W. and Zhang, Y. "Allocation of Layer Bandwidths and FECs for Video Multicast Over Wired and Wireless Networks" IEEE Transactions on Circuits and System for Video Technology, Vol. 12, No. 12, December 2002.
49. Li, M. Koutsopoulos, I. and Poovendran,R. "Optimal Jamming Attacks and Network Defense Policies in Wireless Sensor Networks", INFOCOM 2007. 26th IEEE International Conference on Computer Communications.
50. Liang, Y. Apostolopoulos, J. and Girod, B. "Analysis of Packet Loss for Compressed Video: Effect of Burst Losses and Correlation Between Error Frames" IEEE Transactions on Circuits and System for Video Technology, Vol. 18, No. 7, July 2008.
51. Liu, C. Shu, Y. Yang, W. and Wang, O. , "Throughput Modeling and Analysis of IEEE 802.11 DCF with Selfish Node", Global Telecommunications Conference, 2008. IEEE GLOBECOM 2008.
52. Ma, R. Misra, V. and Rubenstein, D. "Modeling and Analysis of Generalized Slotted-Aloha MAC Protocols in Cooperative, Competitive and Adversarial Environments" Proceedings of the 26th IEEE International Conference on Distributed Computing Systems (ICDCS'06)Competitive and Adversarial Environments.
53. MacKenzie, R., Hands, D. and Farrell, T. 'Packet Handling Strategies to Improve Video QoS over 802.11e WLANs', IEEE 20th International Symposium on Personal, Indoor and Mobile Radio Communications, 2009.
54. Malone, Duffy and Leith, "Modeling the 802.11 Distributed Coordination Function in Non-saturated Heterogeneous Conditions"IEEE/ACM Transactions on Networking, Vol. 15, No. 1, February 2007.
55. Nasipuri, A. Ye, S. You, J. and Hiromoto, R. "A MAC Protocol for Mobile Ad Hoc Networks Using Directional Antennas", Wireless Communications and Networking Conference, 2000.

56. Navda, V. Bohra, A. Ganguly, S. and Rubenstein, D. “Using Channel Hopping to Increase 802.11 Resilience to Jamming Attacks”, INFOCOM 2007. 26th IEEE International Conference on Computer Communications.
57. Politis, I. Tsagkaropoulos, M. Pliakas, T. and Dagiuklas, T. "Distortion Optimized Packet Scheduling and Prioritization of Multiple Video Streams over 802.11e Networks" Hindawi Publishing Corporation Advances in Multimedia, Volume 2007.
58. Radosavac, S. Cárdenas, A., Baras, J. and Moustakides, G. “Detecting IEEE 802.11 MAC layer misbehavior in ad hoc networks: Robust strategies against individual and colluding attackers”, Journal of Computer Security 15 (2007) 103–128.
59. Ramanathan, R."On the performance of Ad Hoc Networks with Beamforming Antennas", MobiHoc '01 , the 2nd ACM international symposium on Mobile ad hoc networking & computing.
60. Ramanathan, R. Redi, J. Santivanez, C. Wiggins, D. and Polit, S. “Ad hoc networking with directional antennas a complete system solution”, MobiHoc’04, May 24–26, 2004, Roppongi, Japan.
61. Raya, M. Aad, I. Hubaux, J. And Fawal, A. “DOMINO: Detecting MAC Layer Greedy Behavior in IEEE 802.11 Hotspots”, IEEE Transactions on Mobile Computing, Vol. 5, No. 12, December 2006
62. Raya, M., Hubaux,J. and Aad, I “DOMINO: a system to detect greedy behavior in IEEE 802.11 hotspots”, MobiSys '04, the 2nd international conference on Mobile systems, applications, and services, 2004.
63. Rong, Y. Lee, S. and Choi, H. “Detecting Stations Cheating on Backoff Rules in 802.11 Networks Using Sequential”, 25th IEEE International Conference on Computer Communications.
64. Schaar, M. Krishnamachari, S. Choi, S. and Xu, X. "Adaptive Cross-Layer Protection Strategies for Robust Scalable Video Transmission Over 802.11 WLANs" IEEE Journal on Selected Area in Communications, Vol. 21, No. 10, December 2003.

65. Setton, E. Zhu, X. and Girod, B. "Confestion Optimized Multi-Path Streaming of Video Over AD Hoc Wireless Networks", 2004 IEEE International Conference on Multimedia and Expo (ICME)
66. Shan, Y. "Cross-Layer Techniques for Adaptive Video Streaming over Wireless Networks " EURASIP Journal on Applied Signal Processing 2005.
67. So, J. and Vaidya, N. "Multi-Channel MAC for Ad Hoc Networks: Handling Multi-Channel Hidden Terminals Using A Single Transceiver ", IEEE Transactions on Mobile Computing, Vol. 5, No. 5, MAY 2006.
68. Spyropoulos, A. and Raghavendra, C. "Capacity bounds for ad-hoc networks using directional antennas", ICC '03. IEEE International Conference on Communications, 2003.
69. Subramanian, A. and Das, S. Addressing deafness and hidden terminal problem in directional antenna based wireless, IEEE Journal on Selected Areas in Communications, Vol. 23, No. 3, March 2005.
70. Sundaresan, K. and Sivakumar, R. "A unified MAC layer framework for ad-hoc networks with smart antennas", IEEE Transactions on Mobile Computing, Vol. 7, No. 2, February 2008.
71. Takai, M. Martin , J. Ren A. and Bagrodia, R. Directional virtual carrier sensing for directional antennas in mobile ad hoc networks, Proceedings of the 24th International Conference on Distributed Computing Systems Workshops (ICDCSW'04).
72. Tian, D. Li, X. Regib, G. Altunbasak, Y. and Jackson, J. "Optimal Packet Scheduling for Wireless Video Streaming with Error-Prone Feedback", IEEE Wireless Communications and Networking Conference, 2004.
73. Yeo, J. Youssef, M. and Agrawala, A. "A Framework for Wireless LAN Monitoring and Its Applications", WiSe '04 Proceedings of the 3rd ACM workshop on Wireless security.

74. Yi, S. Pei, Y. and Kalyanaraman, S. “On the Capacity Improvement of Ad Hoc Wireless Networks Using Directional Antennas”, MobiHOC 2001, Long Beach, CA, USA

75. You, F. Zhang, W. and Xiao, J. Packet Loss Pattern and Parametric Video Quality Model for IPTV, Eighth IEEE/ACIS International Conference on Computer and Information Science,2009.

76. Yu, X. Modestino, J. and Bajic, I. "Performance Analysis of the Efficacy of Packet-level EFC in Improving Video Transport Over Networks" , IEEE International Conference on Image Processing, ICIP 2005.

77. Yu, W. Sun, Y. and Liu, K. “HADOF: Defense Against Routing Disruptions in Mobile Ad Hoc Networks”, INFOCOM 2005. 24th Annual Joint Conference of the IEEE Computer and Communications Societies.

78. Zhang, R. Regunathan, S. and Rose, K. 'End-to-end Distortion Estimation for RD-based Robust Delivery of Pre-compressed Video", Thirty-Fifth Asilomar Conference on Signals, Systems and Computers, 2001.

79. Zhu, X. and Girod, B."Subjective Evaluation of Multi-user rate Allocation for Streaming Heterogeneous Video Contents over Wireless Networks",15th IEEE International Conference on Image Processing, 2008.

80. www.google.com